Novel Methods for the Synthesis and C-H Functionalization of Imidazopyridines and Coumarins

THESIS

Submitted in partial fulfillment of the requirements for the degree

of

DOCTOR OF PHILOSOPHY

by

Neha Meena

ID. NO. 2018PHXF0416P

Under the supervision of

Prof. Anil Kumar

DEPARTMENT OF CHEMISTRY
BIRLA INSTITUTE OF TECHNOLOGY AND SCIENCE, PILANI
PILANI CAMPUS, RAJASTHAN (INDIA)
April 2024

Dedicated to

My Beloved Family

BIRLA INSTITUTE OF TECHNOLOGY AND SCIENCE,
PILANI (RAJASTHAN)

CERTIFICATE

This is to certify that the thesis titled "**Novel Methods for the Synthesis and C-H Functionalization of Imidazopyridines and Coumarins**" submitted by **Neha Meena** ID No **2018PHXF0416P** for the award of Ph.D. of the Institute embodies original work done by her under my supervision.

Signature of the Supervisor:

Name in capital letters: DR. ANIL KUMAR

Designation: Professor

Date:

Acknowledgment

At the beginning, I express my heartfelt devotion to ***"God"*** for giving me strength, knowledge, and the capability to embark on and complete this research study. Now, it is the time of pleasure to recollect the countless cherished moments and the individuals who stood beside me throughout. Their unwavering support, guidance, motivation, and blessings at every stage have helped me to achieve this significant milestone in my life.

Next, I sincerely thank Prof. Anil Kumar, whose guidance and mentorship were important throughout my Ph.D. journey. I am grateful to sir for allowing me to work in the laboratory without any pressure. I consider it a great opportunity to have done my doctoral program under his guidance and to learn from his research expertise. His inspiring hard work and constant motivation helped me to understand better and remain optimistic throughout my Ph.D. tenure. I am also thankful for the opportunities he provided to mentor undergraduate and newcomer students in his laboratory, which added valuable experience to my Ph.D. journey. Sir, I express my heartfelt thanks for all your help and support.

I express my gratitude to the past and current Vice chancellors, Directors, Deans and Associate Deans of Birla Institute of Technology & Science, Pilani (BITS Pilani), for allowing me to pursue my doctoral studies by providing the necessary facilities. I extend my heartfelt appreciation to the office staff of AGSRD, whose secretarial assistance helped me in submitting the various evaluation documents on time. I would also like to acknowledge the former and current Head of the Department, DRC members, Department of Chemistry, BITS Pilani, Pilani Campus for their official support and encouragement. I sincerely thank Dr. Ranjan Sinha Thakur, the Librarian at BITS Pilani, and the entire library staff for their support and help while utilizing the library facilities.

I am grateful to the members of my Doctoral Advisory Committee, Prof. Ajay K. Sah and Prof. Rajeev Sakhuja for their great cooperation during my Ph.D. At the onset, their valuable suggestion for refining my proposal and seminar greatly impacted my research. I acknowledge them for continuous suggestions and corrections for improving my thesis without any time limits. The other respectful faculty members of chemistry department Prof. S. C. Sivasubramanian, Prof. Dalip Kumar, Prof. Indresh Kumar, Prof. Saumi Ray, Prof. R. K. Roy, Prof. Inamur R. Laskar, Prof. Madhushree Sarkar, Prof. Bharti Khungar, Prof. Paritosh Shukla, Prof. Surojit Pande, Prof. Shamik

Chakraborty, and Dr. Bibhas R. Sarkar, Dr. Prashant Uday Manohar, Dr. Mrinmoyee Basu, Dr. Partha Sarathi Addy, Dr. Avik Kumar Pati, Dr. Pritam Jana, Dr. Satyajit Patra, Dr. Nikita Grover are respected for their cooperation during my PhD Programme. I am also thankful to Dr. Kiran Bajaj for her inspirational support during my research. Special appreciation goes to Mrs. Pusphlata Ji, Mr. Suresh Ji, and Mr. Nandalal Ji for their guidance in performing lab experiments in the Chemistry Lab and access to lab equipment and providing essential general chemicals.

I acknowledge Prof. R. Krishnan from Department of Chemistry, BITS Pilani, Hyderabad Campus for providing us with a single X-ray crystal analysis.

My special thanks to former members of my lab colleague Dr. Kasiviswanadharaju Pericherla, Dr. Pinku, Dr. Poonam for their achievement and inspiration to my professional life at BITS Pilani. I would also like to show my sincere thanks to Dr. Santosh Khandagale, Dr. Manish Kumar, Dr. Vishal, Dr. Vaishali Saini, Dr. Vimal, Dr. Moyna Das, Dr. Rishika, Dr. Sayantan, Dr. Chavvi, Dr. Mamta Devi Sharma, Dr. Jagriti for their moral support during my practical work.

I extend my warm thanks to research scholars and friends belonging from BITS Pilani, Dr. Amol Pawar, Dr. Jyothi, Dr. Bintu Kumar, Ms. Aishwarya, Ms. Prachi, Dr. Dhritabrata, Dr. Santosh Mishra, Dr. Pramod, for their continuous direct or indirect support in my research work. I also thank my departmental colleagues Ms. Soumona, Ms. Divya, Mr. Narsimha, Ms. Nidhi, Mr. Ram Prasad Bhatta, Ms. Shivani, Ms. Vishakha, Ms. Anuvasitha, Ms. Heena, Mr. Bharat, Ms. Mamta Katewa, Ms. Sonika, Ms. Shilpa, Ms. Sakshi Jangir, Ms. Sakshi Bajaj, Mr. Ajeet Sheoran, Mr. Ajeet Singh, Ms. Aastha, Ms. Nandani, Mr. Saurajit, Mr. Somnath, Ms. Manisha, Mr. Imtiyaz, Ms. Disha, Ms. Annu, Ms. Susmita, Ms. Ritu, Ms. Khushika, Mr. Sumit, Mr. Atul, Ms. Aarjoo, Ms. Nidhi, Ms. Niti, Ms. Mahima, Ms. Anakshi, Ms. Ritu, Ms. Vinita. I am also thankful to all my pharmacy department (BITS, Pilani) friends for their help.

The friendly and encouraging atmosphere and the remarkable achievements made in Lab 3145 have left an indelible mark on my life. I am immensely proud and grateful to express my heartfelt thanks to my labmates, Dr. Om Prakash Patel, Dr. Shiv Dhiman, Dr. Saroj Budania, Dr. Nitesh Nandwana, Dr. Khima Pandey, Dr. Hitesh Kumar Saini, Dr. Vikki Shinde, Dr. Sonam, Mr. Dhananjay Nipate, Ms. Bhawani, Mr. Prakash Swami, Mr. Amol Gadekar, Ms. Diksha Rohilla, Mr. Tarun Jangir and Ms. Vaani Dhyani for their love and support. I thank each of you individually for your cooperation, caring, and company, which made my Ph.D. journey more comfortable at

BITS Pilani. I also extend my gratitude to graduate students, Mr. Shivanshu, Ms. Radhika, and Ms. Neha, Mr. Himanshu Saini, Mr. Sachin, and Mr. Subhash Verma for their patience and support during our interactions.

I am extremely thankful to Dr. Hemant Joshi for discussing transition-metal complexes based on the pincer system and helping design and synthesize these ligands and their metal complex. His guidance and motivation throughout my Ph.D. helped me to work smartly toward my goals. His valuable suggestions and help are truly appreciated.

My thesis would be incomplete without acknowledging the invaluable contributions of my friends, Ms. Gunjan Dadhich, Ms. Priyanka Choudhary, Mr. Vinod Khatri, and Mr. Manoj Maharia, for their continuous and unwavering support during my Ph.D. years.

I express profound gratitude to Ms. Pragya, and Mr. Dhananjay Nipate for their unwavering moral support during challenging times, which motivated me to reach my destination. Their continuous support in course work, insightful discussions, and cheering me up all the time. I will forever cherish their valuable suggestions and help throughout my journey.

I extend my sincere gratitude to Dr. C.K. Mahesha, Ms. Kavya, Ms. Gurpreet, Mr. Sumit, Ms. Sushma Naharwal, Dr. Amol, Dr. Pramod, Mr. Prakash Pandurang Taur, Ms. Monika Malik, Ms. Prakriti Saraf, Mr. Narendra Kharat, and Mr. Yadav Nagre for their moral support and timely help.

I am deeply grateful to my parents, Mr. Ganesh Kumar Meena and Mrs. Manju Meena for their unwavering love, endless patience, and sacrifices to educate and prepare me to reach this milestone. Their presence has always been a source of comfort during stressful times. Words and this limited space cannot effectively express my gratitude to my parents. My wholehearted thanks to my wonderful siblings, Seema, Mohit, and Abhishek Meena, who celebrated my success as their own and provided me with immense love and care over the years. Also, thanks to my cousins Jyoti, Heena, Yuvraj, Punit, Yashraj, Rimjhim, and Aman Meena. They have always been there for me, offering guidance, providing a listening ear, and helping me through difficult times. Their unwavering faith in me helped me overcome obstacles and strive for success. I am truly blessed to have such loving cousins, and I could not have reached this point without them.

I want to express my sincere gratitude to my teachers from school, college, and post-graduation who supported me directly or indirectly in reaching this level of achievement. I would also like to thank my well-wishers, including teachers, relatives, and friends, whose faith, encouragement, and constant moral support contributed significantly to completing this work. I am deeply grateful to all of them.

I duly acknowledge valuable financial support in the form of a research fellowship from CSIR-New Delhi. DST-FIST is also sincerely acknowledged for providing instrumentation facilities in the department.

Finally, I humbly bow my head to the Almighty, who gave me the strength to work hard and overcome challenging situations.

Neha Meena

ABSTRACT

Heterocyclic compounds play a pivotal role in diverse scientific domains, including medicine, pharmaceuticals, and material chemistry. Transition-metal catalyzed C-H functionalization and oxidative annulation reactions play important role in the synthesis of heterocyclic motif in synthetic organic chemistry. The thesis titled "**Novel Methods for the Synthesis and C-H Functionalization of Imidazopyridines and Coumarins**" deals with the synthesis and C-H functionalization of heterocyclic compounds using transition-metal catalyst. The thesis is divided into five chapters.

The first chapter of the thesis presents a detailed exploration of transition-metal catalyzed C-H bond functionalization and oxidative C-H/C-H coupling reactions. The Co(II)-catalyzed intramolecular alkenylation *via* Knoevenagel condensation between active methylene azoles and β-bromocinnamaldehydes or 2-bromobenzaldehydes afforded imidazopyridine-fused isoquinoline derivatives. Through the implementation of this approach, a diverse array of twenty-nine scaffolds was successfully synthesized in moderate to good (74-36%) yields. The method exhibited tolerance for various functional groups and is amenable for scale up. Additionally, the developed methodology has potential to be extended for the synthesis of thioaroyl-substituted imidazo[1,5-*a*]pyridines and imidazo[1,5-*a*]isoquinolines derivatives, which could provide a novel class of medicinally relevant imidazopyridine-based fused heterocycles.

The second chapter of the thesis demonstrates a Ru(II)-catalyzed [4+2] annulation of 2-alkenyl/2-aryl imidazoles with maleimides for the synthesis of imidazo-fused polyheterocycles in moderate to good (49-81%) yields. The developed protocol features a broad substrate scope, with high functional group tolerance and is scalable. Moreover, annulation of 2-alkenyl/2-aryl imidazoles with 1,4-naphthoquinones under standard conditions delivered 9,12-dihydrobenzo[*b*]imidazo[1,2-*f*]phenanthridine-8,13-dione derivatives.

The third chapter of the thesis describes a regioselective oxidative annulation of 2-arylimidazo[1,2-*a*]pyridines with cinnamaldehyde derivatives. A Rh(III)-catalyzed annulation afforded 5-arylnaphtho[1',2':4,5]imidazo[1,2-*a*]pyridine-6-carbaldehydes while Pd(II)-catalyzed annulation reaction produced 1,7-diarylimidazo[5,1,2-*cd*]indolizine-6-carbaldehydes. The developed synthetic approach produced annulated products in moderate to good (51-80%) yields and exhibited broad substrate scope and excellent functional group tolerance. The method provided two different isomeric annulated products bearing an aldehyde functionality which can be elaborated into an array of functionalities leading to valuable compounds.

The **fourth chapter** of the thesis describes molecular rotor-based complexes and their applications. This chapter is divided into two parts: **Part A** describes a brief introduction of molecular rotor-based complexes and their applications. A new molecular rotor based Pd(II)-complex was synthesized and characterized with the help of NMR, IR, HRMS, and single-crystal X-ray crystallography study. The Pd(II)-complex was found to be the efficient catalyst for regioselective annulation of 2-arylimidaz[1,2-*a*]pyridines with alkynes. The catalyst showed high functional group tolerance and 1.5 mol % of the catalyst loading is required to achieve good yields of annulated products under mild reaction conditions. **Part B** presents the synthesis of three novel Pd(II)-complex of bulky selenium ligands. These complexes were characterized by NMR, HRMS, UV-Vis., IR, and elemental analysis. Moreover, the structure of one of the complex (C2) was validated by single crystal-X-ray study. Notably, the molecular rotor C2 was found to be the most efficient catalyst for the decarboxylative Heck-coupling under mild reaction conditions. The protocol proved to be adaptable to a broad range of substrates with large functional group tolerance and low catalyst loading (2.5 mol %). The catalyst was also found effective for the decarboxylative Suzuki-Miyaura complex leading to corresponding products in good yields. The mechanism behind the decarboxylative Heck-coupling reaction was investigated through both experimental and computational studies. The reaction was found to proceed under silver-free conditions, reducing the overall cost of the protocol.

Finally, in **the fifth chapter** of the thesis, summary of the thesis is presented along with the future scope of the research work.

TABLE OF CONTENTS

Appendices

LIST OF TABLES

LIST OF FIGURES

LIST OF ABBREVATIONS

Abbreviation	Description
AcOH	Acetic acid
acac	Acetylacetonate
ACN	Acetonitrile
Ar	Aryl
Aq	Aqueous
AgOAc	Silver acetate
AdCOOH	1-Adamantane carboxylic acid
atm	Atmosphere
BHT	Butylated hydroxy toluene
Bn	Benzyl
t-BuOK	Potassium *tert*-butoxide
^{13}C	Carbon-13
$CDCl_3$	Deuterated chloroform
Cp*	1,2,3,4,5-Pentamethylcyclopenta-1,3-diene
p-Cymene	1-Methyl-4-(propan-2-yl)benzene
$Cu(OAc)_2$	Cupric acetate
Calc.	Calculated
CCDC	Cambridge crystallographic data center
d	Doublet
dd	Doublet of doublet

DCB	1,4-Dichlorobenzene
DCE	1,2-Dichloroethane
DCM	Dichloromethane
DG	Directing group
DMA	Dimethylacetamide
DME	Dimethoxyethane
DMF	*N,N*-Dimethylformamide
DMSO-d_6	Deuterated dimethylsulfoxide
DMSO	Dimethylsulfoxide
ESI-MS	Electron spray ionization-mass spectrometry
Et_2O	Diethyl ether
EtOAc	Ethyl acetate
EtOH	Ethanol
EWG	Electron withdrawing group
EDG	Electron donating group
equiv.	Equivalent
FID	Free induction decay
FT-IR	Fourier transform infrared
g	Gram
h	Hours
HFIP	Hexafluoroisopropanol
HRMS	High resolution mass spectrometry

Hz	Hertz
^{i}Pr	Isopropyl
IBD	Iodobenzene diacetate
J	Coupling constant
KOAc	Potassium acetate
KIE	Kinetic isotopic effect
k_H	Protonated rate constant
k_D	Deuterated rate constant
Lit.	Literature
mp	Melting point
m	Meta
m	Multiplet
mL	Millilitre
mg	Milligram
MHz	Megahertz
min	Minutes
mmol	Millimole
mol %	Mole percent
MeOH	Methanol
NaOAc	Sodium acetate
NMR	Nuclear magnetic resonance
Nu	Nucleophile

o	Ortho
ORTEP	Oak ridge thermal ellipsoid plot
p	Para
Phen	1,10-Phenanthroline
PIDA	Phenyl iodonium diacetate
PivOH	Pivalic acid
ppm	Parts per million
Q-TOF	Quadrupole time of flight
rt	Room temperature
s	Singlet
t	Triplet
td	Triplet of doublets
TFA	Trifluoroacetic acid
TEMPO	(2,2,6,6-Tetramethylpiperidin-1-yl)oxyl
TFE	Trifluoroethanol
TBHP	*tert*-Butyl hydroperoxide
THF	Tetrahydrofuran
TLC	Thin layer chromatography
p-TSA or *p*-TsOH	*p*-Toluenesulfonic acid
UV	Ultraviolet
XRD	X-Ray diffraction
$Zn(OAc)_2$	Zinc acetate

Chapter 1

Cobalt-Catalyzed One-Pot Synthesis of Imidazo[1,5-*a*]pyridines/Isoquinolines Derivatives

Chapter 1

1.1 INTRODUCTION

Heterocyclic compounds are highly desirable in chemistry due to their prevalence in natural products and extensive pharmaceutical usage.[1-4] Furthermore, the heterocyclic scaffolds play a significant role as versatile building blocks in organic synthesis. Their distinct reactivity is utilized to prepare pharmaceuticals, agrochemicals, dyes, polymers, and other industrially relevant molecules. For centuries, these compounds have been regarded as privileged substances, and their synthesis is often accomplished through functional group transformation. *N*-heterocycles, which are widely present in biologically active natural products, pharmaceutical drugs, and agrochemicals. For example, over 59% of the small-molecule FDA-approved medicines have at least one *N*-heterocycle.[5-7] *N*-heterocycles have various physiological and pharmacological properties that make them attractive for drug design. Therefore, synthesizing *N*-fused heterocycles with different structural modifications is an active area of research. For example, polysubstituted imidazole-fused heterocycles is one such group among different *N*-heterocycles which contain extensive conjugated systems, making them optically attractive and utilized as fluorescent probes.[8-10] Aside from that, imidazo-fused heterocycles enriched in aryl-aryl bonds and electron-rich are frequently found in biological systems. These arylated imidazo-fused heterocycles have been found in many natural compounds and therapeutic prospects. The imidazo-fused heterocycles scaffolds are natural products that act as an inhibitor and anti-cancer agent. The indole/imidazole-fused isoquinolines core has also demonstrated various interesting biological activities such as, anti-cancer, analgesic, and anti-inflammatory (**Figure 1.1)**.[11-13]

Furthermore, researchers have utilized imidazo[1,5-*a*]heteroaromatics as novel dye structures with the promising application as fluorescent probes,[14-18] precursors of *N*-heterocyclic carbenes,[19-21] and organic light-emitting diodes.[22-24] Thus, developing novel and efficient methods for the synthesis of this crucial scaffold has long been a topic of interest in synthetic organic chemistry.

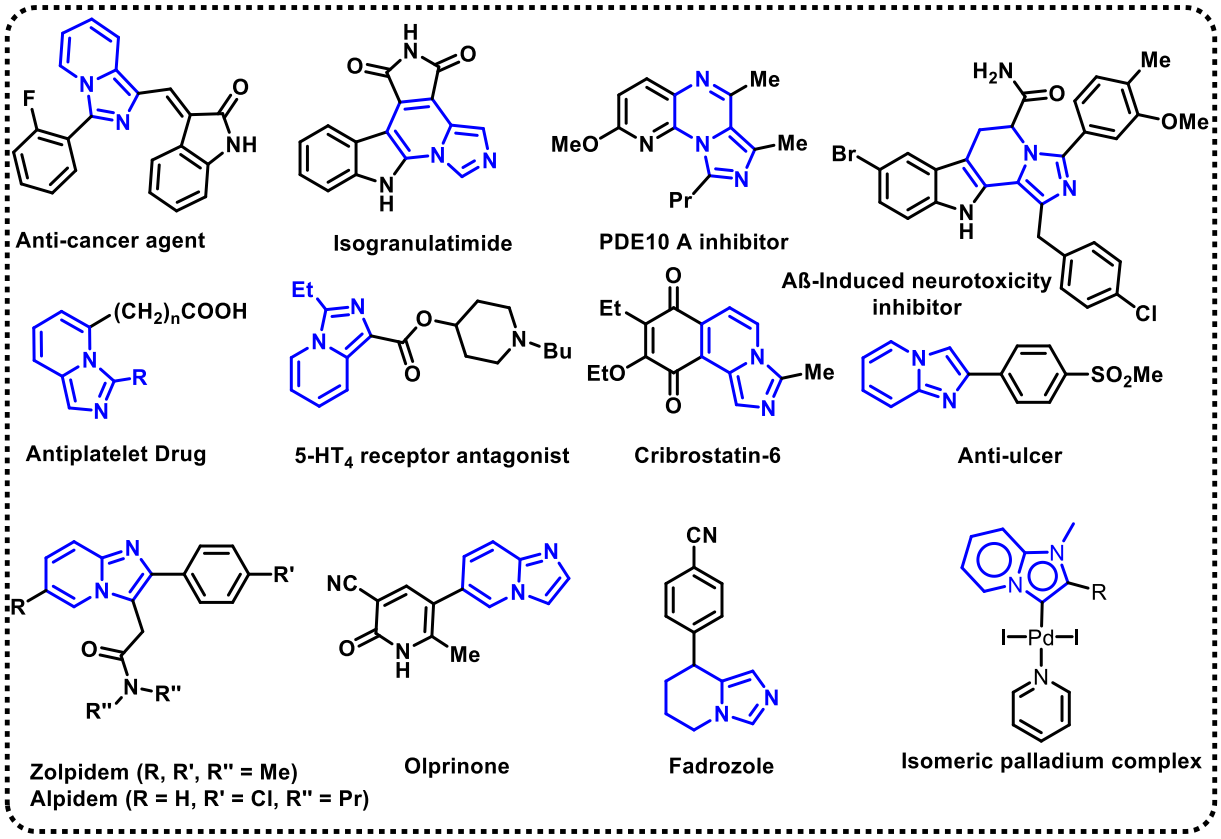

Figure 1.1: Representative examples of biologically active imidazo-fused *N*-heteroaromatics

Despite their enormous synthetic, commercial, and medical potential, the traditional techniques for synthesizing imidazo[1,5-*a*]pyridine derivatives are unexpectedly limited. Consequently, synthesis of imidazo-fused heterocycle has received particular attention from numerous research groups due to the potential uses of fused heterocycles. To obtain these scaffolds, a variety of approaches utilizing transition metal-catalyzed C-H bond activation have been disclosed. In recent years, C-H bond activation (C-H activation) has become a promising method for functionalizing organic moieties in pharmaceuticals, material science, and biochemistry.

Chen group prepared imidazo[1,5-*a*]pyridines (**3**) through Rh-catalyzed regioselective C-H bond activation of the imidazole ring. The *N*-vinylimidazole (**1**) and alkynes (**2**) underwent rhodium-catalyzed oxidative annulation in the presence of $Cu(OAc)_2 \cdot H_2O$ to deliver imidazo-fused[1,5-*a*]pyridines in yields upto 99%. Interestingly, *N*-arylpyrroles on annulation of alkynes also afforded imidazo-fused quinolone derivatives in good yields under these conditions (**Scheme 1.1**).[25]

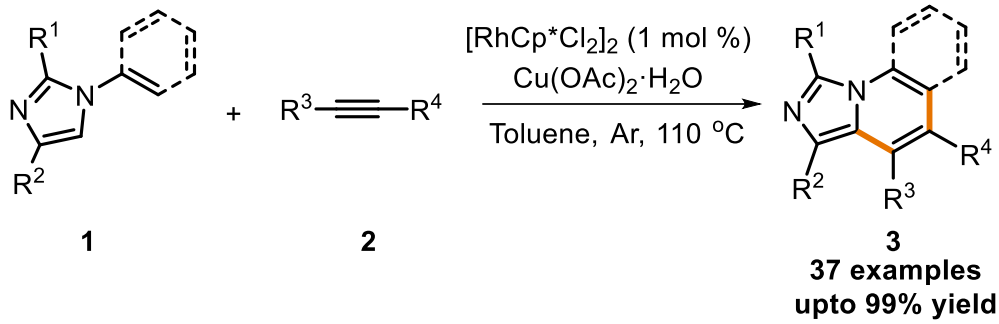

Scheme 1.1: Rh(III)-catalyzed synthesis of imidazo[1,5-*a*]pyridines from *N*-vinylimidazoles

Gevorgyan and coworkers have developed rhodium(II) catalyzed transannualtion of pyridotriazoles (**7**) with nitriles (**6**) to produce pyrrolo or imidazopyridines derivatives (**3**) in moderate to good yield (51-89%) *via* ylide formation followed by (2+2) cycloaddition with broad functional group tolerance (**Scheme 1.2a**).[26] Similarly, Joshi *et al*., have also described a synthetic method to produce imidazo[1,5-*a*]pyridines through a denitrogenative transannulation reaction involving pyridotriazoles (**5**) and derivatives of amines and amino acids (**4**). In their study, they utilized copper salt (CuI) as a catalyst, conducting the reaction at elevated temperatures in a sealed vessel. However, it should be noted that this approach proved unsuitable for aza-heterocyclic and simple aliphatic amines. The denitrogenation process entailed the formation of a Cu-carbene complex, which subsequently underwent migratory insertion, oxidative dehydrogenation, and aromatization, ultimately leading to the formation of the desired product. The molecular oxygen present in the surrounding air facilitated the oxidation reactions (**Scheme 1.2b**).[27]

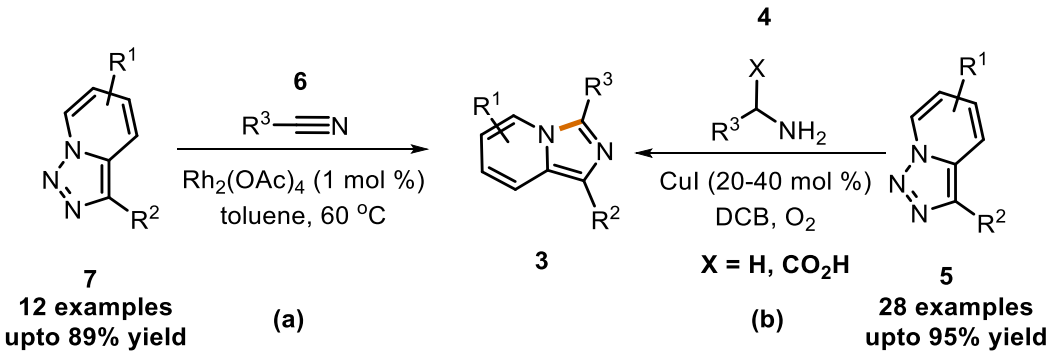

Scheme 1.2: Rh(II)/Cu(I)-catalyzed synthesis of imidazo[1,5-*a*]pyridines from pyridotriazoles

Adimurthy and co-workers disclosed an efficient copper-catalyzed aerobic oxidative amination of C(sp^3)–H bonds to afford imidazo[1,5-*a*]pyridine-1-carboxylates derivatives in upto 93% yield from pyridyl esters (**8**) and benzylamine (**4**) or amino acids In the presence of atmospheric air Cu(I) is oxidized to Cu(II) (**Scheme 1.3**).[28]

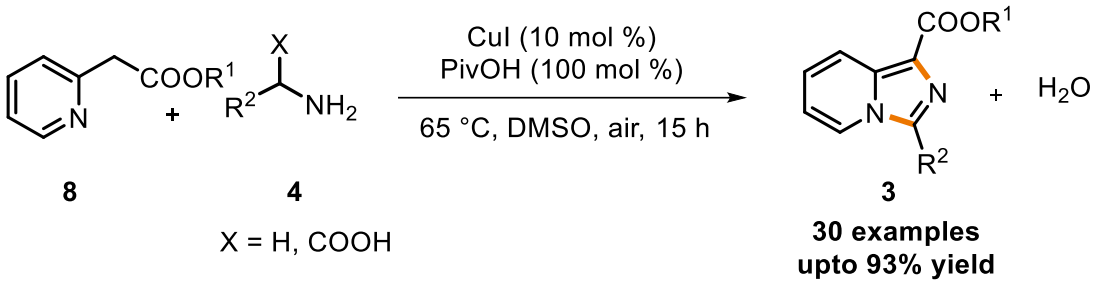

Scheme 1.3: Synthesis of imidazo[1,5-*a*]pyridine-1-carboxylates *via* Cu(I)-catalyzed aerobic oxidative amination

Alternatively, Zeng and Xu's group independently synthesized imidazo[1,5-*a*]-*N*-heteroaromatics *via* Cu-catalyzed domino condensation-amination-oxidative dehydrogenation reaction between 2-benzoylpyridines or 2-benzoylquinolines and benzylamine or *α*-amino acids **(Scheme 1.4a, b or c)**.[29, 30]

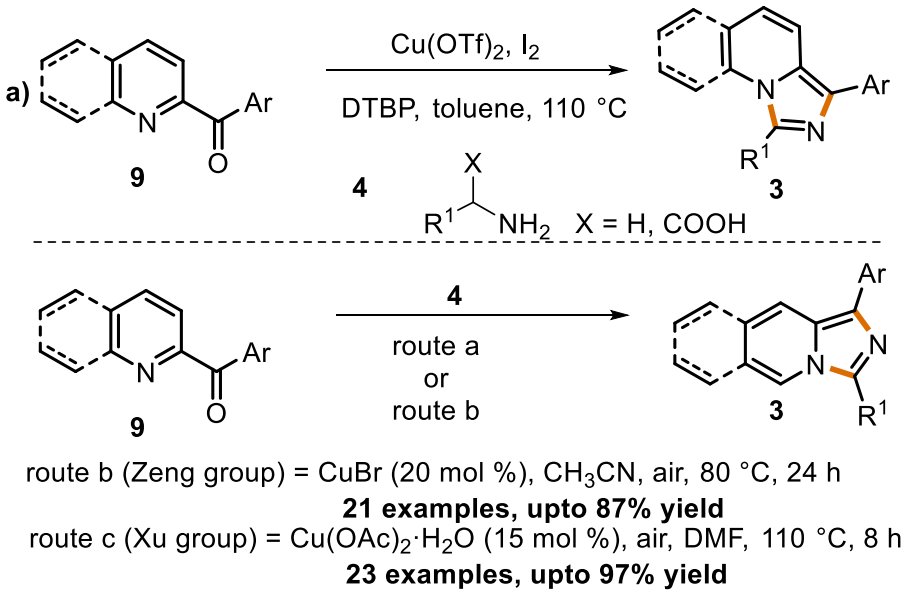

Scheme 1.4: Synthesis of imidazo[1,5-*a*]-*N*-heteroaromatics from 2-benzoylpyridines or 2-benzoylquinolines and benzylamine

Reddy and colleagues also established a copper(II)-catalyzed method to synthesize imidazo[1,5-*a*]quinolones and imidazo[5,1-*a*]isoquinolines **(11)** from 2-methylquinolines **(10)** and benzylamines **(4)**. Initially, an *in-situ* imine intermediate was formed; which underwent intramolecular amination and delivered the respective derivatives in upto 85% yields (**Scheme 1.5**).[31]

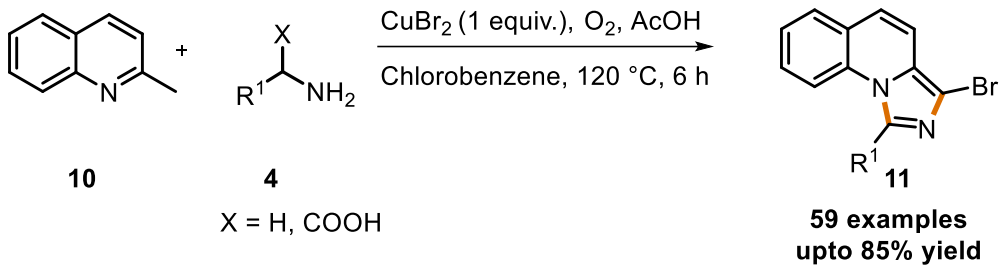

Scheme 1.5: Cu(II)-catalyzed synthesis of imidazo[1,5-*a*]quinolones and isoquinolines from 2-methylquinolines and benzylamine

Simple and elegant approach for the synthesis of polysubstituted imidazo[1,5-*a*]pyridines (**13** or **14**) from (2-pyridinyl)methanols (**12**) and benzylamines (**4**) or amino-acids (**4**) has been reported by Sekar and co-workers. This reaction proceeds *via* alcohol oxidation, condensation followed by oxidative amination in the presence of Cu(I)-catalyst to deliver imidazo[1,5-*a*]pyridines in moderate to excellent yields (68-97%) (**Scheme 1.6**).[32]

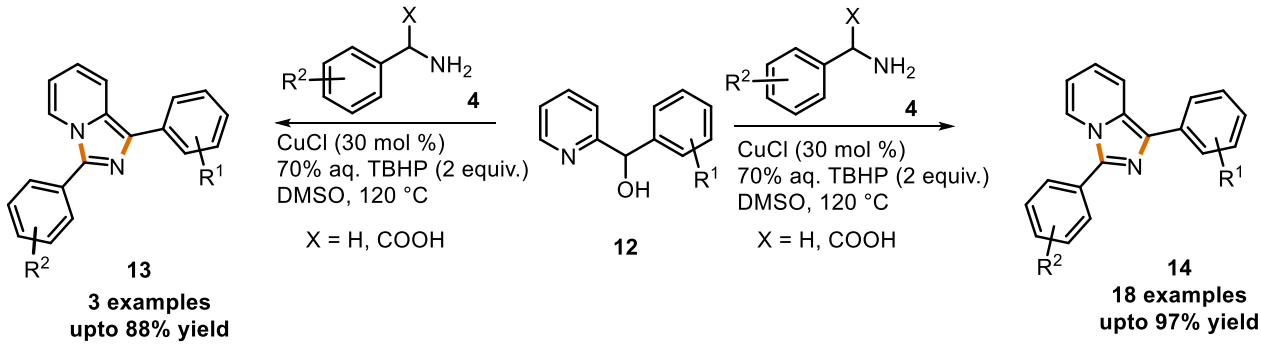

Scheme 1.6: Synthesis of 1,3-disubstituted imidazo[1,5-*a*]pyridines from (2-pyridinyl)methanols and benzylamine/amino acids

Kumar group has developed an efficient route for the synthesis of pyrazolo[5,1-*a*]isoquinolines (**17**) *via* nickel-catalyzed tandem reaction and intramolecular direct arylation of 1-aryl-2-(1*H*-pyrazol-1yl)ethan-1-ones (**16**) and 2-bromoaldehydes (**15**) (**Scheme 1.7a**).[33] Earlier, they have also synthesized imidazole/benzimidazo-fused isoquinolines (**19**) by condensation of 2-(1*H*-

imidazol-1-yl/benzimidazolyl-1-yl)-1-arylethanones (**18**) followed by palladium-catalyzed intramolecular dehydrogenative coupling (**Scheme 1.7b**).[34]

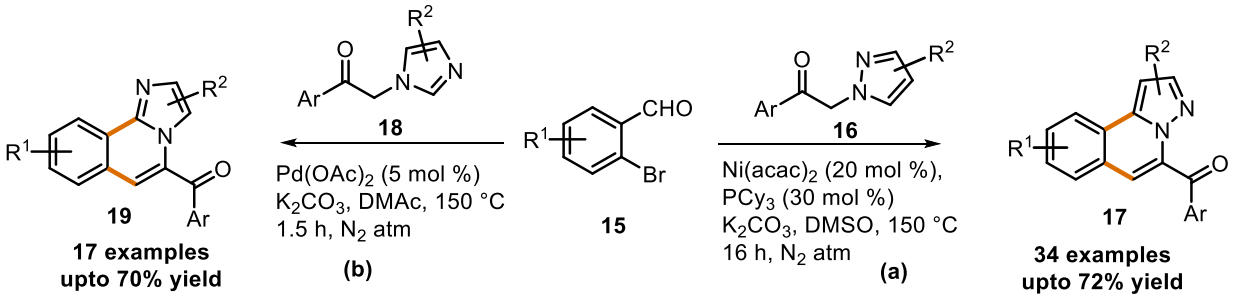

Scheme 1.7: Pd(II) or Ni(II)-catalyzed synthesis of imidazo-fused-isoquinolines from 2-bromobenzaldehydes

Li *et al.* reported a facile synthesis of imidazo[1,2-*a*:3,4-*a*]dipyridinium (**22**) from 2*H*-[1,2′-bipyridin]-2-ones (**20**) and 2-bromoacetophenones (**21**) *via* cobalt/copper-catalyzed tandem C(sp^2)–H alkylation and intramolecular annulation (**Scheme 1.8**).[35]

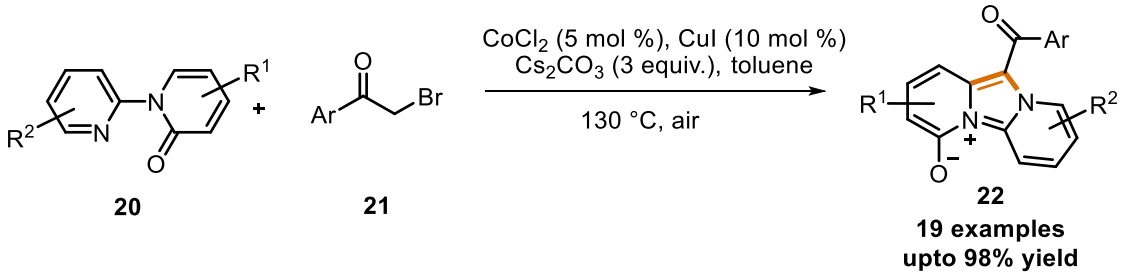

Scheme 1.8: Co(II)-catalyzed synthesis of dipyridinium salt using CuI

Typically, C-H bond activation strategies have relied on rare and expensive 4d and 5d transition metals like platinum, iridium, and rhodium, which have been categorized as EU-critical raw materials. However, 3d transition metals, which are more abundant and less expensive, have been explored relatively less for C-H activation. As researchers strive to develop more environmentally friendly methods for synthesizing organic molecules, 3d transition metal-catalyzed C-H activation has become a popular topic in 21st-century chemistry. Cobalt has been identified as a promising catalyst for C-H activation[36-39] and is found in enzymes that metabolize cholesterols, carbohydrates, and amino acids. Compared to other transition metals like platinum and iridium, cobalt is more cost-effective and less toxic, making it a better alternative.

In this chapter we have described a novel cobalt-catalyzed cascade reaction for synthesis of imidazo[1,5-*a*]pyridine/isoquinolines (**22**) from (2-methyl-1*H*-imidazol-1-yl)-1-arylethan-1-one (**23a**) and 3-bromo-3-aryl-acrylaldehyde **(24)** (**Scheme 1.9**). This method employs direct C-H arylation and classic Knoevenagel condensation to build two C-C bonds in one pot**.**

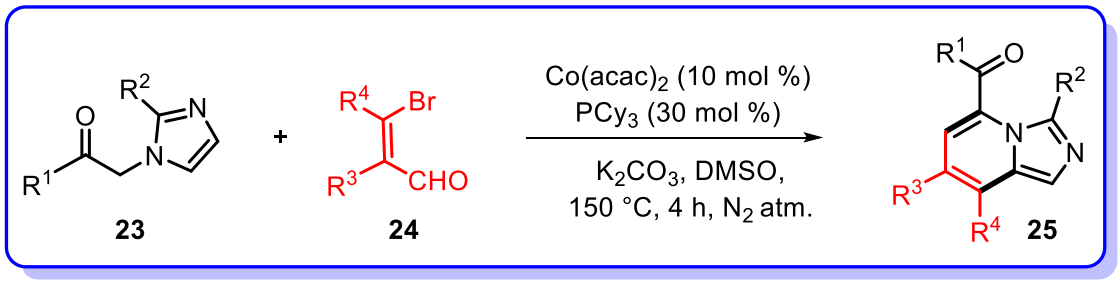

Scheme 1.9: Synthesis of imidazo[1,5-*a*]-pyridine/isoquinolines *via* Co(II)-catalyzed intramolecular C-H alkenylation

1.2 RESULTS AND DISCUSSION

We commenced our investigation by selecting 2-(2-methyl-1*H*-imidazol-1-yl)-1-phenylethan-1-one (**23a**) and 3-bromo-3-phenyl-acrylaldehyde (**24a**) as model substrates. The reaction of **23a** with **24a** was carried out in the presence of $Co(acac)_2$ (20 mol %), PPh_3 (30 mol %), and K_2CO_3 (3.0 equiv) in DMSO at 150 °C for 4 h under nitrogen atmosphere (**Table 1.1**, entry1). To our satisfaction, (3-methyl-8-phenylimidazo[1,5-*a*]pyridin-5-yl)(phenyl)methanone (**25aa**) was isolated in 45% yield. The structure of **25aa** was authenticated by different spectroscopic data like NMR (^1H, $^{13}C\{^1H\}$), HRMS, and IR. In the ^1H NMR spectrum of **25aa**, one singlet appeared at δ 2.45 ppm for methyl protons and rest of protons well matched with the corresponding structure (**Figure 1.2**). The carbonyl carbon and methyl carbon of **25aa** appeared at δ 187.3 ppm, along with the rest of the carbon of the compound (**Figure 1.3**). The mass spectrum of **25aa** showed a peak at *m/z* = 312.1263 for $[M+H]^+$ ion, which also validated its structure. In the IR spectrum of **25aa**, a strong peak appeared at 1651 cm^{-1} for C=O stretching.

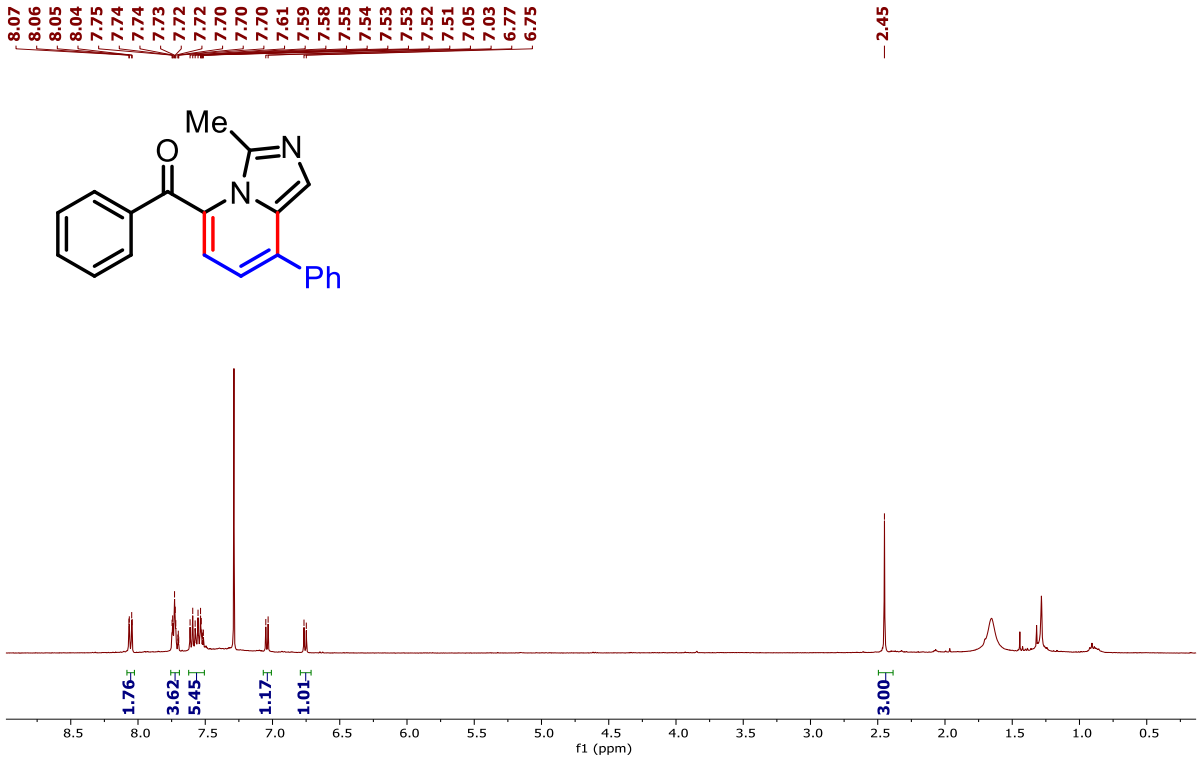

Figure 1.2: ^{1}H-NMR spectrum of (4-methoxyphenyl)(3-methyl-8-phenylimidazo[1,5-*a*]pyridin-5-yl)methanone (**25aa**) recorded in $CDCl_3$

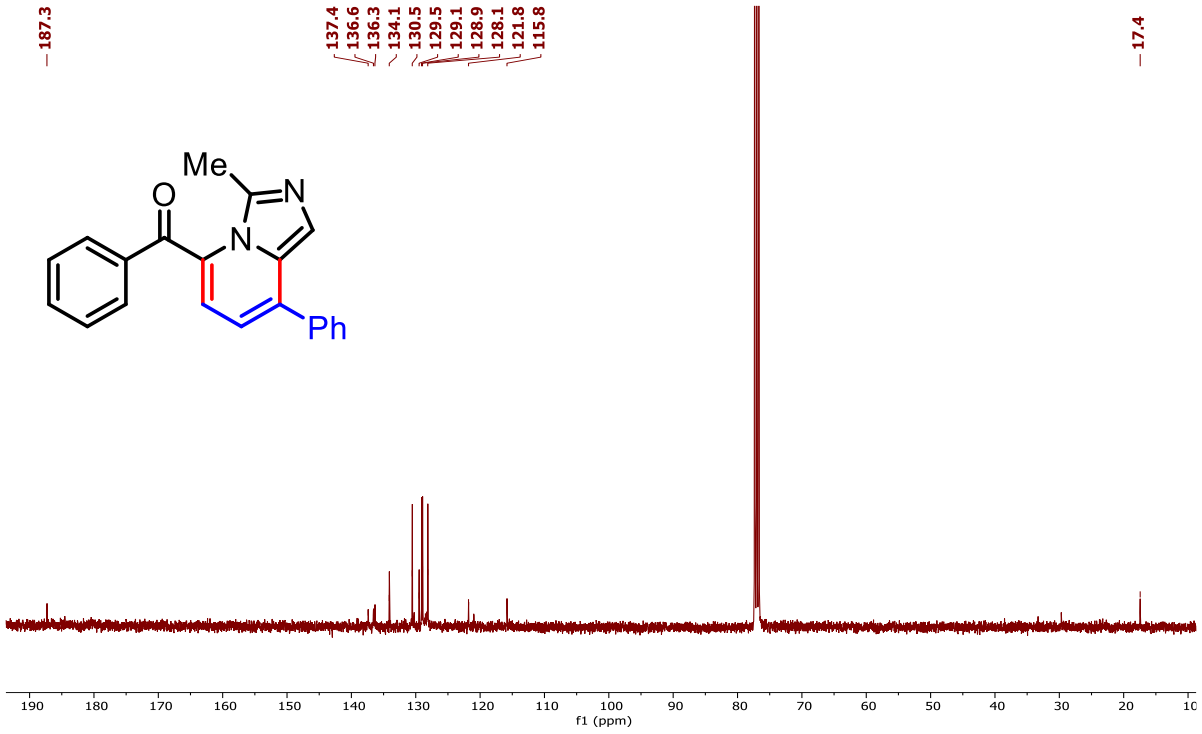

Figure 1.3: ^{13}C{^{1}H}-NMR spectrum of (4-methoxyphenyl)(3-methyl-8-phenylimidazo[1,5-*a*]pyridin-5-yl)methanone (**25aa)** recorded in $CDCl_3$

Basedon this exciting finding, we further explored the optimal conditions by varying the different catalysts, ligands, bases, and solvents to obtain a higher yield of the desired product (**Table 1.1)**. First, we screened for the dependency on various ligands such as PBu_3, PCy_3, $PCy_3 \cdot HBF_4$, P(*o*-tolyl)$_3$, and 1,10-phenathroline (1,10-Phen) (**Table 1.1**, entries 2–6). The highest yield (70%) of **25aa** was obtained using PCy_3 as the ligand (**Table 1.1**, entry 3). Next, we examined the effect of various metal catalysts such as $Co(OAc)_2$, $CoCl_2$, $Co(PCy_3)_2Cl_2$, $V(acac)_3$, $Fe(acac)_3$, $Ni(acac)_2$, and $Cu(acac)_2$ (**Table 1.1**, entries 7–13). The desired product **25aa** could be obtained in low to moderate yields with these catalysts but $Co(acac)_2$ was the most efficient. Furthermore, catalyst loading varied from 10 mol % to 30 mol % and based on the yield of **25aa**, it was found that 20 mol % $Co(acac)_2$ was the optimum catalyst loading for this reaction (**Table 1.1**, entry 3). Examination of different bases such as Cs_2CO_3, K_3PO_4, Na_2CO_3 and DIPEA for the model reaction indicated that K_2CO_3 was the best base for this transformation (**Table 1.1**, entries 3 and 14–17). The reaction of **23a** with **24a** using $Co(acac)_2$ as the catalyst in various organic solvents revealed that the best yield of **25aa** was obtained using DMSO as the solvent (**Table 1.1**, entries 3 and 18–20). The Knoevenagel product 5-bromo-5-(phenyl)-2-(2-methyl-1*H*-imidazol-1-yl)-1-phenyl-penta-2,4-dien-1-one (**28aa**) was isolated in 34% yield as the major product when the reaction of **23a** with **24a** was performed in toluene under these conditions (**Table 1.1**, entry 20). Notably, the reaction failed to produce **25aa** in the absence of K_2CO_3 or $Co(acac)_2$ (**Table 1.1**, entries 21 and 22). The Knoevenagel adduct **28aa** was obtained in 18% yield when the reaction was performed without $Co(acac)_2$ under the standard reaction conditions (**Table 1.1**, entry 22). The yield of **25aa** also reduced to 17% when the model reaction was performed without a ligand (**Table 1.1**, entry 23). Furthermore, the yield of **25aa** reduced to 32% (along with 17% of **28aa**) when the reaction was performed at 100 °C under otherwise similar reaction conditions (**Table 1.1**, entry 24).

Table 1.1 Optimization of reaction condition for the synthesis of **25aa**.

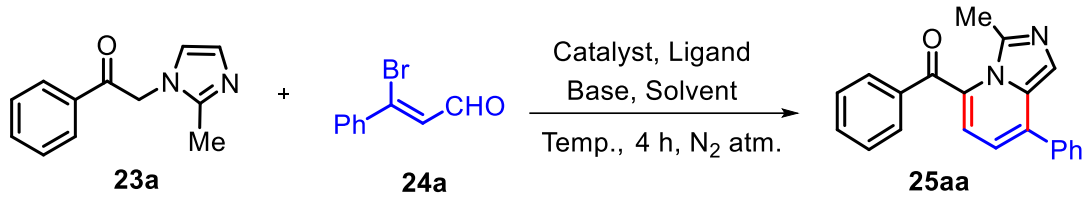

23a **24a** **25aa**

Entry	Catalyst	Ligand	Base	Solvent	% Yield 25aa[b]
1	$Co(acac)_2$	PPh_3	K_2CO_3	DMSO	45
2	$Co(acac)_2$	PBu_3	K_2CO_3	DMSO	25
3[c,d]	$Co(acac)_2$	PCy_3	K_2CO_3	DMSO	70
4	$Co(acac)_2$	$PCy_3{\cdot}HBF_4$	K_2CO_3	DMSO	39
5	$Co(acac)_2$	P(*o*-tolyl)$_3$	K_2CO_3	DMSO	trace
6	$Co(acac)_2$	1,10-Phen	K_2CO_3	DMSO	NR
7	$Co(OAc)_2$	PCy_3	K_2CO_3	DMSO	10
8	$CoCl_2$	PCy_3	K_2CO_3	DMSO	7
9	$Co(PCy_3)_2Cl_2$	PCy_3	K_2CO_3	DMSO	NR
10	$Ni(acac)_2$	PCy_3	K_2CO_3	DMSO	40
11	$V(acac)_3$	PCy_3	K_2CO_3	DMSO	62
12	$Cu(acac)_2$	PCy_3	K_2CO_3	DMSO	trace
13	$Fe(acac)_3$	PCy_3	K_2CO_3	DMSO	29
14	$Co(acac)_2$	PCy_3	Cs_2CO_3	DMSO	45
15	$Co(acac)_2$	PCy_3	K_3PO_4	DMSO	30
16	$Co(acac)_2$	PCy_3	Na_2CO_3	DMSO	46
17	$Co(acac)_2$	PCy_3	DIPEA	DMSO	NR
18	$Co(acac)_2$	PCy_3	K_2CO_3	DMF	30
19	$Co(acac)_2$	PCy_3	K_2CO_3	PEG-400	-
20[e]	$Co(acac)_2$	PCy_3	K_2CO_3	Toluene	trace
21	$Co(acac)_2$	PCy_3	-	DMSO	-
22[f]	-	PCy_3	K_2CO_3	DMSO	-
23	$Co(acac)_2$	-	K_2CO_3	DMSO	17
24[g]	$Co(acac)_2$	PCy_3	K_2CO_3	DMSO	32

[a]Reagents and reaction conditions: **23a** (0.25 mmol), **24a** (0.30 mmol), base (3.0 equiv), catalyst (20 mol %), ligand (30 mol %), solvent (3 mL) at 150 ºC for 4 h. [b]Isolated yield. [c]**25aa** was obtained in 47% yield when 10 mol % $Co(acac)_2$ and 20 mol % PCy_3 was added. [d]3aa was obtained in 65% yield when 30 mol % $Co(acac)_2$ and 50 mol % PCy_3 was added. [e]Knoevenagel adduct (**28aa**) was obtained in 34%. [f]Knoevenagel adduct (**28aa**) was obtained in 18%. [g]at 100 ºC, **28aa** was also obtained in 17% yield.

With the optimal reaction conditions in hand, we investigated the scope of the protocol by reacting *N*-aroyl-2-methyl-imidazoles (**23**) and 3-bromoacrylaldehydes (**24a**), as summarized in **Table 1.2**. First, *N*-aroyl-2-methylimidazoles (**23a–g**) were reacted with **24a** under the standard conditions to afford the related products **25aa–ga** in moderate to good (43–74%) yields. Substrate **23e** bearing the *para*-nitrobenzoyl group failed to produce the desired product **25ea** under standard conditions. It is worthwhile to mention that the reaction of 2-(1*H*-imidazol-1-yl)-1-phenylethan-1-one (**23g**) with **24a** produced a mixture of two regioisomers, phenyl(8-phenylimidazo[1,5-*a*]pyridin-5-yl)methanone (**25ga**) and phenyl(8-phenylimidazo[1,2-*a*]pyridin-5-yl)methanone (**25ga**'), in 43% and 36% yields, respectively. The reaction of 1-phenyl-2-(2-phenyl-1*H*-imidazol-1-yl)ethan-1-one (**23h**) with **24a** also afforded the desired product **25ha** in 63% yield. Next, the scope of 3-bromoacrylaldehydes (**24b–j**) was investigated. Higher yields of imidazo[1,5-*a*]pyridines were obtained from 3-bromo-3-arylacrylaldehydes with electron-donating groups on the benzene ring compared to those with electron-withdrawing groups (compare **25ab–ac** and **25ag** *vs*. **25ad–af**). This was further demonstrated by the competitive reaction of **23a** with **24c** and **24f** under the optimal reaction conditions, producing **25ac** and **25af** in 43% and 18% yields, respectively. The reaction of **23a** with 3-bromo-3-(thiophen-2-yl)acrylaldehyde (**24h**) and 3-bromo-3-(furan-2-yl)acrylaldehyde (**24i**) produced (3-methyl-8-(thiophen-2-yl)imidazo[1,5-*a*]pyridin-5-yl)(phenyl)methanone (**25ah**) and (3-methyl-8-(furan-2-yl)imidazo[1,5-*a*]pyridin-5-yl)(phenyl)methanone (**25ai**) in 57% and 61% yields, respectively. Similarly, the reaction of **23a** with 3-bromo-3-(4-bromophenyl)-2-methylacrylaldehyde (**24j**) afforded (8-(4-bromophenyl)-3,7-dimethylimidazo[1,5-*a*]pyridin-5-yl)(phenyl)methanone (**25aj**) in 47% yield. Other *N*-aroyl-2-methyl-imidazoles also reacted smoothly with substituted 3-bromo-3-arylacrylaldehydes to afford the corresponding imidazo[1,5-*a*]pyridines (**25bc–jd**) in moderate to good (39–66%) yields. The structure of all the compounds were ascertained by NMR and HRMS analysis. Furthermore, the structure of **25ah** was unambiguously confirmed by single crystal X-ray analysis (**Figure 1.4**, CCDC 2159571).

Table 1.2: Substrate scope for the synthesis of imidazo[1,5-*a*]pyridines.[a,b]

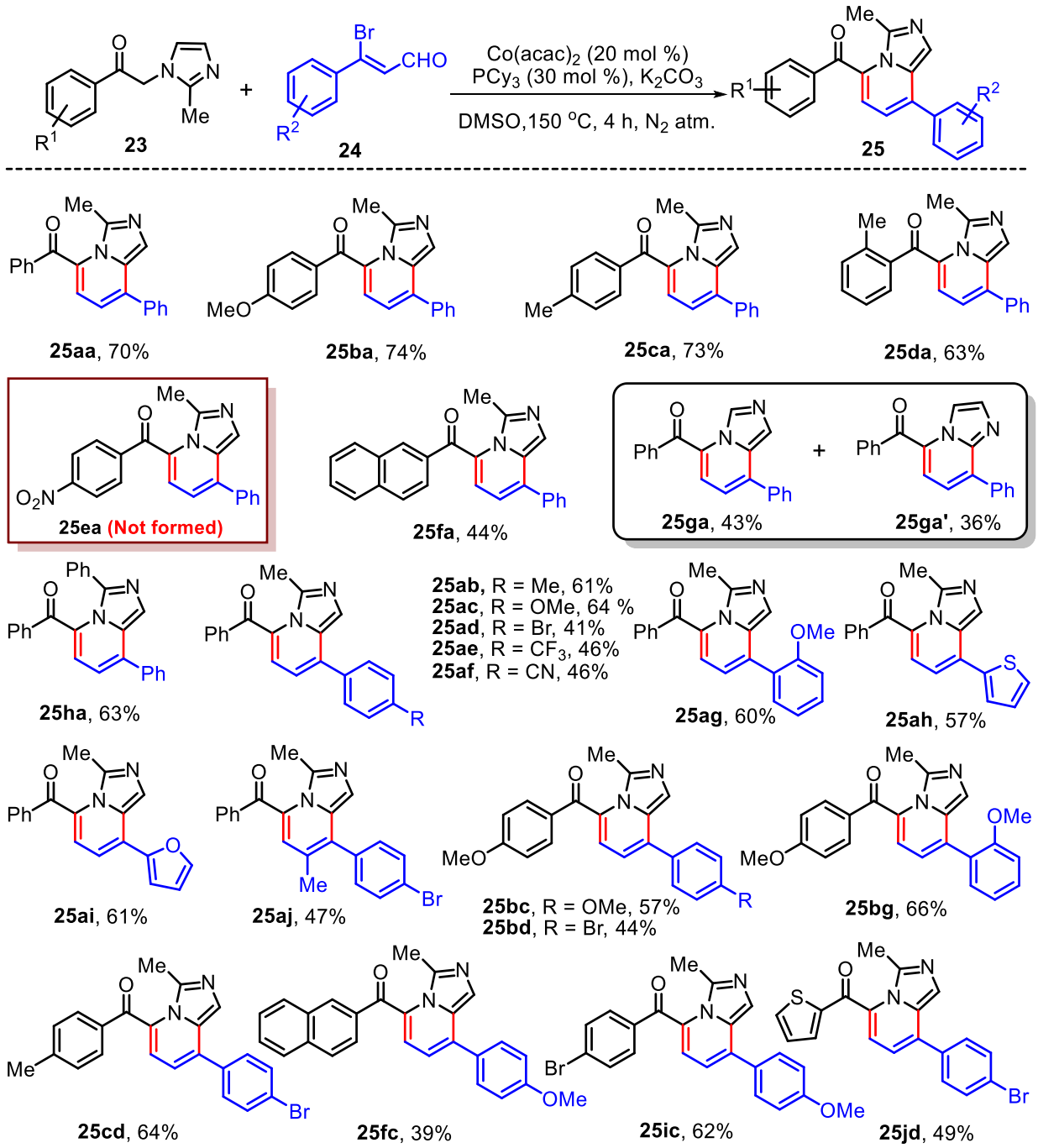

[a]Reaction conditions: **23** (0.25 mmol), **24** (0.30 mmol), K_2CO_3 (3.0 mmol), $Co(acac)_2$ (20 mol %), PCy_3 (30 mol %), DMSO (3 mL) at 150 °C for 4 h. [b]Isolated yields.

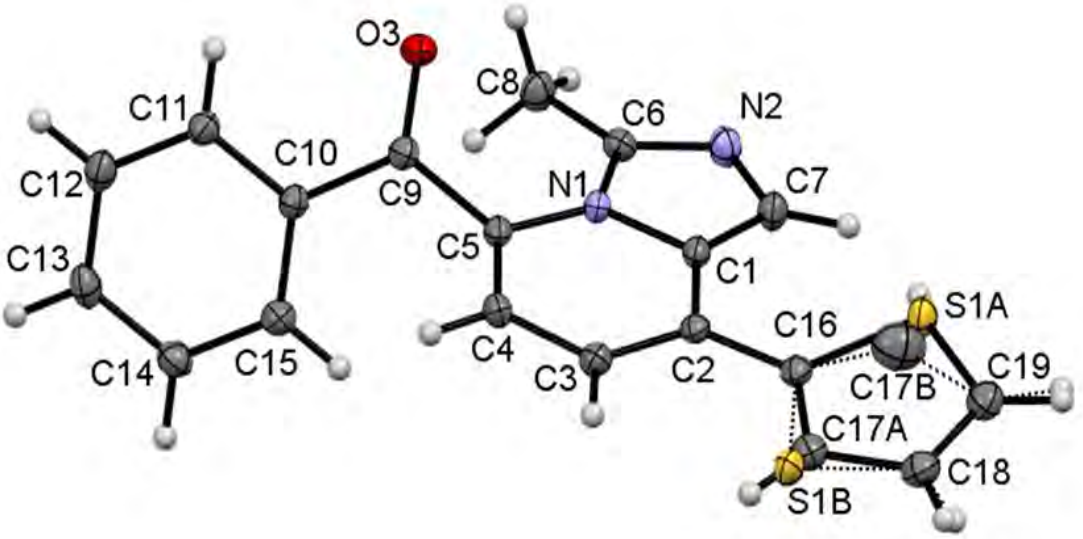

Figure 1.4: Single crystal ORTEP diagram of compound **25ah**. The thermal ellipsoids are drawn to a 50 % probability level (CCDC 2159571)

To demonstrate the generality of the developed approach, 2-(2-methyl-1*H*-imidazol-1-yl)-1-phenylethanethione (**23m**) was allowed to react with **24c** under the optimized reaction conditions (**Scheme 1.10**). The reaction furnished the corresponding imidazo[1,5-*a*]pyridine (**26**) in 46% yield.

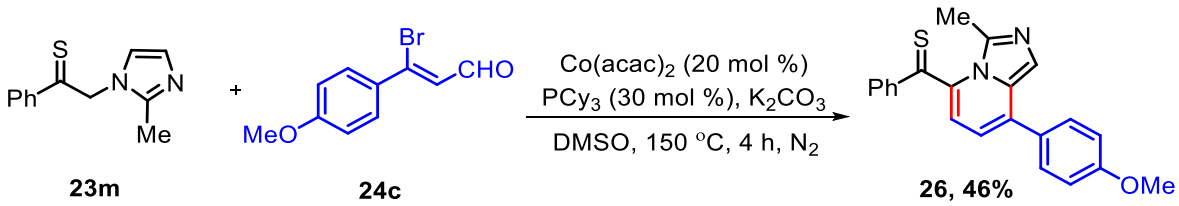

Scheme 1.10: Synthesis of (8-(4-methoxyphenyl)-3-methylimidazo[1,5-*a*]pyridin-5-yl)(phenyl)methanethione **(26)**

To extend the application of this protocol, we then investigated the reaction of 2-bromobenzaldehydes (**15**) with **23** to prepare imidazo[1,5-*a*]isoquinolines (**27**) and the results are summarized in **Table 1.3**. Substituted 2-bromobenzaldehydes (**15a–d**) possessing substituents such as 3,4-di-OMe, –OCH_2O– and –F reacted smoothly with **23a** under the optimized reaction conditions to afford 5-aroyl-3-methylimidazo[5,1-*a*]isoquinolines (**27aa–ad**) in moderate to good (40–65%) yields. Similarly, the reaction of selected substituted *N*-

aroyl-2-methylimidazoles (**23b, 23f, 23k, 23l**) with 1**5a** also produced the corresponding 3-methylimidazo[5,1- *a*]isoquinolines (**27ba–la**) in good (53–63%) yields. As noted earlier, the reaction of **23k** bearing the 2-nitrobenzoyl group with **15a** failed to produce the desired product **27ka** under the standard reaction conditions.

Table 1.3: Substrate scope for the synthesis of imidazo[1,5-*a*]isoquinolines.[a,b]

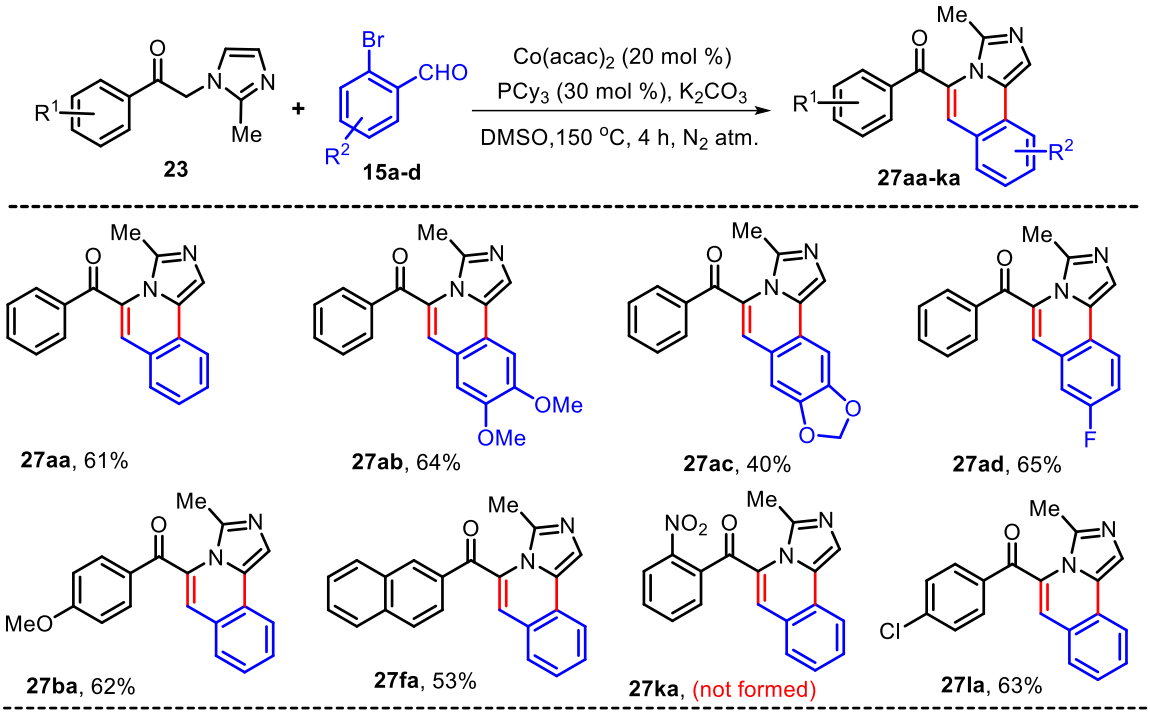

[a]Reaction conditions: **23** (0.25 mmol), **15** (0.30 mmol), K_2CO_3 (3.0 mmol), $Co(acac)_2$ (20 mol %), PCy_3 (30 mol %), DMSO (3 mL) at 150 ºC for 4 h. [b]Isolated yields.

The scalability of the developed method was demonstrated by the gram scale reaction of **23a** with **24a** (**Scheme 1.11**). Interestingly, the reaction was scalable and produced **25aa** in 63% (1.061 g) yield.

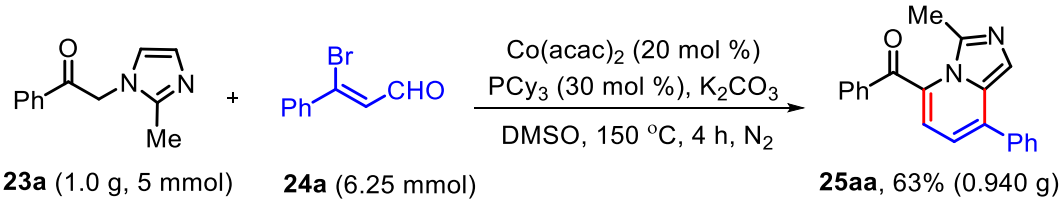

Scheme 1.11: Gram scale synthesis of **25aa**

To investigate the primary mechanism of the tandem process, several control experiments were carried out. First, performing the reaction of **23a** with **24c** under the standard conditions at 50 °C produced the Knoevenagel adduct **28ac** in 61% yield after 30 min (**Scheme 1.12a**). Next, the reaction of the isolated **28ac** in the presence of $Co(acac)_2$ and K_2CO_3 in DMSO at 150 °C for 4 h produced **25ac** in 75% yield (**Scheme 1.12b**). This indicated that initially the Knoevenagel condensation adduct is formed in the reaction which subsequently undergoes the Co-catalyzed intramolecular C–H alkenylation reaction. The formation of **25aa** in 66% and 58% yields in the presence of TEMPO and BHT under the standard reaction conditions revealed that the reaction followed a non-radical pathway (**Scheme 1.12c**). The yield of **25aa** increased from 7% to 41% using $CoCl_2$ as the catalyst and PCy_3 as the ligand in DMSO in the presence of acetylacetone (**Scheme 1.12d**). This result indicated that the Co(0) species is the active catalyst in this reaction.[52,53]

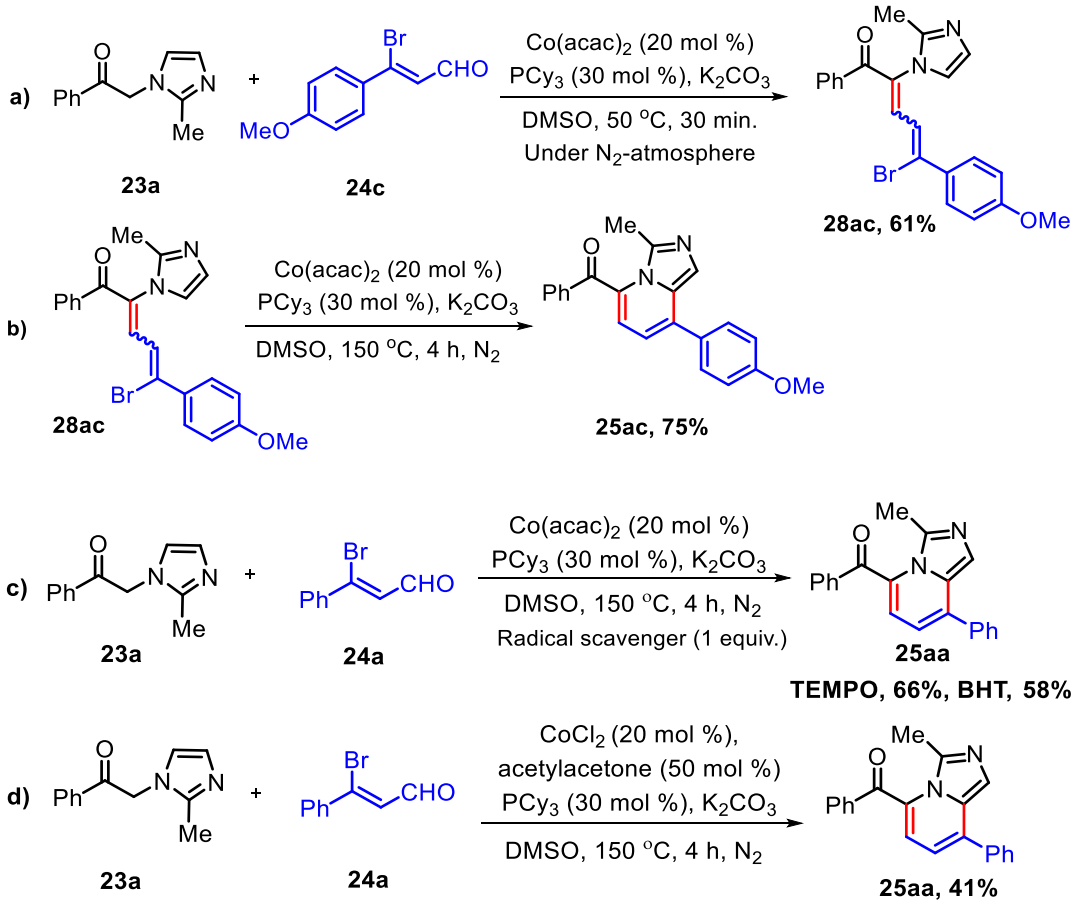

Scheme 1.12: Control experiments

Based on the results of control experiments and literature reports, a plausible mechanism of the Co(II)-catalyzed tandem one-pot transformation is depicted in (**Scheme 1.13)**. It is believed that the Knoevenagel adduct **28** was initially formed bythe reaction of **23** and **24** in the presence of a base. Meanwhile, $Co(acac)_2$ reacts with the phosphine ligand $P(Cy)_3$ to form the Co(0) complex, which is the starting point of the catalytic cycle. The oxidative addition of the Co(0) species with the Knoevenagel adduct **28** generates intermediate **A**. Intramolecular cyclization *via* C4–H bond activation of intermediate **A** produces the seven-membered cobaltacycle **B**, whichon reductive elimination leads to the formation of the desired product **25** with the regeneration of the Co(0) species.

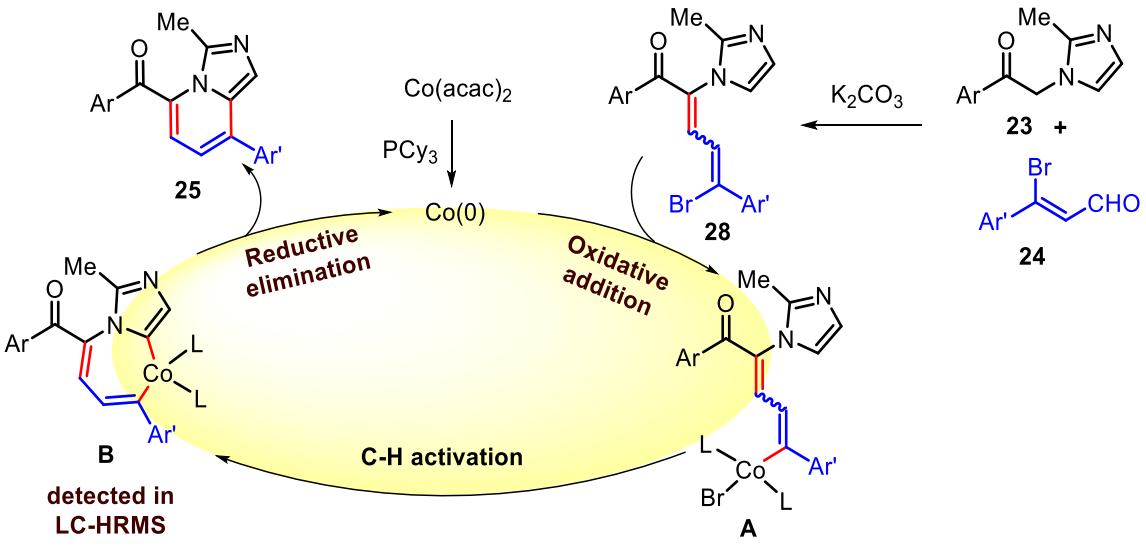

Scheme 1.13: Proposed reaction mechanism

1.3 CONCLUSION

In summary, we have developed a new approach for the one-pot synthesis of polysubstituted imidazo[1,5-*a*]pyridines and imidazo[1,5-*a*]isoquinolines from the cobalt-catalyzed reaction of 3-(2-methyl-1*H*-imidazole-1yl)-1-arylpropane-1-ones with β-bromocinnamaldehydes and 2-bromobenzaldehydes, respectively. This developed reaction involves Knoevenagel condensation followed by cobalt-catalyzed intramolecular cyclization. The ease of operation, use of a cost-effective catalyst, easily obtainable starting materials, and scalability are the salient features that make this protocol very useful for synthesizing biologically relevant aroyl- and thiaroyl-substituted imidazo[1,5-*a*]pyridines and imidazo[1,5-*a*]isoquinolines.

1.4 EXPERIMENTAL SECTION

1.4.1 General Information

All reagents and solvents were purchased commercially and used without further purification. Melting points were measured using an automatic capillary point apparatus and were uncorrected. The thin layer chromatography (TLC) was performed on 0.25 mm silica gel 60-F254 and were visualized using a UV lamp. All reactions were performed in a pressure tube under a nitrogen atmosphere. The products were purified by column chromatography over silica gel (100-200 mesh) using ethyl acetate/hexane as eluent. The ^{1}H NMR (400 MHz) and ^{13}C NMR (100 MHz) spectra were recorded on a Bruker Advance 400 spectrometer using $CDCl_3$ (TMS as an internal standard) as the solvent. High-resolution mass spectra (HRMS) were recorded on an Agilent Q-TOF LC-MS spectrometer in positive electrospray ionization (ESI) mode. X-ray crystal structures were obtained with Rigaku Oxford XtaLAB AFC12 (RINC): Kappa dual home/near diffractometer.

1.4.2 General Procedure for the Synthesis of Imidazo[1,5-*a*]pyridines (25) and Imidazo[1,5-*a*]isoquinolines (27).

An oven-dried sealed tube with a rubber septum was charged with 2-(2-methyl-1*H*-imidazol-1-yl)-1-phenylethan-1-one (**23**) (0.25 mmol), 3-bromo-3-arylacrylaldehyde (**24**) or 2-bromo-benzaldehydes (**15**) (0.30 mmol), K_2CO_3 (3.0 equiv.) and dry DMSO (3 mL). The resulting reaction mixture was stirred at room temperature and degassed by purging nitrogen gas. Then, PCy_3 (30 mol %) was added and again degassed for 15 minutes, followed by the addition of $Co(acac)_2$ (20 mol %) and degassing for 5 minutes. After that, the tube was sealed, and the reaction mixture was heated at 150 °C for 4 h. On completion of the reaction, the reaction mixture was cooled to room temperature, diluted with ice-cold water, and extracted with EtOAc (3 × 10 mL). The organic layer was separated and dried over anhydrous Na_2SO_4 and evaporated under reduced pressure on a rotatory evaporator. The crude product was purified by column chromatography on silica gel (100–200 mesh) using ethyl acetate:hexanes as the eluent.

(3-Methyl-8-phenylimidazo[1,5-*a*]pyridin-5-yl)(phenyl)methanone (25aa). Purification by column chromatography on silica gel (eluent: EtOAc/hexanes, 1:4 *v/v*); Yellow semi-solid; 55 mg (70%); ^{1}H NMR (400 MHz, $CDCl_3$) δ 8.06 (dd, *J* = 8.3, 1.3 Hz, 2H), 7.76–7.69 (m, 3H), 7.63–7.49 (m, 5H), 7.04 (d, *J* = 7.0 Hz, 1H), 6.76 (d, *J* = 7.0 Hz, 1H), 2.45 (s, 3H); ^{13}C{^{1}H} NMR (100 MHz, $CDCl_3$) δ 187.3, 137.4, 136.6, 136.3, 134.1, 130.5, 130.2, 129.5, 129.1, 128.9, 128.1, 121.8, 121.0, 115.8, 17.4; HRMS (ESI) *m/z*: $[M+H]^+$ Calcd for $C_{21}H_{16}N_2O$ 313.1335; Found 313.1313.

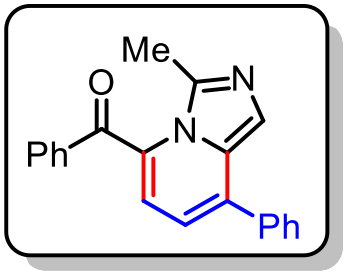

(4-Methoxyphenyl)(3-methyl-8-phenylimidazo[1,5-*a*]pyridin-5-yl)methanone (25ba). Purification by column chromatography on silica gel (eluent: EtOAc/hexanes, 3:7 *v/v*); Yellow solid; 63 mg (74%); mp = 161–163 °C; ^{1}H NMR (400 MHz, $CDCl_3$) δ 8.01 (d, *J* = 8.8 Hz, 2H), 7.70 (d, *J* = 6.8 Hz, 3H), 7.56–7.44 (m, 3H), 7.03 (d, *J* = 8.8 Hz, 2H), 6.95 (d, *J* = 6.9 Hz, 1H), 6.73 (d, *J* = 6.9 Hz, 1H), 3.93 (s, 3H), 2.41 (s, 3H); ^{13}C{^{1}H} NMR (100 MHz, $CDCl_3$) δ 186.7, 164.4, 137.1, 132.9, 129.3, 129.1, 129.0, 128.1, 121.9, 120.4, 119.7, 115.3, 114.2, 55.7, 17.5; HRMS (ESI) *m/z*: $[M+H]^+$ Calcd for $C_{22}H_{19}N_2O$ 343.1441; Found 343.1409.

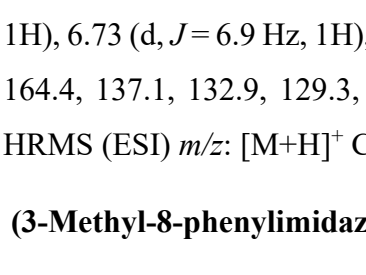

(3-Methyl-8-phenylimidazo[1,5-*a*]pyridin-5-yl)(*p*-tolyl)methanone (25ca). Purification by column chromatography on silica gel (eluent: EtOAc/hexanes, 1:4 *v/v*); Yellow semi-solid; 59.5 mg (73%); ^{1}H NMR (400 MHz, $CDCl_3$) δ 7.96 (d, *J* = 7.5 Hz, 2H), 7.73 (d, *J* = 6.3 Hz, 2H), 7.61–7.46 (m, 4H), 7.39 (d, *J* = 7.4 Hz, 2H), 7.03 (s, 1H), 6.76 (d, *J* = 6.3 Hz, 1H), 2.51 (s, 3H), 2.41 (s, 3H); ^{13}C{^{1}H} NMR (100 MHz, $CDCl_3$) δ 187.5, 145.1, 137.1, 134.0, 130.7, 129.6, 129.1, 129.0, 128.2, 120.7, 120.7, 115.3, 21.8, 18.0; HRMS (ESI) *m/z*: $[M+H]^+$ Calcd for $C_{22}H_{19}N_2O$ 327.1492; Found 327.1506.

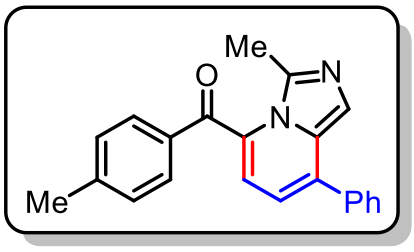

(3-Methyl-8-phenylimidazo[1,5-*a*]pyridin-5-yl)(*o*-tolyl)methanone (25da). Purification by column chromatography on silica gel (eluent: EtOAc/hexanes, 1:3 *v/v*); Yellow semi-solid; 51 mg (63%); ^{1}H NMR (400 MHz, $CDCl_3$) δ 7.90 (s, 1H), 7.69 – 7.64 (m, 3H), 7.59 – 7.56 (m, 3H), 7.44 (d, *J* = 7.6 Hz, 1H), 7.36 (t, *J* = 6.6 Hz, 2H), 7.17 (d, *J* = 6.9 Hz, 1H), 6.95 (d, *J* = 7.0 Hz, 1H), 2.76 (s, 3H), 2.62 (s, 3H); ^{13}C{^{1}H} NMR (100 MHz, $CDCl_3$) δ 188.9, 139.6, 137.8, 136.9, 136.6, 132.2, 131.9, 131.2, 129.3, 129.0, 128.2, 125.6, 122.7, 122.7, 115.2, 20.9, 18.0; HRMS (ESI) *m/z*: $[M+H]^+$ Calcd for $C_{22}H_{19}N_2O$ 327.1492; Found 327.1506.

(3-Methyl-8-phenylimidazo[1,5-*a*]pyridin-5-yl)(naphthalen-2-yl)methanone (25fa). Purification by column chromatography on silica gel (eluent: EtOAc/hexanes, 3:7 *v/v*); Yellow semi-solid; 40 mg (44%); ^{1}H NMR (400 MHz, $CDCl_3$) δ 8.54 (s, 1H), 8.17 (d, *J* = 8.6 Hz, 1H), 8.07 (d, *J* = 8.5 Hz, 1H), 8.03 – 7.97 (m, 2H), 7.87 (s, 1H), 7.72 (d, *J* = 7.4 Hz, 3H), 7.65 (t, *J* = 7.5 Hz, 1H), 7.59 – 7.57 (m, 3H), 7.27 (s, 1H), 6.96 (d, *J* = 6.9 Hz, 1H), 2.64 (s, 3H); ^{13}C{^{1}H} NMR (100 MHz, $CDCl_3$) δ 186.9, 137.5, 136.2, 135.9, 133.5, 133.2, 132.3, 131.5, 130.4, 129.9, 129.8, 129.6, 129.3, 129.3, 128.1, 128.0, 127.5, 125.0, 122.5, 16.7; HRMS (ESI) *m/z*: $[M+H]^+$ Calcd for $C_{25}H_{19}N_2O$ 363.1492; Found 363.1490.

Phenyl(8-phenylimidazo[1,5-*a*]pyridin-5-yl)methanone (25ga). Purification by column chromatography on silica gel (eluent: EtOAc/hexanes, 1:4 *v/v*); Yellow semi-solid; 32 mg (43%); ^{1}H NMR (400 MHz, $CDCl_3$) δ 9.00 (s, 1H), 8.05 (d, *J* = 7.4 Hz, 2H), 7.95 (s, 1H), 7.87 (d, *J* = 7.4 Hz, 2H), 7.69 (t, *J* = 7.4 Hz, 1H), 7.62 – 7.54 (m, 4H), 7.52 (d, *J* = 7.4 Hz, 2H), 7.40 (d, *J* = 7.4 Hz, 1H); ^{13}C{^{1}H} NMR (100 MHz, $CDCl_3$) δ 189.9, 143.9, 137.6, 135.5, 135.3, 134.2, 133.0, 130.8, 129.8, 129.6, 129.4, 128.9, 128.7, 123.2, 121.7, 115.4; HRMS (ESI) *m/z*: $[M+H]^+$ Calcd for $C_{20}H_{15}N_2O$ 299.1179; Found 299.1178.

(3,8-Diphenylimidazo[1,5-*a*]pyridin-5-yl)(phenyl)methanone (25ha). Purification by column chromatography on silica gel (eluent: EtOAc/hexanes, 1:3 *v/v*); Yellow semi-solid; 65 mg (63%); ^{1}H NMR (400 MHz, $CDCl_3$) δ 8.12 (s, 1H), 7.73 (s, 2H), 7.61 (s, 6H), 7.44 (s, 3H), 7.40 – 7.34 (m, 3H), 7.35 – 7.30 (m, 2H), 7.14 (s, 2H) ; ^{13}C{^{1}H} NMR (100 MHz, $CDCl_3$) 186.9, 137.5, 135.3, 135.1, 134.0, 131.4, 131.3, 130.8, 130.2, 129.5, 129.5, 129.2, 129.1, 129.0, 128.0, 127.6, 123.2, 115.4; HRMS (ESI) *m/z*: $[M+H]^+$ Calcd for $C_{26}H_{19}N_2O$ 375.1492; Found 375.1496.

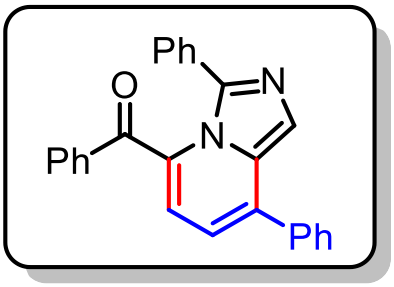

(4-Bromophenyl)(8-(4-methoxyphenyl)-3-methylimidazo[1,5-*a*]pyridin-5-yl)methanone (25ic). Purification by column chromatography on silica gel (eluent: EtOAc/hexanes, 1:3 *v/v*); Yellow semi-solid; 65 mg (62%); ^{1}H NMR (400 MHz, $CDCl_3$) δ 8.06 (d, *J* = 7.3 Hz, 1H), 8.00 (s, 1H), 7.97 – 7.91 (m, 1H), 7.82 – 7.77 (m, 2H), 7.68 – 7.58 (m, 3H), 7.35 (d, *J* = 7.9 Hz, 1H), 7.11 (d, *J* = 7.7 Hz, 2H), 7.10 – 7.02 (m, 2H), 3.94 (s, 3H), 2.77 (s, 3H); ^{13}C{^{1}H} NMR (100 MHz, $CDCl_3$) δ 187.4, 160.5, 146.7, 136.7, 133.8, 131.1, 130.5, 129.4, 129.1, 128.8, 127.5, 127.4, 122.6, 121.8, 114.5, 55.4, 17.8; HRMS (ESI) *m/z*: $[M+H]^+$, $[M+2+H]^+$ Calcd for $C_{22}H_{18}BrN_2O_2$ 421.0546, 423.0526 ; Found 421.0551, 423.0530.

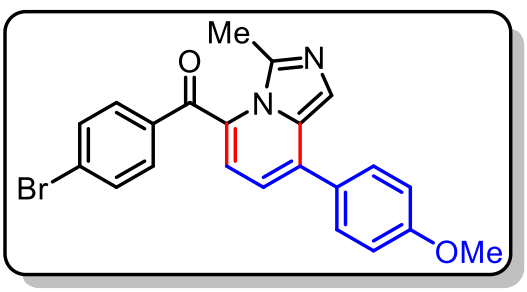

8-(4-Bromophenyl)-3-methylimidazo[1,5-*a*]pyridin-5-yl)(thiophen-2-yl)methanone (25jd). Purification by column chromatography on silica gel (eluent: EtOAc/hexanes, 1:4 *v/v*); Orange semi-solid; 48.5 mg (49%); ^{1}H NMR (400 MHz, $CDCl_3$) δ 8.04 – 8.00 (m, 1H), 7.98 – 7.88 (m, 2H), 7.79 – 7.71 (m, 2H), 7.59 – 7.50 (m, 3H), 7.37 – 7.32 (m, 1H), 7.18 – 7.10 (m, 1H), 2.86 (s, 3H); ^{13}C{^{1}H} NMR (100 MHz, $CDCl_3$) δ 177.9, 141.8, 138.2, 137.6, 136.6, 133.4, 133.0, 130.7, 130.4, 129.7, 129.3, 125.1, 123.1, 119.8, 119.4, 16.3 HRMS (ESI) *m/z*: $[M+H]^+$, $[M+2+H]^+$ Calcd for $C_{19}H_{14}BrN_2OS$ 397.0005, 398.0035; Found 397.0005, 398.0041.

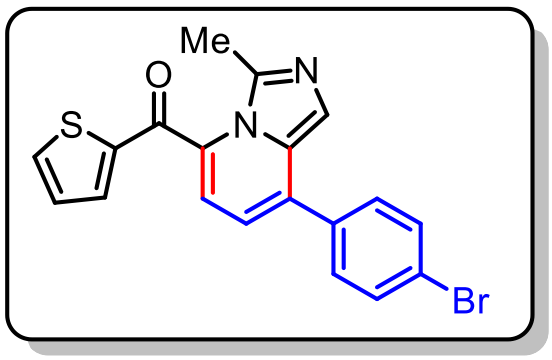

3-Methyl-8-(*p*-tolyl)imidazo[1,5-*a*]pyridin-5-yl)(phenyl)methanone (25ab). Purification by column chromatography on silica gel (eluent: EtOAc/hexanes, 1:4 *v/v*); Yellow semi-solid; 50 mg (61%); ^{1}H NMR (400 MHz, $CDCl_3$) δ 7.95 (d, *J* = 8.1 Hz, 2H), 7.73 (d, *J* = 6.7 Hz, 2H), 7.59 – 7.46 (m, 4H), 7.38 (d, *J* = 7.9 Hz, 2H), 7.01 (d, *J* = 6.4 Hz, 1H), 6.75 (d, *J* = 6.9 Hz, 1H), 2.51 (s, 3H), 2.42 (s, 3H); ^{13}C{^{1}H} NMR (100 MHz, $CDCl_3$) δ 187.5, 139.4, 137.4, 136.7, 134.0, 133.9, 130.5, 130.0, 129.7, 128.8, 128.1, 122.4, 121.7, 114.8, 21.4, 17.7; HRMS (ESI) *m/z*: $[M+H]^+$ Calcd for $C_{22}H_{19}N_2O$ 327.1492; Found 327.1506.

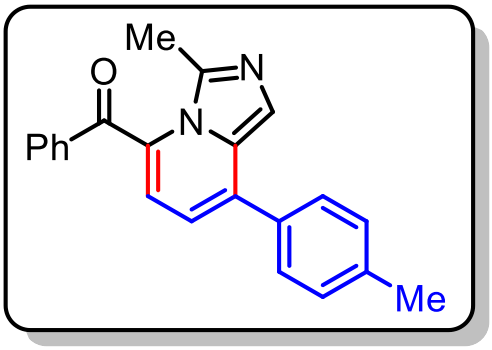

8-(4-Methoxyphenyl)-3-methylimidazo[1,5-*a*]pyridin-5-yl)(phenyl)methanone (25ac). Purification by column chromatography on silica gel (eluent: EtOAc/hexanes, 3:7 *v/v*); Yellow solid; 55 mg (64%); mp = 134-136 ºC; ^{1}H NMR (400 MHz, $CDCl_3$) δ 8.04 (d, *J* = 7.2 Hz, 2H), 7.78 – 7.65 (m, 4H), 7.58 (t, *J* = 7.7 Hz, 2H), 7.13 – 6.97 (m, 3H), 6.71 (d, *J* = 7.0 Hz, 1H), 3.92 (s, 3H), 2.44 (s, 3H); ^{13}C{^{1}H} NMR (100 MHz, $CDCl_3$) δ 187.4, 160.5, 137.1, 136.7, 133.8, 130.7, 130.5, 129.8, 129.4, 129.3, 128.8, 128.5, 122.7, 121.8, 114.4, 114.4, 55.4, 17.9; HRMS (ESI) *m/z*: $[M+H]^+$ Calcd for $C_{21}H_{19}N_2O_2$ 343.1441; Found 343.1409.

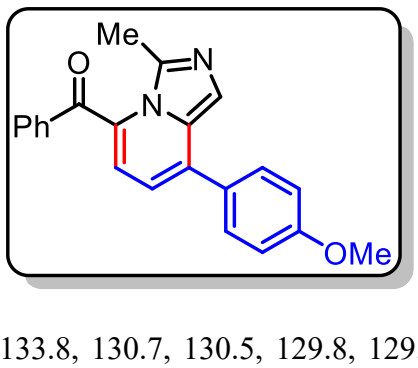

8-(4-Bromophenyl)-3-methylimidazo[1,5-*a*]pyridin-5-yl)(phenyl)methanone (25ad). Purification by column chromatography on silica gel (eluent: EtOAc/hexanes, 1:4 *v/v*); Yellow solid; 40 mg (41%); mp = 140-142 ºC; ^{1}H NMR (400 MHz, $CDCl_3$) δ 8.10 – 8.05 (m, 2H), 7.92 (s, 1H), 7.80 (t, *J* = 7.0 Hz, 1H), 7.74 (d, *J* = 6.5 Hz, 2H), 7.65 (s, 2H), 7.54 (d, *J* = 6.5 Hz, 2H), 7.34 (d, *J* = 5.6 Hz, 1H), 7.08 (d, *J* = 5.6 Hz, 1H), 2.77 (s, 3H); ^{13}C{^{1}H} NMR (100 MHz, $CDCl_3$) δ 186.2, 137.8, 136.5, 135.2, 135.0, 133.5, 132.9, 130.8, 130.8, 130.7, 129.5, 129.4, 125.0, 123.6, 119.3, 113.9, 16.0; HRMS (ESI) *m/z*: $[M+H]^+$, $[M+2+H]^+$ Calcd for $C_{21}H_{16}BrN_2O$ 391.0441, 393.0420; Found 391.0396, 393.0425.

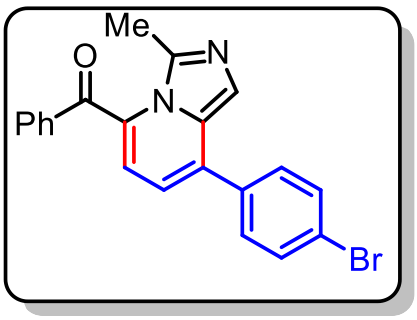

3-Methyl-8-(4-(trifluoromethyl)phenyl)imidazo[1,5-*a*]pyridin-5-yl)(phenyl)methanone

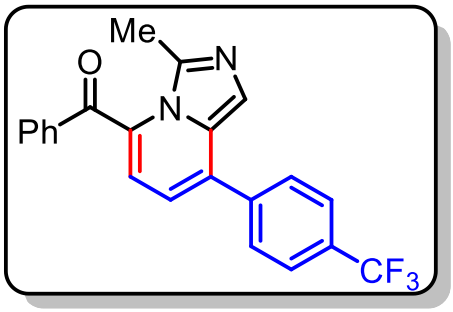

(25ae). Purification by column chromatography on silica gel (eluent: EtOAc/hexanes, 1:3 *v/v*); Yellow solid; 44 mg (46%); mp = 162-164 ºC; ^{1}H NMR (400 MHz, $CDCl_3$) δ 8.03 (d, *J* = 7.1 Hz, 2H), 7.90 – 7.49 (m, 8H), 7.00 (d, *J* = 6.6 Hz, 1H), 6.75 (d, *J* = 6.6 Hz, 1H), 2.42 (s, 3H); ^{13}C{^{1}H} NMR (100 MHz, $CDCl_3$) δ 187.6, 140.6, 139.7, 136.4, 135.4, 134.1, 131.5, 131.0, 130.9, 130.5, 128.9, 128.5, 126.0 (q, J_{C-F} = 3.5 Hz), 125.3, 122.6, 122.2, 120.3, 115.8, 17.8; ^{19}F NMR (376 MHz, $CDCl_3$) δ -62.68; HRMS (ESI) *m/z*: $[M+H]^+$ Calcd for $C_{22}H_{16}N_2F_3O$ 381.1209; Found 381.1220.

4-(3-Methyl-8-phenylimidazo[1,5-*a*]pyridine-5-carbonyl)benzonitrile (25af). Purification by column chromatography on silica gel (eluent: EtOAc/hexanes, 3:7 *v/v*); Orange solid; 39 mg (46%); mp = 167-169 ºC; ^{1}H NMR (400 MHz, $CDCl_3$) δ 8.04 (d, *J* = 7.5 Hz, 2H), 7.85 – 7.83 (s, 4H), 7.74 (t, *J* = 7.3 Hz, 2H), 7.60 (t, *J* = 7.5 Hz, 2H), 7.04 (d, *J* = 6.8 Hz, 1H), 6.81 (d, *J* = 6.6 Hz, 1H), 2.46 (s, 3H); ^{13}C{^{1}H} NMR (100 MHz, $CDCl_3$) δ 187.5, 141.3, 136.1, 134.3, 132.9, 130.5, 129.0, 128.8, 120.2, 118.3, 116.4, 113.0, 17.7; HRMS (ESI) *m/z*: $[M+H]^+$ Calcd for $C_{22}H_{16}N_3O$ 338.1288; Found 338.1279.

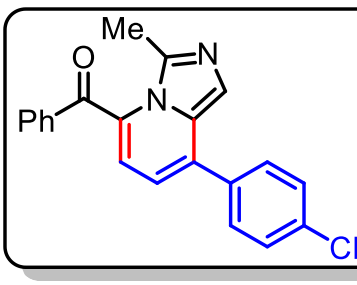

(3-Methoxyphenyl)-3-methylimidazo[1,5-*a*]pyridin-5-yl)(phenyl)methanone (25ag).

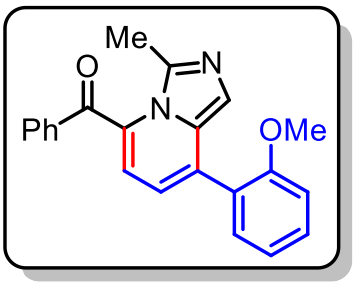

Purification by column chromatography on silica gel (eluent: EtOAc/hexanes, 3:7 *v/v*); Yellow solid; 51 mg (60%); mp = 153-155 ºC; ^{1}H NMR (400 MHz, $CDCl_3$) δ 8.11 – 8.05 (m, 2H), 7.81 – 7.73 (m, 1H), 7.67 – 7.60 (m, 3H), 7.55 – 7.50 (m, 1H), 7.40 (d, *J* = 6.8 Hz, 1H), 7.31 (s, 1H), 7.15 – 7.08 (m, 2H), 7.06 – 7.02 (m, 1H), 3.83 (s, 3H), 2.72 (s, 3H); ^{13}C{^{1}H} NMR (100 MHz, $CDCl_3$) δ 187.6, 156.9, 138.8, 136.7, 134.2, 133.8, 132.4, 130.6, 130.5, 130.3, 130.2, 128.8, 125.5, 122.6, 121.3, 120.8, 116.9, 111.5, 55.6, 17.8; HRMS (ESI) *m/z*: $[M+H]^+$ Calcd for $C_{22}H_{19}N_2O_2$ 343.1441; Found 343.1409.

3-Methyl-8-(thiophen-2-yl)imidazo[1,5-*a*]pyridiyl)(phenyl)methanone (25ah). Purification by column chromatography on silica gel (eluent: EtOAc/hexanes, 1:4 *v/v*); Orange solid; 45 mg (57%); mp = 185-187 ºC; ^{1}H NMR (400 MHz, $CDCl_3$) δ 8.00 (d, *J* = 7.3 Hz, 3H), 7.68 (t, *J* = 7.4 Hz, 1H), 7.63 (d, *J* = 3.7 Hz, 1H), 7.55 (t, *J* = 7.6 Hz, 2H), 7.48 (d, *J* = 5.1 Hz, 1H), 7.21 (t, *J* = 4.4 Hz, 1H), 6.99 – 6.86 (m, 2H), 2.41 (s, 3H); ^{13}C{^{1}H} NMR (100 MHz, $CDCl_3$) δ 187.7, 139.0, 136.8, 134.2, 130.7, 130.5, 130.1, 129.1, 128.4, 127.3, 127.3, 123.0, 121.1, 114.8, 18.1; HRMS (ESI) *m/z*: $[M+H]^+$ Calcd for $C_{19}H_{15}N_2OS$ 319.0900; Found 319.0908.

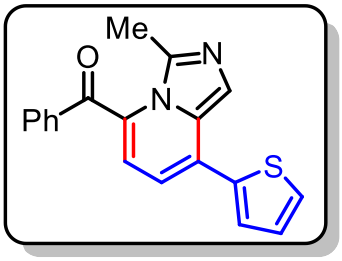

(8-(Furan-2-yl)-3-methylimidazo[1,5-*a*]pyridin-5-yl)(phenyl)methanone (25ai). Purification by column chromatography on silica gel (eluent: EtOAc/hexanes, 1:4 *v/v*); Orange solid; 46 mg (61%); mp = 158-160 ºC; ^{1}H NMR (400 MHz, $CDCl_3$) δ 8.17 (s, 1H), 8.01 (d, *J* = 7.6 Hz, 2H), 7.75 – 7.66 (m, 2H), 7.58 (t, *J* = 7.6 Hz, 2H), 7.22 – 7.04 (m, 3H), 6.68 – 6.61 (m, 1H), 2.55 (s, 3H); ^{13}C{^{1}H} NMR (100 MHz, $CDCl_3$) δ 186.8, 149.2, 144.5, 136.0, 134.3, 130.5, 130.1, 129.0, 125.3, 122.2, 119.4, 113.0, 112.5, 111.4, 17.1; HRMS (ESI) *m/z*: $[M+H]^+$ Calcd for $C_{19}H_{15}N_2O_2$ 303.1128; Found 303.1125.

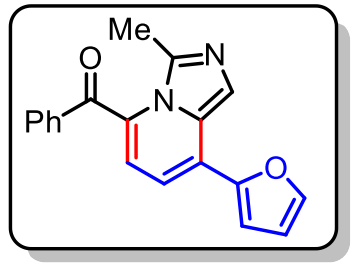

8-(4-Bromophenyl)-3,7-dimethylimidazo[1,5-*a*]pyridin-5-yl)(phenyl)methanone (25aj). Purification by column chromatography on silica gel (eluent: EtOAc/hexanes, 1:3 *v/v*); Yellow semi-solid; 47.5 mg (47%); ^{1}H NMR (400 MHz, $CDCl_3$) δ 8.04 (d, *J* = 7.7 Hz, 2H), 7.72 (t, *J* = 7.4 Hz, 1H), 7.67 (d, *J* = 8.0 Hz, 2H), 7.59 (t, *J* = 7.6 Hz, 2H), 7.32 (d, *J* = 8.0 Hz, 2H), 7.14 (s, 1H), 6.82 (s, 1H), 2.39 (s, 3H), 2.14 (s, 3H); ^{13}C{^{1}H} NMR (100 MHz, $CDCl_3$) δ 187.8, 136.5, 134.7, 134.1, 132.5, 132.0, 130.9, 130.5, 128.9, 123.7, 123.1, 122.6, 120.8, 18.1, 17.5; HRMS (ESI) *m/z*: $[M+H]^+$, $[M+2+H]^+$ Calcd for $C_{22}H_{18}BrN_2O$ 405.0597, 407.0577; Found 405.0553 and 407.0580.

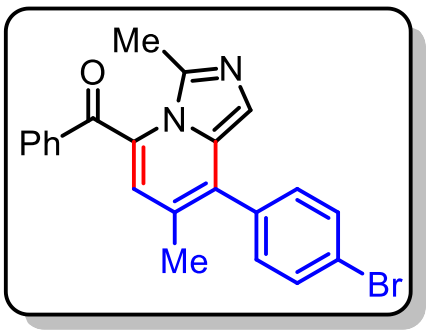

(4-Methoxyphenyl)(8-(4-methoxyphenyl)-3-methylimidazo[1,5-*a*]pyridin-5-yl)methanone

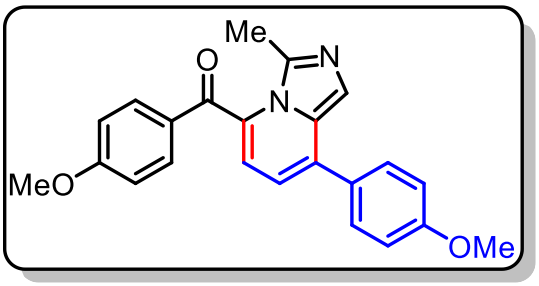

(25bc). Purification by column chromatography on silica gel (eluent: EtOAc/hexanes, 1:3 *v/v*); Yellow solid; 53 mg (57%); mp = 153-155 ºC; ^{1}H NMR (400 MHz, $CDCl_3$) δ 8.03 (d, *J* = 8.5 Hz, 2H), 7.72 (s, 1H), 7.68 (d, *J* = 8.3 Hz, 2H), 7.06 (t, *J* = 7.5 Hz, 4H), 6.98 (d, *J* = 6.8 Hz, 1H), 6.72 (d, *J* = 6.8 Hz, 1H), 3.95 (s, 3H), 3.91 (s, 3H), 2.43 (s, 3H); ^{13}C{^{1}H} NMR (100 MHz, $CDCl_3$) δ 184.7, 165.4, 161.5, 137.0, 133.5, 132.3, 130.0, 129.8, 129.4, 127.8, 126.7, 123.5, 119.1, 115.1, 114.8, 113.9, 113.9, 113.7, 55.9, 55.6, 16.1; HRMS (ESI) *m/z*: $[M+H]^+$ Calcd for $C_{23}H_{21}N_2O_3$ 373.1547; Found 373.1574.

(8-(4-Bromophenyl)-3-methylimidazo[1,5-*a*]pyridin-5-yl)(4-methoxyphenyl)methanone

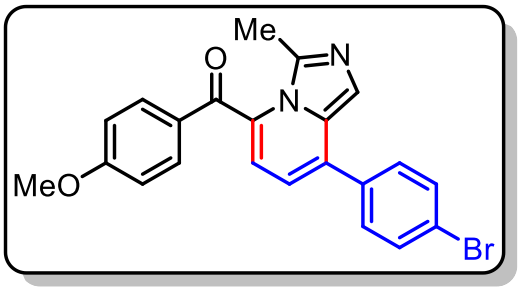

(25bd). Purification by column chromatography on silica gel (eluent: EtOAc/hexanes, 1:3 *v/v*); Yellow semi-solid; 46 mg (44%); NMR (400 MHz, $CDCl_3$) δ 7.92 (d, *J* = 5.92 Hz, 2H), 7.82 – 7.62 (m, 5H), 7.09 – 7.03 (m, 3H), 6.71 (d, *J* = 6.04 Hz, 1H), 3.92 (s, 3H), 2.43 (s, 3H); ^{13}C{^{1}H} NMR (100 MHz, $CDCl_3$) δ 186.1, 160.6, 137.5, 135.5, 132.2, 131.9, 131.8, 129.4, 129.2, 129.2, 129.1, 123.0, 122.1, 114.5, 114.3, 55.4, 17.9; HRMS (ESI) *m/z*: $[M+H]^+$, $[M+2+H]^+$ Calcd for $C_{22}H_{18}BrN_2O_2$ 421.0546, 423.0528; Found 421.0551, 423.0531.

(4-Methoxyphenyl)(8-(2-methoxyphenyl)-3-methylimidazo[1,5-*a*]pyridin-5-yl)methanone

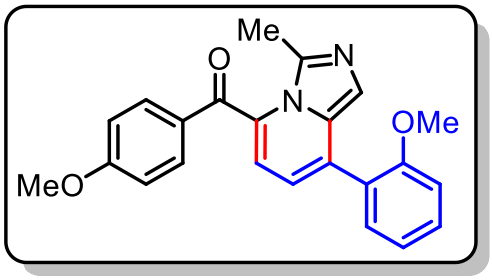

(25bg). Purification by column chromatography on silica gel (eluent: EtOAc/hexanes, 3:7 *v/v*); Yellow semi-solid; 61 mg (66%); ^{1}H NMR (400 MHz, $CDCl_3$) δ 7.97 (d, *J* = 8.1 Hz, 2H), 7.51 – 7.41 (m, 3H), 7.38 (d, *J* = 8.0 Hz, 2H), 7.14 – 7.06 (m, 2H), 6.99 (d, *J* = 6.9 Hz, 1H), 6.76 (d, *J* = 6.9 Hz, 1H), 3.83 (s, 3H), 2.51 (s, 3H), 2.43 (s, 3H); ^{13}C{^{1}H} NMR (100 MHz, $CDCl_3$) δ 187.5, 156.9, 145.0, 138.6, 134.1, 133.8, 132.4, 130.7, 130.7, 130.4, 130.2, 129.5, 125.6, 122.3, 120.7, 120.6, 116.9, 111.5, 55.6, 21.8, 17.7; HRMS (ESI) *m/z*: $[M+H]^+$ Calcd for $C_{23}H_{21}N_2O_3$ 373.1547; Found 373.1574.

8-(4-Bromophenyl)-3-methylimidazo[1,5-*a*]pyridin-5-yl)(*p*-tolyl)methanone (25cd).

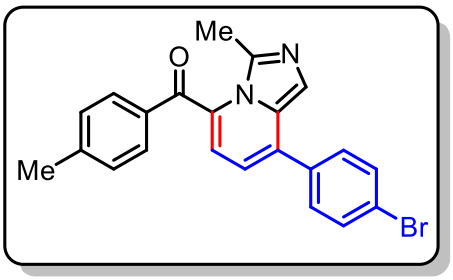

Purification by column chromatography on silica gel (eluent: EtOAc/hexanes, 1:4 *v/v*); Yellow semi-solid; 65 mg (64%); ^{1}H NMR (400 MHz, $CDCl_3$) δ 7.94 (d, J = 8.1 Hz, 2H), 7.70 – 7.64 (m, 3H), 7.61 – 7.56 (m, 2H), 7.41 – 7.35 (m, 2H), 6.99 (d, *J* = 6.9 Hz, 1H), 6.74 (d, *J* = 6.9 Hz, 1H), 2.50 (s, 3H), 2.44 (s, 3H); ^{13}C{^{1}H} NMR (100 MHz, $CDCl_3$) δ 187.3, 145.4, 139.3, 135.8, 135.5, 133.8, 132.2, 131.4, 130.7, 129.7, 129.0, 128.1, 123.4, 121.4, 120.2, 115.5, 21.8, 17.5; HRMS (ESI) *m/z*: $[M+H]^+$, $[M+2+H]^+$ Calcd for $C_{23}H_{17}N_2O$ 405.0597, 407.0577; Found 405.0553, 407.0581.

8-(4-Methoxyphenyl)-3-methylimidazo[1,5-*a*]pyridin-5-yl)(naphthalen-2-yl)methanone (25fc).

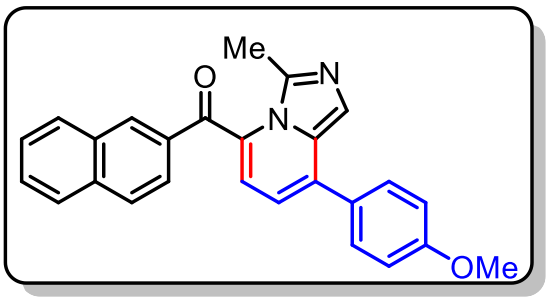

Purification by column chromatography on silica gel (eluent: EtOAc/hexanes, 1:3 *v/v*); Yellow semi-solid; 38 mg (39%); ^{1}H NMR (400 MHz, $CDCl_3$) δ 8.53 (s, 1H), 8.16 (dd, *J* = 8.6, 1.6 Hz, 1H), 8.05 (d, *J* = 8.6 Hz, 1H), 8.01 – 7.97 (m, 2H), 7.78 (s, 1H), 7.73 – 7.67 (m, 3H), 7.65 – 7.60 (m, 1H), 7.13 – 7.10 (m, 1H), 7.10 – 7.06 (m, 2H), 6.76 (d, *J* = 7.0 Hz, 1H), 3.93 (s, 3H), 2.48 (s, 3H); ^{13}C{^{1}H} NMR (100 MHz, $CDCl_3$) δ 187.5, 160.6, 137.0, 135.9, 134.0, 133.1, 132.3, 129.9, 129.7, 129.4, 129.3, 129.1, 129.0, 128.0, 127.2, 125.2, 122.3, 121.7, 114.6, 114.5, 55.4, 17.7; HRMS (ESI) *m/z*: $[M+H]^+$ Calcd for $C_{26}H_{21}N_2O_2$ 393.1598; Found 393.1596.

Phenyl(8-phenylimidazo[1,2-*a*]pyridin-5-yl)methanone (25ga).

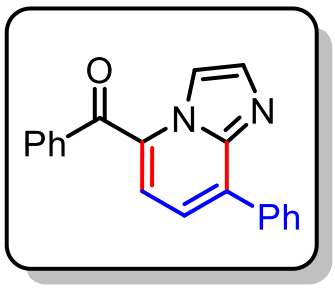

Purification by column chromatography on silica gel (eluent: EtOAc/hexanes, 15:85 *v/v*); Yellow semi-solid; 27 mg (36%); ^{1}H NMR (400 MHz, $CDCl_3$) δ 8.14 (d, *J* = 7.3 Hz, 1H), 7.85 – 7.81 (m, 1H), 7.66 – 7.61 (m, 1H), 7.58 (s, 3H), 7.50 (t, *J* = 7.3 Hz, 2H), 7.47 – 7.40 (m, 5H), 6.53 – 6.49 (m, 1H); ^{13}C{^{1}H} NMR (100 MHz, $CDCl_3$) δ 191.4, 145.3, 140.8, 137.5, 135.7, 133.3, 133.0, 131.6, 130.7, 130.6, 129.6, 129.6, 129.5, 129.4, 129.3, 129.1, 129.1, 128.6, 128.3, 127.7, 121.3; HRMS (ESI) *m/z*: $[M+H]^+$ Calcd for $C_{20}H_{15}N_2O$ 299.1179; Found 299.1178.

8-(4-Methoxyphenyl)-3-methylimidazo[1,5-*a*]pyridin-5-yl)(phenyl)methanethione (26).

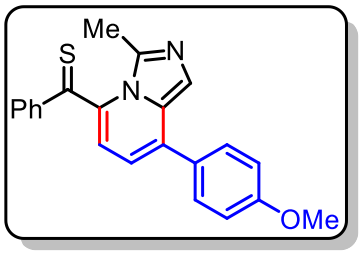

Purification by column chromatography on silica gel (eluent: EtOAc/hexanes, 1:3 *v/v*); Yellow semi-solid; 41 mg (46%); ^{1}H NMR (400 MHz, $CDCl_3$) δ 8.02 (d, *J* = 7.1 Hz, 2H), 7.73 – 7.64 (m, 4H), 7.56 (t, *J* = 7.7 Hz, 2H), 7.07 – 6.99 (m, 3H), 6.69 (d, *J* = 7.0 Hz, 1H), 3.89 (s, 3H), 2.42 (s, 3H); ^{13}C{^{1}H} NMR (100 MHz, $CDCl_3$) δ 187.7, 160.8, 139.8, 137.3, 137.0, 134.1, 132.2, 130.8, 130.1, 129.7, 129.6, 129.1, 123.0, 122.1, 114.7, 114.7, 55.7, 18.2; HRMS (ESI) *m/z*: $[M+H]^+$ Calcd for $C_{22}H_{19}N_2OS$ 359.1213; Found 359.1226.

(3-Methylimidazo[5,1-*a*]isoquinolin-5-yl)(phenyl)methanone (27aa). Purification by column chromatography on silica gel (eluent: EtOAc/hexanes, 1:3 *v/v*); Yellow solid; 44 mg (61%); mp = 126-128 ºC; ^{1}H NMR (400 MHz, $CDCl_3$) δ 8.11 – 8.03 (m, 3H), 7.92 (s, 1H), 7.73 (t, *J* = 7.4 Hz, 1H), 7.63 – 7.58 (m, 4H), 7.43 (t, *J* = 7.7 Hz, 1H), 7.04 (s, 1H), 2.40 (s, 3H); ^{13}C{^{1}H} NMR (100 MHz, $CDCl_3$) δ 188.7, 140.1, 136.2, 134.4, 131.5, 130.5, 130.2, 129.8, 129.0, 128.1, 126.8, 126.2, 125.0, 122.0, 120.4, 119.8, 17.5; HRMS (ESI) *m/z*: $[M+H]^+$ Calcd for $C_{19}H_{15}N_2O$ 287.1179; Found 287.1146.

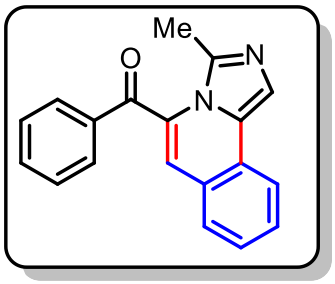

8,9-Dimethoxy-3-methylimidazo[5,1-*a*]isoquinolin-5-yl)(phenyl)methanone (27ab).

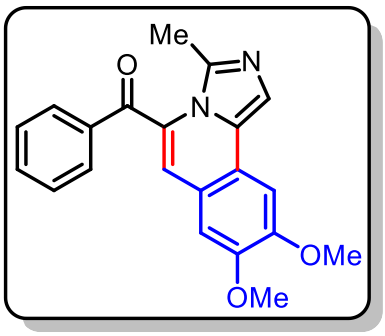

Purification by column chromatography on silica gel (eluent: EtOAc/hexanes, 2:3 *v/v*); Yellow solid; 55 mg (64%); mp = 156-158 ºC; ^{1}H NMR (400 MHz, $CDCl_3$) δ 8.06 (d, *J* = 7.4 Hz, 2H), 7.82 (s, 1H), 7.73 (t, *J* = 7.4 Hz, 1H), 7.59 (t, *J* = 7.7 Hz, 2H), 7.44 (s, 1H), 7.06 (s, 1H), 7.00 (s, 1H), 4.10 (s, 3H), 3.95 (s, 3H), 2.41 (s, 3H); ^{13}C{^{1}H} NMR (100 MHz, $CDCl_3$) δ 188.3, 151.9, 149.0, 139.7, 136.6, 134.0, 130.4, 130.0, 129.8, 128.9, 121.2, 120.9, 118.9, 118.8, 108.8, 103.1, 56.3, 56.0, 17.7; HRMS (ESI) *m/z*: $[M+H]^+$ Calcd for $C_{21}H_{19}N_2O_3$ 347.1390; Found 347.1385.

3-Methyl-[1,3]dioxolo[4,5-*g*]imidazo[5,1-*a*]isoquinolin-5-yl)(phenyl)methanone (27ac).

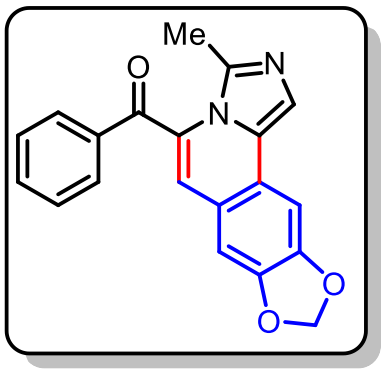

Purification by column chromatography on silica gel (eluent: EtOAc/hexanes, 1:1 *v/v*); Yellow solid; 33 mg (40%); mp = 162-164 ºC; ^{1}H NMR (400 MHz, $CDCl_3$) δ 8.03 (d, *J* = 7.5 Hz, 2H), 7.77 (s, 1H), 7.72 (t, *J* = 7.3 Hz, 1H), 7.58 (t, *J* = 7.6 Hz, 2H), 7.43 (s, 1H), 6.98 – 6.95 (m, 2H), 6.10 (s, 2H), 2.38 (s, 3H); ^{13}C{^{1}H} NMR (100 MHz, $CDCl_3$) δ 188.2, 150.4, 147.5, 136.4, 134.1, 130.4, 129.9, 128.9, 122.6, 120.8, 120.1, 119.0, 106.3, 101.8, 101.1, 17.6; HRMS (ESI) *m/z*: $[M+H]^+$ Calcd for $C_{20}H_{15}N_2O_3$ 331.1077; Found 331.1068.

8-Fluoro-3-methylimidazo[5,1-*a*]isoquinolin-5-yl)(phenyl)methanone (27ad). Purification by column chromatography on silica gel (eluent: EtOAc/hexanes, 3:7 *v/v*); Yellow solid; 50 mg (65%); mp = 191-193 ºC; ^{1}H NMR (400 MHz, $CDCl_3$) δ 8.10 – 8.02 (m, 3H), 7.85 (s, 1H), 7.74 (t, *J* = 7.4 Hz, 1H), 7.60 (t, *J* = 7.6 Hz, 2H), 7.38 – 7.31 (m, 1H), 7.30 – 7.24 (m, 1H), 6.95 (s, 1H), 2.38 (s, 3H); ^{13}C{^{1}H} NMR (100 MHz, $CDCl_3$) δ 188.7, 162.4 (d, J_{C-F} = 245.6 Hz), 160.0, 139.9, 135.9, 134.6, 132.5, 130.5, 129.3, 129.1, 126.6 (d, J_{C-F} = 8.7 Hz), 124.2 (d, J_{C-F} = 8.4 Hz), 122.7, (d, J_{C-F} = 2.4 Hz), 119.8, 118.5 (d, J_{C-F} = 29.3 Hz), 118.1 (d, J_{C-F} = 2.74 Hz), 113.3 (d, J_{C-F} = 21.9 Hz), 17.4; HRMS (ESI) *m/z*: $[M+H]^+$ Calcd for $C_{19}H_{14}FN_2O$ 305.1085; Found 305.1051.

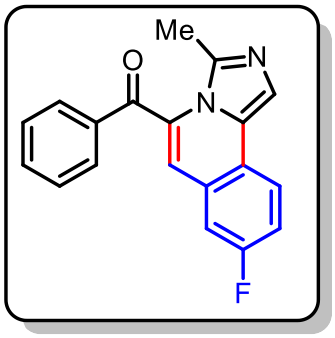

(4-Methoxyphenyl)(3-methylimidazo[5,1-*a*]isoquinolin-5-yl)methanone (27ba). Purification by column chromatography on silica gel (eluent: EtOAc/hexanes, 2:3 *v/v*); Yellow solid; 50 mg (62%); mp = 152-154 ºC; ^{1}H NMR (400 MHz, $CDCl_3$) δ 8.08 (d, *J* = 7.9 Hz, 1H), 8.04 (d, *J* = 8.7 Hz, 2H), 7.96 (s, 1H), 7.67 – 7.59 (m, 2H), 7.48 (t, *J* = 7.3 Hz, 1H), 7.09 – 7.05 (m, 2H), 7.04 (s, 1H), 3.95 (s, 3H), 2.47 (s, 3H); ^{13}C{^{1}H} NMR (100 MHz, $CDCl_3$) 187.2, 164.9, 139.6, 133.0, 131.2, 130.3, 129.7, 128.8, 128.1, 127.5, 125.5, 125.3, 122.3, 119.5, 118.1, 114.5, 55.8, 16.7; HRMS (ESI) *m/z*: $[M+H]^+$ Calcd for $C_{20}H_{17}N_2O_2$ 317.1285; Found 317.1253.

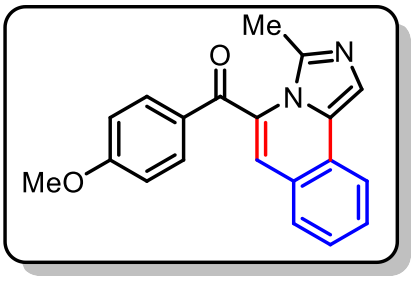

3-Methylimidazo[5,1-*a*]isoquinolin-5-yl)(naphthalen-2-yl)methanone (27fa). Purification by column chromatography on silica gel (eluent: EtOAc/hexanes, 2:3 *v/v*); Yellow solid; 44.5 mg (53%); mp =184-186 °C; ^{1}H NMR (400 MHz, $CDCl_3$) δ 8.54 (s, 1H), 8.18 (d, *J* = 8.4 Hz, 1H), 8.12 (d, *J* = 8.0 Hz, 1H), 8.06 (d, *J* = 8.6 Hz, 1H), 8.01 – 7.96 (m, 2H), 7.74 – 7.60 (m, 5H), 7.49 (t, *J* = 7.5 Hz, 1H), 7.19 (s, 1H), 2.49 (s, 3H); ^{13}C{^{1}H} NMR (100 MHz, $CDCl_3$) δ 187.9, 136.3, 133.6, 133.0, 132.3, 131.1, 130.9, 129.9, 129.7, 129.5, 128.7, 128.3, 128.1, 127.5, 125.3, 124.8, 122.6, 122.0, 16.4; HRMS (ESI) *m/z*: $[M+H]^+$ Calcd for $C_{23}H_{17}N_2O$ 337.1335; Found 337.1300.

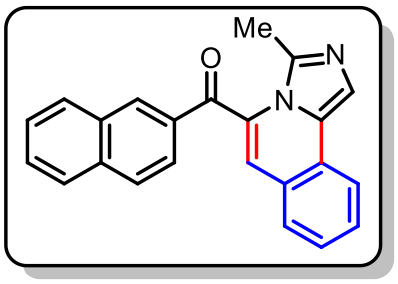

(4-Chlorophenyl)(3-methylimidazo[5,1-*a*]isoquinolin-5-yl)methanone (27la). Purification by column chromatography on silica gel (eluent: EtOAc/hexanes, 3:7 *v/v*); Yellow solid; 51 mg (63%); mp = 170-172 ºC; ^{1}H NMR (400 MHz, $CDCl_3$) δ 8.07 (d, *J* = 8.0 Hz, 1H), 8.01 (d, *J* = 8.6 Hz, 2H), 7.92 (s, 1H), 7.65 – 7.54 (m, 4H), 7.47 – 7.40 (m, 1H), 7.03 (s, 1H), 2.39 (s, 3H); ^{13}C{^{1}H} NMR (100 MHz, $CDCl_3$) δ 187.4, 141.1, 134.6, 131.7, 131.1, 130.4, 129.4, 128.2, 126.9, 126.3, 124.9, 122.1, 120.5, 120.0, 17.5; HRMS (ESI) *m/z*: $[M+H]^+$ Calcd for $C_{19}H_{14}ClN_2O$ 321.0789; Found 321.0744.

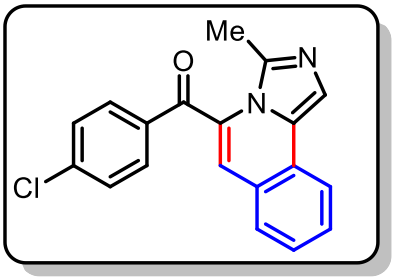

1.4.3 General Procedure for Preparation of 5-Bromo-5-(4-methoxyphenyl)-2-(2-methyl-1*H*-imidazol-1-yl)-1-phenylpenta-2,4-dien-1-one (28ac).

A mixture of **23a** (0.50 mmol), **24c** (0.60 mmol), K_2CO_3 (3.0 equiv), EtOH (3 mL) were added in a 25 mL round bottom flask. The reaction mixture was stirred at room temperature for 24 h. After completion of the reaction, the solvent was evaporated on a rotatory evaporator. The residue obtained was diluted with water and extracted by ethyl acetate (3 × 10 mL). The organic layer was separated and dried over anhydrous Na_2SO_4 and evaporated under reduced pressure on a rotatory evaporator. The crude product was purified by column chromatography on silica gel (100-200 mesh) using a mixture of hexanes and ethyl acetate (7:3 *v/v*) as eluent.

5-Bromo-5-(4-methoxyphenyl)-2-(2-methyl-1*H*-imidazol-1-yl)-1-phenylpenta-2,4-dien-1-one (28ac). Yellow solid; 91 mg (43%); mp = 102-104 ºC; ^{1}H NMR (400 MHz, $CDCl_3$) δ 7.80 – 7.73 (m, 3H), 7.65 – 7.59 (m, 1H), 7.56 – 7.49 (m, 4H), 7.13 (s, 1H), 6.97 (s, 1H), 6.90 – 6.86 (m,

2H), 6.67 – 6.64 (m, 1H), 3.85 (s, 3H), 2.28 (s, 3H); $^{13}C\{^{1}H\}$ NMR (100 MHz, $CDCl_3$) δ 190.7, 161.9, 145.8, 139.6, 139.5, 136.9, 134.1, 132.8, 130.4, 129.8, 129.2, 128.8, 128.7, 128.1, 121.2, 120.0, 114.1, 55.5, 13.3; HRMS (ESI) *m/z*: $[M+H]^+$, $[M+2+H]^+$ Calcd for $C_{22}H_{20}BrN_2O_2$ 423.0703, 425.0682; Found 423.0661, 425.0678.

1.4.4 Sample Preparation and Crystal Measurement of 25ah. The single crystals of the compound **25ah** were obtained as needles. The crystal data collection and reduction were performed using CrysAlis PRO on a single crystal Rigaku Oxford XtaLab Pro diffractometer. The crystals were kept at 93(2) K during data collection using CuKα (λ = 1.54184) radiation. Using Olex2, the structure was solved with the ShelXT structure solution program using Intrinsic Phasing and refined with the ShelXL refinement package using Least Squares minimization. Single crystal ORTEP diagram of compound **25ah**, due to the rotation of the thiophene ring along C2-C16 bond the occupancies of S1A and S1B are fixed to 70 % and 30 % respectively, and similarly C17A and C17B occupancies are fixed to 70 % and 30 % respectively. The thermal ellipsoids are drawn to a 50 % probability level.

Table 1.4: Crystal data for **25ah**.

Identification code	**25ah**
Empirical formula	$C_{19}H_{14}N_2OS$
Formula weight	318.38
Temperature/K	93(2)
Crystal system	triclinic
Space group	P-1
a/Å	7.6918(2)
b/Å	7.7847(2)
c/Å	13.7184(3)
α/°	90.026(2)
β/°	97.054(2)
γ/°	114.557(3)
Volume/$Å^3$	740.27(4)
Z	2
$\rho_{calc}g/cm^3$	1.428

μ/mm^{-1}	1.982
F(000)	332.0
Crystal size/mm^3	0.1 × 0.08 × 0.05
Radiation	Cu Kα (λ = 1.54184)
2Θ range for data collection/°	12.522 to 160.416
Index ranges	$-7 \leq h \leq 9$, $-9 \leq k \leq 9$, $-17 \leq l \leq 17$
Reflections collected	7457
Independent reflections	3095 [R_{int} = 0.0340, R_{sigma} = 0.0402]
Data/restraints/parameters	3095/2/227
Goodness-of-fit on F^2	1.113
Final R indexes [I>=2σ (I)]	R_1 = 0.0487
	wR_2 = 0.1375
Final R indexes [all data]	R_1 = 0.0505
	wR_2 = 0.1397
Largest diff. peak/hole / e $Å^{-3}$	0.26/-0.51

1.5 REFERENCES

1. Taylor, A. P.; Robinson, R. P.; Fobian, Y. M.; Blakemore, D. C.; Jones, L. H.; Fadeyi, O., *Organic & Biomolecular Chemistry* **2016**, *14*, 6611-6637.
2. Najmi, A.; Javed, S. A.; Al Bratty, M.; Alhazmi, H. A., *Molecules* **2022**, *27*, 349.
3. Kerru, N.; Gummidi, L.; Maddila, S.; Gangu, K. K.; Jonnalagadda, S. B., *Molecules* **2020**, *25*, 1909.
4. Tran, T. N.Henary, M., *Molecules* **2022**, *27*, 2700.
5. Pantaine, L. R.; Milligan, J. A.; Matsui, J. K.; Kelly, C. B.; Molander, G. A., *Organic Letters* **2019**, *21*, 2317-2321.
6. Liu, J.; Jiang, J.; Zheng, L.; Liu, Z. Q., *Advanced Synthesis & Catalysis* **2020**, *362*, 4876-4895.
7. Barraza, S. J.Denmark, S. E., *Journal of the American Chemical Society* **2018**, *140*, 6668-6684.
8. Godula, K.Sames, D., *Science* **2006**, *312*, 67-72.
9. McMurray, L.; O'Hara, F.; Gaunt, M. J., *Chemical Society Reviews* **2011**, *40*, 1885-1898.

10. Gutekunst, W. R.Baran, P. S., *Chemical Society Reviews* **2011**, *40*, 1976-1991.
11. Chaudhari, K.; Surana, S.; Jain, P.; Patel, H. M., *European Journal of Medicinal Chemistry* **2016**, *124*, 160-185.
12. Akhtar, J.; Khan, A. A.; Ali, Z.; Haider, R.; Yar, M. S., *European Journal of Medicinal Chemistry* **2017**, *125*, 143-189.
13. Martins, P.; Jesus, J.; Santos, S.; Raposo, L. R.; Roma-Rodrigues, C.; Baptista, P. V.; Fernandes, A. R., *Molecules* **2015**, *20*, 16852-16891.
14. Bori, J.; Behera, N.; Mahata, S.; Manivannan, V., *ChemistrySelect* **2017**, *2*, 11727-11731.
15. Hutt, J. T.; Jo, J.; Olasz, A.; Chen, C.-H.; Lee, D.; Aron, Z. D., *Organic Letters* **2012**, *14*, 3162-3165.
16. Volpi, G.; Lace, B.; Garino, C.; Priola, E.; Artuso, E.; Vioglio, P. C.; Barolo, C.; Fin, A.; Genre, A.; Prandi, C., *Dyes and Pigments* **2018**, *157*, 298-304.
17. Song, G.-J.; Bai, S.-Y.; Dai, X.; Cao, X.-Q.; Zhao, B.-X., *RSC Advances* **2016**, *6*, 41317-41322.
18. Ge, Y.; Ji, R.; Shen, S.; Cao, X.; Li, F., *Sensors and Actuators B: Chemical* **2017**, *100*, 875-881.
19. Alcarazo, M.; Roseblade, S. J.; Cowley, A. R.; Fernández, R.; Brown, J. M.; Lassaletta, J. M., *Journal of the American Chemical Society* **2005**, *127*, 3290-3291.
20. Burstein, C.; Lehmann, C. W.; Glorius, F., *Tetrahedron* **2005**, *61*, 6207-6217.
21. Hahn, F. E., *Angewandte Chemie International Edition* **2006**, *45*, 1348-1352.
22. Weber, M. D.; Garino, C.; Volpi, G.; Casamassa, E.; Milanesio, M.; Barolo, C.; Costa, R. D., *Dalton Transactions* **2016**, *45*, 8984-8993.
23. Salassa, L.; Garino, C.; Albertino, A.; Volpi, G.; Nervi, C.; Gobetto, R.; Hardcastle, K. I., *Organometallics* **2008**, *27*, 1427-1435.
24. Sheng, H.; Hu, Y.; Zhou, Y.; Fan, S.; Cao, Y.; Zhao, X.; Yang, W., *Dyes and Pigments* **2019**, *160*, 48-57.
25. Huang, J.-R.; Zhang, Q.-R.; Qu, C.-H.; Sun, X.-H.; Dong, L.; Chen, Y.-C., *Organic Letters* **2013**, *15*, 1878-1881.
26. Chuprakov, S.; Hwang, F. W.; Gevorgyan, V., *Angewandte Chemie International Edition* **2007**, *46*, 4757-4759.
27. Joshi, A.; Chandra Mohan, D.; Adimurthy, S., *Organic Letters* **2016**, *18*, 464-467.
28. Mohan, D. Rao, S., *Organic & Biomolecular Chemistry* **2015**, *13*, 5602-5607.

29. Li, M.; Xie, Y.; Ye, Y.; Zou, Y.; Jiang, H.; Zeng, W., *Organic letters* **2014**, *16*, 6232-6235.
30. Wang, H.; Xu, W.; Wang, Z.; Yu, L.; Xu, K., *The Journal of Organic Chemistry* **2015**, *80*, 2431-2435.
31. Sandeep, M.; Swati Dushyant, P.; Sravani, B.; Rajender Reddy, K., *European Journal of Organic Chemistry* **2018**, *2018*, 3036-3047.
32. Chandrasekar, S.; Sangeetha, S.; Sekar, G., *ChemistrySelect* **2019**, *4*, 5651-5655.
33. Dhiman, S.; Nandwana, N. K.; Saini, H. K.; Kumar, D.; Rangan, K.; Robertson, K. N.; Jha, M.; Kumar, A., *Advanced Synthesis & Catalysis* **2018**, *360*, 1973-1983.
34. Dhiman, S.; Pericherla, K.; Nandwana, N. K.; Kumar, D.; Kumar, A., *The Journal of Organic Chemistry* **2014**, *79*, 7399-7404.
35. Li, T.; Fu, C.; Ma, Q.; Sang, Z.; Yang, Y.; Yang, H.; Lv, R.; Li, B., *The Journal of Organic Chemistry* **2017**, *82*, 10263-10270.
36. Wei, D.; Zhu, X.; Niu, J. L.; Song, M. P., *ChemCatChem* **2016**, *8*, 1242-1263.
37. Yoshino, T.Matsunaga, S., *Advanced Synthesis & Catalysis* **2017**, *359*, 1245-1262.
38. Li, T.; Zhang, C.; Tan, Y.; Pan, W.; Rao, Y., *Organic Chemistry Frontiers* **2017**, *4*, 204-209.
39. Gandeepan, P.; Rajamalli, P.; Cheng, C. H., *Angewandte Chemie* **2016**, *128*, 4380-4383.

Chapter 2

Ru(II)-Catalyzed Annulation of 2-Alkenyl-/Aryl-imidazoles with *N*-Maleimides and Quinones

2.1 INTRODUCTION

Imidazo-fused heterocyclic compound possess significant biological properties such as a strong affinity for peripheral benzodiazepine receptors, regulation of potassium-ion channels, and cytotoxicity against specific human cancer cell lines.[1-7] The synthesis of fused-imidazo-derivatives has received considerable attention due to their usefulness and unusual activity. Several synthetic methods have been developed for constructing imidazo[1,2-*a*]pyridines/isoquinolines and fused benzimidazoles.

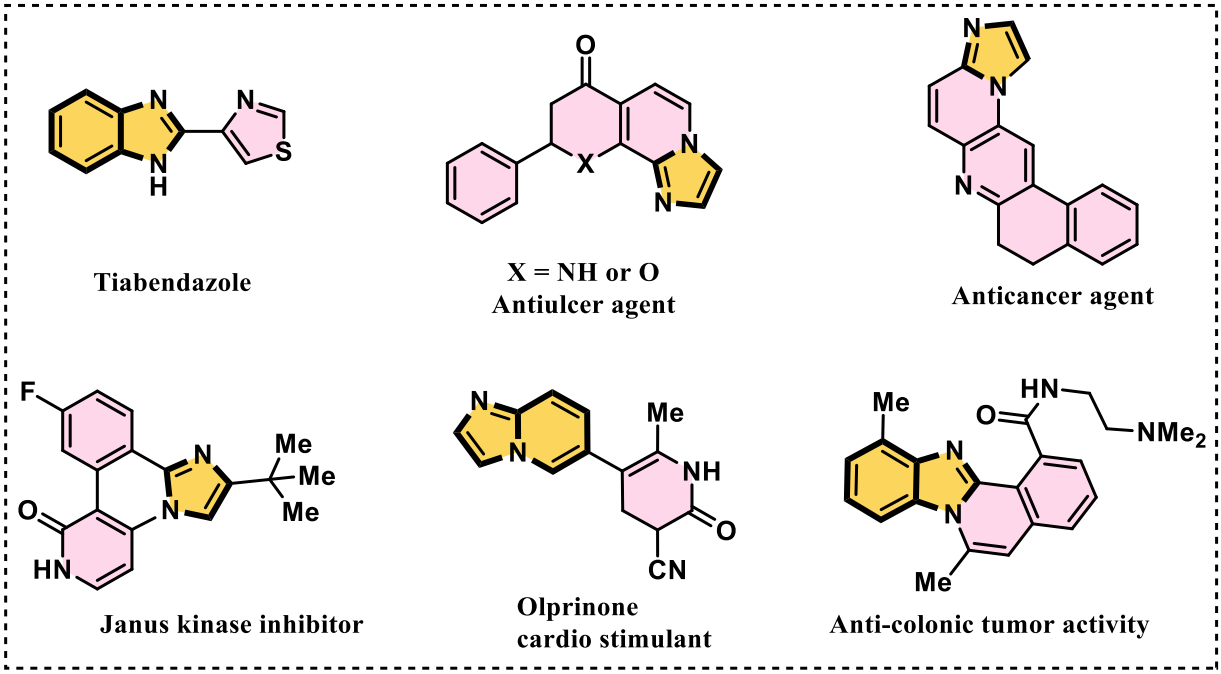

Figure 2.1: Selected examples of biologically active imidazo-fused heterocycles

The transition metal-catalyzed cascade annulation reactions have gained remarkable attention over the past few decades as a convincing and efficient method for synthesizing fused heterocyclic compounds.[8-12] This approach combines different pharmacophores and natural product scaffolds to create diverse structures.[13-15] Rhodium and ruthenium-catalyzed oxidative annulation reactions have been demonstrated very well in the literature for the synthesis of fused imidazo[1,2-*a*]pyridine/isoquinolines or benzimidazole-fused heterocyclic compounds by using 2-alkenyl/2-arylimidazoles, 2-arylbenzimidazoles, with internal alkynes, olefins, maleimides, quinones, sulfoxonium ylide, and diazo carbonyl compounds.[16-21]

Ellman and colleagues developed a new way to synthesize [5,6]-bicyclic heterocycles with nitrogen at the ring junction. Using Rh(III) as a catalyst, the C-H bond of C-alkenyl azoles **(1)** was activated and reacted with different electrophiles such as alkynes **(2)**, diazoketone **(3)**, and sulfoxonium ylides **(4)** to produce corresponding bicyclic heterocycles **5** and **6 (Scheme 2.1)**.[22] This method allowed them to use alkenyl imidazoles, pyrazoles, or triazoles as starting materials. This method was beneficial for making new compounds for drug discovery as it enables consumption of heterocycles with different nitrogen positions and substitutions was crucial for finding new drugs.

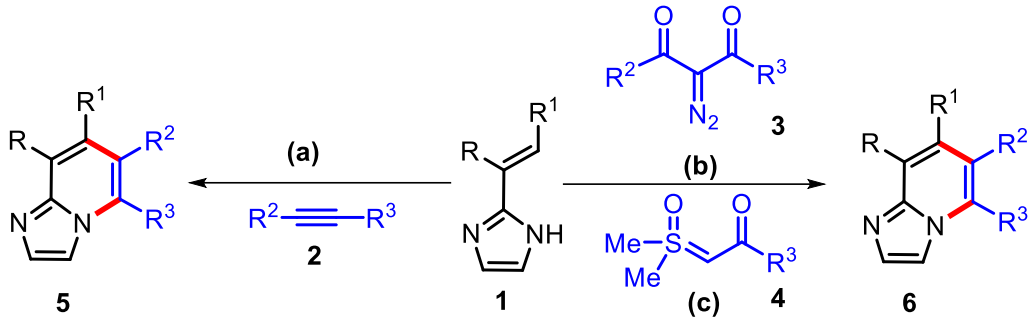

No.	Condition	Examples	Yield%
a)	$[RhCp^*Cl_2]_2$, $Cu(OAc)_2{\cdot}H_2O$, $AgSbF_6$, MeOH, 60 °C, 12 h	18	upto 88
b)	$[RhCp^*Cl_2]_2$, $AgSbF_6$, THF, 40 °C, 16 h	11	upto 92
c)	$[RhCp^*(MeCN)_3](SbF_6)_2$, PivOH, NaOAc, toluene, 120 °C, 16 h	25	upto 96

Scheme 2.1: Rh(III)-catalyzed synthesis of bicyclic bridgehead nitrogen heterocycles from C-alkenyl azoles

Subsequently, same group reported the synthesis of imidazo-fused pyrimidine derivatives, through Rh(III)-catalyzed annulations of *N*-azoloimines **(7)** (**Scheme 2.2a**).[23] This approach allowed for the selective activation of the imidoyl C-H bond, enabling efficient coupling with different coupling partners, like alkynes **(2)**, diazo compounds **(3)**, and sulfoxonium ylides **(4)** producing various imidazo-fused pyrimidines derivatives. The reaction exhibited compatibility with both electron-donating and electron-withdrawing coupling partners, leading to the formation of products in good to excellent yields.

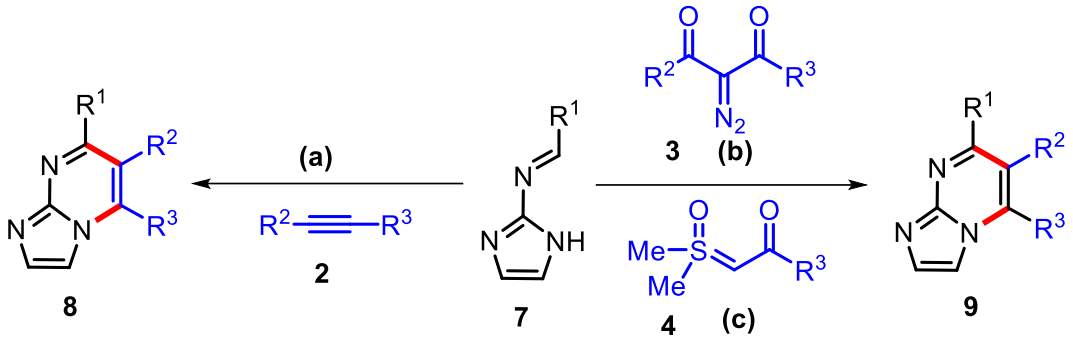

No.	Condition	Examples	Yield%
a)	$[RhCp^*Cl_2]_2$, $Cu(OAc)_2$, TFE, 60 °C, 16 h	13	upto 93
b)	$[RhCp^*(MeCN)_3](SbF_6)_2$, PivOH, NaOAc, 1,4-dioxane, 100 °C, 16 h	10	upto 94
c)	$[RhCp^*(MeCN)_3](SbF_6)_2$, PivOH, NaOAc, 1,4-dioxane, 100 °C, 16 h	20	upto 88

Scheme 2.2: Rh(III)-catalyzed synthesis of imidazo-fused pyrimidines from *N*-azoloimines

Dutta and Sen demonstrated C-H/N-H annulation of 2-arylbenzimidazoles **(10)** and various diarylacetylenes **(2)** with a Co(III) catalyst and silver acetate as an oxidant, producing imidazo-fused isoquinoline derivatives in (**11**) up to 93% yields (**Scheme 2.3a**).[24] Chatani *et al.* used nickel complexes to achieve a similar reaction with diphenylacetylene **(2)** and developed different protocols with or without a base (**Scheme 2.3b**).[25] Chandrasekhar and Gandhi groups independently reported a related synthesis with $[RuCl_2(p\text{-cymene})]_2$ as a catalyst, giving products in moderate to good yields (43% to 92%) yields (**Scheme 2.3c and Scheme 2.3d**).[26] Ackermann *et al*., also developed a ruthenium-catalyzed process that used an innovative electrochemical oxidation method for the synthesis of azo-fused-isoquinolines **(4)**. This process had molecular hydrogen as the only byproduct and gave yields from 50% to 93%. The researchers isolated and characterized a key catalytic intermediate, aza-ruthena(II)-bicyclo-[3.2.0]-heptadiene, which helped to understand the mechanism of the reaction better yields (**Scheme 2.3e**).[27] Instead of Ru(II) Hua and group, used $[RhCp^*Cl_2]_2$ as a catalyst and obtained compound **11** in yields up to 93% (**Scheme 2.3f**).[28] Another multicomponent approach for the synthesis of phenanthraimidazo scaffolds, by using Rh(III), was documented by Yu *et al.* (**Scheme 2.3g**).[29] Additionally, the combination of a $[RhCp^*Cl_2]_2$ catalyst with silver acetate as the oxidant was described by da Silva Júnior *et al*., yielding products in the range of 49% to 75% (**Scheme 2.3h**).[30]

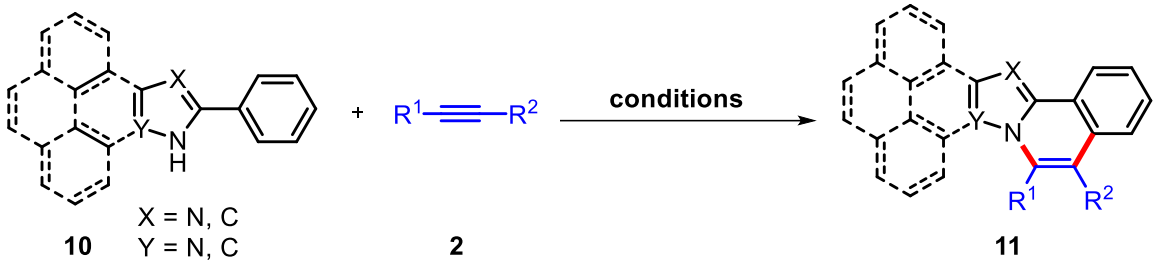

No.	Condition	Examples	Yield%
a)	$[CoCp^*I_2]_2$, AgOAc, NaOAc, TFE, 60 °C, 12 h	31	upto 95
b)	$Ni(OAc)_2$, dtbbpy, ^tBuOK, toluene, 160 °C, 14-48 h	9	upto 95
c)	$[RuCl_2(p\text{-cymene})]_2$, $Cu(OAc)_2{\cdot}H_2O$, toluene, 110 °C, 12 h	18	upto 92
d)	$[RuCl_2(p\text{-cymene})]_2$, 1-AdCOOH, $Cu(OAc)_2$, K_2CO_3, xylenes, 120 °C, 16 h	8	upto 60
e)	$[RuCl_2(p\text{-cymene})]_2$, 1-AdCOOH, KOAc, *t*-AmOH, H_2O, 100 °C, 4 h, CCE@8 mA	36	upto 93
f)	$[RhCp^*Cl_2]_2$, $Cu(OAc)_2{\cdot}H_2O$, acetone, 120 °C, 12 h	14	upto 93
g)	$[RhCp^*Cl_2]_2$, $Cu(OAc)_2{\cdot}H_2O$, TFE, 120°C, 16 h	2	upto 53
h)	$[RhCp^*Cl_2]_2$, AgOAc, MeOH, 100 °C, 24 h	16	upto 75

Scheme 2.3: Oxidative annulation of 2-arylbenzimidazoles and fused homologs with alkynes

Maleimides **(13)** are the key core motif exclusively found in numerous natural and pharmaceuticals compounds, exhibiting diverse biological activities.[31] Furthermore, maleimides can be easily transformed into biologically potent pyrrolidines, succinimides, and lactams.[32-34] Notably, in recent years maleimides have played a crucial role as the two-carbon electrophilic coupling partner in various organic transformations, such as C-H activation, annulation, and spirocyclization reactions facilitated by metal catalyst. With recent developments, transition metal-catalyzed annulation and spirocyclization of several dipolarophile substrates with maleimides have been explored to construct polyheterocyclic compounds. For instance, Jeganmohan and co-workers demonstrated the Rh(III)-catalyzed construction of isoindolinone spirosuccinimides (**14**) by monodentate amide ligand assisted 1,1-cyclization of N-methoxybenzamides (**12**) with maleimides (**13**) through C-H/N-H/O-H bond activation (**Scheme 2.4**).[35] Notably, the reaction was

carried out in a redox-free manner by employing an internal oxidant. The methodology showcased wide functional group tolerance and with no requirement for external oxidants. The tentative mechanism of this approach has been identified through the isolation of metallocycle intermediate, deuterium labelling experiment (H/D), and DFT studies. These experiments revealed that the internally generated AcOH played a crucial role in the cleavage of the N-OMe bond and oxidation of Rh(I) to Rh(III) species.

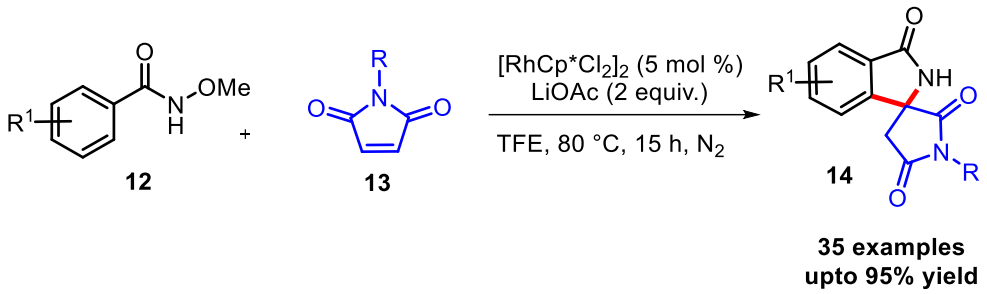

Scheme 2.4: Rh(III)-catalyzed synthesis of isoindolinone spirosuccinimides

Lee *et al.* developed a novel and efficient Rh(III)-catalyzed route to synthesize of biologically active spiro-fused pyrrolidinedione heterocycles **(16)** through cascade C-H activation and spirocyclization of 2-arylquinazolin-4(3*H*)-ones **(15)** with maleimides **(13) (Scheme 2.5)**.[36] The sequential *ortho* C-H functionalization and spirocyclization followed by aza-Michael addition to form C-C and C-N bond in single-step process were the main steps of the protocol. The notable features include one-step synthesis, broad substrate scope, high atom economy, regioselectivity, and broad functional group tolerance.

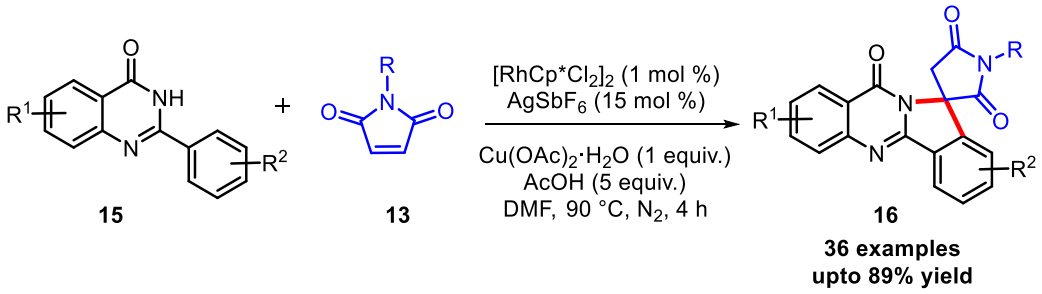

Scheme 2.5: Rh(III)-catalyzed synthesis of spiro-fused pyrrolidinedione heterocycles

Bao and colleagues demonstrated a highly effective protocol for the construction of pyrrolo[3,4-*b*]indole-1,3-diones (**18**) by using Rh(III)-catalyzed C-H activation and annulation process involving arylhydrazines (**17**) with maleimides (**13**) (**Scheme 2.6**).[37] The easily accessible starting

materials, compatibility of various functional groups, mild reaction conditions, and overall experimental simplicity enhance the demand for this protocol to synthesize fused heterocycles.

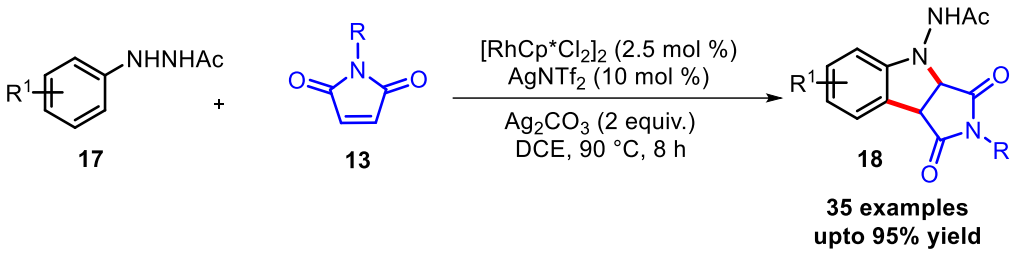

Scheme 2.6: Rh(III)-catalyzed synthesis of pyrrolo[3,4-*b*]indole-1,3-diones

Our group also described a Rh(III)-catalyzed dehydrogenative annulation and spirocyclization or 2-arylimidazo[1,2-*a*]pyridines[38] **(19)** and 2-arylindoles[11] **(21)** with maleimides **(13) (Scheme 2.7)**. This protocol shows a broad substrate scope for both the 2-arylimidazo[1,2-*a*]pyridines/indoles and maleimides and delivers the annulated and spirocyclized product in good to excellent yields. Furthermore, the absorption and fluorescence properties of annulated products were studied and validated by quantum chemical calculations.

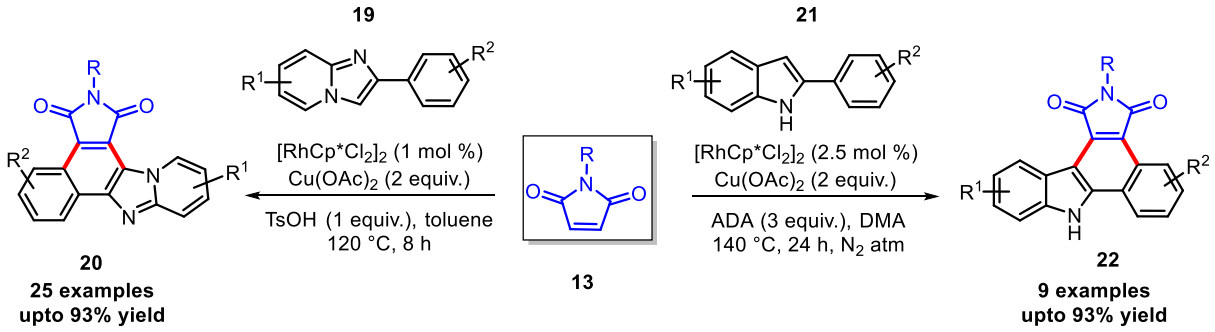

Scheme 2.7: Rh(III)-catalyzed annulation of 2-arylimidazo[1,2-*a*]pyridines/2-arylindoles with maleimides

In 2021, Lee and colleagues developed a novel method to connect various maleimides (**13**) with 2-arylbenzimidazoles (**23**) *via* Rh(III)-catalyzed C-H activation/annulation approach. Depending on the acidic and basic reaction conditions, two different types of polyheterocycles **24** and **25** were produced in good yield (**Scheme 2.8a or Scheme 2.8b**).[39] The synthesized compounds were used to develop a fluorescent on-off chemosensor. This chemosensor exhibited exceptional sensitivity in detecting Hg^{2+}, Cu^{2+}, and Fe^{3+} heavy-metal ions in a mixed aqueous solution, even at nanomolar concentration.

Huang *et al*. described Rh(III)-catalyzed synthesis of benzimidazole-fused isoquinolines (**25**) and benzimidazoles-spiroisoindoles (**26**) through a cascade reaction involving C-H activation and cyclization of 2-arylbenzimidazoles (**23**) with maleimides (**13**) (**Scheme 2.8c)**.[40] The selectivity towards the formation of these two distinct products can be altered by using unsubstituted or substituted benzimidazoles at the *ortho*-position of the phenyl ring. The mechanism involves the C-H activation followed by migratory insertion of maleimide forming a Heck-type intermediate. A similar type of work was also reported by Zhou and co-workers through Rh(III)-catalyzed [4+2]-cyclization of 2-arylbenzimidazoles **(23)** with maleimides **(13)** through C-H bond activation process (**Scheme 2.8d).**[41]

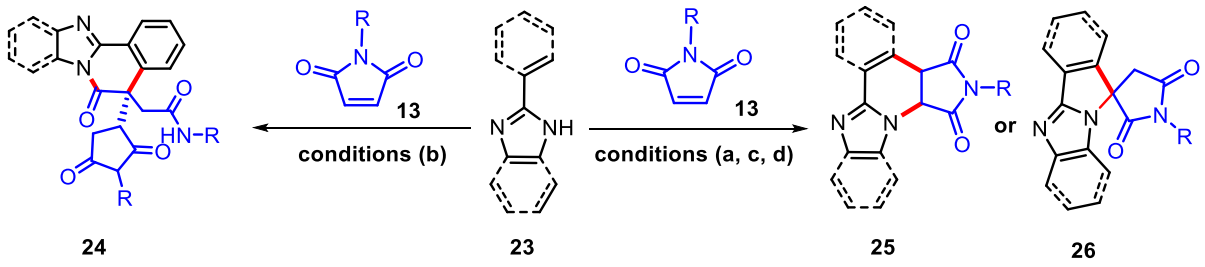

No.	Condition	Examples	Yield%
a)	$[RhCp^*Cl_2]_2$, $AgSbF_6$, AcOH, DCE, 100 °C, 12 h	12	upto 78
b)	$[RhCp^*Cl_2]_2$, $AgSbF_6$, NaOAc, PhCl, 120 °C, 12 h	23	upto 86
c)	$[RhCp^*Cl_2]_2$, AgOAc, DCE, 100 °C, 5 h	28	upto 90
d)	$[RhCp^*Cl_2]_2$, $AgSbF_6$, AgOAc, DCE, 120 °C, 12 h	23	upto 85

Scheme 2.8: Rh(III)-catalyzed annulation of 2-arylbenzimidazoles with maleimides

Quinones are organic compounds found in various living organisms, including bacteria, flowering plants, and arthropods.[42-44] They possess various applications, including critical pharmacological properties, participation in redox reactions, and advanced electrochemical energy storage utilization. Benzoquinone and 1,4-naphthoquinone are the most straightforward and essential quinones among the reported ones.[45-47]

1,4-Benzoquinone (**27**) has demonstrated remarkable selectivity in acting as a coupling partner with certain (hetero)arenes under transition metals catalysis. For instance, in 2015, Zhou and co-workers demonstrated the innovative a C-H bond functionalization reaction, wherein quinone

acted as a C1 synthon. This groundbreaking discovery shows the amide-directed C-H activation of 3-arylisoquinolones through Ir(III), followed by their subsequent incorporation into quinone substrates, as illustrated in **Scheme 2.9a**.[48] Subsequently, protodemetalation delivered arylated dihydroquinone, and a second C-H metalation happened at the most acidic C(sp^3)-H bond of the dihydroquinone. C-N reductive elimination yielded spirocyclic adducts **(28)**, requiring the use of a sacrificial equivalent of benzoquinone **(27)** to oxidize Ir(I) to Ir(III). This reaction consistently yielded near-quantitative yields across a variety of isoquinolone substrates. Naphthoquinones also produced spirocyclic products, although two equivalents of $Cu(OAc)_2$ were needed to achieve high-yield product formation, attributed to the reduced oxidizing capacity of naphthoquinone.

In 2019, the Fan group reported the Rh(III)-catalyzed arylation of 2-phenylindole **(21)** with quinones **(27)** (**Scheme 2.9b**).[49] Depending on substituents at C-3 position of 2-arylindole, the quinone substrates behaved as either a C1 or C2 synthon. The arylated 2,3-dihydroquinone products underwent nucleophilic attack by indole without any substituent, followed by aromatization to produce annulated products (**30**). In an alternative pathway, the Rh(III)-catalyst underwent a second C-H insertion into the acidic C-H bond of the arylated 2,3-dihydroquinone to afford spirocyclic products (**29**), with a regeneration of Rh(III) *via* quinone. Surprisingly, when they used $[IrCp^*Cl_2]_2$ catalyst and $Zn(OAc)_2$ as an additive, the 2,3-diphenylindoles participated in an [4+2] annulation with quinones at the nitrogen of the indole, producing indolopheanthridine scaffolds **(31)** (**Scheme 2.9c**).[50]

Moon *et al.* revealed an easy and efficient method for the direct C-H/C-H cross-coupling reaction of various (hetero)arenes with quinones **(27)** (**Scheme 2.9d**).[51] This versatile cross-coupling method accommodates a wide array of substrates and directing groups, offering a convenient and potent synthetic approach for generating a diverse range of aryl-substituted quinones (**32**) with significant synthetic applications. Furthermore, this synthetic pathway facilitates the rapid construction of the carbazole quinone motif, which has been recognized as a novel inhibitor scaffold for GSKβ.[52]

Recently, Sakhuja and co-workers developed a Ru(II)-catalyzed methodology for the [4+1] and [4+2] oxidative coupling between *N*-aryl-2,3-dihydrophthalazine-1,4-diones and 1,4-benzoquinones **(27)**, to produce spiro-indazolones **(33)** and fused cinnolines **(34)** derivatives

(**Scheme 2.9e**).[53] Notably, these transformations occurred under mild, aerobic conditions without the need for an external oxidant.

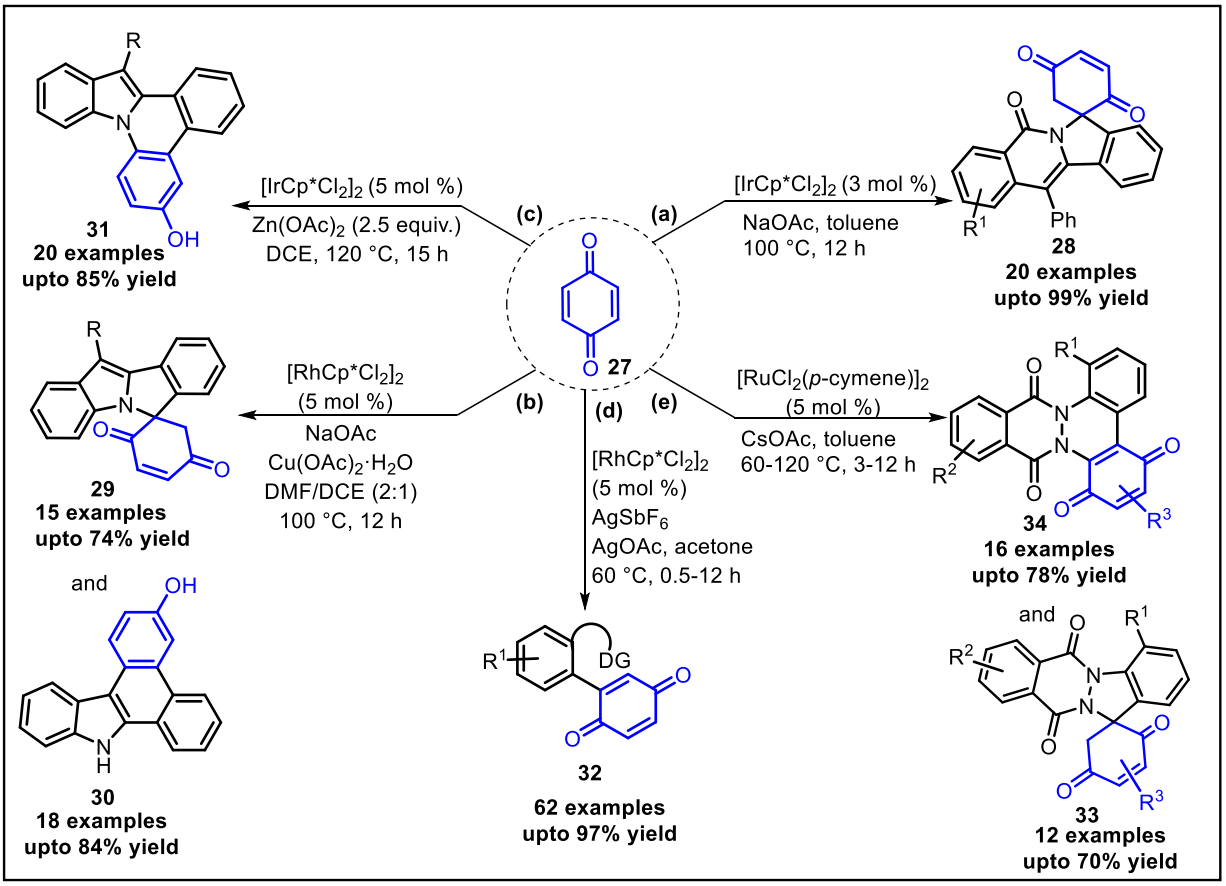

Scheme 2.9: Transition-metal catalyzed C-H functionalization of (hetero)arenes with quinones

Sankaram *et al*. demonstrated an efficient approach for the preparation of benzo[4,5]imidazo[1,2-*f*]phenanthridine-1,4-diones derivatives **(35)** *via* Rh(III)-catalyzed oxidative annulation of 2-aryl-1*H*-benzo[*d*]imidazo **(23)** with 1,4-quinones **(27)** (**Scheme 2.10**).[54] A wide range of fused phenanthridine derivatives were prepared in good yields through this C-H/N-H annulation reaction.

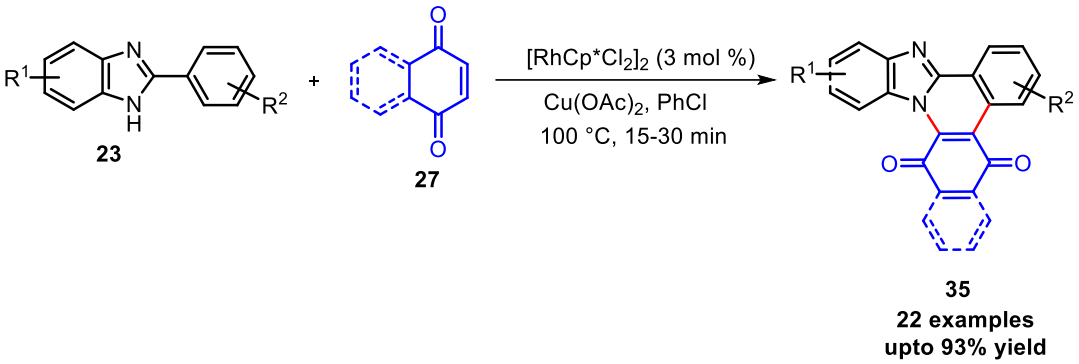

Scheme 2.10: Rh(III)-catalyzed synthesis of benzo[4,5]imidazo[1,2-*f*]phenanthridine-1,4-diones

As part of our interest in the synthesis of *N*-heterocyclic compounds under transition-metal catalysis, we have developed a ruthenium-catalyzed C−H/N−H annulation of 2-alkenyl-/2-aryl-imidazoles **(1** or **23)** with maleimides **(13)** and quinones **(38)** to construct a series of imidazo-fused polyheterocyclic frameworks (**36** or **39**) (**Scheme 2.11**).

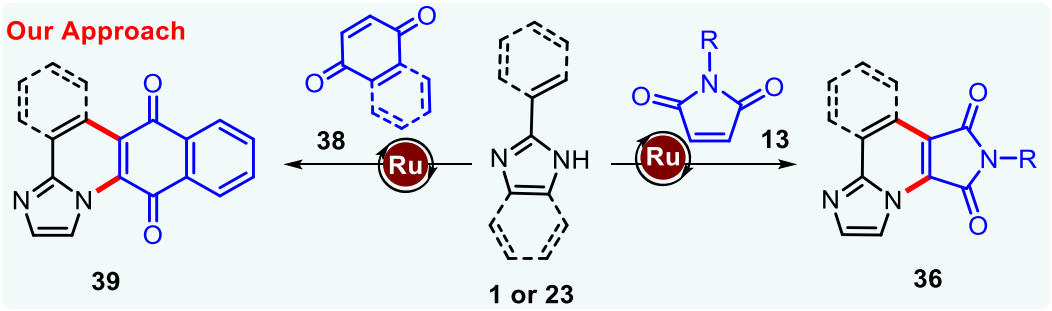

Scheme 2.11: Synthesis of imidazo-fused heterocycles *via* Ru(II)-catalyzed annulation of 2-alkenyl/aryl imidazoles with maleimides and quinones

2.2 RESULTS AND DISCUSSION

We commenced our investigation by selecting (*E*)-2-(1-phenylprop-1-en-2-yl)-1*H*-imidazole (**1a**) and *N*-methylmaleimide (**13a**) as model substrates. Initially, reaction of **1a** with **13a** in the presence of $[RuCl_2(p\text{-cymene})]_2$, $Cu(OAc)_2$, $AgSbF_6$ and HOAc in methanol at 70 °C for 12 h gave annulated product **36aa** and spiro-annulated product **36aa′** in 52% and 33% yields, respectively (**Table 2.1**, entry 1**)**. The structures of **36aa** and **36aa′** were ascertained by ^{1}H NMR and $^{13}C\{^1H\}$ NMR and ESI-HRMS data. Further, the structure of **36aa** was unambiguously confirmed by single crystal X-ray diffraction analysis (**CCDC** 2297100).

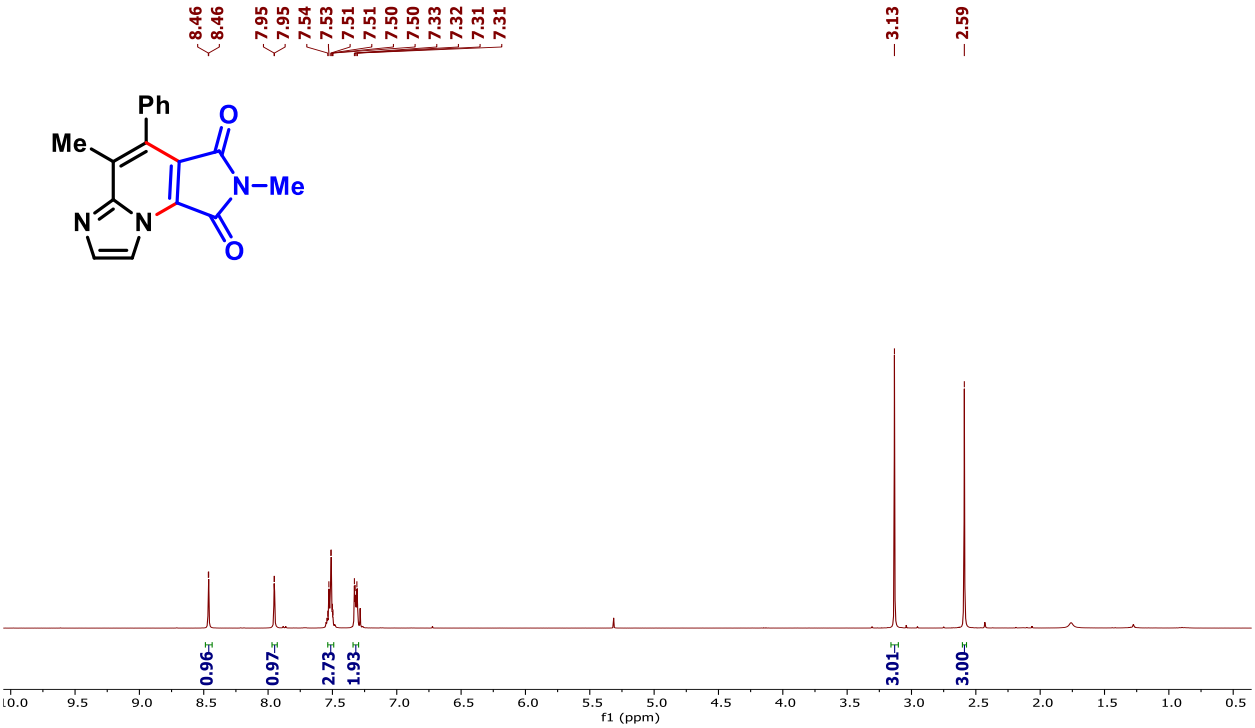

Figure 2.2: ^{1}H-NMR spectrum of 2,5-dimethyl-4-phenyl-1*H*-imidazo[1,2-*a*]pyrrolo[3,4-*e*]pyridine-1,3(2*H*)-dione **(36aa)** recorded in $CDCl_3$

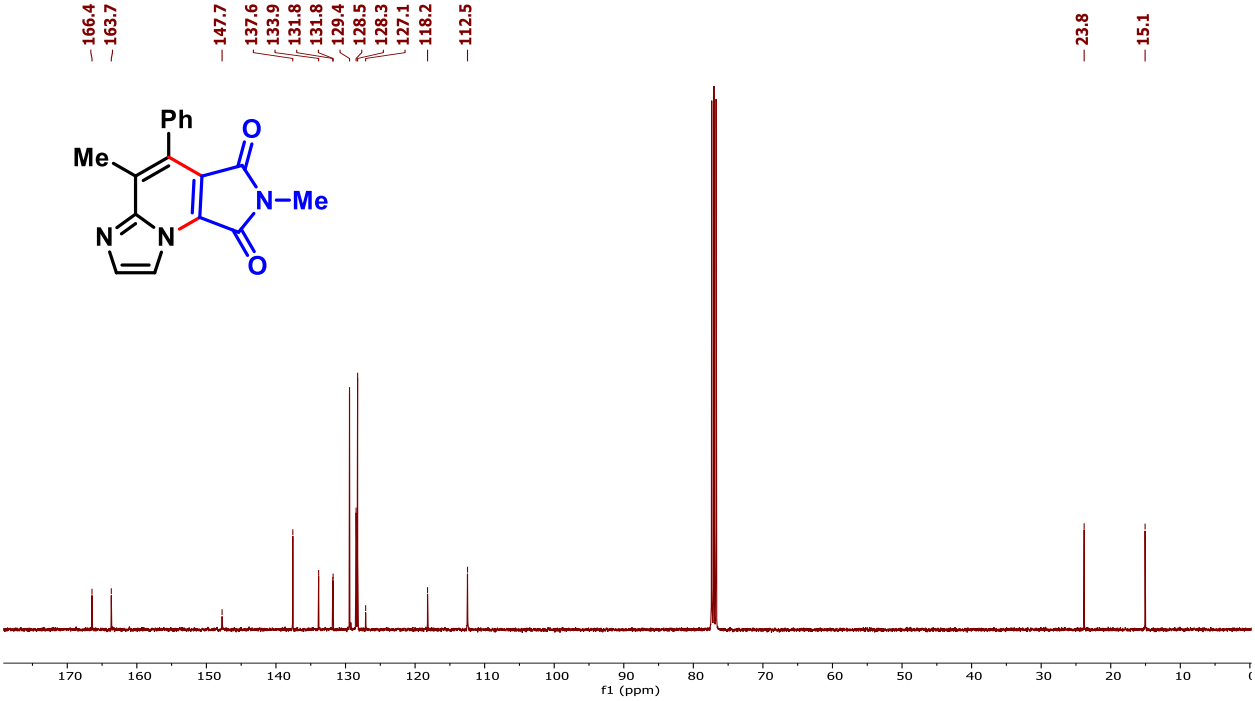

Figure 2.3: ^{13}C-NMR spectrum of 2,5-dimethyl-4-phenyl-1*H*-imidazo[1,2-*a*]pyrrolo[3,4-*e*]pyridine-1,3(2*H*)-dione **(36aa)** recorded in $CDCl_3$

Table 2.1: Optimization of reaction conditions.[a]

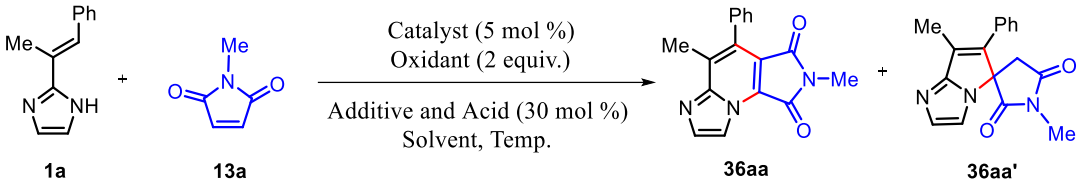

Entry	Catalyst	Additive	Acid	Oxidant	Solvent	% Yield[b]	
						36aa	36aa′
1	$[RuCl_2(p\text{-cymene})]_2$	$AgSbF_6$	AcOH	$Cu(OAc)_2$	MeOH	52	33
2	$[RuCl_2(p\text{-cymene})]_2$	$AgSbF_6$	AcOH	AgOAc	MeOH	15	trace
3	$[RuCl_2(p\text{-cymene})]_2$	$AgSbF_6$	AcOH	IBD	MeOH	NR	-
4	$[RuCl_2(p\text{-cymene})]_2$	$AgSbF_6$	AcOH	$Cu(OAc)_2{\cdot}H_2O$	MeOH	25	10
5	$[RhCp^*Cl_2]_2$	$AgSbF_6$	AcOH	$Cu(OAc)_2$	MeOH	40	15
6	$[Cp^*Co(CO)I_2]_2$	$AgSbF_6$	AcOH	$Cu(OAc)_2$	MeOH	-	nd
7	$Pd(OAc)_2$	$AgSbF_6$	AcOH	$Cu(OAc)_2$	MeOH	-	-
8	$Ni(OTf)_2$	$AgSbF_6$	AcOH	$Cu(OAc)_2$	MeOH	-	-
9	$[RuCl_2(p\text{-cymene})]_2$	$AgSbF_6$	AcOH	$Cu(OAc)_2$	EtOH	37	15
10	$[RuCl_2(p\text{-cymene})]_2$	$AgSbF_6$	AcOH	$Cu(OAc)_2$	DCE	nd	-
11	$[RuCl_2(p\text{-cymene})]_2$	$AgSbF_6$	AcOH	$Cu(OAc)_2$	*t*-AmOH	50	-
12	$[RuCl_2(p\text{-cymene})]_2$	$AgSbF_6$	AcOH	$Cu(OAc)_2$	TFE	35	-
13	$[RuCl_2(p\text{-cymene})]_2$	$AgSbF_6$	AcOH	$Cu(OAc)_2$	IPA	trace	-
14	$[RuCl_2(p\text{-cymene})]_2$	$AgSbF_6$	AcOH	$Cu(OAc)_2$	DMF	trace	-
15	**$[RuCl_2(p\text{-cymene})]_2$**	**KPF_6**	**AcOH**	**$Cu(OAc)_2$**	**MeOH**	**80**	**-**
16	$[RuCl_2(p\text{-cymene})]_2$	KPF_6	TFA	$Cu(OAc)_2$	MeOH	trace	
17	$[RuCl_2(p\text{-cymene})]_2$	KPF_6	PTSA	$Cu(OAc)_2$	MeOH	67	-
18	$[RuCl_2(p\text{-cymene})]_2$	KPF_6	PivOH	$Cu(OAc)_2$	MeOH	40	-
19	$[RuCl_2(p\text{-cymene})]_2$	KPF_6	AcOH	-	MeOH	37	-
20	$[RuCl_2(p\text{-cymene})]_2$	KPF_6	-	$Cu(OAc)_2$	MeOH	22	
21	$[RuCl_2(p\text{-cymene})]_2$	-	AcOH	$Cu(OAc)_2$	MeOH	27	
22	-	KPF_6	AcOH	$Cu(OAc)_2$	MeOH	-	

[a]Reaction conditions: **1a** (0.27 mmol), **13a** (0.54 mmol), oxidant (2.0 equiv), catalyst (5 mol %), additive (30 mol %), acid (30 mol %), and solvent (2 mL) at 70 ºC for 12 h. [b]Isolated yields.

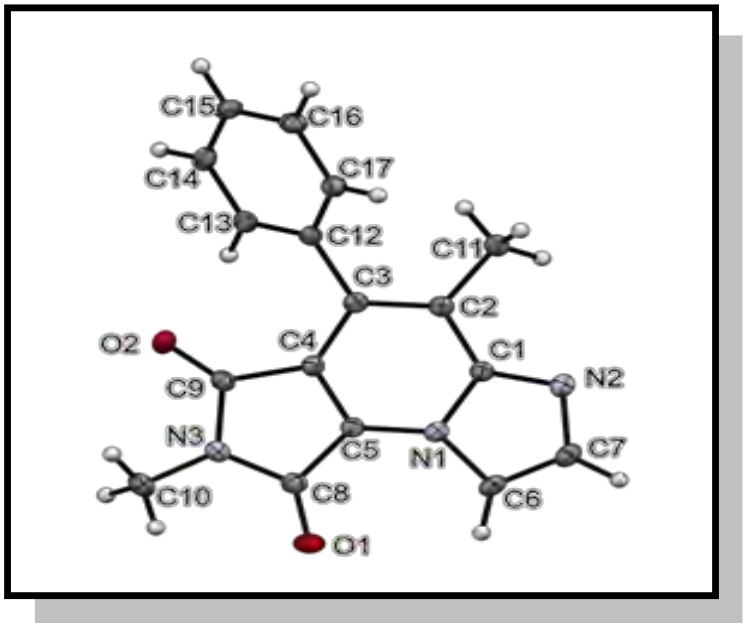

Figure 2.4: The ORTEP diagram of **36aa** [CCDC: 2297100]. Thermal ellipsoids are drawn at 50 % probability level

To improve the yield and selectivity of the reaction various experiments were performed. Among different oxidants such as AgOAc, IBD, and $Cu(OAc)_2 \cdot H_2O$ screened (**Table 2.1**, entry 2-4), $Cu(OAc)_2$ was found to be the most suitable oxidant for this reaction, delivering **36aa** in 52% yield. Changing catalysts (**Table 2.1**, entry 5-8) and solvents (**Table 2.1**, entry 9-14) did not improve the yield of **36aa**. It is worth mentioning that the reaction of **1a** with **2a** in the presence of $[Ru(p\text{-cymene})Cl_2]_2$ (5 mol %), $Cu(OAc)_2 \cdot H_2O$ (2 equiv.), $AgSbF_6$ (30 mol %), AcOH (30 mol %) in DMF at 70 °C for 12 h did not produce annulated product **36aa** (Table 1, entry 14) which is in sharp contrast to annulation of **13a** with 2-phenylbenzimidazole to produce 2-methyl-3*a*,13*a*-dihydro-1*H*-benzo[4,5]imidazo[2,1-*a*]pyrrolo[3,4-*c*]isoquinoline-1,3(2*H*)-dione under similar conditions at 140 °C. Interestingly, changing $AgSbF_6$ with KPF_6 lead to a significant improvement in the yield (80%) and selectivity of **36aa** (**Table 2.1**, entry 15). Next, a series of acids namely TFA, PTSA and PivOH were evaluated and all of them were found to be less efficient than AcOH (**Table 2.1**, entries 16–18). The yield of **36aa** significantly decreased in the absence of oxidant and additives (**Table 2.1**, entry 19-21) while annulated product **36aa** was not formed in the absence of the catalyst (**Table 2.1**, entry 22). Thus, the optimized conditions for the annulation reaction are as follows: $[RuCl_2(p\text{-cymene})]_2$ (5 mol %), $Cu(OAc)_2 \cdot H_2O$ (2 equiv.), KPF_6 (30 mol %), AcOH (30 mol %) in the methanol at 70 °C for 12 h.

Table 2.2. Substrate scope for the synthesis of imidazo[1,2-*a*]pyrrolo[3,4-*e*]pyridines, imidazo[2,1-*a*]pyrrolo[3,4-*c*]isoquinolines and benzo[*g*]imidazo[1,2-*a*]quinoline-6,11-diones.[a]

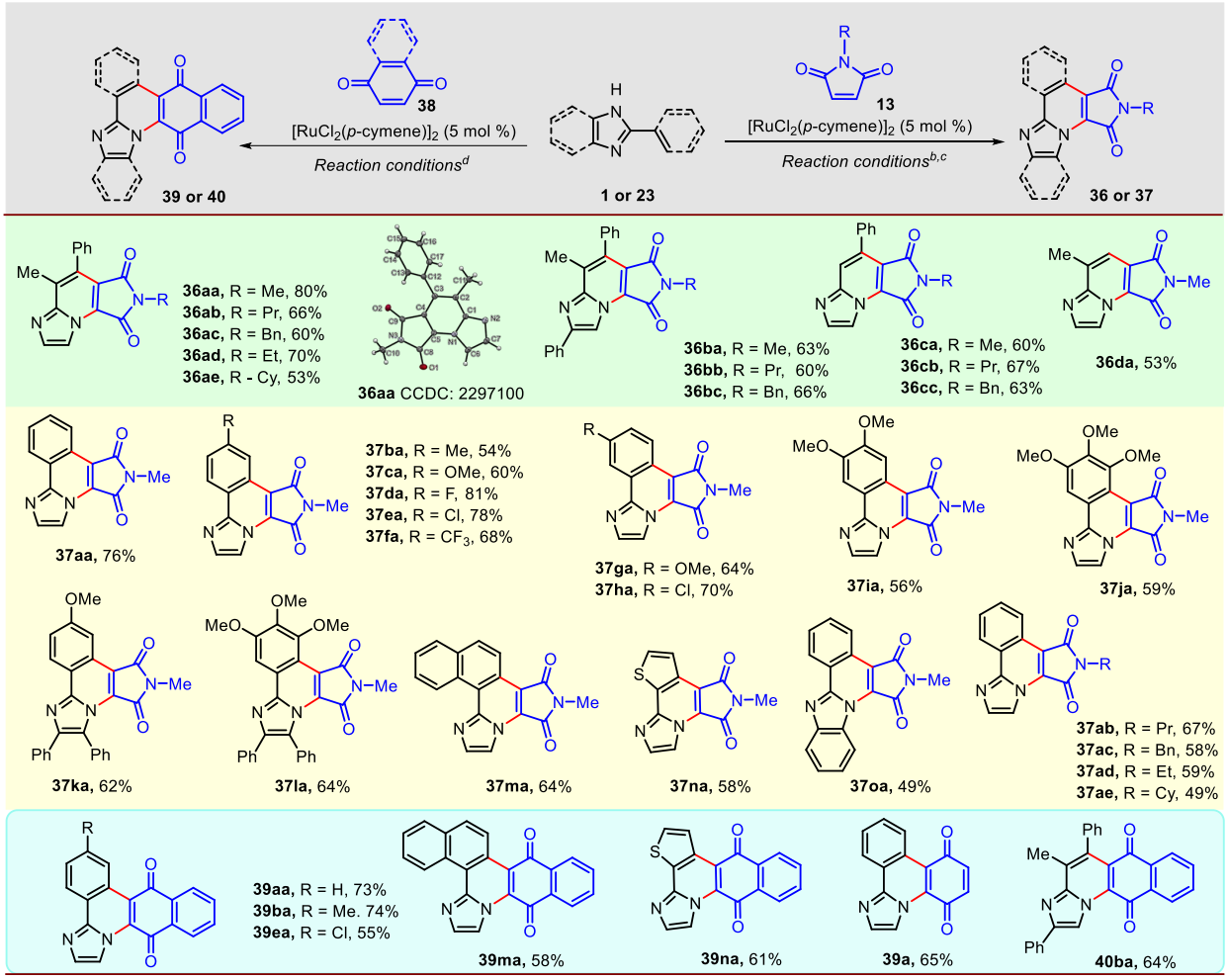

[a]Isolated yields.

[b]Reaction conditions for preparation of **36**: **1** (0.34 mmol), **13** (0.68 mmol), $Cu(OAc)_2$ (2.0 equiv), $RuCl_2$(*p*-cymene)$_2$ (5 mol %), KPF_6 (30 mol %), AcOH (30 mol %) in MeOH (2 mL) at 70 ºC for 12 h.

[c]Reaction conditions for preparation of **37**: **23** (0.34 mmol), **13** (0.68 mmol), $Cu(OAc)_2$ (2.0 equiv), $RuCl_2$(*p*-cymene)$_2$ (5 mol %), $AgSbF_6$ (30 mol %), AcOH (30 mol %) in DMA (2 mL) at 140 ºC for 24 h.

[d]Reaction conditions for preparation of **39** and **40**: **23** or **1b** (0.34 mmol), **38** (0.68 mmol), $Cu(OAc)_2$ (2.0 equiv), $RuCl_2$(*p*-cymene)$_2$ (5 mol %), $AgSbF_6$ (30 mol %), AcOH (30 mol %) in DMA (2 mL) at 140 ºC for 4-6 h.

With the optimized reaction conditions in hand, we explored the generality of the developed protocol against a variety of *N*-substituted maleimides and 2-alkenylimidazoles (**Table 2.2**). As shown in **Table 2.2**, reaction of 2-alkenylimidazole (**1a**) with *N*-substituted maleimides (**13a-e**) produced corresponding annulated products **36aa-36ae** in moderate to very good (53-80%) yields. Unfortunately, maleimide with free N-H and *N*-arylmaleimides failed to produce the desired products under the standard conditions. The reaction of other 2-alkenylimidazoles (**1b-d**) with maleimides (**13a-c**) also delivered corresponding imidazo[1,2-*a*]pyrrolo[3,4-*e*]pyridine-1,3(2*H*)-diones (**36ba-36da**) in moderate to good (53-67%) yields.

Next, we extended the scope of this protocol to 2-aryl-1*H*-imidazoles. Initially, reaction of 2-phenyl-1*H*-indazole (**23a**) with **13a** produced phenylimidazo[2,1-*a*]pyrrolo[3,4-*c*]isoquinoline-5,7(6*H*)-dione (**37aa**) in low (21%) yield and thus the reaction conditions were re-optimized. To our satisfaction reaction of **23a** with **13a** in the presence of $[RuCl_2(p\text{-cymene})]_2$, $Cu(OAc)_2$, $AgSbF_6$, AcOH in DMA at 140 °C for 24 h produced **37aa** in 76% yield. This condition was similar to the conditions reported by Sun group for the annulation of maleimides with 2-arylbenzimidazoles. As summarized **in Table 2.2**, an array of 2-arylimidazoles (**23b-l**) having substituents such as Me, OMe, F, and Cl on the 2-phenyl ring reacted well with **13a** producing corresponding imidazo[2,1-*a*]pyrrolo[3,4-*c*]isoquinoline-5,7(6*H*)-dione derivatives (**37ba-la**) in moderate to very good (54-82%) yields. The reaction of 2-(naphthalen-1-yl)-1*H*-imidazole (**23m**) and 2-(thiophen-2-yl)-1*H*-imidazole (**23n**) with **13a** furnished the corresponding annulated products **37ma** and **37na** in 64% and 58% yields, respectively. Moreover, 2-phenyl-1*H*-benzo[*d*]imidazole (**23o**) also reacted smoothly with **13a** under the standard condition to deliver the corresponding annulated products **37oa** in 49% yield. The reaction of **23a** with other *N*-substituted maleimides (**13b-e**) successfully produced the corresponding annulated products **37ab-37ae** in moderate to good (49-67%) yields. The structure of all the products was ascertained by ^1H NMR, ^{13}C NMR and HRMS data.

High therapeutic potential and unique reactivity of the naphthoquinones make them attractive for the development of new type of compounds.[55] In recent years, benzoquinones and 1,4-naphthoquinones have emerged as competent coupling partners in transition metal-catalyzed C-H functionalization reactions,[56-60] but their reaction with 2-alkenyl-/2-aryl-imidazoles are rarely explored. Thus, we examined the annulation reaction of 1,4-napthoquinone (**38a**) with **23a** in the

presence of Ru-catalyst. A preliminary investigation, revealed that the reaction of **23a** and **38a** in the presence of $[RuCl_2(p\text{-cymene})]_2$, $Cu(OAc)_2$, $AgSbF_6$, AcOH in DMA at 140 °C for 4 h produced **39aa** in 73% yield. Similarly, annulation of other 2-arylimidazoles *viz* **23b**, **23e**, **23m**and **23n** with **38a** proceeded well producing desired annulated products **39ba**, **39ea**, **39ma** and **39na** in 74%, 55%, 58% and 61% yields, respectively. Moreover, reaction of **23a** with 1,4-benzoquinone (**27**) under standard conditions produced corresponding annulated product **39a** in 65% yield. To our satisfaction, **1b** also reacted smoothly with **38a** under optimal reaction conditions producing corresponding annulated product **40ba** in 64% yield after 6 h.

A few control experiments were performed to gain better insight into the mechanism of the oxidative annulation reaction. Initially, the reaction of **1a** or **13a** was performed under optimized reaction conditions in the presence of radical inhibitors TEMPO and BHT (**Scheme 2.12a**). Notably, no significant reduction in the yield of **36aa** was observed by the presence of TEMPO or BHT, revealing that the reaction does not follow the radical pathway. Next, competitive reaction between **23c** (*p*-OMe) and **23f** (*p*-CF_3) with **13a** and between **23g** (*m*-OMe) and **23g** (*m*-Cl) with **13a** under the optimized reaction conditions produced corresponding products **37ca** and **37fa** in the 1: 3 ratios and **37ga** and **37ha** in 1: 10 ratios, respectively, (**Scheme 2.12b**), suggested that the reaction might be proceeding through concerted metalation deprotonation (CMD)[61] pathway rather than Friedel-Crafts type electrophilic aromatic substitution. Exchange of C_1-proton of 2-alkenyl group of (*E*)-2-(1-phenylprop-1-en-2-yl)-1*H*-imidazole (**1a**) with deuterium (70%) when reacted with $[Ru(p\text{-cymene})Cl_2]_2$ without **13a** in the presence of D_2O under standard reaction conditions (**Scheme 2.12c**) indicated that the C-H bond cleavage is a reversible process. Further, a stoichiometric reaction of **1a** (1.0 equiv.) with $[Ru(p\text{-cymene})Cl_2]_2$ (0.5 equiv.) in MeOH at room temperature for 24 h under nitrogen atmosphere produced ruthenacycle **Ru-I** (**Scheme 2.12d**). Finally, formation of **36aa** in 64% yield from the reaction of **1a** and **13a** under optimal conditions using **Ru-I** (5 mol %) instead of $[RuCl_2(p\text{-cymene})]_2$ confirmed that **Ru-I** is an intermediate in this transformation.

a) Radical scavanger experiment

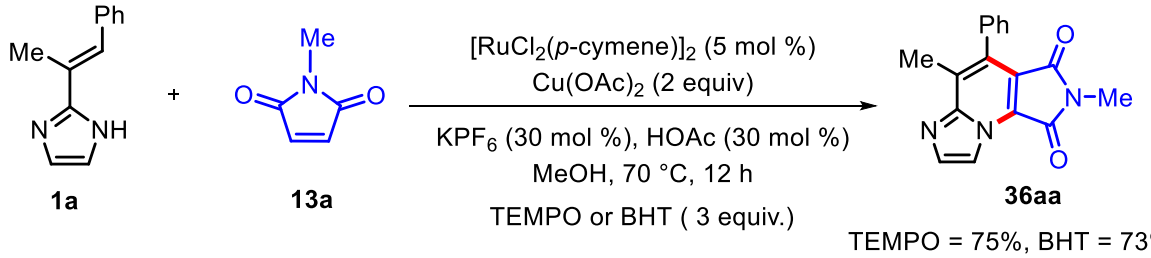

b) Competitive experiment

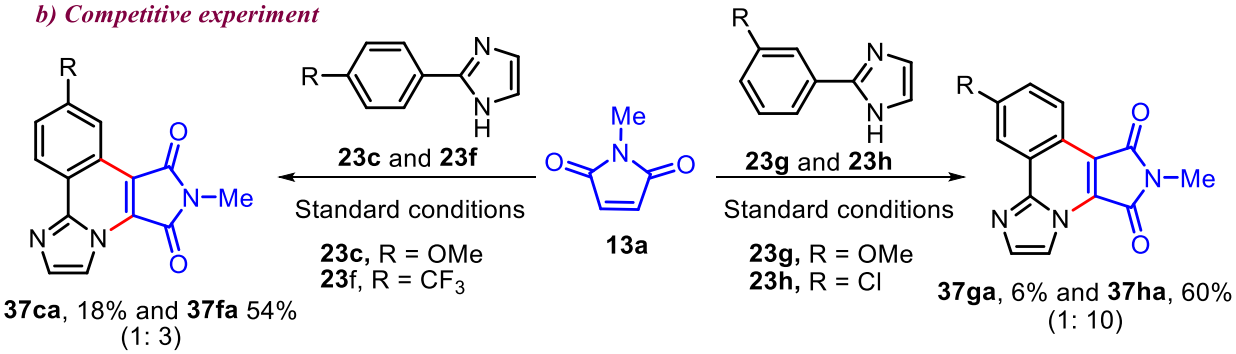

c) H/D exchange experiment

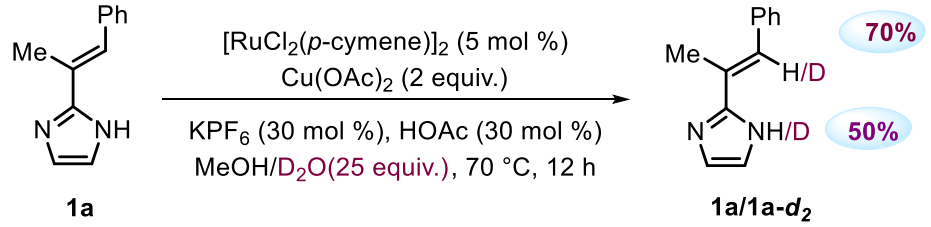

d) Ruthenium complex synthesis

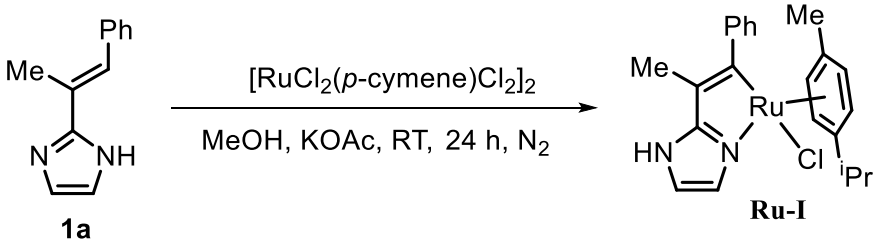

e) Standard reaction performed with Ru-I

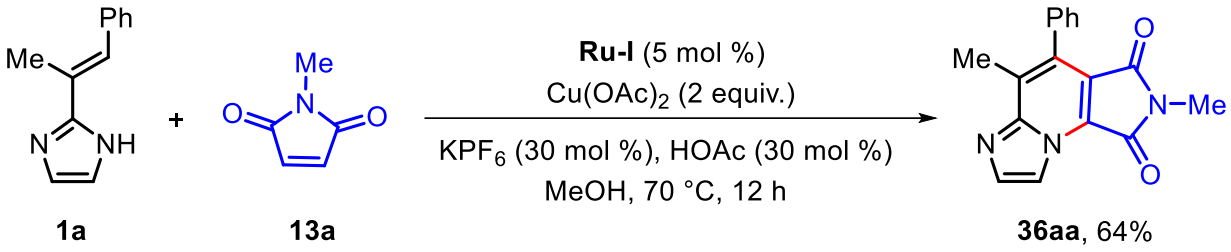

Scheme 2.12: Control experiments

To demonstrate the synthetic applicability of this protocol, a gram scale experiment was carried out. The reaction of **13a** with **1a** (5.43 mmol) and **23a** (6.94 mmol) under standard reaction conditions produced corresponding annulated products **36aa** and **37aa** in 1.0 g (63%) and 1.2 g (72%) yield, respectively **(Scheme 2.13a)**. Furthermore, partial reduction of **36aa** with sodium borohydride in methanol produced 3-hydroxy-2,5-dimethyl-4-phenyl-2,3-dihydro-1*H*-imidazo[1,2-*a*]pyrrolo[3,4-*e*]pyridin-1-one (**41**) in 72% yield **(Scheme 2.13b)**.

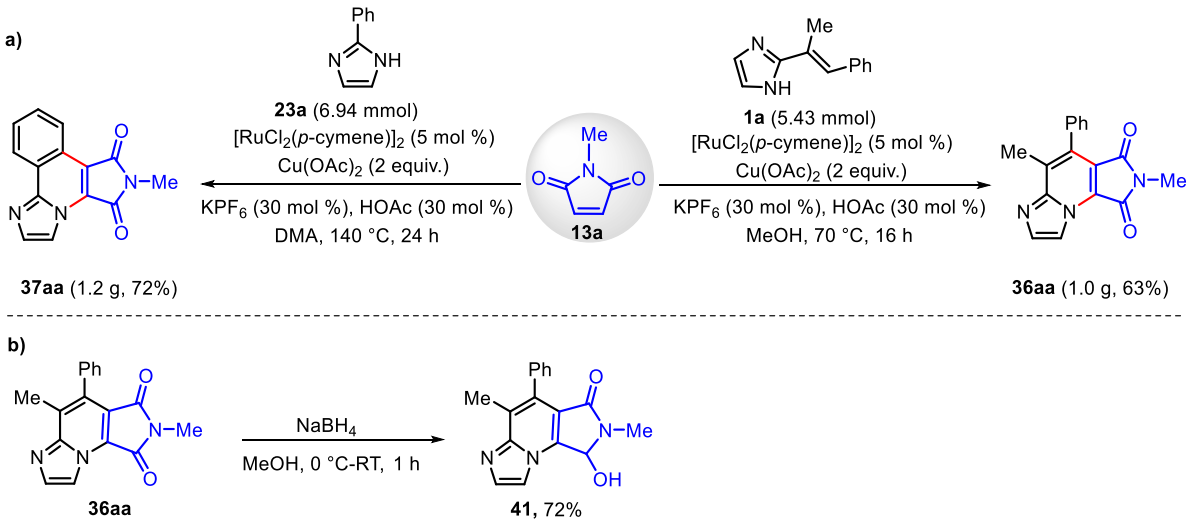

Scheme 2.13: Gram scale experiment and partial reduction of **34aa**

Based on previous reports[41, 62-66] and control experiments, a plausible reaction mechanism for the formation of annulated product is depicted in **Scheme 2.14**. Initially, in the presence of AcOH and KPF_6, the dimeric $[RuCl_2(p\text{-cymene})]_2$ is converted an active ruthenium complex **A**. The active ruthenium complex **A** reacts with **1** to form an intermediate **B**, which on subsequent reversible C-H bond activation forms the six-membered ruthenacycle intermediate **Ru-I**. Intermediate **Ru-I** further coordinates with maleimide **13** to afford intermediate **C**. Coordination of **13** prompts its migratory insertion into the Ru–C bond of **Ru-I** leading to formation of seven membered ruthenacycle intermediate **D**. Eventually, reductive elimination of **D** provides intermediate **E** and a ruthenium(0) species. Oxidation of intermediate **E** generates product **36** and oxidation of Ru(0)L species regenerates the catalytically active ruthenium(II) complex.

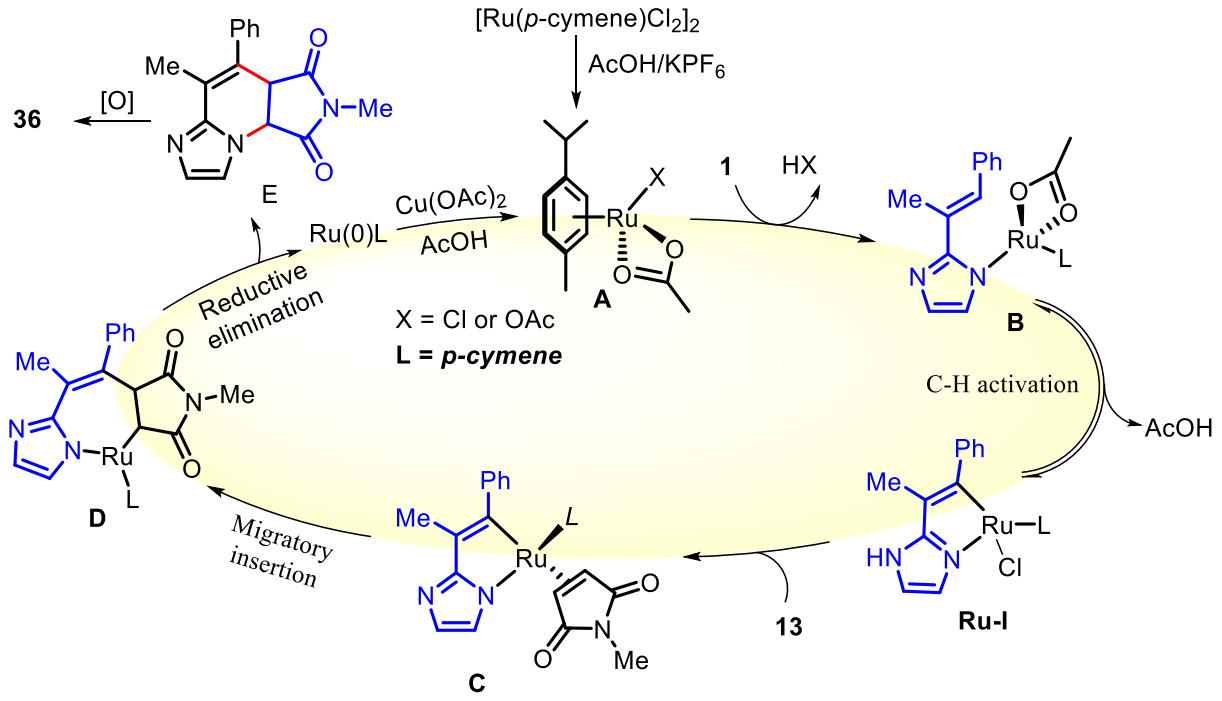

Scheme 2.14: Proposed Reaction Mechanism.

2.3 CONCLUSIONS

In summary, we have successfully developed a novel protocol for the synthesis of imidazo[1,2-*a*]pyrrolo[3,4-*e*]pyridines, imidazo[2,1-*a*]pyrrolo[3,4-*c*]isoquinolines and benzo[*g*]imidazo[1,2-*a*]quinoline-6,11-diones by the Ru(II)-catalyzed [4+2] C−H/N−H annulation of 2-alkenyl/2-aryl-imidazoles with maleimides and 1,4-naphthoquinones. The developed protocol is operationally simple, exhibits broad substrate scope for 2-alkenyl-/aryl-imidazoles, maleimides and 1,4-naphthoquinones with excellent functional group tolerance, provides annulated products in moderate to very good yields and is scalable. The mechanistic investigation revealed that the annulation reaction involves formation of C-C bond through Ru-catalyzed C(sp^2)-H bond activation followed intramolecular cyclization.

2.4 EXPERIMENTAL SECTION

2.4.1 General Information

2-Alkenylimidazoles and 2-arylimidazoles were synthesized by using a previously reported method.[22] *N*-substituted maleimides were prepared from the reaction of maleic anhydride with the corresponding primary amines using the reported procedure.[67] 1,4-Naphthoquinones, 1,4-

benzoquinone and all other chemicals and catalysts were commercially available and were used as received without further purification. Thin layer chromatography (TLC) was performed on Merck pre-coated TLC (silica gel 60 F254) plates. The products were purified by column chromatography over silica gel (100-200 mesh) using ethyl acetate/hexanes as eluent. Melting points were determined in open capillary tubes on an automated apparatus and were uncorrected. The ^{1}H NMR (400 MHz) and $^{13}C\{^{1}H\}$ NMR (100 MHz) spectra were recorded using $CDCl_3$ as the solvent on a Bruker Advance 400 spectrometer. The ^{1}H and $^{13}C\{^{1}H\}$ shifts were referenced at 7.26 ppm and 77.6 ppm for $CDCl_3$ respectively. Chemical shifts (δ) and coupling constants (J) are reported in parts per million (ppm) and hertz, respectively. The chemical multiplicities were reported as: singlet (s), doublet (d), triplet (t), quartet (q), quintet (quint), sextet (sext), septet (sept) and multiplet (m) and their combinations of them as well. HRMS data were acquired with an Agilent Q-TOF LC-MS spectrometer in positive mode using an electrospray ionization (ESI) ion source. Single crystal X-ray data was obtained using the Rigaku Oxford XtaLAB AFC12 (RINC): Kappa dual home/near diffractometer.

2.4.2 General Experimental Procedure for the Synthesis of 36.

A 10 mL pressure tube was charged with **1** (0.27 mmol, 1 equiv) and **13** (0.54 mmol, 2 equiv), $Cu(OAc)_2$ (98 mg, 0.54 mmol, 2.0 equiv), KPF_6 (15 mg, 0.08 mmol, 30 mol %), HOAc (5 μL, 30 mol %), $[RuCl_2(p\text{-cymene})]_2$ (7.7 mg, 0.013 mmol, 5.0 mol %) and methanol (2 mL). The reaction tube was capped tightly, and the resulting reaction mixture was stirred at 70 °C in an oil bath for 12 h. Upon completion of the reaction, the reaction mixture was cooled to ambient temperature and methanol was evaporated under reduced pressure. The resulting mixture was diluted with EtOAc (5 mL) and washed with water (2 × 5 mL). The ethyl acetate layer was dried over anhydrous Na_2SO_4, filtered, and evaporated to yield the crude product, which was purified by column chromatography on silica gel (100-200 mesh size) using EtOAc/hexanes as eluent to afford the desired annulated product **36**.

2,5-Dimethyl-4-phenyl-1*H*-imidazo[1,2-*a*]pyrrolo[3,4-*e*]pyridine-1,3(2*H*)-dione (36aa).

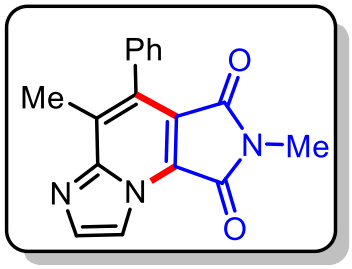

Purification by column chromatography on silica gel (eluent: EtOAc/hexanes, 1:3 *v/v*); Yellow solid; 63 mg (80%); mp = 233-235 °C; ^{1}H NMR (400 MHz, $CDCl_3$) δ 8.46 (d, *J* = 0.9 Hz, 1H), 7.95 (d, *J* = 0.8 Hz, 1H), 7.54 – 7.50 (m, 3H), 7.33 – 7.30 (m, 2H), 3.13 (s, 3H), 2.59 (s, 3H); ^{13}C{^{1}H} NMR (100 MHz, $CDCl_3$) δ 166.4, 163.7, 147.7, 137.6, 133.9, 131.83, 131.78, 129.4, 128.5, 128.3, 127.1, 118.2, 112.5, 23.8, 15.1; HRMS (ESI) *m/z*: $[M + H]^+$ Calcd for $C_{17}H_{14}N_3O_2^+$ 292.1081; Found 292.1071.

5-Methyl-4-phenyl-2-propyl-1*H*-imidazo[1,2-*a*]pyrrolo[3,4-*e*]pyridine-1,3(2*H*)-dione (36ab).

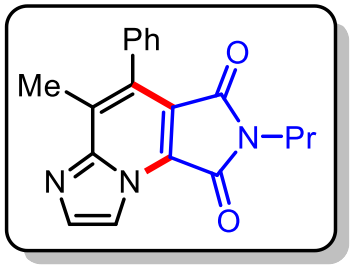

Purification by column chromatography on silica gel (eluent: EtOAc/hexanes, 1:3 *v/v*); Yellow solid; 57 mg (66%); mp = 203-205 °C; ^{1}H NMR (400 MHz, $CDCl_3$) δ 8.47 (s, 1H), 7.96 (s, 1H), 7.55 – 7.50 (m, 3H), 7.33 – 7.32 (m, 2H), 3.60 (t, *J* = 7.26 Hz, 2H), 2.59 (s, 3H), 1.72 – 1.66 (m, 2H), 0.94 (t, *J* = 7.4 Hz, 3H); ^{13}C{^{1}H} NMR (100 MHz, $CDCl_3$) δ 166.4, 163.8, 137.5, 133.9, 133.4, 131.9, 131.7, 129.5, 128.4, 128.2, 118.0, 112.4, 39.7, 21.9, 15.0, 11.3; HRMS (ESI) *m/z*: $[M + H]^+$ Calcd for $C_{19}H_{18}N_3O_2^+$ 320.1394; Found 320.1386.

2-Benzyl-5-methyl-4-phenyl-1*H*-imidazo[1,2-*a*]pyrrolo[3,4-*e*]pyridine-1,3(2*H*)-dione (36ac).

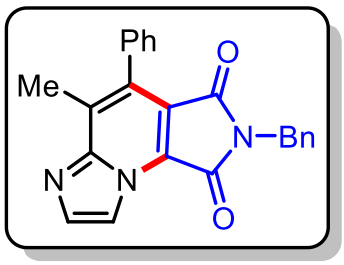

Purification by column chromatography on silica gel (eluent: EtOAc/hexanes, 4:6 *v/v*); Yellow solid; 59 mg (60%); mp =180-182 °C; ^{1}H NMR (400 MHz, $CDCl_3$) δ 8.45 (s, 1H), 7.93 (s, 1H), 7.54 – 7.48 (m, 3H), 7.42 – 7.38 (m, 2H), 7.33 – 7.27 (m, 5H), 4.77 (s, 2H), 2.57 (s, 3H); ^{13}C{^{1}H} NMR (100 MHz, $CDCl_3$) δ 166.0, 163.4, 147.7, 137.6, 136.0, 133.8, 132.0, 131.9, 129.5, 128.7, 128.5, 128.3, 128.0, 127.0, 118.1, 112.5, 41.7, 15.1; HRMS (ESI) *m/z*: $[M + H]^+$ Calcd for $C_{23}H_{18}N_3O_2^+$ 368.1394; Found 368.1402.

2-Ethyl-5-methyl-4-phenyl-1*H*-imidazo[1,2-*a*]pyrrolo[3,4-*e*]pyridine-1,3(2*H*)-dione (36ad).

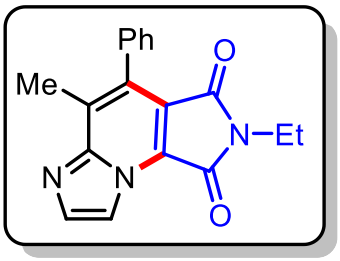

Purification by column chromatography on silica gel (eluent: EtOAc/hexanes, 1:3 *v/v*); Yellow solid; 57 mg (70%); mp = 184-186 °C; ^{1}H NMR (400 MHz, $CDCl_3$) δ 8.47 (s, 1H), 7.96 (s, 1H), 7.55 – 7.49 (m, 3H), 7.33 (dd, *J* = 7.6, 1.8 Hz, 2H), 3.69 (q, *J* = 7.2 Hz, 2H), 2.59 (s, 3H), 1.27 (t, *J* = 7.2 Hz, 3H); ^{13}C{^{1}H} NMR (100 MHz, $CDCl_3$) δ 166.2, 163.5, 147.8, 137.5, 133.9, 131.8, 131.7, 129.5, 128.4, 128.3, 127.1, 118.1, 112.4, 33.0, 15.1, 14.0; HRMS (ESI) *m/z*: $[M + H]^+$ Calcd for $C_{18}H_{16}N_3O_2^+$ 306.1237; Found 306.1230.

2-Cyclohexyl-5-methyl-4-phenyl-1*H*-imidazo[1,2-*a*]pyrrolo[3,4-*e*]pyridine-1,3(2*H*)-dione (36ae).

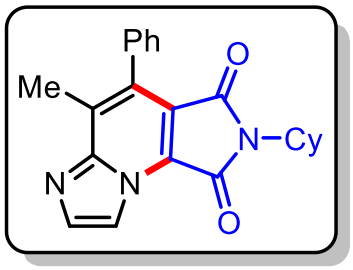

Purification by column chromatography on silica gel (eluent: EtOAc/hexanes, 1:4 *v/v*); Yellow solid; 50 mg (53%); mp = 196-198 °C; ^{1}H NMR (400 MHz, $CDCl_3$) δ 8.45 (s, 1H), 7.93 (s, 1H), 7.54 – 7.46 (m, 3H), 7.33 – 7.29 (m, 2H), 4.06 – 3.96 (m, 1H), 2.56 (s, 3H), 2.18 – 2.05 (m, 2H), 1.87 – 1.80 (m, 2H), 1.76 – 1.69 (m, 2H), 1.36 – 1.29 (m, 2H), 1.26 – 1.18 (m, 2H); ^{13}C{^{1}H} NMR (100 MHz, $CDCl_3$) δ 166.4, 163.7, 147.8, 137.4, 134.0, 131.8, 131.6, 129.4, 128.4, 128.2, 126.9, 117.7, 112.3, 51.1, 30.1, 26.0, 25.0, 15.0; HRMS (ESI) *m/z*: $[M + H]^+$ Calcd for $C_{22}H_{22}N_3O_2^+$ 360.1707; Found 360.1712.

2,5-Dimethyl-4,7-diphenyl-1*H*-imidazo[1,2-*a*]pyrrolo[3,4-*e*]pyridine-1,3(2*H*)-dione (36ba).

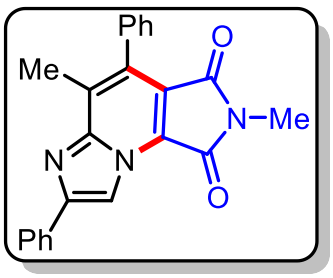

Purification by column chromatography on silica gel (eluent: EtOAc/hexanes, 2:3 *v/v*); Yellow solid; 44 mg (63%); mp =190-192 °C; ^{1}H NMR (400 MHz, $CDCl_3$) δ 8.74 (s, 1H), 8.14 – 8.10 (m, 2H), 7.54 – 7.50 (m, 5H), 7.45 – 7.41 (m, 1H), 7.34 (dd, *J* = 7.5, 1.8 Hz, 2H), 3.15 (s, 3H), 2.64 (s, 3H); ^{13}C{^{1}H} NMR (100 MHz, $CDCl_3$) δ 166.5, 163.8, 150.3, 148.1, 134.1, 133.0, 132.0, 131.3, 129.4, 128.93, 128.91, 128.4, 128.3, 126.6, 126.5, 117.9, 108.0, 23.8, 15.1; HRMS (ESI) *m/z*: $[M + H]^+$ Calcd for $C_{23}H_{18}N_3O_2^+$ 368.1394; Found 368.1401.

5-Methyl-4,7-diphenyl-2-propyl-1*H*-imidazo[1,2-*a*]pyrrolo[3,4-*e*]pyridine-1,3(2*H*)-dione

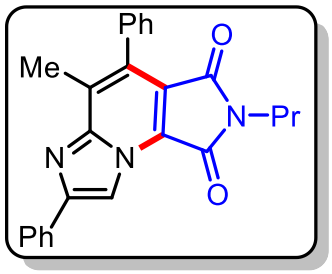

(36bb). Purification by column chromatography on silica gel (eluent: EtOAc/hexanes, 3:7 *v/v*); Yellow solid; 46 mg (60%); mp = 188-190 °C; ^{1}H NMR (400 MHz, $CDCl_3$) δ 8.74 (s, 1H), 8.11 (d, *J* = 7.3 Hz, 2H), 7.56 – 7.49 (m, 5H), 7.42 (t, *J* = 7.4 Hz, 1H), 7.36 – 7.34 (m, 2H), 3.61 (t, *J* = 7.3 Hz, 2H), 2.64 (s, 3H), 1.71 – 1.66 (m, 2H), 0.96 (t, *J* = 7.4 Hz, 3H); ^{13}C{^{1}H} NMR (100 MHz, $CDCl_3$) δ 166.5, 163.9, 150.2, 148.1, 134.1, 133.0, 132.0, 131.2, 129.5, 128.9, 128.4, 128.2, 126.6, 126.4, 117.6, 108.0, 39.7, 22.0, 15.1, 11.3; HRMS (ESI) *m/z* Calcd for $C_{25}H_{22}N_3O_2^+$ $[M+H]^+$ 396.1707; Found 396.1713.

2-Benzyl-5-methyl-4,7-diphenyl-1*H*-imidazo[1,2-*a*]pyrrolo[3,4-*e*]pyridine-1,3(2*H*)-dione

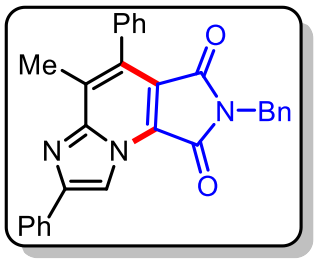

(36bc). Purification by column chromatography on silica gel (eluent: EtOAc/hexanes, 2:3 *v/v*); Yellow solid; 56 mg (66%); mp =202-204 °C; ^{1}H NMR (400 MHz, $CDCl_3$) δ 8.74 (s, 1H), 8.11 – 8.08 (m, 2H), 7.53 – 7.48 (m, 5H), 7.44 – 7.40 (m, 3H), 7.36 – 7.29 (m, 5H), 4.80 (s, 2H), 2.63 (s, 3H); ^{13}C{^{1}H} NMR (100 MHz, $CDCl_3$)δ 166.0, 163.6, 150.3, 148.1, 136.1, 134.0, 133.0, 132.1, 131.5, 129.5, 128.94, 128.91, 128.8, 128.7, 128.4, 128.3, 128.0, 126.6, 117.7, 108.0, 41.7, 15.1; HRMS (ESI) *m/z*: $[M + H]^+$ Calcd for $C_{29}H_{22}N_3O_2^+$ 444.1712; Found 444.1720.

2-Methyl-4-phenyl-1*H*-imidazo[1,2-*a*]pyrrolo[3,4-*e*]pyridine-1,3(2*H*)-dione (36ca).

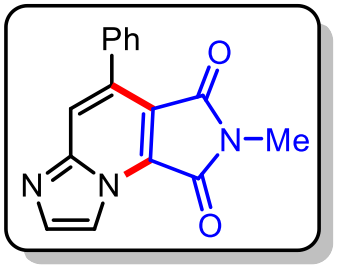

Purification by column chromatography on silica gel (eluent: EtOAc/hexanes, 2:3 *v/v*); Yellow solid; 49 mg (60%); mp = 237-239 °C; ^{1}H NMR (400 MHz, $CDCl_3$) δ 8.51 (s, 1H), 8.00 (s, 1H), 7.90 (s, 1H), 7.63 – 7.60 (m, 2H), 7.53 – 7.50 (m, 3H), 3.21 (s, 3H); ^{13}C{^{1}H} NMR (100 MHz, $CDCl_3$) δ 166.2, 163.5, 138.9, 134.7, 130.1, 129.2, 129.1, 128.3, 122.0, 116.8, 112.0, 24.0; HRMS (ESI) *m/z*: $[M + H]^+$ Calcd for $C_{16}H_{12}N_3O_2^+$ 278.0924; Found 278.0920.

4-Phenyl-2-propyl-1*H*-imidazo[1,2-*a*]pyrrolo[3,4-*e*]pyridine-1,3(2*H*)-dione (36cb).

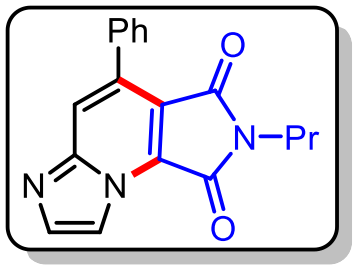

Purification by column chromatography on silica gel (eluent: EtOAc/hexanes, 1:3 *v/v*); Yellow solid; 60 mg (67%); mp = 196-198 °C; ^{1}H NMR (400 MHz, $CDCl_3$) δ 8.50 (s, 1H), 7.98 (s, 1H), 7.89 (s, 1H), 7.63 (dd, *J* = 7.4, 2.2 Hz, 1H), 7.55 – 7.50 (m, 3H), 3.67 (t, *J* = 7.2 Hz, 2H), 1.74 (m, 2H), 0.98 (t, *J* = 7.4 Hz, 3H); ^{13}C{^{1}H} NMR (100 MHz, $CDCl_3$) δ 166.2, 163.5, 138.8, 134.8, 130.0, 129.2, 129.0, 128.3, 122.0, 116.6, 111.9, 39.9, 21.9, 11.3; HRMS (ESI) *m/z*: $[M + H]^+$ Calcd for $C_{18}H_{16}N_3O_2^+$ 306.1237; Found 306.1229.

2-Benzyl-4-phenyl-1*H*-imidazo[1,2-*a*]pyrrolo[3,4-*e*]pyridine-1,3(2*H*)-dione (36cc).

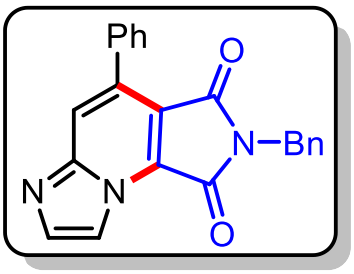

Purification by column chromatography on silica gel (eluent: EtOAc/hexanes, 2:3 *v/v*); Yellow solid; 65 mg (63%); mp = 231-233 °C; ^{1}H NMR (400 MHz, $CDCl_3$) δ 8.49 (s, 1H), 7.98 (s, 1H), 7.89 (s, 1H), 7.63 (d, *J* = 2.4 Hz, 1H), 7.61 (d, *J* = 1.6 Hz, 1H), 7.52 – 7.51 (m, 2H), 7.46 – 7.44 (m, 2H), 7.36 – 7.29 (m, 4H), 4.86 (s, 2H); ^{13}C{^{1}H} NMR (100 MHz, $CDCl_3$) δ 165.5, 162.9, 147.2, 138.6, 135.5, 134.5, 134.4, 129.7, 129.0, 128.8, 128.5, 128.5, 128.1, 127.8, 121.9, 116.4, 41.6; HRMS (ESI) *m/z*: $[M + H]^+$ Calcd for $C_{22}H_{16}N_3O_2^+$ 354.1237; Found 354.1230.

2,5-Dimethyl-1*H*-imidazo[1,2-*a*]pyrrolo[3,4-*e*]pyridine-1,3(2*H*)-dione (36da). Purification by column chromatography on silica gel (eluent: EtOAc/hexanes, 2:3 *v/v*); Yellow solid; 53 mg (53%); mp =142-144 °C; ^{1}H NMR (400 MHz, $CDCl_3$) δ 8.38 (d, *J* = 1.1 Hz, 1H), 7.90 (d, *J* = 1.2 Hz, 1H), 7.40 (d, d, *J* = 1.0 Hz, 1H), 3.20 (s, 3H), 2.78 (d, *J* = 0.9 Hz, 3H); ^{13}C{^{1}H}NMR (100 MHz, $CDCl_3$) δ 167.0, 163.8, 147.6, 137.1, 134.1, 127.5, 120.3, 115.7, 112.6, 24.0, 18.1; HRMS (ESI) *m/z*: $[M + H]^+$ Calcd for $C_{11}H_{10}N_3O_2^+$ 216.0768; Found 216.0769.

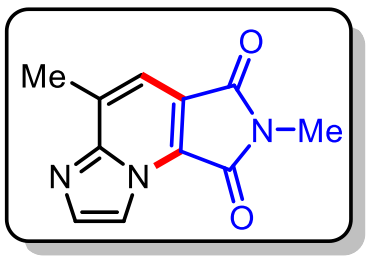

2.4.3 General Procedure for the Synthesis of 37.

A 10 mL pressure tube was charged with 2-arylimidazole **23** (0.34 mmol, 1 equiv), maleimide **13** (0.68 mmol, 2 equiv), $Cu(OAc)_2$ (123 mg, 0.68 mmol, 2 equiv), KPF_6 (19 mg, 0.1 mmol, 30 mol

%), HOAc (6 µL, 0.1 mmol, 30 mol %), $[RuCl_2(p\text{-cymene})]_2$ (10.5 mg, 0.017 mmol, 5.0 mol %) and DMA (2 mL). The resulting reaction mixture was stirred at 140 °C in an oil bath for 24 h. Upon completion of the reaction, the reaction mixture was cooled to ambient temperature and diluted with ice cold water (5 mL) and extracted with ethyl acetate (3 × 5 mL). The combined organic layer was dried over anhydrous Na_2SO_4, filtered, and evaporated to yield the crude product, which was purified by column chromatography on silica gel (100-200 mesh size) using EtOAc/hexanes as eluent to afford the desired annulated product **37**.

6-Methyl-5*H*-imidazo[2,1-*a*]pyrrolo[3,4-*c*]isoquinoline-5,7(6*H*)-dione (37aa). Purification by column chromatography on silica gel (eluent: EtOAc/hexanes, 1:3 *v/v*); Yellow solid; 66 mg (76%); mp =196-198 °C; ^{1}H NMR (400 MHz, $CDCl_3$) δ 8.72 – 8.62 (m, 2H), 8.35 (d, J = 1.4 Hz, 1H), 7.83 – 7.69 (m, 3H), 3.24 (s, 3H); $^{13}C\{^1H\}$ NMR (100 MHz, $CDCl_3$) δ 167.6, 164.0, 144.9, 134.5, 130.7, 129.7, 128.7, 125.3, 124.9, 124.2, 123.0, 115.8, 113.0, 23.9; HRMS (ESI) *m/z*: $[M + H]^+$ Calcd for $C_{14}H_{10}N_3O_2^+$ 252.0768; Found 252.0763.

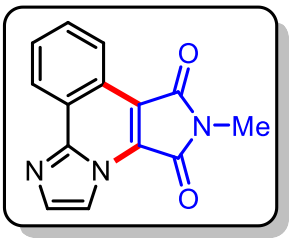

6,9-Dimethyl-5*H*-imidazo[2,1-*a*]pyrrolo[3,4-*c*]isoquinoline-5,7(6*H*)-dione (37ba). Purification by column chromatography on silica gel (eluent: EtOAc/hexanes, 1:3 *v/v*); Yellow solid; 45 mg (54%); mp =211-213 °C; ^{1}H NMR (400 MHz, $CDCl_3$) δ 8.56 (d, J = 8.3 Hz, 1H), 8.42 (s, 1H), 8.32 (d, J = 1.4 Hz, 1H), 7.76 (d, J = 1.4 Hz, 1H), 7.60 (dd, J = 8.4, 1.8 Hz, 1H), 3.24 (s, 3H), 2.59 (s, 3H); $^{13}C\{^1H\}$ NMR (100 MHz, $CDCl_3$) δ 167.8, 164.1, 145.1, 140.4, 134.4, 132.4, 128.7, 124.4, 124.0, 123.2, 123.1, 115.5, 112.7, 23.9, 21.9; HRMS (ESI) *m/z*: $[M + H]^+$ Calcd for $C_{15}H_{12}N_3O_2^+$ 266.0930; Found 266.0922.

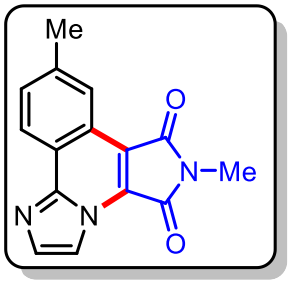

9-Methoxy-6-methyl-5*H*-imidazo[2,1-*a*]pyrrolo[3,4-*c*]isoquinoline-5,7(6*H*)-dione (37ca). Purification by column chromatography on silica gel (eluent: EtOAc/hexanes, 1:3 *v/v*); Yellow solid; 48 mg (60%); mp =206-208 °C; ^{1}H NMR (400 MHz, $CDCl_3$) δ 8.62 (d, J = 9.0 Hz, 1H), 8.33 (d, J = 1.2 Hz, 1H), 8.08 (d, J = 2.6 Hz, 1H), 7.77 (s, 1H), 7.39 (dd, J = 8.9, 2.6 Hz, 1H), 4.02 (s, 3H), 3.25 (s, 3H); $^{13}C\{^1H\}$ NMR (100 MHz, $CDCl_3$) δ 168.0, 164.1, 160.9, 142.5, 134.5, 129.1, 125.9, 124.9, 121.2, 119.6, 115.1, 112.4, 105.1, 55.7, 23.9; HRMS (ESI) *m/z*: $[M + H]^+$ Calcd for $C_{15}H_{12}N_3O_3^+$ 282.0873; Found 282.0877.

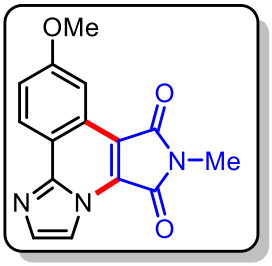

9-Fluoro-6-methyl-5*H*-imidazo[2,1-*a*]pyrrolo[3,4-*c*]isoquinoline-5,7(6*H*)-dione (37da).

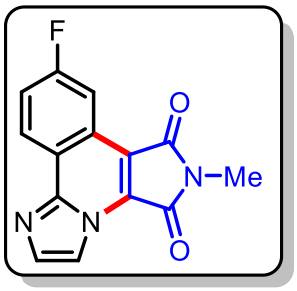

Purification by column chromatography on silica gel (eluent: EtOAc/hexanes, 1:3 *v/v*); Yellow solid; 69 mg (83%); mp =246-248 °C; ^{1}H NMR (400 MHz, $CDCl_3$) δ 8.76 – 8.73 (m, 1H), 8.39 (s, 1H), 8.36 (d, J = 2.6 Hz, 1H), 7.81 (s, 1H), 7.57 – 7.54 (m, 1H), 3.27 (s, 3H); ^{13}C{^{1}H} NMR (100 MHz, $CDCl_3$) δ 167.4, 163.8, 163.2 (d, $J_{C\text{-}F}$ = 250 Hz), 134.7, 129.8, 126.9 (d, $J_{C\text{-}F}$ = 9.2 Hz), 124.7, 124.6, 122.0, 119.7 (d, $J_{C\text{-}F}$ = 23.9 Hz), 113.0, 110.4 (d, $J_{C\text{-}F}$ = 31.7 Hz), 24.0; HRMS (ESI) *m/z*: $[M + H]^+$ Calcd for $C_{14}H_9FN_3O_2^+$ 270.0673; Found 270.0668.

9-Chloro-6-methyl-5*H*-imidazo[2,1-*a*]pyrrolo[3,4-*c*]isoquinoline-5,7(6*H*)-dione (37ea).

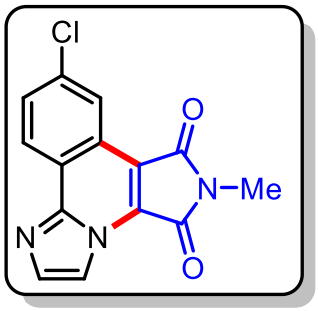

Purification by column chromatography on silica gel (eluent: EtOAc/hexanes, 1:3 *v/v*); Yellow solid; 63 mg (78%); mp =225-227 °C; ^{1}H NMR (400 MHz, $CDCl_3$) δ 8.65 (d, J = 2.2 Hz, 1H), 8.62 (d, J = 8.7 Hz, 1H), 8.37 (d, J = 1.4 Hz, 1H), 7.80 (d, J = 1.3 Hz, 1H), 7.73 (dd, J = 8.7, 2.1 Hz, 1H), 3.26 (s, 3H); ^{13}C{^{1}H}NMR (100 MHz, $CDCl_3$) δ 167.2, 163.7, 144.5, 136.3, 134.9, 131.2, 129.6, 125.7, 124.2, 123.9, 123.5, 114.6, 113.2, 24.1; HRMS (ESI) *m/z*: $[M + H]^+$ Calcd for $C_{14}H_9ClN_3O_2^+$ 286.0378; Found 286.0369.

6-Methyl-9-(trifluoromethyl)-5*H*-imidazo[2,1-*a*]pyrrolo[3,4-*c*]isoquinoline-5,7(6*H*)-dione

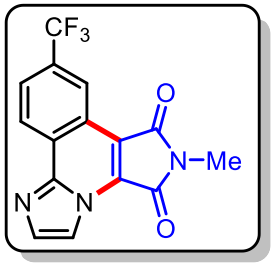

(**37fa**). Purification by column chromatography on silica gel (eluent: EtOAc/hexanes, 1:4 *v/v*); Yellow solid; 51 mg (68mp = 230-232 °C; ^{1}H NMR (400 MHz, $CDCl_3$) δ 8.97 (s, 1H), 8.82 (d, J = 8.6 Hz, 1H), 8.43 (d, J = 1.3 Hz, 1H), 8.01 – 7.97 (m, 1H), 7.87 (d, J = 1.3 Hz, 1H), 3.28 (s, 3H); ^{13}C{^{1}H} NMR (100 MHz, $CDCl_3$) 167.1, 163.6, 144.0, 135.3, 131.6 (q, $J_{C\text{-}F}$ = 33.0 Hz), 129.9, 127.1, 126.7 (q, $J_{C\text{-}F}$ = 3.3 Hz), 125.1, 123.6 (q, $J_{C\text{-}F}$ = 271.2 Hz), 122.6, 122.4 (q, $J_{C\text{-}F}$ = 4.2 Hz), 115.3, 113.8, 24.1; HRMS (ESI) *m/z*: $[M + H]^+$ Calcd for $C_{15}H_9F_3N_3O_2^+$ 320.0641; Found 320.0648.

10-Methoxy-6-methyl-5*H*-imidazo[2,1-*a*]pyrrolo[3,4-*c*]isoquinoline-5,7(6*H*)-dione (37ga).

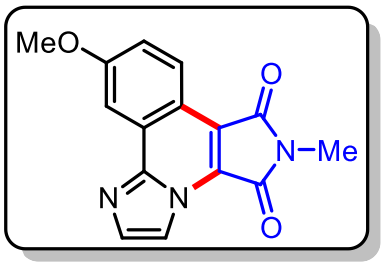

Purification by column chromatography on silica gel (eluent: EtOAc/hexanes, 3:7 *v/v*); Yellow solid; 51 mg (64%); mp =186-188 °C; ^{1}H NMR (400 MHz, $CDCl_3$) δ 8.62 (d, *J* = 8.9 Hz, 1H), 8.38 (s, 1H), 8.10 (s, 1H), 7.80 (s, 1H), 7.34 (dd, *J* = 6.8, 2.0 Hz, 1H), 4.06 (s, 3H), 3.24 (s, 3H); ^{13}C{^{1}H} NMR (100 MHz, $CDCl_3$) δ 167.9, 164.3, 161.7, 134.2, 127.5, 126.7, 120.8, 117.2, 116.6, 113.3, 104.5, 55.9, 23.9; HRMS (ESI) *m/z* Calcd for $C_{15}H_{12}N_3O_3^+$ 282.0873; Found 282.0879.

10-Chloro-6-methyl-5*H*-imidazo[2,1-*a*]pyrrolo[3,4-*c*]isoquinoline-5,7(6H)-dione (37ha).

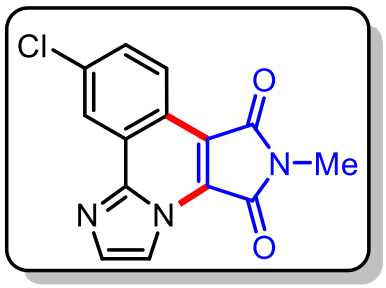

Purification by column chromatography on silica gel (eluent: EtOAc/hexanes, 3:7 *v/v*); Yellow solid; 56 mg (70%); mp = 192-194 °C; ^{1}H NMR (400 MHz, $CDCl_3$) δ 8.76 (t, *J* = 7.0 Hz, 2H), 8.42 (s, 1H), 7.85 – 7.76 (m, 2H), 3.27 (s, 3H); ^{13}C{^{1}H} NMR (100 MHz, $CDCl_3$) δ 167.8, 164.2, 134.5, 134.1, 130.8, 129.8, 125.4, 125.0, 124.3, 123.2, 116.0, 113.1, 24.0; HRMS (ESI) *m/z*: $[M + H]^+$ Calcd for $C_{14}H_9ClN_3O_2^+$ 286.0378; Found 286.0367.

9,10-Dimethoxy-6-methyl-5*H*-imidazo[2,1-*a*]pyrrolo[3,4-*c*]isoquinoline-5,7(6*H*)-dione

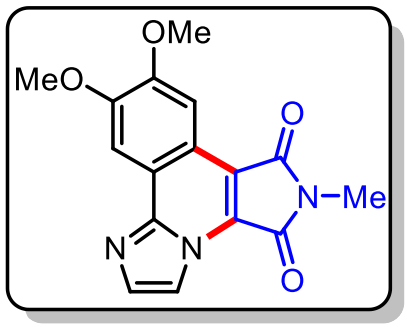

(37ia). Purification by column chromatography on silica gel (eluent: EtOAc/hexanes, 3:7 *v/v*); Yellow solid; 43mg (56%); mp =213-215 °C; ^{1}H NMR (400 MHz, $CDCl_3$) δ 8.33 (s, 1H), 8.04 (s, 2H), 7.76 (s, 1H), 4.13 (s, 3H), 4.10 (s, 3H), 3.24 (s, 3H); ^{13}C{^{1}H} NMR (100 MHz, $CDCl_3$) δ 168.2, 164.2, 152.6, 151.9, 144.6, 134.2, 126.4, 120.9, 118.1, 115.7, 112.6, 104.5, 104.4, 56.5, 56.3, 23.8; HRMS (ESI) *m/z*: $[M + H]^+$ Calcd for $C_{16}H_{14}N_3O_4^+$ 312.0979; Found 312.0982.

8,9,10-Trimethoxy-6-methyl-5*H*-imidazo[2,1-*a*]pyrrolo[3,4-*c*]isoquinoline-5,7(6*H*)-dione

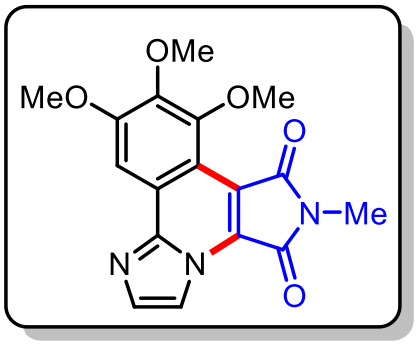

(37ja). Purification by column chromatography on silica gel (eluent: EtOAc/hexanes, 1:3 *v/v*); Yellow solid; 40 mg (59%); mp = 203-205 °C; ^{1}H NMR (400 MHz, $CDCl_3$) δ 8.50 (s, 1H), 8.04 (s, 1H), 7.77 (s, 1H), 4.14 (s, 3H), 4.13 (s, 3H), 4.03 (s, 3H), 3.26 (s, 3H); ^{13}C{^{1}H} NMR (100 MHz, $CDCl_3$) δ 165.2, 163.9, 156.6, 150.4, 144.8, 144.3, 134.3, 128.1, 122.7, 116.4, 113.9, 113.2, 101.4, 62.1, 61.1, 56.5, 24.2; HRMS (ESI) *m/z*: $[M + H]^+$ Calcd for $C_{17}H_{16}N_3O_5^+$ 342.1084; Found 342.1086.

9-Methoxy-6-methyl-2,3-diphenyl-5*H*-imidazo[2,1-*a*]pyrrolo[3,4-*c*]isoquinoline-5,7(6*H*)-dione (37ka). Purification by column chromatography on silica gel (eluent: EtOAc/hexanes, 1:3 *v/v*); Off-white solid; 41 mg (62%); mp = 214-216 °C; ^{1}H NMR (400 MHz, $CDCl_3$) δ 8.72 (d, *J* = 7.6 Hz, 1H), 8.05 (d, *J* = 8.0 Hz, 1H), 7.76 (d, *J* = 6.9 Hz, 2H), 7.61 (d, *J* = 8.6 Hz, 2H), 7.62 – 7.49 (m, 4H), 7.45 – 7.41 (m, 1H), 7.03 (d, *J* = 8.6 Hz, 2H), 3.92 (s, 3H), 3.09 (s, 3H); ^{13}C{^{1}H} NMR (100 MHz, $CDCl_3$) δ 167.9, 162.1, 160.9, 144.9, 143.3, 133.7, 131.7, 131.5, 130.1, 129.3, 128.3, 128.2, 128.1, 127.7, 126.2, 124.7, 123.9, 121.5, 119.7, 117.2, 104.8, 55.7, 23.9; HRMS (ESI) *m/z* Calcd for $C_{27}H_{20}N_3O_3^+$ $[M+H]^+$ 434.1505; Found 434.1498.

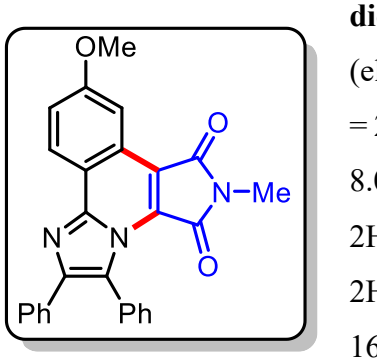

8,9,10-Trimethoxy-6-methyl-2,3-diphenyl-5*H*-imidazo[2,1-*a*]pyrrolo[3,4-*c*]isoquinoline-5,7(6*H*)-dione (37la). Purification by column chromatography on silica gel (eluent: EtOAc/hexanes, 1:3 *v/v*); Yellow solid; 67 mg (64%); mp = 182-184 °C; ^{1}H NMR (400 MHz, $CDCl_3$) δ 8.21 (s, 1H), 7.62 – 7.60 (m, 2H), 7.57 – 7.55 (m, 1H), 7.53 – 7.49 (m, 2H), 7.46 – 7.43 (m, 2H), 7.32 – 7.26 (m, 3H), 4.18 (s, 3H), 4.17 (s, 3H), 4.03 (s, 3H), 3.04 (s, 3H); ^{13}C{^{1}H} NMR (100 MHz, $CDCl_3$) δ 165.1, 161.9, 156.7, 150.4, 144.9, 144.3, 143.8, 133.7, 131.8, 131.2, 129.2, 129.0, 128.4, 128.3, 128.2, 127.7, 124.8, 123.3, 119.1, 113.4, 101.6, 62.1, 61.1, 56.6, 24.3; HRMS (ESI) *m/z*: $[M + H]^+$ Calcd for $C_{29}H_{24}N_3O_5^+$ 494.1710; Found 494.1739.

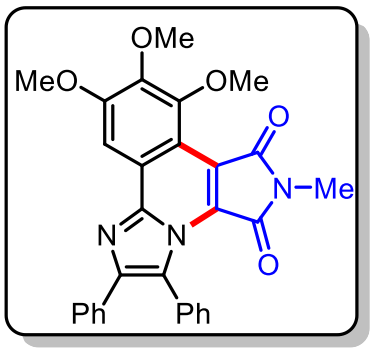

2-Methyl-1*H*-benzo[*h*]imidazo[2,1-*a*]pyrrolo[3,4-*c*]isoquinoline-1,3(2*H*)-dione (37ma).

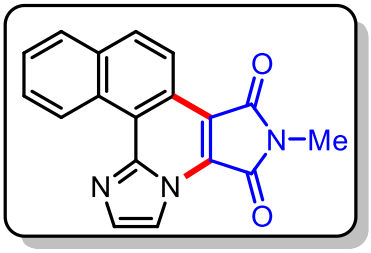

Purification by column chromatography on silica gel (eluent: EtOAc/hexanes, 1:3 *v/v*); Yellow solid; 49 mg (64%); mp = 190-192 °C; ^{1}H NMR (400 MHz, $CDCl_3$) δ 10.57 (d, *J* = 7.9 Hz, 1H), 8.63 (d, *J* = 7.9 Hz, 1H), 8.41 (s, 1H), 8.03 – 7.87 (m, 3H), 7.86 – 7.75 (m, 1H), 7.73 – 7.63 (m, 1H), 3.16 (s, 3H); ^{13}C{^{1}H} NMR (100 MHz, $CDCl_3$) δ 167.8, 163.8, 145.0, 135.3, 133.7, 131.0, 128.95, 128.89, 128.6, 128.4, 128.3, 123.1, 121.8, 120.9, 115.5, 112.1, 24.0; HRMS (ESI) *m/z*: $[M + H]^+$ Calcd for $C_{18}H_{12}N_3O_2^+$ 302.0924; Found 302.0929.

6-Methyl-5*H*-imidazo[1,2-*a*]pyrrolo[3,4-*e*]thieno[2,3-*c*]pyridine-5,7(6*H*)-dione (37na).

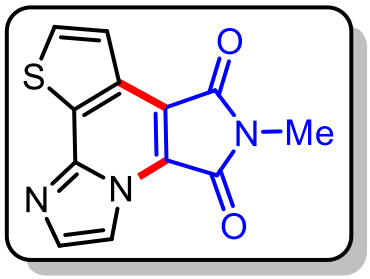

Purification by column chromatography on silica gel (eluent: EtOAc/hexanes, 1:3 *v/v*); Yellow solid; 50 mg (58%); mp =220-222 °C; ^{1}H NMR (400 MHz, $CDCl_3$) δ 8.40 (s, 1H), 7.94 (d, *J* = 5.3 Hz, 1H), 7.84 (s, 1H), 7.76 (d, *J* = 5.3 Hz, 1H), 3.25 (s, 3H); ^{13}C{^{1}H} NMR (100 MHz, $CDCl_3$) δ 166.8, 164.2, 143.0, 135.8, 132.8, 130.4, 128.9, 127.4, 122.3, 115.2, 112.4, 24.0; HRMS (ESI) *m/z*: $[M + H]^+$ Calcd for $C_{12}H_8N_3O_2S^+$ 258.0332; Found 258.0328.

2-Methyl-1*H*-benzo[4,5]imidazo[2,1-*a*]pyrrolo[3,4-*c*]isoquinoline-1,3(2*H*)-dione (37oa).

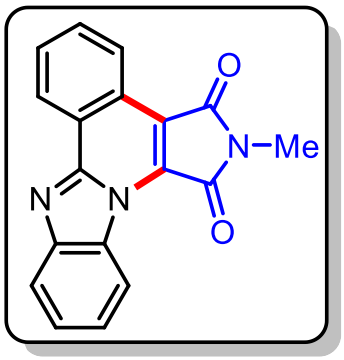

Purification by column chromatography on silica gel (eluent: EtOAc/hexanes, 1:3 *v/v*); Orange solid; 38 mg (49%); mp = 209-211°C; ^{1}H NMR (400 MHz, $CDCl_3$) δ 9.25 (d, *J* = 8.3 Hz, 1H), 8.93 – 8.90 (m, 1H), 8.83 – 8.81 (m, 1H), 8.05 (d, *J* = 8.0 Hz, 1H), 7.86 – 7.81 (m, 2H), 7.63 (t, *J* = 7.2 Hz, 1H), 7.54 (t, *J* = 8.2 Hz, 1H), 3.31 (s, 3H); ^{13}C{^{1}H} NMR (100 MHz, $CDCl_3$) δ 167.6, 163.9, 144.2, 132.3, 131.3, 130.6, 126.3, 125.8, 125.1, 124.9, 124.8, 123.79, 123.76, 119.9, 116.2, 115.0, 114.9, 24.1; HRMS (ESI) *m/z*: $[M + H]^+$ Calcd for $C_{18}H_{12}N_3O_2^+$ 302.0930; Found 302.0921.

6-Propyl-5*H*-imidazo[2,1-*a*]pyrrolo[3,4-*c*]isoquinoline-5,7(6*H*)-dione (37ab). Purification by column chromatography on silica gel (eluent: EtOAc/hexanes, 1:3 *v/v*); Yellow solid; 66 mg (67%); mp =136-138 °C; ^{1}H NMR (400 MHz, $CDCl_3$) δ 8.74 – 8.67 (m, 2H), 8.38 (d, *J* = 1.4 Hz, 1H), 7.81 – 7.80 (m, 1H), 7.77 (dd, *J* = 4.9, 1.6 Hz, 1H), 7.75 – 7.73 (m, 1H), 3.71 (t, *J* = 7.2 Hz, 2H), 1.83 – 1.74 (m, 2H), 1.02 (t, *J* = 7.4 Hz, 3H); ^{13}C{^{1}H} NMR (100 MHz, $CDCl_3$) δ 167.8, 164.2, 145.0, 134.5, 130.7, 129.7, 128.6, 125.4, 124.9, 124.2, 123.2, 115.6, 113.0, 39.8, 22.1, 11.3; HRMS (ESI) *m/z*: $[M + H]^+$ Calcd for $C_{16}H_{14}N_3O_2^+$ 280.1086; Found 280.1079.

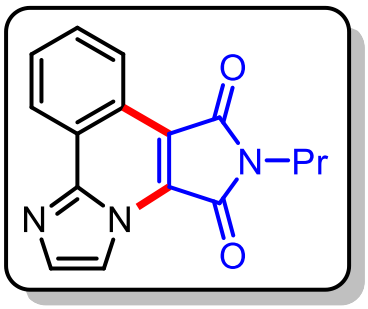

6-Benzyl-5*H*-imidazo[2,1-*a*]pyrrolo[3,4-*c*]isoquinoline-5,7(6*H*)-dione (37ac). Purification by column chromatography on silica gel (eluent: EtOAc/hexanes, 1:3 *v/v*); Orange solid; 66 mg (58%); mp = 209-211°C; mp = 180-182 °C; ^{1}H NMR (400 MHz, $CDCl_3$) δ 8.71 (d, *J* = 8.3 Hz, 2H), 8.39 – 8.37 (m, 1H), 7.82 – 7.72 (m, 3H), 7.48 (d, *J* = 7.2 Hz, 2H), 7.39 – 7.28 (m, 3H), 4.90 (s, 2H); ^{13}C{^{1}H} NMR (100 MHz, $CDCl_3$) δ 167.1, 163.6, 135.8, 133.4, 131.2, 130.3, 128.9, 128.6, 128.4, 128.2, 125.1, 124.8, 124.5, 123.4, 116.4, 113.2, 41.8; HRMS (ESI) *m/z*: $[M + H]^+$ Calcd for $C_{20}H_{14}N_3O_2^+$ 328.1081; Found 328.1074.

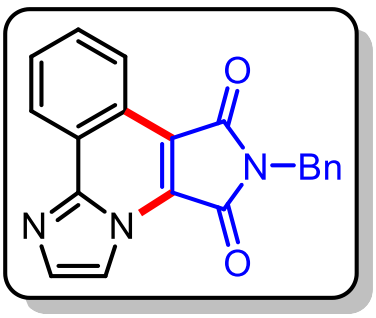

6-Ethyl-5*H*-imidazo[2,1-*a*]pyrrolo[3,4-*c*]isoquinoline-5,7(6*H*)-dione (37ad). Purification by column chromatography on silica gel (eluent: EtOAc/hexanes, 1:3 *v/v*); Yellow solid; 54 mg (59%); mp =198-200 °C; ^{1}H NMR (400 MHz, $CDCl_3$) δ 8.76 (d, *J* = 8.4 Hz, 2H), 8.45 (s, 1H), 7.82 – 7.76 (m, 3H), 3.83 (q, *J* = 7.2 Hz, 2H), 1.37 (t, *J* = 7.2 Hz, 3H); ^{13}C{^{1}H} NMR (100 MHz, $CDCl_3$) δ 167.6, 163.9, 145.0, 134.5, 130.7, 129.8, 128.7, 125.3, 124.9, 124.2, 123.2, 115.7, 113.0, 33.1, 14.1; HRMS (ESI) *m/z*: $[M + H]^+$ Calcd for $C_{15}H_{12}N_3O_2^+$ 266.0924; Found 266.0919.

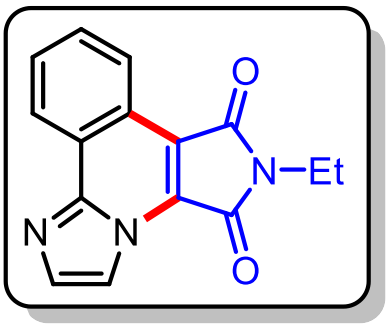

6-Cyclohexyl-5*H*-imidazo[2,1-*a*]pyrrolo[3,4-*c*]isoquinoline-5,7(6*H*)-dione (37ae). Purification

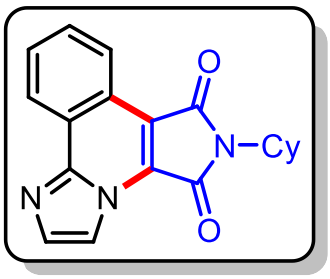

by column chromatography on silica gel (eluent: EtOAc/hexanes, 1:3 *v/v*); Yellow solid; 54 mg (49%); mp = 237-239 °C; ^{1}H NMR (400 MHz, $CDCl_3$) δ 8.74 (d, *J* = 8.1 Hz, 2H), 8.41 (d, *J* = 1.4 Hz, 1H), 7.82 – 7.74 (m, 3H), 4.20 – 4.12 (m, 1H), 2.28 – 2.18 (m, 2H), 1.95 – 1.91 (m, 2H), 1.87 – 1.83 (m, 2H), 1.77 – 1.73 (m, 1H), 1.49 – 1.26 (m, 3H); ^{13}C{^{1}H} NMR (100 MHz, $CDCl_3$) δ 167.8, 164.2, 145.0, 134.4, 130.6, 129.8, 128.6, 125.4, 124.9, 124.2, 123.3, 115.4, 113.0, 51.2, 30.2, 26.0, 25.1; HRMS (ESI) *m/z*: $[M + H]^+$ Calcd for $C_{19}H_{18}N_3O_2^+$ 320.1394; Found 320.1401.

2.4.4 General Procedure for the Synthesis of 39.

A 10 mL pressure tube was charged with 2-arylimidazole **23** (0.27 mmol, 1 equiv) and 1,4-naphthoquinone **38** (0.54 mmol, 2 equiv), $Cu(OAc)_2$ (98 mg, 0.54 mmol, 2.0 equiv), KPF_6 (15 mg, 0.08 mmol, 30 mol %), HOAc (5 µL, 30 mol %), $[RuCl_2(p\text{-cymene})]_2$ (7.7 mg, 0.013 mmol, 5.0 mol %) and DMA (2 mL). The resulting reaction mixture was stirred at 140 °C in an oil bath for 4 h. Upon completion of the reaction, the reaction mixture was cooled to ambient temperature and diluted with ice cold water (5 mL) and extracted with ethyl acetate (3 × 5 mL). The combined organic layer was dried over anhydrous Na_2SO_4, filtered, and evaporated to yield the crude product, which was purified by column chromatography on silica gel (100-200 mesh size) using EtOAc/hexanes as eluent to afford the desired annulated product **39**.

Benzo[*b*]imidazo[1,2-*f*]phenanthridine-8,13-dione (39aa). Purification by column

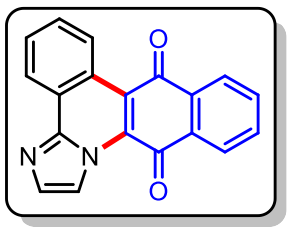

chromatography on silica gel (eluent: EtOAc/hexanes, 1:7 *v/v*); Red solid; 75 mg (73%); mp = 205-207 °C; ^{1}H NMR (400 MHz, $CDCl_3$) δ 9.45 (dd, *J* = 8.3, 1.4 Hz, 1H), 9.35 (d, *J* = 1.6 Hz, 1H), 8.79 (dd, *J* = 7.8, 1.7 Hz, 1H), 8.25 (dd, *J* = 5.9, 1.9 Hz, 2H), 7.87 – 7.74 (m, 5H); ^{13}C{^{1}H} NMR (100 MHz, $CDCl_3$) δ 184.8, 180.1, 144.6, 134.7, 134.5, 134.0, 133.1, 131.43, 131.38, 131.1, 129.9, 129.2, 127.0, 126.6, 126.4, 125.1, 123.7, 122.2, 117.3; HRMS (ESI) *m/z*: $[M + H]^+$ Calcd for $C_{19}H_{11}N_2O_2^+$ $[M+H]^+$ 299.0815; Found 299.0809.

6-Methylbenzo[*b*]imidazo[1,2-*f*]phenanthridine-8,13-dione (39ba). Purification by column chromatography on silica gel (eluent: EtOAc/hexanes, 3:7 *v/v*); Red solid; 74 mg (74%); mp = 196-198 °C; ^{1}H NMR (400 MHz, $CDCl_3$) δ 9.21 (d, *J* = 1.5 Hz, 1H), 9.12 – 9.10 (m, 1H), 8.53 (d, *J* = 8.2 Hz, 1H), 8.18 – 8.12 (m, 2H), 7.81 – 7.74 (m, 2H), 7.72 (d, *J* = 1.5 Hz, 1H), 7.52 (dd, *J* = 8.3, 1.7 Hz, 1H), 2.54 (s, 3H); ^{13}C{^{1}H} NMR (100 MHz, $CDCl_3$) δ 184.7, 179.8, 144.6, 140.1, 134.5, 134.4, 133.8, 132.9, 132.6, 131.3, 131.2, 128.5, 126.8, 126.4, 125.0, 124.1, 123.4, 121.6, 116.9, 22.2; HRMS (ESI) *m/z*: $[M + H]^+$ Calcd for $C_{20}H_{13}N_2O_2^+$ 313.0972; Found 313.0979.

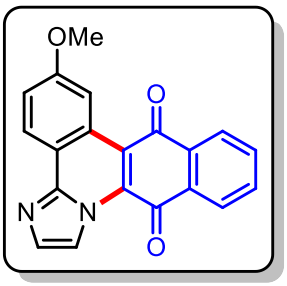

6-Chlorobenzo[*b*]imidazo[1,2-*f*]phenanthridine-8,13-dione (39ea). Purification by column chromatography on silica gel (eluent: EtOAc/hexanes, 3:7 *v/v*); Red solid; 51 mg (55%); mp = 215-217 °C; ^{1}H NMR (400 MHz, $CDCl_3$) δ 9.60 (d, *J* = 2.0 Hz, 1H), 9.36 (d, *J* = 1.5 Hz, 1H), 8.76 (d, *J* = 8.7 Hz, 1H), 8.31 – 8.27 (m, 2H), 7.91 – 7.84 (m, 3H), 7.79 (dd, *J* = 8.7, 2.0 Hz, 1H); ^{13}C{^{1}H} NMR (100 MHz, $CDCl_3$) δ 184.5, 180.0, 147.2, 144.2, 136.4, 135.0, 134.2, 132.9, 132.2, 131.6, 131.3, 128.5, 127.1, 126.8, 126.1, 125.2, 124.7, 120.8, 117.5; HRMS (ESI) *m/z*: $[M + H]^+$ Calcd for $C_{19}H_{10}ClN_2O_2^+$ 333.0425; Found 333.0418.

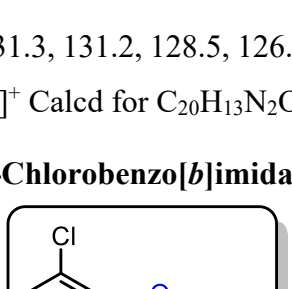

Dibenzo[*b*,*i*]imidazo[1,2-*f*]phenanthridine-9,14-dione (39ma). Purification by column chromatography on silica gel (eluent: EtOAc/hexanes, 1:9 *v/v*); Red solid; 52 mg (58%); mp = 202-204 °C; ^{1}H NMR (400 MHz, $CDCl_3$) δ 10.86 (d, *J* = 8.6 Hz, 1H), 9.60 – 9.58 (m, 1H), 9.32 (d, *J* = 9.2 Hz, 1H), 8.31 – 8.26 (m, 2H), 8.11 – 8.05 (m, 2H), 8.02 – 7.98 (m, 1H), 7.89 – 7.82 (m, 3H), 7.78 (t, *J* = 7.3 Hz, 1H); ^{13}C{^{1}H} NMR (100 MHz, $CDCl_3$) δ 185.1, 179.7, 144.6, 135.5, 134.6, 133.9, 133.8, 133.5, 131.6, 130.5, 129.9, 128.8, 128.6, 128.1, 128.0, 127.1, 126.6, 125.2, 124.4, 123.6, 122.7, 116.2; HRMS (ESI) *m/z*: $[M + H]^+$ Calcd for $C_{23}H_{13}N_2O_2^+$ 349.0972; Found 349.0978.

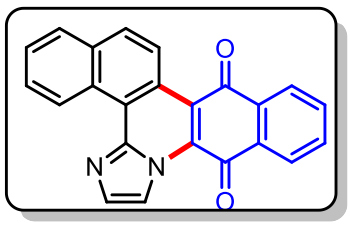

Benzo[*g*]imidazo[1,2-*a*]thieno[2,3-*c*]quinoline-8,13-dione (39na). Purification by column chromatography on silica gel (eluent: EtOAc/hexanes, 2:8 *v/v*); Orange solid; 62 mg (61%); mp = 188-190 °C; ^{1}H NMR (400 MHz, $CDCl_3$) δ 9.35 (s, 1H), 8.25 – 8.17 (m, 2H), 8.03 – 7.98 (m, 2H), 7.85 – 7.77 (m, 3H); ^{13}C{^{1}H} NMR (100 MHz, $CDCl_3$) δ 182.5, 178.3, 143.2, 138.2, 135.7, 134.7, 134.4, 132.8, 132.2, 131.1, 130.0, 127.5, 127.2, 126.9, 121.6, 120.7, 116.1; HRMS (ESI) *m/z*: $[M + H]^+$ Calcd for $C_{17}H_9N_2O_2S^+$ 305.0379; Found 302.0382.

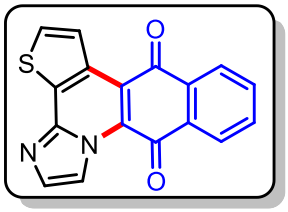

Imidazo[1,2-*f*]phenanthridine-5,8-dione (39a). Purification by column chromatography on silica gel (eluent: EtOAc/hexanes, 1:4 *v/v*); Red solid; 56 mg (65%); mp = 201-203 °C; ^{1}H NMR (400 MHz, DMSO-d_6) δ 9.26 – 9.19 (m, 1H), 9.07 (s, 1H), 8.66 (d, J = 9.2 Hz, 1H), 7.88 – 7.80 (m, 3H), 7.09 (s, 2H); ^{13}C{^{1}H} NMR (100 MHz, DMSO-d_6) δ 187.7, 182.4, 150.2, 144.0, 138.6, 136.1, 134.9, 131.2, 130.4, 128.4, 125.7, 124.8, 123.6, 116.9, 116.1; HRMS (ESI) *m/z*: $[M + H]^+$ Calcd for $C_{15}H_9N_2O_2^+$ 249.0659; Found 249.0660.

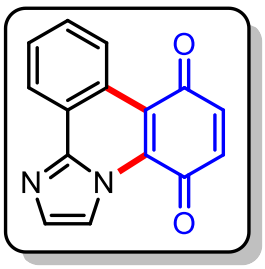

4-Methyl-2,5-diphenylbenzo[*g*]imidazo[1,2-*a*]quinoline-6,11-dione (40ba). Compound **39ba** was prepared by the reaction of **1b** (50 mg, 0.192 mmol) and **37** (33 mg, 0.211 mmol) for 6 h following same procedure as for **7**. Purification by column chromatography on silica gel (eluent: EtOAc/hexanes, 1:9 *v/v*); Red solid; 51 mg (64%); mp = 194-196 °C; ^{1}H NMR (400 MHz, $CDCl_3$) δ 9.89 (s, 1H), 8.28 (dd, J = 7.6, 1.4 Hz, 1H), 8.17 – 8.14 (m, 2H), 8.03 (dd, J = 7.6, 1.4 Hz, 1H), 7.80 – 7.70 (m, 2H), 7.58 – 7.54 (m, 2H), 7.53 – 7.49 (m, 3H), 7.44 – 7.39 (m, 1H), 7.24 – 7.22 (m, 2H), 2.54 (s, 3H); ^{13}C{^{1}H} NMR (100 MHz, $CDCl_3$) δ 182.5, 179.4, 150.4, 147.3, 139.4, 135.0, 134.5, 134.3, 133.9, 133.3, 132.6, 132.0, 128.92, 128.87, 128.8, 128.5, 128.1, 127.2, 127.1, 126.5, 126.4, 123.6, 112.7, 15.8; HRMS (ESI) *m/z*: $[M + H]^+$ Calcd for $C_{28}H_{19}N_2O_2^+$ 415.1441; Found 415.1448.

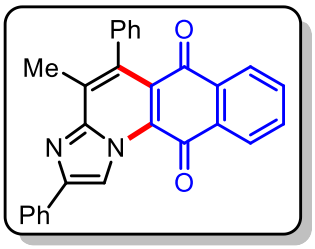

2.4.5 Synthesis of 3-Hydroxy-2,5-dimethyl-4-phenyl-2,3-dihydro-1*H*-imidazo[1,2-*a*]pyrrolo[3,4-*e*]pyridin-1-one (41). A solution of **36aa** (25 mg, 0.086 mmol) in 2 mL of methanol was cooled to 0 °C and $NaBH_4$ (9.55 mg, 3 equiv.) was added to this solution. The

resulting mixture was allowed to reach room temperature and kept under stirring for 1 h. After completion of reaction, H_2O (3 mL) was added and extracted with dichloromethane (3 × 5 mL). The combined organic layer was dried over anhydrous Na_2SO_4, filtered, and evaporated to yield the crude product. The crude product was purified by column chromatography on silica gel (100-200 mesh size) using hexane/ethyl acetate (3: 7 *v/v*) as eluent to give white solid (18 mg, 72%); mp = 250-252 °C; ^{1}H NMR (400 MHz, $CDCl_3$) δ 8.49 (s, 1H), 7.77 (s, 1H), 7.56 – 7.46 (m, 3H), 7.36 (d, *J* = 7.2 Hz, 2H), 5.69 (s, 1H), 3.11 (s, 3H), 2.53 (s, 3H); ^{13}C{^{1}H} NMR (100 MHz, $CDCl_3$) δ 162.2, 146.6, 135.7, 134.6, 132.5, 131.4, 128.4, 128.3, 127.8, 125.0, 111.4, 81.4, 25.9, 14.7; FT-IR ν_{max} (neat) 3368, 2924, 1705, 1442, 1257, 1080, 794, 702, 509 cm^{-1}; HRMS (ESI) *m/z*: $[M + H]^+$ Calcd for $C_{17}H_{16}N_3O_2^+$ 294.1237; Found 294.1233.

2.4.6 Synthesis of Intermediate Ru-I:[68] A 10 mL round bottom flask was charged with **1a** (20.0 mg, 0.10 mmol), $[RuCl_2(p\text{-cymene})]_2$ (33.0 mg, 0.05 mmol), KOAc (21.0 mg, 0.20 mmol) and MeOH (2.0 mL). The resulting mixture was stirred at room temperature for 24 h under an argon atmosphere. After completion of reaction, methanol was evaporated on rota-evaporatory. The crude product obtained by purified by column chromatography (DCM/MeOH, 99: 1 *v/v*) to provide intermediate **Ru-I** as yellow solid; ^{1}H NMR (400 MHz, $CDCl_3$) δ 10.32 (s, 1H), 7.40 – 7.31 (m, 4H), 7.20 – 7.11 (m, 1H), 7.06 (s, 1H), 6.44 (s, 1H), 5.29 – 5.23 (m, 2H), 4.86 (d, *J* = 5.5 Hz, 1H), 4.29 (d, *J* = 5.5 Hz, 1H), 2.23 – 2.14 (m, 1H), 1.92 (s, 3H), 1.54 (s, 3H), 0.95 (d, *J* = 6.9 Hz, 3H), 0.78 (d, *J* = 6.9 Hz, 3H); ^{13}C{^{1}H} NMR (100 MHz, $CDCl_3$) δ 187.0, 157.4, 153.2, 129.3, 128.3, 128.2, 127.4, 125.7, 124.4, 121.2, 115.5, 96.8, 95.9, 89.0, 87.5, 84.2, 83.1, 30.8, 23.1, 20.9, 18.6, 13.3.

2.4.7 Sample Preparation and Crystal Measurement of 36aa. Single crystals of **36aa** $[C_{17}H_{13}N_3O_2]$ were grown from slow evaporation of ethyl acetate/hexane solution. A suitable crystal was selected and mounted on a XtaLAB AFC12 (RINC): Kappa dual home/near diffractometer. The crystal was kept at 93(2) K during data collection. Using Olex2[69], the structure was solved with the ShelXT[70] structure solution program using Intrinsic phasing and refined with the ShelXL[71] refinement package using least squares minimisation.

Table 2.3. Crystal data for **36aa.**

Identification code	**36aa**
Empirical formula	$C_{17}H_{13}N_3O_2$
Formula weight	291.30
Temperature/K	93(2)
Crystal system	orthorhombic
Space group	Pbca
a/Å	18.0859(3)
b/Å	7.37450(10)
c/Å	20.0210(3)
α/°	90
β/°	90
γ/°	90
Volume/Å^3	2670.29(7)
Z	8
ρ_{calc}g/cm^3	1.449
μ/mm^{-1}	0.798
F(000)	1216.0
Crystal size/mm^3	0.2 × 0.08 × 0.04
Radiation	Cu Kα (λ = 1.54184)
2Θ range for data collection/°	8.834 to 159.34
Index ranges	-22 ≤ h ≤ 22, -9 ≤ k ≤ 4, -25 ≤ l ≤ 23
Reflections collected	9778
Independent reflections	2827 [R_{int} = 0.0264, R_{sigma} = 0.0281]
Data/restraints/parameters	2827/0/201
Goodness-of-fit on F^2	1.067
Final R indexes [I>=2σ (I)]	R_1 = 0.0348, wR_2 = 0.0933
Final R indexes [all data]	R_1 = 0.0377, wR_2 = 0.0954
Largest diff. peak/hole / e Å^{-3}	0.21/-0.25

2.5 REFERENCES

1. Sun, Q.LaVoie, E. J., *Heterocycles* **1996**, *4*, 737-743.
2. Zhe Xiong, L.; Nurul Huda, Q.; Leslie W, D.; Gideon M, P., **1996**.
3. Deady, L. W.; Rodemann, T.; Finlay, G. J.; Baguley, B. C.; Denny, W. A., *Anti-cancer drug Design* **2000**, *15*, 339-346.
4. Rodgers, J.; Robinson, D.; Arvanitis, A.; Maduskuie, T.; Shepard, S.; Storace, L.; Wang, H.; Rafalski, M.; Jalluri, R.; Combs, A., *Journal*, **2006**.
5. Andaloussi, M.; Moreau, E.; Masurier, N.; Lacroix, J.; Gaudreault, R. C.; Chezal, J.-M.; El Laghdach, A.; Canitrot, D.; Debiton, E.; Teulade, J.-C., *European Journal of Medicinal Chemistry* **2008**, *43*, 2505-2517.
6. Nafie, M. S.; Tantawy, M. A.; Elmgeed, G. A., *Steroids* **2019**, *152*, 108485.
7. Palmer, A. M.; Grobbel, B.; Jecke, C.; Brehm, C.; Zimmermann, P. J.; Buhr, W.; Feth, M. P.; Simon, W.-A.; Kromer, W., *Journal of Medicinal Chemistry* **2007**, *50*, 6240-6264.
8. Muniraj, N.Prabhu, K. R., *Organic Letters* **2019**, *21*, 1068-1072.
9. Kumar, S. V.; Banerjee, S.; Punniyamurthy, T., *Organic Chemistry Frontiers* **2020**, *7*, 1527-1569.
10. Ackermann, L., *Accounts of Chemical Research* **2014**, *47*, 281-295.
11. Shinde, V. N.; Rangan, K.; Kumar, D.; Kumar, A., *The Journal of Organic Chemistry* **2021**, *86*, 2328-2338.
12. Zhu, C.; Wang, C.-Q.; Feng, C., *Tetrahedron Letters* **2018**, *59*, 430-437.
13. Ouyang, W.; Rao, J.; Li, Y.; Liu, X.; Huo, Y.; Chen, Q.; Li, X., *Advanced Synthesis & Catalysis* **2020**, *362*, 5576-5600.
14. Kumar, S.; Kumar, N.; Roy, P.; Sondhi, S. M., *Molecular Diversity* **2013**, *17*, 753-766.
15. Wang, S.; Fang, K.; Dong, G.; Chen, S.; Liu, N.; Miao, Z.; Yao, J.; Li, J.; Zhang, W.; Sheng, C., *Journal of Medicinal Chemistry* **2015**, *58*, 6678-6696.
16. Wood, J. M.; de Carvalho, R. L.; da Silva Júnior, E. N., *The Chemical Record* **2021**, *21*, 2604-2637.
17. Twardy, D. J.; Wheeler, K. A.; Török, B.; Dembinski, R., *Molecules* **2022**, *27*, 2062.
18. Bhorali, P.; Sultana, S.; Gogoi, S., *Asian Journal of Organic Chemistry* **2022**, *11*, e202100754.
19. Manoharan, R.Jeganmohan, M., *Asian Journal of Organic Chemistry* **2019**, *8*, 1949-1969.

20. Xiang, Y.; Wang, C.; Ding, Q.; Peng, Y., *Advanced Synthesis & Catalysis* **2019**, *361*, 919-944.
21. Ushakov, P. Y.; Ioffe, S. L.; Sukhorukov, A. Y., *Organic Chemistry Frontiers* **2022**, *9*, 5358-5382.
22. Halskov, K. S.; Roth, H. S.; Ellman, J. A., *Angewandte Chemie International Edition* **2017**, *56*, 9183-9187.
23. Hoang, G. L.Ellman, J. A., *Tetrahedron* **2018**, *74*, 3318-3324.
24. Dutta, P. K.Sen, S., *European Journal of Organic Chemistry* **2018**, *2018*, 5512-5519.
25. Obata, A.; Sasagawa, A.; Yamazaki, K.; Ano, Y.; Chatani, N., *Chemical Science* **2019**, *10*, 3242-3248.
26. Kavitha, N.; Sukumar, G.; Kumar, V. P.; Mainkar, P. S.; Chandrasekhar, S., *Tetrahedron Letters* **2013**, *54*, 4198-4201.
27. Yang, L.; Steinbock, R.; Scheremetjew, A.; Kuniyil, R.; Finger, L. H.; Messinis, A. M.; Ackermann, L., *Angewandte Chemie International Edition* **2020**, *59*, 11130-11135.
28. Zheng, L.Hua, R., *The Journal of Organic Chemistry* **2014**, *79*, 3930-3936.
29. Yu, T.; Li, X.; Zhao, Y.; Yang, Q.; Li, Y.; Zhang, H.; Li, Z., *Journal of Photochemistry and Photobiology A: Chemistry* **2018**, *360*, 58-63.
30. Dias, G. G.; Paz, E. R.; Kadooca, J. Y.; Sabino, A. A.; Cury, L. A.; Torikai, K.; De Simone, C. A.; Fantuzzi, F.; da Silva Júnior, E. N., *The Journal of Organic Chemistry* **2020**, *86*, 264-278.
31. Bin, J. W.; Wong, I. L.; Hu, X.; Yu, Z. X.; Xing, L. F.; Jiang, T.; Chow, L. M.; Biao, W. S., *Journal of Medicinal Chemistry* **2013**, *56*, 9057-9070.
32. Miura, W.; Hirano, K.; Miura, M., *Organic Letters* **2015**, *17*, 4034-4037.
33. Zhao, H.; Shao, X.; Wang, T.; Zhai, S.; Qiu, S.; Tao, C.; Wang, H.; Zhai, H., *Chemical Communications* **2018**, *54*, 4927-4930.
34. Yuan, Y.-C.; Goujon, M.; Bruneau, C.; Roisnel, T.; Gramage-Doria, R., *The Journal of Organic Chemistry* **2019**, *84*, 16183-16191.
35. Ramesh, B.; Tamizmani, M.; Jeganmohan, M., *The Journal of Organic Chemistry* **2019**, *84*, 4058-4071.
36. Devkota, S.; Lee, H. J.; Kim, S. H.; Lee, Y. R., *Advanced Synthesis & Catalysis* **2019**, *361*, 5587-5595.

37. Li, H.; Zhang, S.; Feng, X.; Yu, X.; Yamamoto, Y.; Bao, M., *Organic Letters* **2019**, *21*, 8563-8567.
38. Shinde, V. N.; Kanchan Roy, T.; Jaspal, S.; Nipate, D. S.; Meena, N.; Rangan, K.; Kumar, D.; Kumar, A., *Advanced Synthesis & Catalysis* **2020**, *362*, 5751-5764.
39. Aslam, M.; Mohandoss, S.; Lee, Y. R., *Organic Letters* **2021**, *23*, 6206-6211.
40. Huang, Y.-T.; Barve, I. J.; Huang, Y.-T.; Dhole, S.; Chiu, W.-J.; Sun, C.-M., *Organic & Biomolecular Chemistry* **2022**, *20*, 6854-6862.
41. Deng, C.; Li, C.; Yao, J.; Jin, Q.; Miao, M.; Zhou, H., *European Journal of Organic Chemistry* **2021**, *2021*, 3552-3558.
42. Wang, D.; Yu, X.; Wang, L.; Yao, W.; Xu, Z.; Wan, H., *Tetrahedron Letters* **2016**, *57*, 5211-5214.
43. Zhang, S.-S.; Jiang, C.-Y.; Wu, J.-Q.; Liu, X.-G.; Li, Q.; Huang, Z.-S.; Li, D.; Wang, H., *Chemical Communications* **2015**, *51*, 10240-10243.
44. Song, G.; Wang, F.; Li, X., *Chemical Society Reviews* **2012**, *41*, 3651-3678.
45. Qi, Z.Li, X., *Chinese Journal of Catalysis* **2015**, *36*, 48-56.
46. Dandawate, P. R.; Vyas, A. C.; Padhye, S. B.; Singh, M. W.; Baruah, J. B., *Mini Reviews in Medicinal Chemistry* **2010**, *10*, 436-454.
47. Wu, Y.; Sun, P.; Zhang, K.; Yang, T.; Yao, H.; Lin, A., *The Journal of Organic Chemistry* **2016**, *81*, 2166-2173.
48. Zhou, T.; Li, L.; Li, B.; Song, H.; Wang, B., *Organic Letters* **2015**, *17*, 4204-4207.
49. Zhang, Q.; Li, Q.; Wang, C., *RSC Advances* **2021**, *11*, 13030-13033.
50. Guo, S.; Liu, Y.; Zhang, X.; Fan, X., *Advanced Synthesis & Catalysis* **2020**, *362*, 3011-3020.
51. Moon, Y.; Jeong, Y.; Kook, D.; Hong, S., *Organic & Biomolecular Chemistry* **2015**, *13*, 3918-3923.
52. Pecoraro, C.; Faggion, B.; Balboni, B.; Carbone, D.; Peters, G. J.; Diana, P.; Assaraf, Y. G.; Giovannetti, E., *Drug Resistance Updates* **2021**, *58*, 100779.
53. Naharwal, S.; Karishma, P.; Mahesha, C. K.; Bajaj, K.; Mandal, S. K.; Sakhuja, R., *Organic & Biomolecular Chemistry* **2022**, *20*, 4753-4764.
54. Siva Sankaram, G.; Sridhar, B.; Subba Reddy, B., *European Journal of Organic Chemistry* **2022**, *2022*, e202201113.

55. Aminin, D.Polonik, S., *Chemical and Pharmaceutical Bulletin* **2020**, *68*, 46-57.
56. Kumar, S.; Nair, A. M.; Patra, J.; Volla, C. M. R., *Organic Letters* **2023**, *25*, 1114-1119.
57. Nale, S. D.; Maiti, D.; Lee, Y. R., *Organic Letters* **2021**, *23*, 2465-2470.
58. Guo, S.; Liu, Y.; Zhang, X.; Fan, X., *Advanced Synthesis & Catalysis* **2020**, *362*, 3011-3020.
59. Zhou, T.; Li, L.; Li, B.; Song, H.; Wang, B., *Organic Letters* **2015**, *17*, 4204-4207.
60. Srinivas, L.; Chary, D. Y.; Ajay, C.; Sridhar, B.; Reddy, B. J. M.; Reddy, B. V. S., *Journal of Molecular Structure* **2023**, *1289*.
61. David, L.Keith, F., *Chemistry Letters* **2010**, *39*, 1118-1126.
62. Duarah, G.; Kaishap, P. P.; Begum, T.; Gogoi, S., *Advanced Synthesis & Catalysis* **2019**, *361*, 654-672.
63. Kang, J. Y.; An, W.; Kim, S.; Kwon, N. Y.; Jeong, T.; Ghosh, P.; Kim, H. S.; Mishra, N. K.; Kim, I. S., *Chemical Communications* **2021**, *57*, 10947-10950.
64. Guo, S.; Liu, Y.; Zhao, L.; Zhang, X.; Fan, X., *Organic letters* **2019**, *21*, 6437-6441.
65. Song, L.; Zhang, X.; Tang, X.; Van Meervelt, L.; Van der Eycken, J.; Harvey, J. N.; Van der Eycken, E. V., *Chemical Science* **2020**, *11*, 11562-11569.
66. Wang, R.Falck, J. R., *Journal of Organometallic Chemistry* **2014**, *759*, 33-36.
67. Mandal, R.; Emayavaramban, B.; Sundararaju, B., *Organic Letters* **2018**, *20*, 2835-2838.
68. Yang, L.; Steinbock, R.; Scheremetjew, A.; Kuniyil, R.; Finger, L. H.; Messinis, A. M.; Ackermann, L., *Angewandte Chemie International Edition* **2020**, *59*, 11130-11135.
69. Dolomanov, O. V.; Bourhis, L. J.; Gildea, R. J.; Howard, J. A. K.; Puschmann, H., *Journal of Applied Crystallography* **2009**, *42*, 339-341.
70. Sheldrick, G., *Acta Crystallographica Section A* **2015**, *71*, 3-8.
71. Sheldrick, G., *Acta Crystallographica Section C* **2015**, *71*, 3-8.

Chapter 3

Catalyst-Controlled Regiodivergent Annulation of 2-Arylimidazo[1,2-*a*]pyridines with Cinnamaldehyde

3.1 INTRODUCTION

Imidazo[1,2-*a*]pyridine constitutes an interesting class of privileged chemical moiety found in several marketed drugs such as Zolpidem, Alpidem (sedative and hypnotic),[1] Necopidem, Saripidem (treat anxiety and insomnia),[2] Minodronic acid (for the treatment of osteoporosis),[3] Olprinone[4] and GSK812397 (CXCR4 receptor antagonist)[5] etc. (**Figure 3.1**). Notably, imidazo[1,2-*a*]pyridine framework also forms the backbone for synthesizing complex organic architectures that have exhibited profound applications in medicinal and materials chemistry.[6-8] Imidazo[1,2-*a*]pyridines with extended π-systems have also shown interesting optical and electronic properties.[9-11] Due to the significant importance of imidazo[1,2-*a*]pyridines in medicinal chemistry and materials chemistry, the synthesis and functionalization of this framework have attracted considerable interest from organic chemists.[12-19] The functionalization of this heterocycle plays an important role in advancing pharmaceutical research. Notably, due to its inherent electron-rich nature, the imidazopyridine ring has gained more interest from synthetic chemists, particularly in terms of direct functionalization at the C3-carbon site, and other positions.

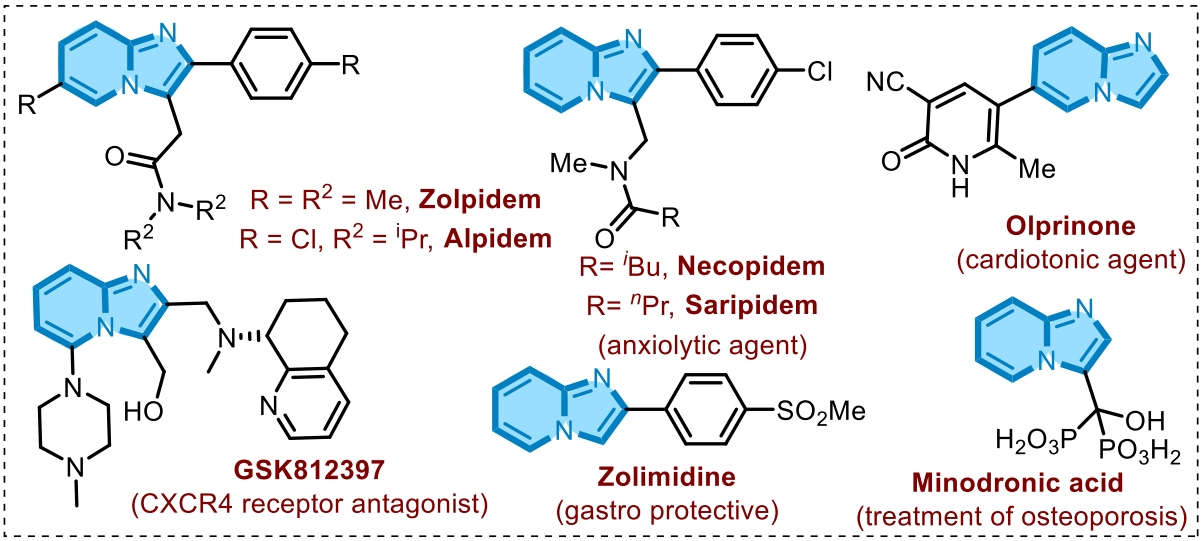

Figure 3.1: Marketed drugs with imidazo[1,2-*a*]pyridine framework

C–H functionalization is a powerful technique that can form new C–C/C–N/C–O bonds from unactivated C–H bonds. One of the challenges in organic chemistry is to selectively modify C-H bonds in molecules that have many of them. Heterocycles can have specific reactivity at certain sites due to the heteroatoms.[20-23]

The C–H functionalization can lead to the creation and diversification of various functional molecules. One way to achieve this is by using transition-metal catalysts that activate specific C−H bonds and transform them into other functional groups. Regioselective C-H bond functionalization is significant because it allows the formation of a single desired product among many options. To ensure efficiency and atom economy, progress in regio-divergent C-H bond functionalization of *N*-heterocycles is crucial because these compounds are common in natural products and drugs.[24, 25] Furthermore, numerous methods for C-H functionalization of imidazo[1,2-*a*]pyridine have been developed in the scientific literature over the past few decades. These methods have been used to enhance the structural diversity of imidazo[1,2-*a*]pyridine, synthesizing more potent bioactive compounds.[26-30] Most previous studies on the C−H bond functionalization of imidazo[1,2-*a*]pyridines are focused on the C-3 position, which is more reactive than the other positions. What makes this research exciting is the pursuit of selective *ortho*-functionalization without protecting the active C-3 site.

In recent years, efforts have also been directed towards *ortho*-C-H bond functionalization, including amidation, cyanation, alkylation, and bisallylation, often involving the formation of five-membered metallacycle intermediates or chelation assistance. Remarkable contributions have been made by researchers like Reddy, Ackermann, Glorious, Chatani, and others, who have achieved selective C-H bond functionalization through careful selection of catalysts, oxidants, additives, and solvents. Selected recent examples for *ortho*-functionalization of imidazo[1,2-*a*]pyridines are given below.

The bis-allylation of imidazopyridine was recently recognized by the Song group. They described *ortho*-bis-allylation of 2-arylimidazo[1,2-*a*]pyridines **(1)** by using [Ru(*p*-cymene)Cl_2]$_2$ as catalyst with vinylcyclopropanes **(2)** (**Scheme 3.1)**.[32] Imidazopyridine undergoes chelation assisted-mechanism and produces the bisallylated products **(3)** in excellent yields *via* dual C-H and C-C activation. The developed approach shows a broad substrate scope, good functional group tolerance.

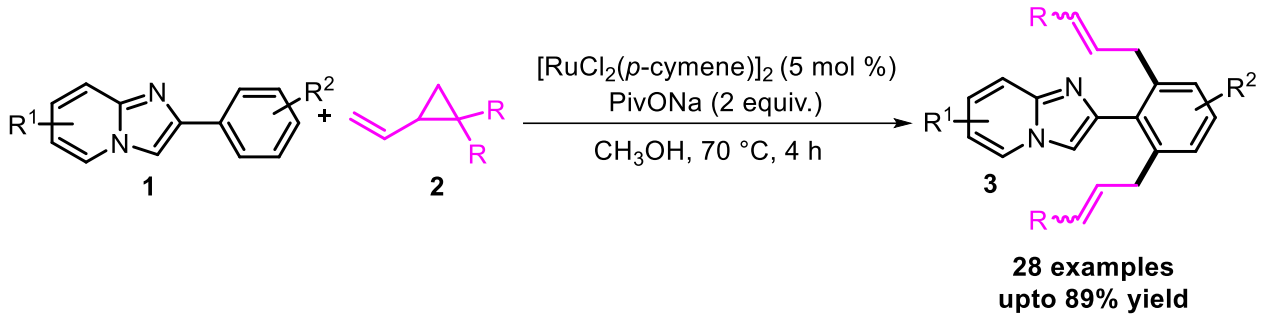

Scheme 3.1: Ru(II)-catalyzed bis-allylation of 2-arylimidazopyridines with vinylcyclopropanes

Zhang and co-workers developed an efficient Pd(II) and Rh(III)-controlled site-selective C-H bond alkynylation of 2-arylimidazopyridines **(1)** by using (bromoethynyl)triisopropylsilane **(4)** (**Scheme 3.2**).[33] The efficient C-H alkynylation of 2-arylimidazopyridines, providing access at the C3-and *ortho* positions of the phenyl ring. This developed methodology has been used in the development of a versatile framework (**5** or **6**) that could be applied effectively for introducing modifications at later stage of a synthesis process, which is also used in medicinal as well as in material chemistry.

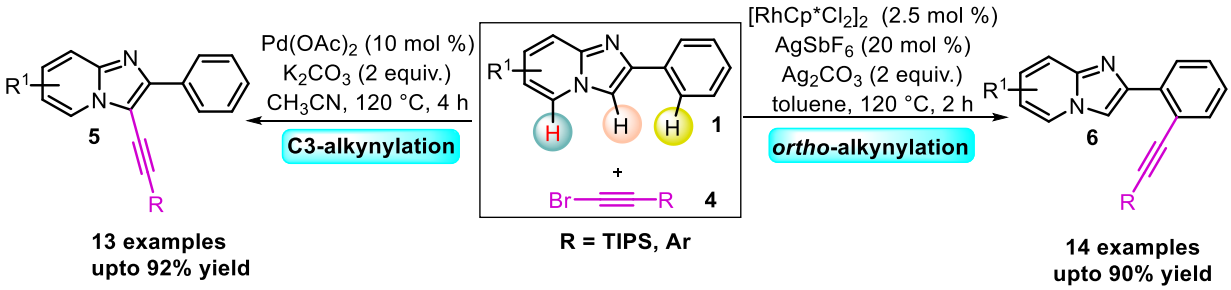

Scheme 3.2: Regioselective alkylation of 2-arylimidazopyridines

In addition, recently, our group also developed a mechanochemical protocol for bis alkenylation of products **(8)** of 2-arylimidazopyridines **(1)** with alkynes **(7)** by using Ru(II)-catalyzed, under solvent-free conditions (**Scheme 3.3**).[34] Good functional group tolerance, reduced reaction times, a broad range of applicable substrates, and solvent-free conditions are silent feature of this protocol. The method can be used for the gram scale preparation of corresponding products.

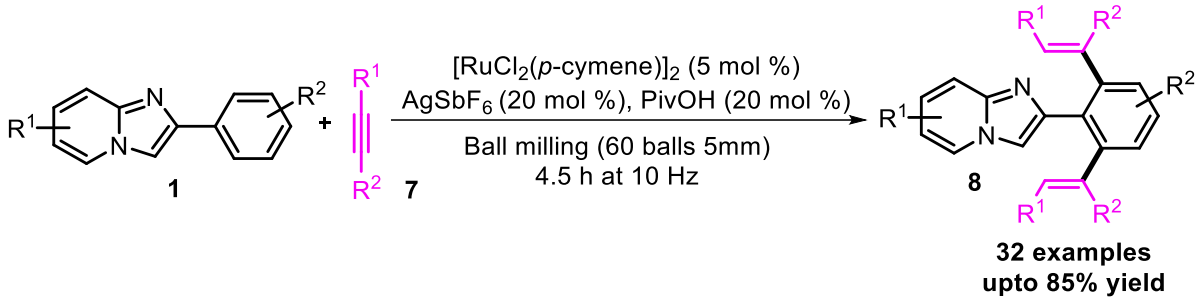

Scheme 3.3: Ru(II)-catalyzed bis-alkenylation of 2-arylimidazo[1,2-*a*]pyridine by using alkynes

Transition metal-catalyzed C-H bond functionalization approach has been extensively explored in organic synthesis, proving particularly impactful in building complex cyclic scaffolds from readily available raw materials. Despite its successes, the challenge of selective C-H bond activation remains a major concern, which has been partially addressed using directing groups. While directing groups enhance selectivity in C-H bond functionalization, the removal of these groups poses a significant challenge. To overcome this limitation, an annulation strategy has rapidly gained prominence in recent years for constructing both hetero- and carbocycles. Transition metal-catalyzed C-H annulation and spirocyclization have attracted considerable interest among chemists, offering a rapid and sustainable approach to synthesizing diverse cyclic molecules. In this context, the use of heteroatoms as directing groups in annulation reactions has proven effective in avoiding the need for subsequent removal. The strong coordination of heteroatoms with metals, followed by cyclometallation at adjacent positions, facilitates C-H functionalization/annulation with various partners, making the protocol more practical. In particular, transition metal-catalyzed annulation of imidazo[1,2-*a*]pyridines to generate polyheterocycles is of special interest as these molecules have been less explored, and also these molecules hold significant optical properties.[36-43]

Liu and his group demonstrated a Rh(III)-catalyzed [4+2] annulation reaction of 2-arylimidazo[1,2-*a*]pyridine **(1)** with methyl-2-chloroacetate **(9)** as a coupling reagent for the successful construction of naptho[1′,2′:4,5]imidazo[1,2-*a*]pyridine frameworks **(10)** (**Scheme 3.4)**.[35]

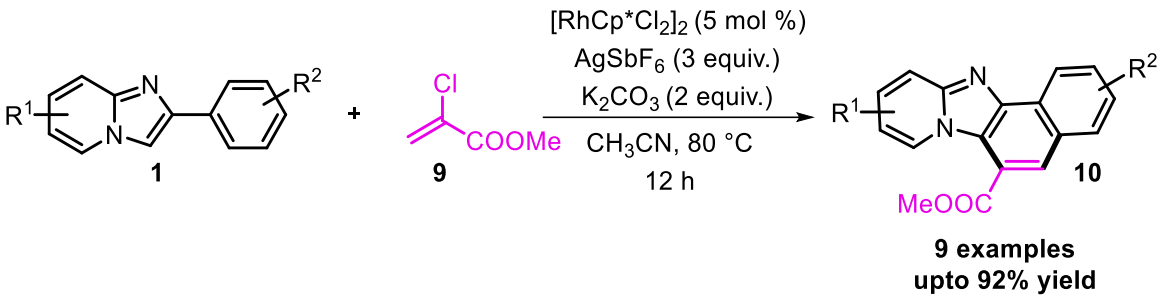

Scheme 3.4: Rh(III)-catalyzed annulation of imidazo[1,2-*a*]pyridine with methyl 2-chloroacrylate

The regioselectivity of this cycloaromatization reaction depends on the mode of action of the catalyst. For example, Pd(II)-catalyzed oxidative annulation has been successfully utilized by Fan and colleagues to synthesize napthofused-imidazo[1,2-*a*]pyridine (**11**) and imidazo[5,1,2-*cd*]indolizine (**12**) derivatives. Through dehydrogenative coupling, imidazo[1,2-*a*]pyridines (**1**) are cycloaromatized with internal alkynes (**7**), resulting in the formation of the desired products (**11**) by selectively breaking C-H bonds within 2-arylimidazo[1,2-*a*]pyridines structures at different positions. Importantly, this reaction exhibits a wide range of applicable substrates, demonstrates good compatibility with various functional groups, and utilizes molecular oxygen as the oxidant, forming the annulated products with poor to good yields (7-86%) **(Scheme 3.5a)**.[44] In 2015, Ghosh *et al*. achieved dual functionalization of 2-arylimidazo[1,2-*a*]pyridines (**1**) using an ionic salt of Pd-catalyst, $Cu(OAc)_2$ as an oxidant, and TBAB. As a result of the reaction, the desired product **(12)** and a minor regioisomeric product (**11**) were obtained, with an overall yield of 85%. This methodology also demonstrated applicability to other heterocyclic substrates. Mechanistic investigations suggested that initially, the catalyst binds at the C-3 position, leading to the formation of an intermediate. Subsequent alkyne insertion and reductive elimination furnished the desired product and Pd(0). The Pd(0) species was then oxidized back to Pd(II) by $Cu(OAc)_2$, enabling its reutilization in the catalytic cycle (**Scheme 3.5b)**.[45] Additionally, Hajra and coworkers achieved the dual C-H bond activation by using imidazo[1,2-*a*]pyridines (**1**) and alkynes (**7**), resulting in the formation of diaza-cyclopenta[*cd*]indene derivatives **(12)**. The method showed high regioselectivity and broad functional group compatibility with moderate to good yields (61-79%) (**Scheme 3.5c)**.[46]

Li *et al.* also documented a noteworthy discovery involving the Rh(III)-catalyzed control of

conditions for dual C-H activation of 2-phenylimidazo[1,2-*a*]pyridines with substituted alkynes (**7**). In the presence of AgOAc, naptho[1',2':4,5]imidazo[1,2-*a*]pyridine (**11**) products were produced with impressive yields *via* chelation-assisted C-H activation at the *ortho* position of the phenyl ring, followed by rollover C-H activation (**Scheme 3.5d**).[47] Conversely, when $AgBF_4$ was used in standard reaction conditions, the reaction produced fused isoquinolinium derivatives (**13**) through C-C and C-X coupling (**Scheme 3.5e**).[47] As a result of this well-designed approach, polyazaheterocycles were synthesized effectively.

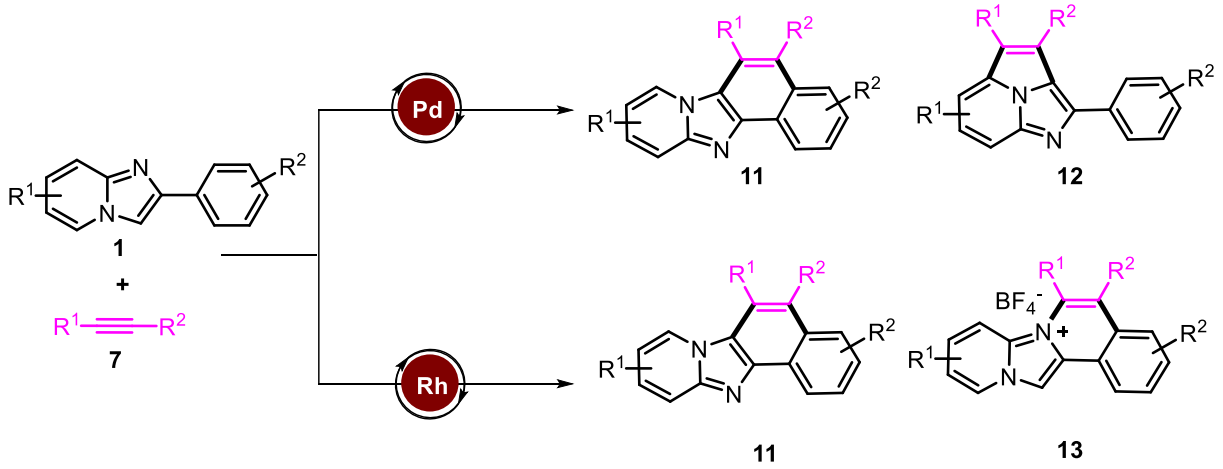

No.	Condition	Examples	Yield%
a)	$Pd(OAc)_2$, $Cu(OAc)_2$, TBAB, DMF, O_2, 100 °C, 12 h	25	upto 86
b)	NHC-based Pd-complex, TBAB, DMA, 90 °C, 12 h	4	upto 89
c)	$Pd(OAc)_2$, $Cu(OAc)_2{\cdot}H_2O$ $_2$, DMSO, 1110 °C, 12 h	19	upto 79
d)	$[RhCp^*Cl_2]_2$, AgOAc, $AgSbF_6$, DCE, 100 °C, 12 h	39	upto 93
e)	$[RhCp^*Cl_2]_2$, $Cu(OAc)_2$, $AgBF_4$, DCE, 100 °C, 24 h	6	upto 88

Scheme 3.5: Pd(II)/Rh(III)-catalyzed oxidative annulation of imidazo[1,2-*a*]pyridines with alkynes

Mu and his group reported a new Pd(II)-catalyzed method for the synthesis of 6*H*-benzo[*b*]imidazo-[5,1,2-*de*]quinolizin-6-one derivatives **(15)** through annulation of imidazo[1,2-*a*]pyridine **(1)** with 2-chlorobenzaldehydes **(14)** (**Scheme 3.6**).[48] They used a $Pd(OAc)_2$ (10 mol %) with Xanthphos ligand and a tetra-butylammonium bromide (NBu_4Br) surfactant in water and air to perform this reaction, which involved two steps: arylation and acylation. Remarkably, both imidazo[1,2-*a*]pyridines (**1**) and 2-chlorobenzaldehydes **(14)** with electron-donating or electron-

withdrawing groups yielded excellent yields of the desired product. This developed methodology commenced with the oxidative addition of the aldehyde to the Pd-ligand complex, generating an intermediate species. Subsequently, this intermediate engaged with imidazo[1,2-*a*]pyridine and later reacted with K_2CO_3, forming the arylated product through reductive elimination. The arylated product then underwent palladation again, creating a Pd-O bond with the carbonyl group of the aldehyde. Ultimately, this sequence of reactions terminated in the formation of the dehydrogenative cyclized product through *β*-elimination.

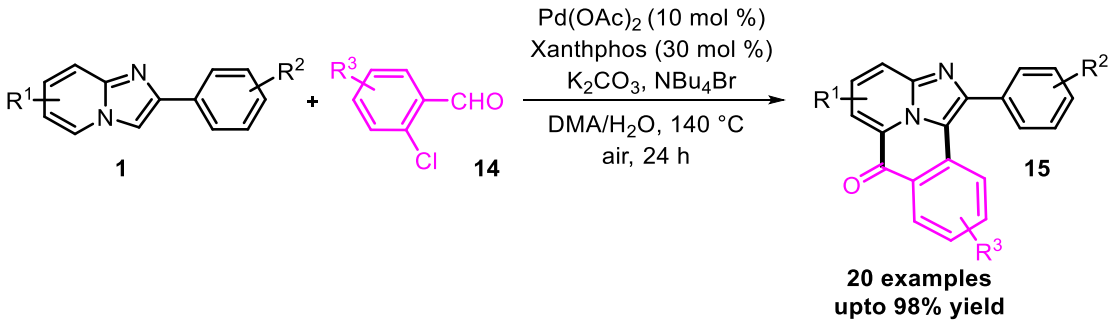

Scheme 3.6: Pd(II)-catalyzed dehydrogenative annulation reaction for the synthesis of 6H-benzo[*b*]imidazo[5,1,2-*de*]quinolizin-6-ones

Li group explored the Rh(III)-catalyzed annulative coupling between 2-phenylimidazo[1,2-*a*]pyridines (**1**) and sulfoxonium ylides (**16**) for synthesis of structurally diverse naphtho fused imidazopyridines (**17**) under mild reaction conditions **(Scheme 3.7).**[49]

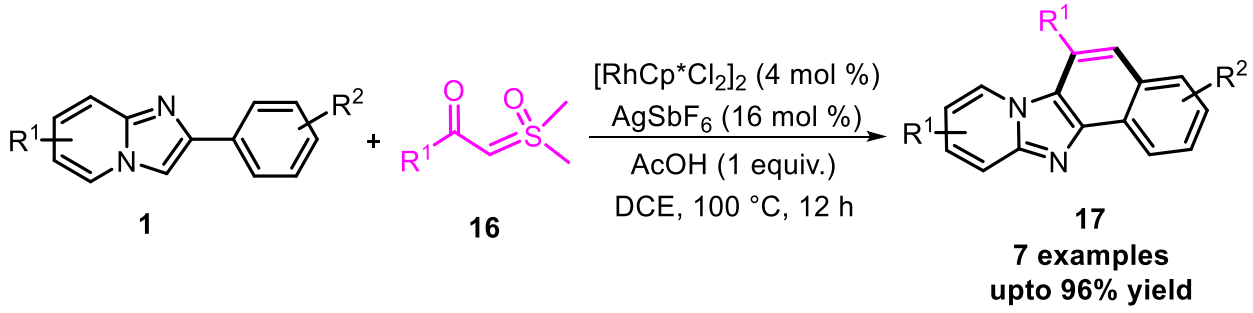

Scheme 3.7: Rh(III)-catalyzed annulation of 2-arylimidazopyidines with sulfoxonium ylides

In 2019, Reddy and his colleagues successfully developed the synthesis of bridged heterocycles by employing Rh(III)-catalyzed bicyclizations of 2-arylimidazo[1,2-*a*]pyridines (**1**) and cyclic enones (**18**) (**Scheme 3.8**).[50] The developed protocol delivered bridged imidazopyridine derivatives (**19**) in good to excellent yields (84-95%) with high regioselectivity. The reaction

pathway involved a sequential conjugate addition of the aryl group's *ortho* C-H bond, followed by a highly regioselective intramolecular C3-alkylation of the imidazopyridine ring.

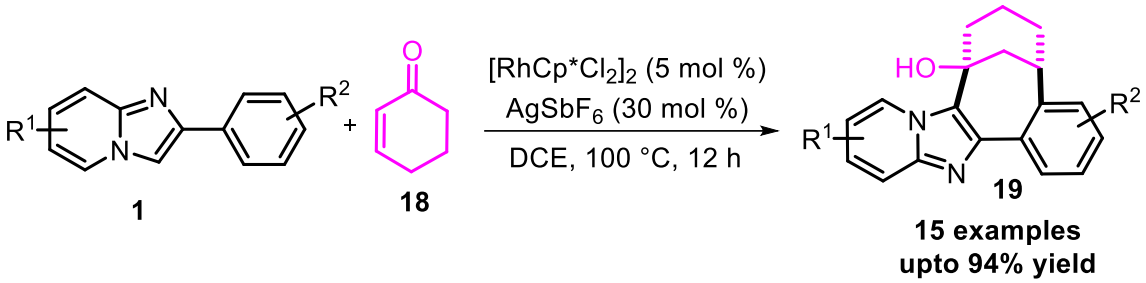

Scheme 3.8: Rh(III)-catalyzed annulation of enones with imidazopyridines

Miura and coworkers reported the Rh(III)-catalyzed oxidative annulation of 2- phenylimidazo[1,2-*a*]pyridines **(1)** with vinylene carbonate **(20)** to afford naphtho- [1′,2′:4,5]imidazo[1,2-*a*]pyridines **(21)** (**Scheme 3.9).**[43] The designed strategy provided an efficient and straightforward tool for the construction of biologically important polyaromatic scaffolds. The present strategy has shown significant features like no need for external oxidants and bases. Interestingly, the unsubstituted vinylene-fused scaffold could be assembled in single-step operation with high regioselectivity.

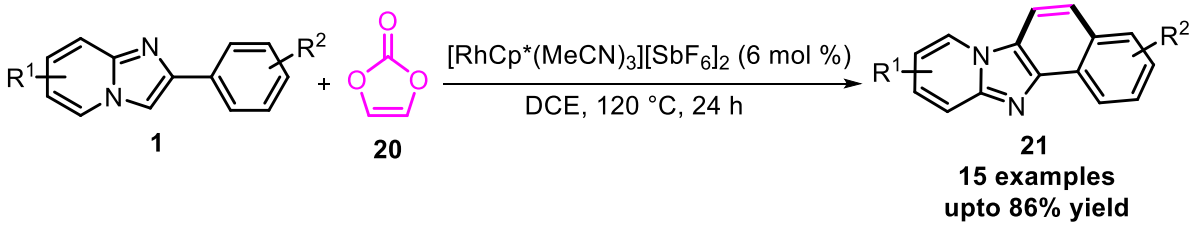

Scheme 3.9: Rh(III)-catalyzed cyclizations of 2-arylimidazopyridines with vinylene carbonate

Wang and co-workers developed a palladium-catalyzed approach for diarylation and intramolecular dehydrogenative coupling reactions of imidazo[1,2-*a*]pyridine **(1)** with diaryliodonium salts (**22**) (**Scheme 3.10**).[51] This strategy has been applied for synthesizing phenanthrol-imidazopyridine fused heterocycles (**23**).

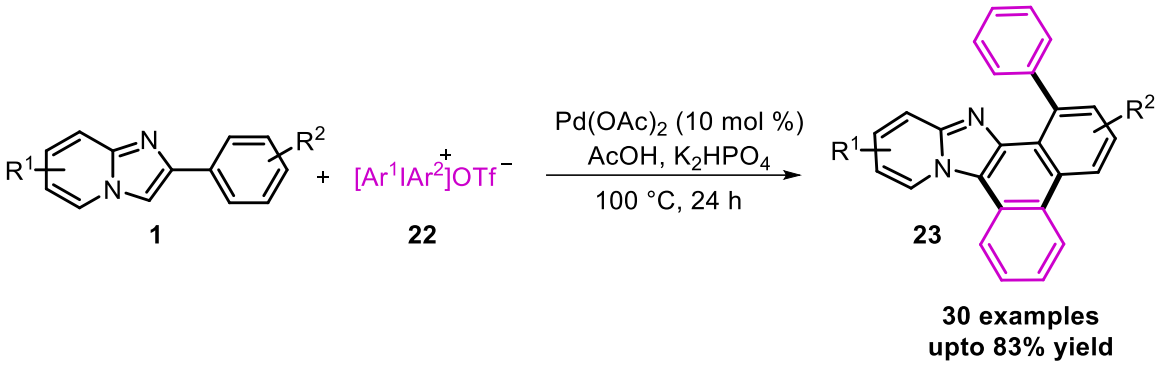

Scheme 3.10: Pd(II)-catalyzed arylation/annulation reaction of 2-arylimidazo[1,2-*a*]pyridine

A cyclized scaffold containing imidazopyridine moiety was obtained in 2020 *via* double C2' and C3 bond activation. The methodology developed by our group, *via* an effective Rh(III)-catalyzed C-H bond functionalization of 2-phenylimidazo[1,2-*a*]pyridines **(1)** by using *N*-substituted maleimides **(24)** as coupling partner produced substituted 1*H*-benzo[e]pyrido[1',2':1,2]imidazo[4,5-*g*]isoindole-1,3(2*H*)-diones **(25)** in good to excellent yields (**Scheme 3.11**).[52] Furthermore, the photophysical properties of certain annulated compounds were investigated by recording both UV-visible absorption and fluorescence spectra. Their observations revealed that most of these compounds exhibited noticeable emission with a maximum wavelength of 419-498 nm, accomplished by high fluorescence quantum yields.

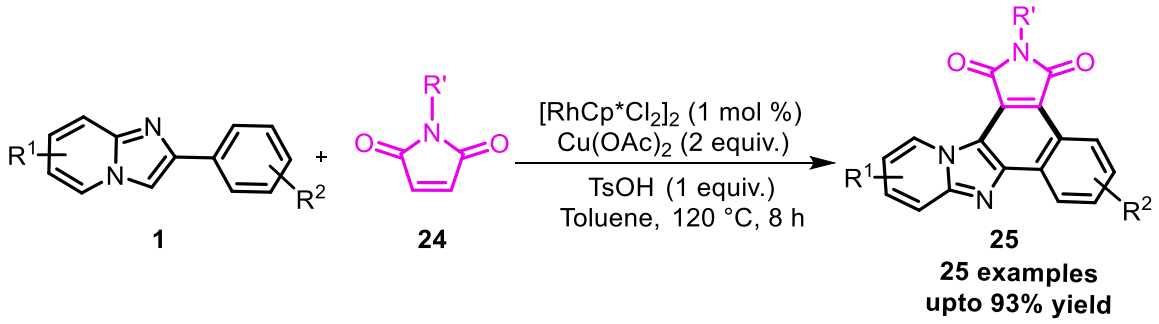

Scheme 3.11: Rh(III) mediated cross-dehydrogenative reaction of imidazo[1,2-*a*]pyridine with substituted maleimides

Li group disclosed a Rh(III)-catalyzed dialkylation-annulation of 2-arylimidazo[1,2-*a*]pyridine **(1)** with diazo compounds (**26**) (**Scheme 3.12**).[53] The reaction proceeded through the formation of a dialkylated arene, followed by an intramolecular nucleophilic attack of the C-3 position of imidazopyridine at the proximal carbonyl group. Further, mechanistic investigations revealed that

the final nucleophilic cyclization step is the rate-determining step. These coupling systems utilized readily available arenes and unsaturated coupling partners to prepare carbocycles **(27)**. This methodology holds promise for applications in the synthesizing of complex molecular structures.

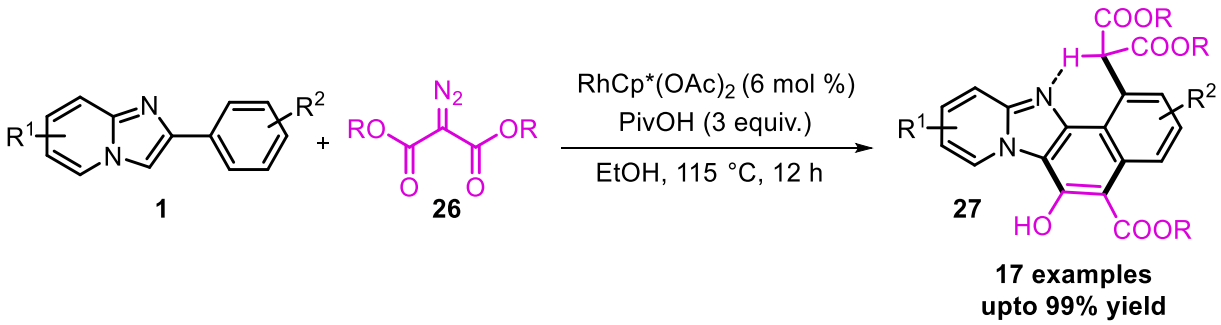

Scheme 3.12: Rh(III)-catalyzed dialkylation-annulation reaction of 2-arylimidazo[1,2-*a*]pyridine

A diastereoselective cascade reaction involving Rh(III)-catalyzed annulation of 2-arylimidazo[1,2-*a*]pyridines **(1)** with *p*-quinol **(28)** has been accomplished by Nayani and colleagues (**Scheme 3.13**).[54] This methodology produced bridged heterocycles with three nearby stereocenters facilitated by a twofold conjugate addition process. Initially, the phenyl ring's *ortho* C-H bond in imidazo[1,2-*a*]pyridines undergoes functionalization through Rh(III)-catalysis, with the involvement of *p*-quinol in the process. Subsequently, an intramolecular conjugate addition occurs, yielding a diverse array of novel bridged heterocycles **(29)**.

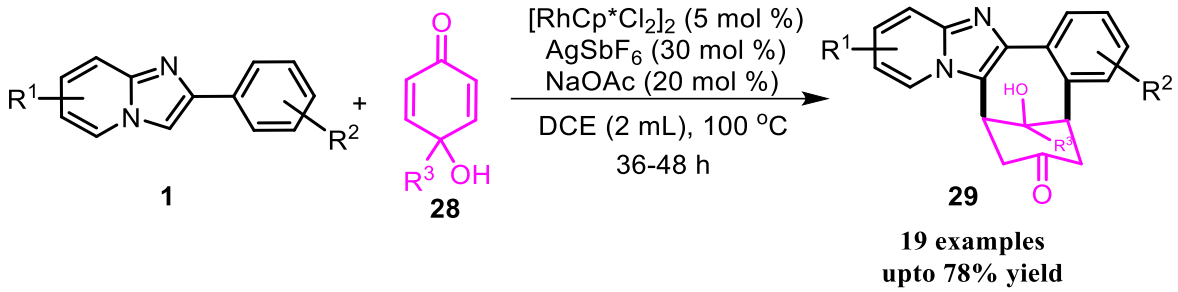

Scheme 3.13: Rh(III)-catalyzed annulation reaction of 2-arylimidazo[1,2-*a*]pyridines with cyclic enones

In this chapter, we developed the catalyst dependent regioselective oxidative annulation of 2-arylimidazo[1,2-*a*]pyridines with cinnamaldehyde derivatives to afford 5-arylnaphtho[1',2':4,5]imidazo[1,2-*a*]pyridine-6-carbaldehyde and 1,7-diarylimidazo[5,1,2-*cd*]indolizine-6-carbaldehyde, respectively (**Scheme 3.14**). Surprisingly, there have been no

reports of site-selective annulation at the *ortho* and C-3 positions of imidazo[1,2-*a*]pyridine using a cinnamaldehyde as a coupling partner.

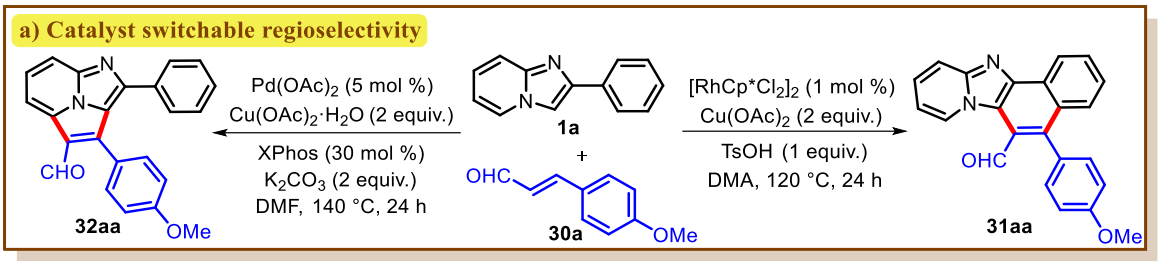

Scheme 3.14: Rh(III) and Pd(II)-catalyzed annulation approach for the synthesis of naphtho and indazolo-fused imidazopyridines.

3.2 RESULTS AND DISCUSSIONS

Initially, we performed reaction of 2-phenylimidazo[1,2-*a*]pyridine (**1a**) with *trans*-4-methoxycinnamaldehyde (**30a**) in the presence of $[RhCp^*Cl_2]_2$ (1 mol %) as a catalyst, $Cu(OAc)_2$ (2 equiv.) as oxidant, TsOH (1 equiv.) as an additive in toluene at 120 °C for 24 h. Interestingly, 5-(4-methoxyphenyl)naphtho[1',2':4,5]imidazo[1,2-*a*]pyridine-6-carbaldehyde **(31aa)** was observed in 39% yield as the sole annulated product (**Table 3.1**, entry 1). The compound **31aa** was characterized by ^1H, $^{13}C\{^1H\}$ NMR, HRMS and single crystal X-ray (**CCDC No.** 2107392). To further improve yield of the annulated product **31aa**, various reaction parameters such as oxidants, catalysts, additives, and solvents were screened. Examination of different solvents such as THF, DCE, TFE, DMF, DMSO, and DMA (**Table 3.1**, entries 2-7) indicated that polar aprotic solvents like DMF, DMSO and DMA were more effective producing **31aa** in 68%, 52%, and 76% yields, respectively. Changing oxidant with $Cu(OAc)_2·H_2O$, AgOAc, Ag_2CO_3, and $K_2S_2O_8$ (**Table 3.1**, entries 8-11) or acidic additive with ADA, PivOH, AcOH, and TFA (**Table 3.1**, entries 12-15) did not improve yield of **31aa**. Reaction of **1a** with **30a** in the absence of catalysts (**Table 3.1**, entry 16) failed to produce any product and starting substrates were recovered in almost quantitative yield indicating indispensable role of the catalyst for this reaction. Further, reaction of **1a** with **30a** using $[RuCl_2(p\text{-cymene})]_2$ (**Table 3.1**, entry 17) and $Pd(OAc)_2$ (**Table 3.1**, entry 18) as catalyst produced **31aa** in lower yields. Interestingly, when $Pd(OAc)_2$ was used as catalyst along with **31aa** (36%) an isomeric product, 7-(4-methoxyphenyl)-1-phenylimidazo[5,1,2-*cd*]indolizine-6-carbaldehyde (**32aa**), was also obtained in 15% yield.

With aforementioned result, we started investigating the optimal reaction conditions for the synthesis of **32aa**. Interestingly, yield of **32aa** improved by replacing acidic additive with K_2CO_3 (2 equiv.) and solvent with DMF (**Table 1**, entries 19-20). Subsequently, the effect of various ligand such as SPhos, PCy_3, PPh_3, Xanthphos and XPhos was examined (**Table 1**, entries 21-25) and it was found that the yield of **32aa** (71%) was significantly increased when Xphos was used as the ligand (**Table 1**, entry 25). The yield of **31aa** drastically decreased when reaction of **1a** and **30a** was performed in the absence of oxidant (**Table 1**, entry 26) or using other palladium catalysts such as $PdCl_2$, $PdCl_2(MeCN)_2$ and $PdCl_2(PPh_3)_2$ (**Table 1**, entries 27-29).

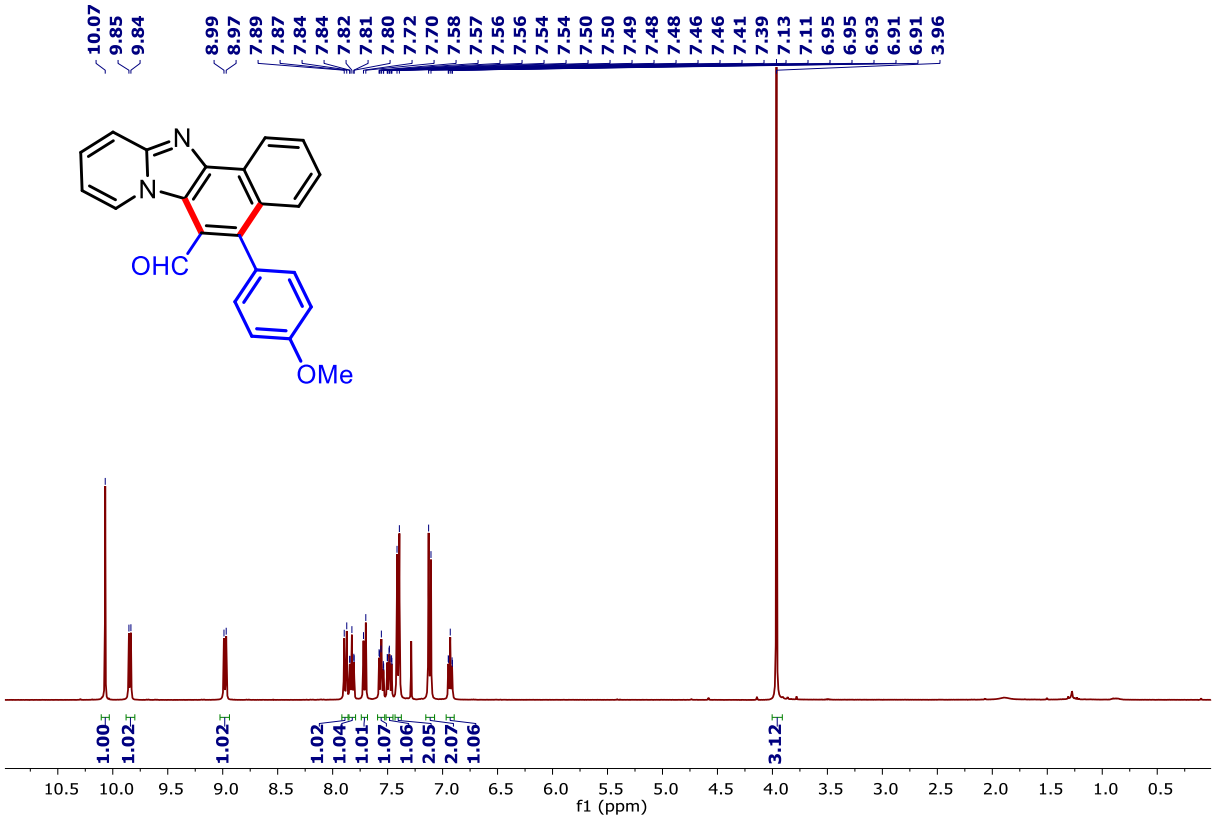

Figure 3.2: ^{1}H-NMR spectrum 5-(4-methoxyphenyl)naphtho[1',2':4,5]imidazo[1,2-*a*]pyridine-6-carbaldehyde (**31aa**) recorded in $CDCl_3$

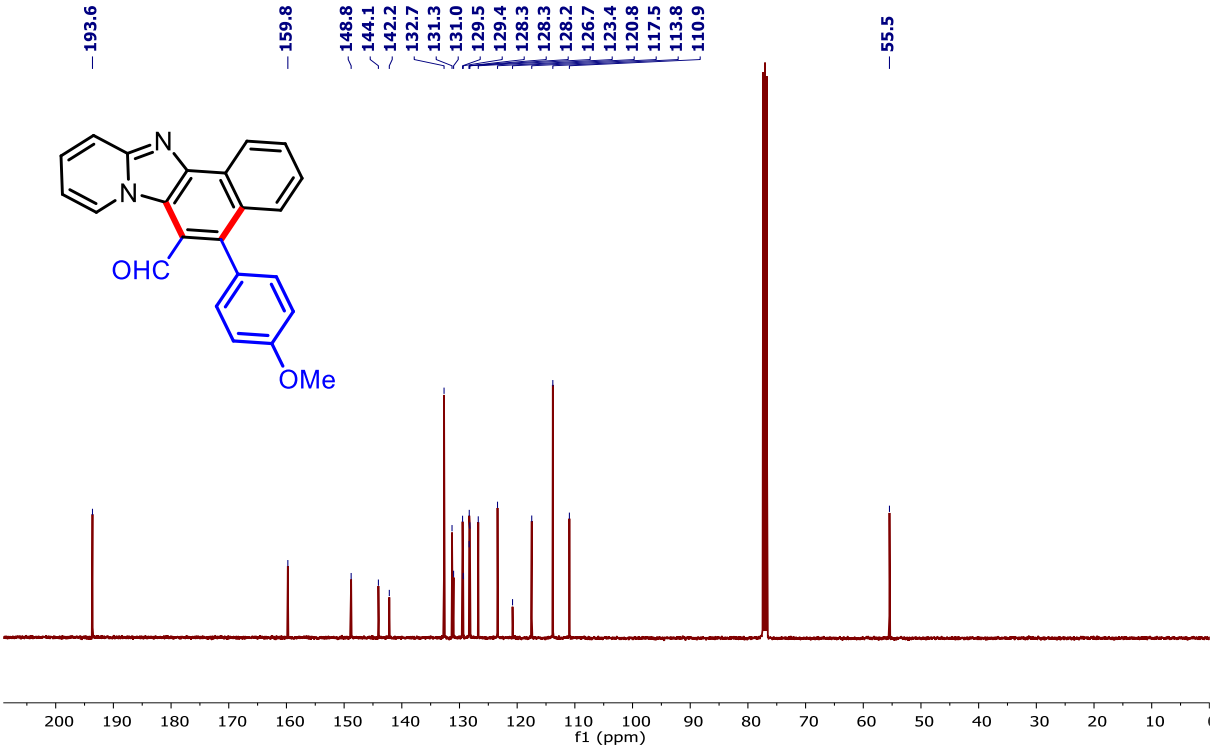

Figure 3.3: $^{13}C\{^{1}H\}$-NMR spectrum of 5-(4-methoxyphenyl)naphtho[1',2':4,5]imidazo[1,2-*a*]pyridine-6-carbaldehyde (**31aa)** recorded in $CDCl_3$

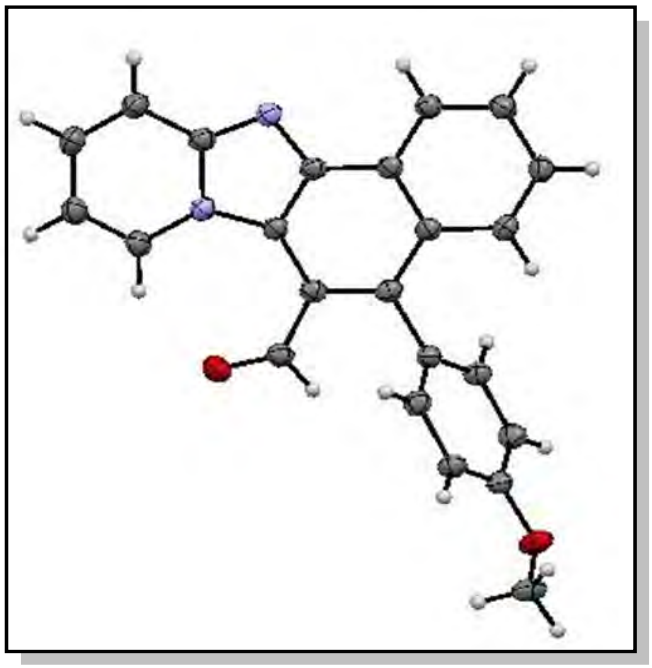

Figure 3.4: The ORTEP diagram of **31aa** [CCDC: 2107392]. Thermal ellipsoids are drawn at 50 % probability level

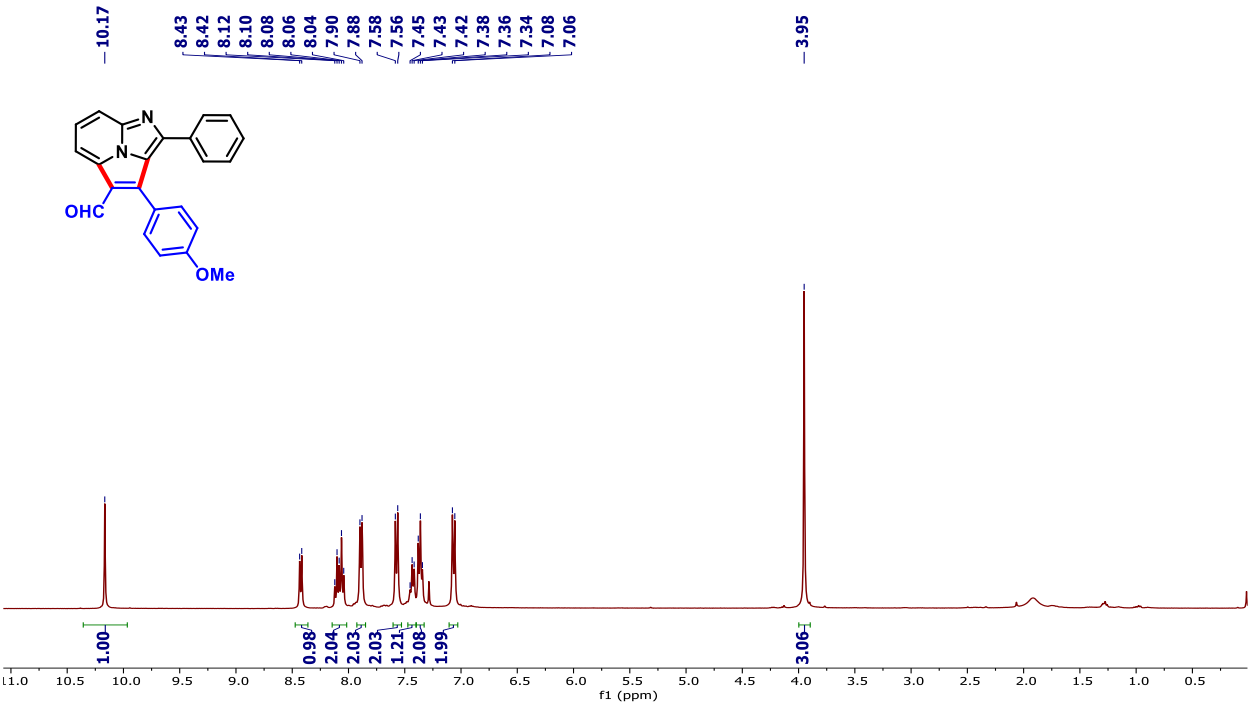

Figure 3.5: ^{1}H-NMR spectrum of 7-(4-methoxyphenyl)-1-phenylimidazo[5,1,2-*cd*]indolizine-6-carbaldehyde (**32aa**) recorded in $CDCl_3$

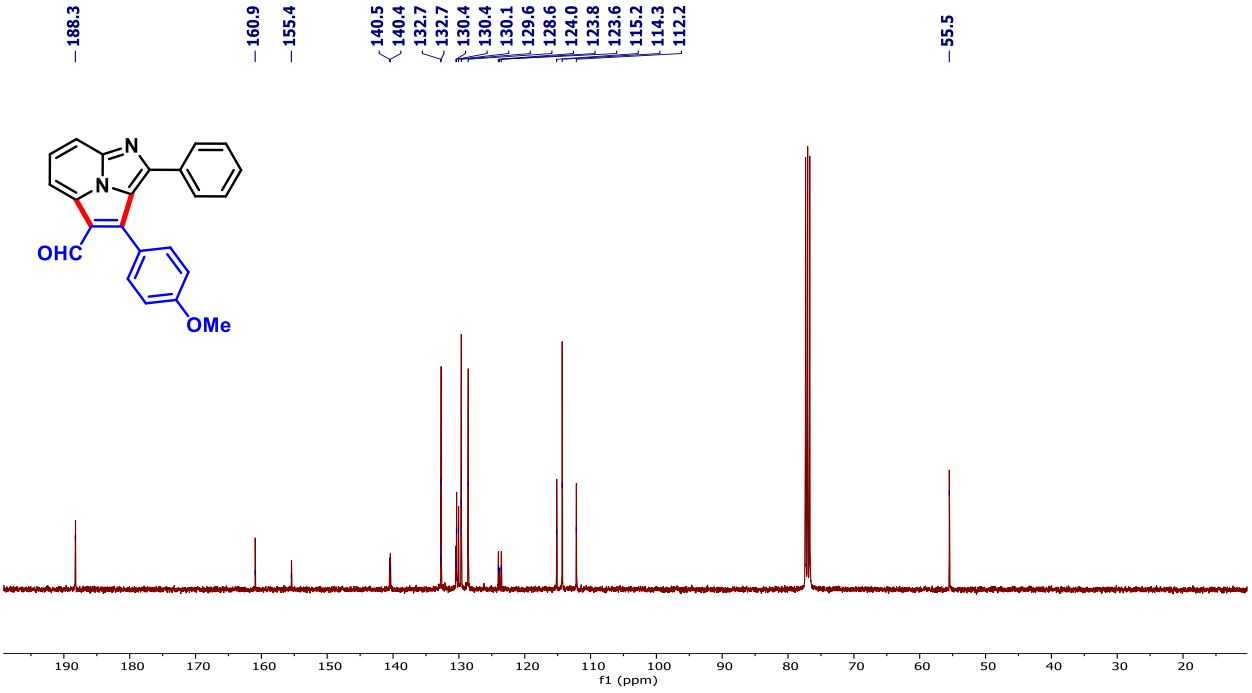

Figure 3.6: ^{13}C{^{1}H}-NMR spectrum of 7-(4-methoxyphenyl)-1-phenylimidazo[5,1,2-*cd*]indolizine-6-carbaldehyde (**32aa)** recorded in CDC

Table 3.1: Optimization of the reaction conditions.

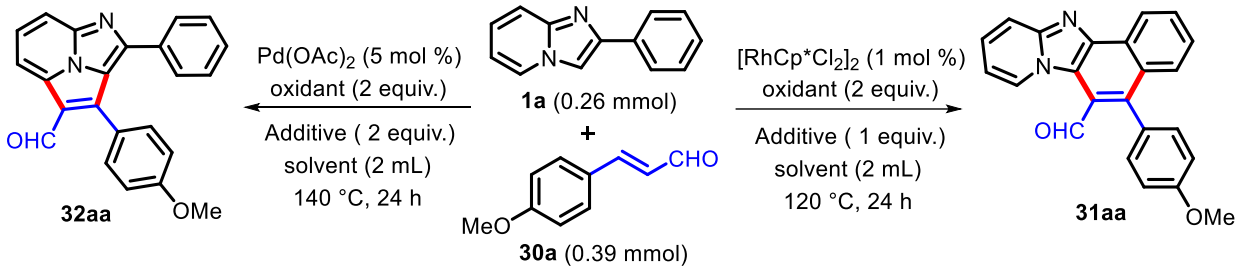

Entry	Catalyst	Oxidant	Ligand	Additive	Solvent	Yield (%)[a]	
						35aa	**36aa**
1	$[RhCp^*Cl_2]_2$	$Cu(OAc)_2$	-	TsOH	toluene	39	-
2	$[RhCp^*Cl_2]_2$	$Cu(OAc)_2$	-	TsOH	DCE	41	-
3	$[RhCp^*Cl_2]_2$	$Cu(OAc)_2$	-	TsOH	THF	trace	-
4	$[RhCp^*Cl_2]_2$	$Cu(OAc)_2$	-	TsOH	TFE	23	-
5	$[RhCp^*Cl_2]_2$	$Cu(OAc)_2$	-	TsOH	DMF	68	-
6	$[RhCp^*Cl_2]_2$	$Cu(OAc)_2$	-	TsOH	DMSO	52	-
7	**$[RhCp^*Cl_2]_2$**	**$Cu(OAc)_2$**	**-**	**TsOH**	**DMA**	**76**	**-**
8	$[RhCp^*Cl_2]_2$	$Cu(OAc)_2.H_2O$	-	TsOH	DMA	71	-
9	$[RhCp^*Cl_2]_2$	$K_2S_2O_8$	-	TsOH	DMA	21	-
10	$[RhCp^*Cl_2]_2$	AgOAc	-	TsOH	DMA	33	-
11	$[RhCp^*Cl_2]_2$	Ag_2CO_3	-	TsOH	DMA	29	-
12	$[RhCp^*Cl_2]_2$	$Cu(OAc)_2$	-	ADA	DMA	66	-
13	$[RhCp^*Cl_2]_2$	$Cu(OAc)_2$	-	PivOH	DMA	62	-
14	$[RhCp^*Cl_2]_2$	$Cu(OAc)_2$	-	AcOH	DMA	41	-
15	$[RhCp^*Cl_2]_2$	$Cu(OAc)_2$	-	TFA	DMA	12	-
16	-	$Cu(OAc)_2$	-	TsOH	DMA	-	-
17	$[Ru(p\text{-cymene})Cl_2]_2$	$Cu(OAc)_2$	-	TsOH	DMA	38	-
18	$Pd(OAc)_2$	$Cu(OAc)_2$	-	TsOH	DMA	36	15
19	$Pd(OAc)_2$	$Cu(OAc)_2{\cdot}H_2O$	-	K_2CO_3	DMA	-	27
20	$Pd(OAc)_2$	$Cu(OAc)_2{\cdot}H_2O$	-	K_2CO_3	DMF	-	41
21	$Pd(OAc)_2$	$Cu(OAc)_2{\cdot}H_2O$	SPhos	K_2CO_3	DMF	-	31
22	$Pd(OAc)_2$	$Cu(OAc)_2{\cdot}H_2O$	PCy_3	K_2CO_3	DMF	-	39
23	$Pd(OAc)_2$	$Cu(OAc)_2{\cdot}H_2O$	PPh_3	K_2CO_3	DMF	-	23
24	$Pd(OAc)_2$	$Cu(OAc)_2{\cdot}H_2O$	Xanthphos	K_2CO_3	DMF	-	35
25	**$Pd(OAc)_2$**	$Cu(OAc)_2{\cdot}H_2O$	**Xphos**	K_2CO_3	**DMF**	-	**71**
26	$Pd(OAc)_2$	-	XPhos	K_2CO_3	DMF	-	47
27	$PdCl_2$	$Cu(OAc)_2{\cdot}H_2O$	Xphos	K_2CO_3	DMF	-	23
28	$PdCl_2(MeCN)_2$	$Cu(OAc)_2{\cdot}H_2O$	XPhos	K_2CO_3	DMF	-	20
29	$PdCl_2(PPh_3)_2$	$Cu(OAc)_2{\cdot}H_2O$	XPhos	K_2CO_3	DMF	-	17

[a]Isolated yield.

Under the best-identified reaction conditions for Rh(III)-catalyzed annulation reaction, we next examined the scope with respect to the 2-arylimidazo[1,2-*a*]pyridines (**Table 3.2**). A variety of 2-arylimidazo[1,2-*a*]pyridines (**1a-i**) bearing both electron-donating as well as electron-withdrawing groups on C2-phenyl ring reacted smoothly with **30a** to afford corresponding annulated products **31aa-31ia** in 51-78% yields. Notably, slightly higher yields of the annulated products were obtained from substrates with electron-donating groups on C2-phenyl ring as compared to those with electron-withdrawing groups on C2-phenyl ring (Compare **31ba** and **31ca** vs **31ea-31ha**). The position of the substituents on the C2-phenyl ring did not have much influence on the yield of the annulated product. 2-Arylimidazo[1,2-*a*]pyridines (**1j-l**) with methyl group on imidazopyridine nucleus produced corresponding annulated products **31ja-la** in good yields.

Table 3.2: Synthesis of 5-arylnaphtho[1',2':4,5]imidazo[1,2-*a*]pyridine-6-carbaldehydes.[a,b]

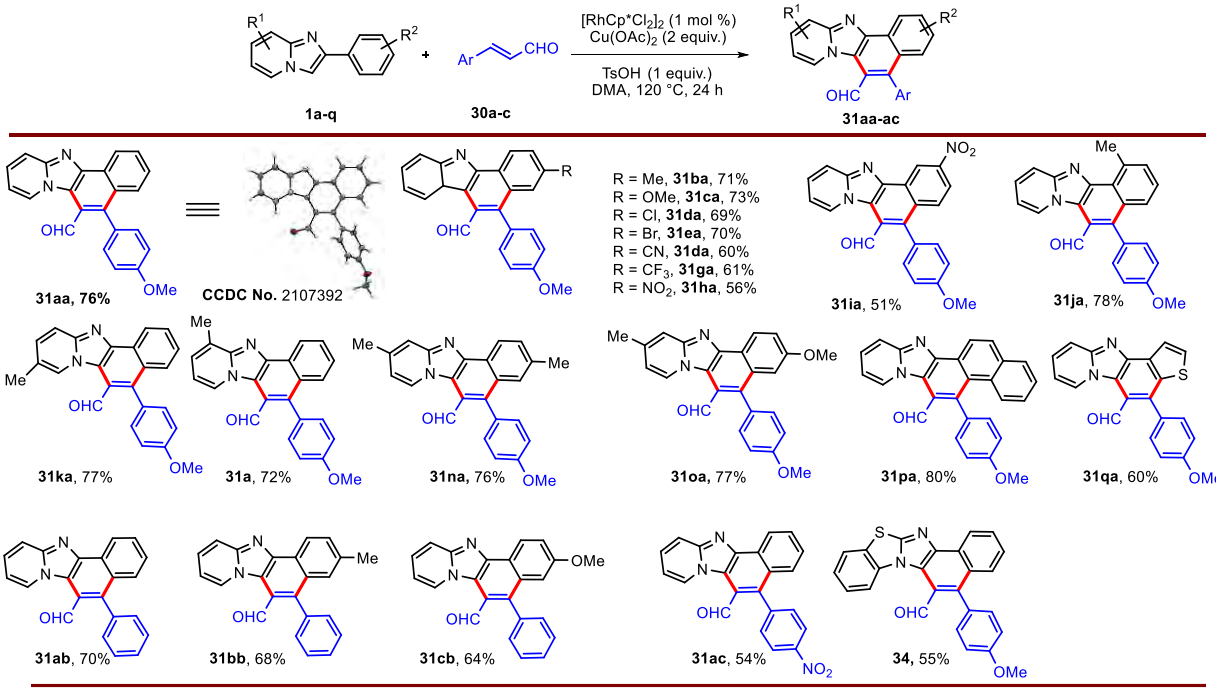

[a]Reaction condition: **1** (0.26 mmol), **30**(0.39 mmol), [RhCp*Cl_2]$_2$ (1 mol %), $Cu(OAc)_2$ (0.52 mmol), TsOH (0.26 mmol), DMA (2 mL), 120 °C for 24 h in oil bath.

[b]Isolated yield

2-(Napthyl-2-yl)imidazo[1,2-*a*]pyridine (**1m**) and 2-(thiophene-2-yl)imidazo[1,2-*a*]pyridine (**1n**) also reacted with **30a** to generate the corresponding products **31ma** and **31na** in 80% and 60% yields, respectively. Subsequently, we probed the scope and generality of the protocol with respect to cinnamaldehyde (**30b**). Reaction of **30b** with **1a-c** produced corresponding annulated products

31ab-ac in good (64-70%) yields. The reaction of (*E*)-3-(4-nitrophenyl)acrylaldehyde (**30c**) with **1a** produced corresponding annulated product **31ac** in 54% yield. To our delight, the developed methodology is also applicable for 2-phenylbenzo[*d*]imidazo[2,1-*b*]thiazole (**33a**), giving corresponding annulated product **34** in 55% yield.

Next, we examined the substrate scope for the synthesis of 7-aryl-1-phenylimidazo[5,1,2-*cd*]indolizine-6-carbaldehydes (**32aa**) by reacting various 2-arylimidazo[1,2-*a*]pyridines (**1a-n**) with **30a** under Pd(II)-catalysis following **Table 3.1**, entry 25 reaction conditions (**Table 3.3**). Annulated products (**32aa-ha**) were obtained in moderate to good (52-71%) yields from 2-arylimidazo[1,2-*a*]pyridines with both electron-donating groups such as Me, OMe as well as electron-withdrawing groups such as Cl, CN, CF_3 and NO_2 at *para*/*meta* positions of C2-phenyl ring. Variations in the electronic properties of C2-phenyl ring did not have a significant effect on the yields of annulated product. The regioselectivity of the annulated product **32ca** was unambiguously confirmed by the single X-ray crystallography (**CCDC No.** 2107376). Similarly, 2-arylimidazo[1,2-*a*]pyridines (**1j-l**) with a methyl group on imidazopyridine nucleus produced corresponding annulated products **32ja-la** in good (62-73%) yields. 2-Napthylimidazo[1,2-*a*]pyridine (**1m**) and 2-thienylimidazo[1,2-*a*]pyridine (**1n**) also furnished corresponding annulated products **32ma** and **32na** in 65% and 53% yields, respectively.

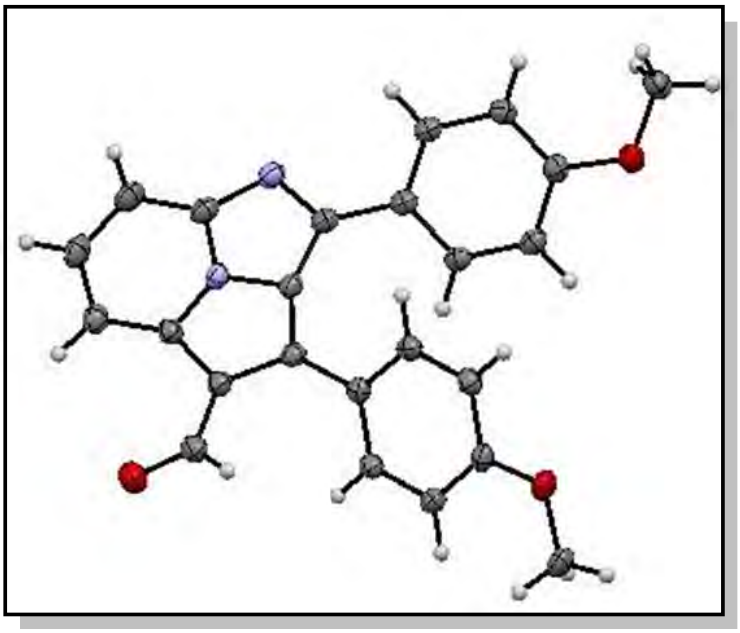

Figure 3.7: The ORTEP diagram of **32ca** [CCDC: 2107376]. Thermal ellipsoids are drawn at 50 % probability level

Table 3.3: Synthesis of 7-aryl-1-phenylimidazo[5,1,2-*cd*]indolizine-6-carbaldehydes.[a,b]

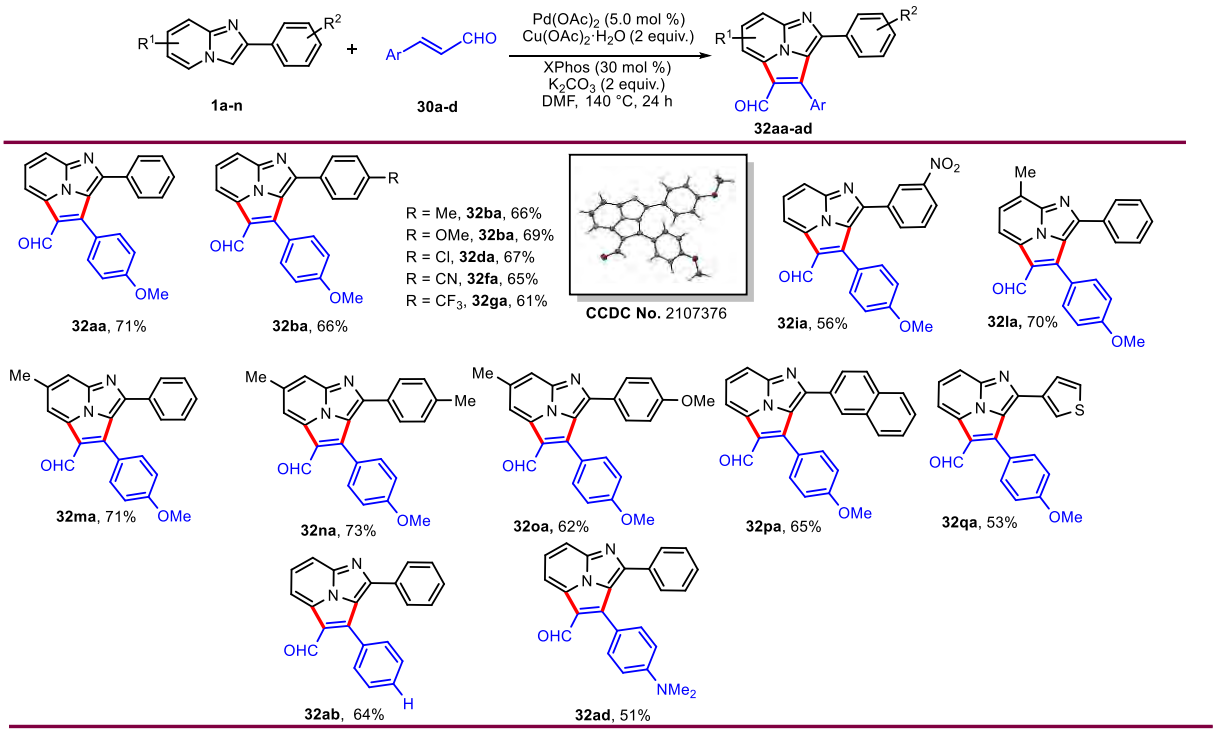

[a]Reaction condition: **1a** (0.26 mmol), **30a** (0.39 mmol), $Pd(OAc)_2$ (5 mol %), $Cu(OAc)_2 \cdot H_2O$ (2 equiv.), XPhos (30 mol %), K_2CO_3 (2.0 equiv.), DMF (2 mL), 140 °C for 24 h in oil bath.

[b]Isolated yield.

Moreover, other cinnamaldehyde derivatives are also suitable substrates for the reactions. For instance, **30b** and (*E*)-3-(4-(dimethylamino)phenyl)acrylaldehyde (**30d**) reacted smoothly with **1a** under optimized conditions to furnish corresponding annulated products **32ab** and **32ad** in 64% and 51% yields, respectively.

To evaluate the synthetic potential of these chemical transformations, gram scale experiments have been demonstrated (**Table 3.4**). The substrate **1a** on reaction with **30a** under optimal conditions afforded the corresponding annulated products 6-(4-methoxyphenyl)naphtho[1',2':4,5]imidazo-[1,2-*a*]pyridine-5-carbaldehyde **(32aa)** and 7-(4-methoxyphenyl)-1-phenylimidazo[5,1,2-*cd*]-indolizine-6-carbaldehyde **(32aa)** in 71% and 68% yields, respectively. The synthetic utility of the protocol was further explored by the reduction of aldehyde moiety (**Table 3.4**). The annulated product **32aa** was treated with $NaBH_4$ in methanol to produce (7-(4-methoxyphenyl)-1-phenylimidazo[5,1,2-*cd*]indolizin-6-yl)methanol (**35**) in 86% yield.

Table 3.4: Gram-scale experiment and synthetic utility.

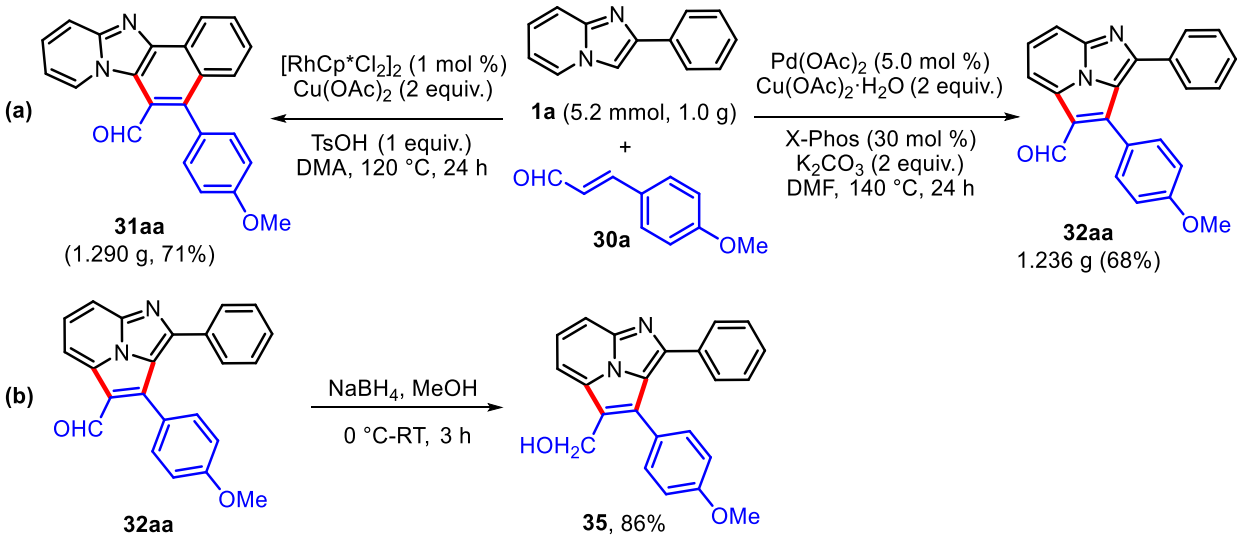

To know the mode of action, we carried out a detailed mechanistic investigation by radical trapping experiment, deuterium labelling, KIE experiment, and intermediate isolation (**Scheme 3.15**). The yield of **31aa** and **32aa** under standard conditions were unaffected by the presence of radical scavengers such as TEMPO (2,2,6,6-tetramethylpiperidine-1-oxyl) and BHT (2,6-di-*tert*-butyl-4-methylphenol) indicating that the reaction does not follow radical pathway (**Scheme 3.15a**). Hydrogen/deuterium (H/D) exchange experiments were conducted both under Rh(III)-catalyzed and Pd(II)-catalyzed conditions (**Scheme 3.15b**). When **1a** was mixed with 25 equivalents of D_2O under standard conditions of Rh(III)-catalysis, H/D exchange was observed at the C3-position and at the *ortho*-positions of C2-phenyl ring in **1a**. On the other hand, mixing **1a** with 25 equivalents of D_2O under standard conditions of Pd(II)-catalysis led to increased H/D exchange at the C3-position of **1a**.

a) Radical trapping experiment

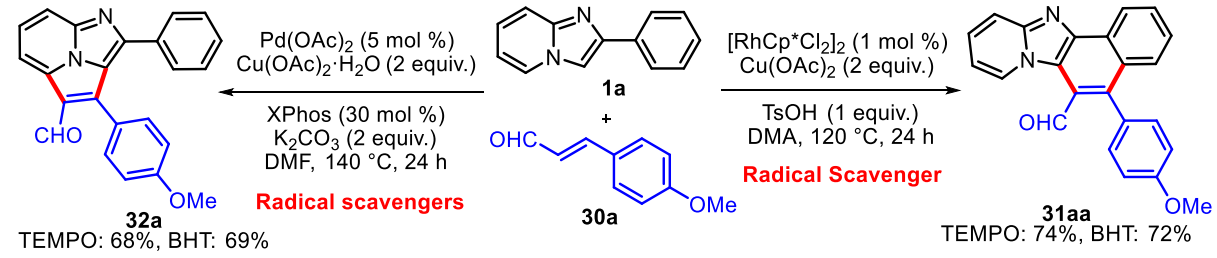

b) Deuterium exchange experiment

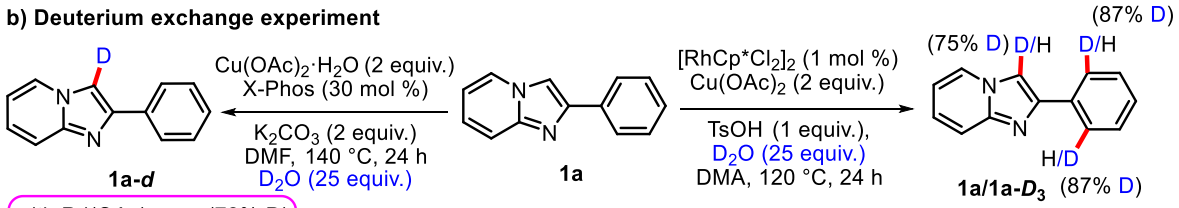

with $Pd(OAc)_2$ (72% D)
without $Pd(OAc)_2$ (22% D)

c) Intermediate detection

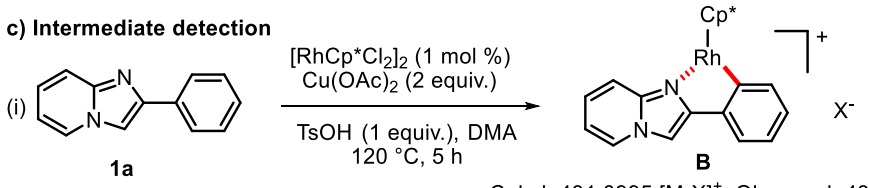

Calcd: 431.0995 $[M-X]^+$, Observed: 431.0992

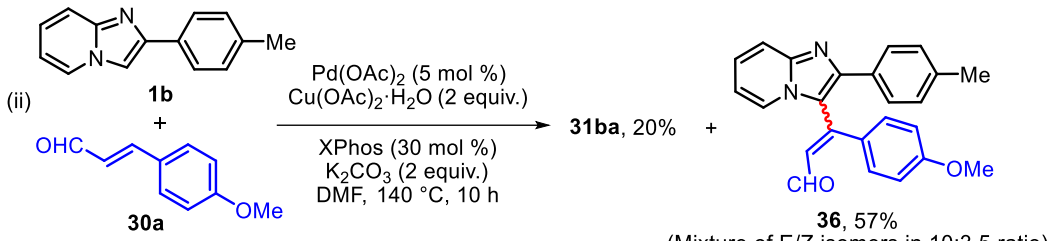

(Mixture of E/Z isomers in 10:3.5 ratio)

d) KIE study (intramolecular competition)

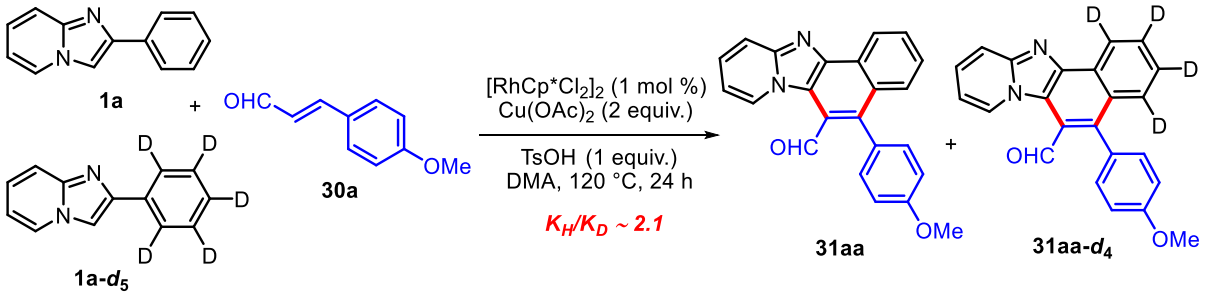

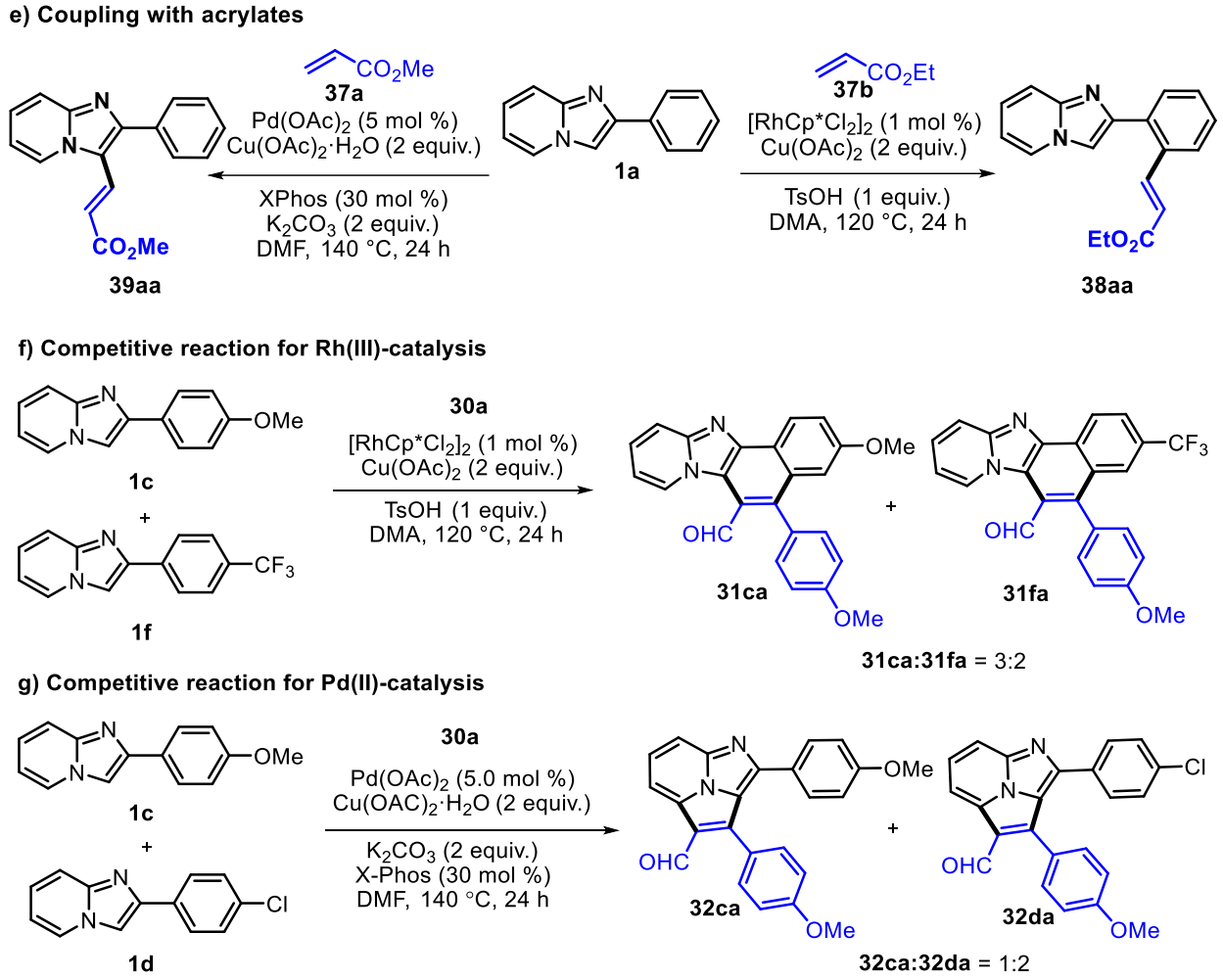

Scheme 3.15: Control experiments

A peak at *m/z* 431.0992 corresponding to $C_{23}H_{24}N_2Rh$ $[M]^+$ ion was observed in the HRMS analysis of the reaction of **1a** in the absence of **30a** using Rh(III)-catalyst under the optimized conditions after 5 h indicated that rhodacycle **B** is an intermediate in this reaction (**Scheme 3.15c (i)**). For intercepted Pd(II)-catalyzed reaction of **1b** and **30a** after 10 h, E/Z mixture of 3-(4-methoxyphenyl)-3-(2-(*p*-tolyl)imidazo[1,2-*a*]pyridin-3-yl)acrylaldehyde (**31**) in 10:3.5 ratio was observed (**Scheme 3.15c (ii)**). An intermolecular kinetic isotope experiment was performed for Rh(III)-catalyzed annulation reaction by subjecting an equimolar mixture of **1a** and its deuterated analogue **1a-*d*$_5$** under standard reaction conditions (**Scheme 3.15d**). An isotope kinetic effect (k_H/k_D) of 2.1 was observed, implying that the Rh-mediated *ortho*-C-H bond cleavage is the rate-determining step. Further, we examined acrylates (**37a** and **37b**) as coupling partners under the standard reaction conditions. The reaction of **1a** with methylacrylate (**37a**) under palladium

catalysis led to formation of C3-functionalized imidazo[1,2-*a*]pyridine derivative **39aa** in 55% yield, while reaction of **1a** with ethylacrylate (**37b**) under Rh catalysis resulted in formation of **38aa** in 60% yield through directed ortho-alkenylation of the C2-phenylringof **1a** (**Scheme 3.15e**).

Competitive reaction of **1c** and **1f** with **30a** under Rh catalysis produced the corresponding products **32ca** and **32fa** in a 1:2 ratio (**Scheme 3.15f**), indicating that the reaction was more favorable for substrates with the C2-phenyl ring substituted with electron-withdrawing groups. Similarly, competitive reaction of **1c** and **1d** with **34a** under Pd catalysis produced the corresponding products **36ca** and **36da** in a 3:2 ratio (**Scheme 3.16g**), indicating that electron-rich imidazo[1,2-*a*]pyridines are more favorable for this reaction.

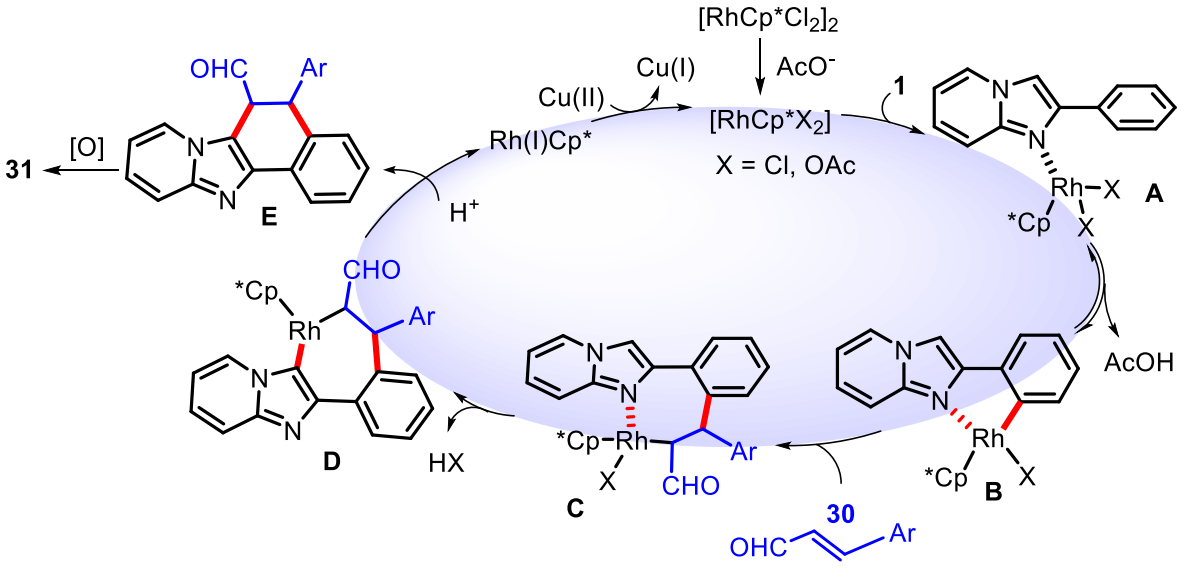

Scheme 3.16: Tentative mechanism for the formation of **31** by Rh(III)-catalyzed annulation of **1** with **32**.

On the basis of control experiments and previous literature reports,[37, 39, 40, 55, 56] the tentative mechanism for the Rh(III)-catalyzed and Pd(II)-catalyzed annulation reactions has been depicted in **Scheme 3.16** and **Scheme 3.17**, respectively. In Rh(III)-catalyzed annulation reaction initially, a monomeric cationic rhodium complex [RhCp*X_2] where X can be Cl or OAc is generated *in situ* from the dimeric [RhCp*Cl_2]$_2$ complex and $Cu(OAc)_2$, which coordinates effectively with the nitrogen atom of **1** to form the intermediate **A** which then forms rhodacycle **B** by *ortho*-C–H bond activation of C2-phenyl ring. Chelation of cinnamaldehyde derivative with Rh(III) followed by oxidative migratory insertion into the Rh–C bond affords intermediate **C**. Rollover C_3–H activation produces a seven-membered rhodacycle **D,** which undergoes reductive elimination under acidic

conditions to generate intermediate **E** and Rh(I) species. Finally, oxidation of **E** in the presence of $Cu(OAc)_2$ would furnish annulated product **31** along with regeneration of active Rh(III) catalyst from Rh(I) species.

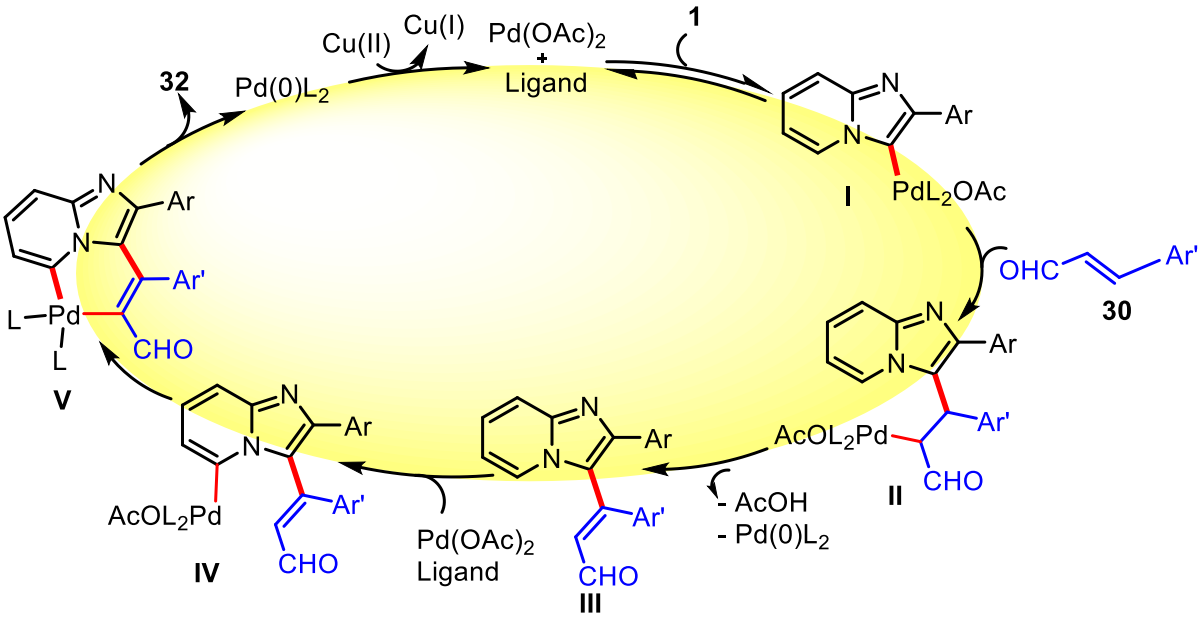

Scheme 3.17: Tentative mechanism for the formation of **32** by Pd(II)-catalyzed annulation of **1** with **30**.

On the other hand, in the case of Pd(II)-catalyzed annulation reaction, initially electrophilic palladation at C3-position of imidazolyl moiety takes place to generate intermediate **I**. After that, the insertion of cinnamaldehyde affords the carbopalladation intermediate **II,** which undergoes the β-hydrogen elimination to produce the alkenylated intermediate **III** and liberates $Pd(0)L_2$ species, which upon oxidation in the presence of $Cu(OAc)_2$ regenerates Pd(II) catalyst. Subsequently, palladation at C7-position generates intermediate **IV,** which then furnishes a seven-membered palladacycle intermediate **V** by concerted metalation deprotonation process. Finally, product **32** is generated from **V** through reductive elimination.

3.3 CONCLUSIONS

In conclusion, we have developed a catalyst-controlled regioselective oxidative annulation of 2-arylimidazo[1,2-*a*]pyridines with cinnamaldehyde derivatives. The annulation reaction afforded 5-arylnaphtho[1',2':4,5]imidazo[1,2-*a*]pyridine-6-carbaldehydes in the presence of $[RhCp^*Cl_2]_2$ as catalyst while 1,7-diarylimidazo[5,1,2-*cd*]indolizine-6-carbaldehydes were

obtained using $Pd(OAc)_2$ as catalyst. The reaction produced annulated products in good yields, exhibited broad substrate scope and excellent functional group tolerance.

3.4 EXPERIMENTAL

3.4.1. General Information

2-Arylimidazo[1,2-*a*]pyridines (**1a**-**1n**) and 2-phenylbenzo[*d*]imidazo[2,1-*b*]thiazole (**33**) were synthesized by following the reported method.[57] All other reagents used were commercially available and used as such without purification. The reactions were performed under air and in a pressure tube. The products were purified by column chromatography over silica gel (100-200 mesh) using ethyl acetate/petroleum ether as eluent. Thin layer chromatography (TLC) was performed on Merck pre-coated TLC (silica gel 60 F254) plates. The ^1H NMR (400 MHz) and $^{13}C\{^1H\}$ NMR (100 MHz) spectra were recorded on a Bruker Advance 400 spectrometer using $CDCl_3$ or DMSO-d_6 as the solvent. Chemical shifts (δ) and coupling constants (*J*) are reported in parts per million (ppm) and hertz, respectively. The chemical multiplicities were reported as singlet (s), doublet (d), triplet (t), quartet (q), and multiplet (m) and combinations of them as well. HRMS data were recorded on a Q-TOF LC-MS spectrometer in positive electrospray ionization (ESI) mode. Melting points were determined in open capillary tubes on EZ-Melt automated melting point apparatus and are uncorrected. Single crystal X-ray analysis was performed on a Rigaku Oxford XtaLAB AFC12 (RINC): Kappa dual home/near diffractometer.

3.4.2. General Procedure for the Rh(III)-Catalyzed Annulation Reaction.

An oven dried 10 mL pressure tube was charged with **1** (0.26 mmol, 1 equiv.), 3-arylacrylaldehyde **30** (0.39 mmol, 1.5 equiv.), $[RhCp^*Cl_2]_2$ (1.6 mg, 1 mol %), $Cu(OAc)_2$ (94 mg, 0.52 mmol, 2 equiv.), TsOH (45 mg, 0.26 mmol, 1 equiv.) and DMA (2 mL). The reaction vial was capped and stirred at 120 °C for 24 h in an oil bath. After completion of the reaction, the reaction mixture was cooled to room temperature, diluted with EtOAc (5 mL), and washed with chilled water (3 × 10 mL). The aqueous layer was again extracted with EtOAc (2 × 3 mL). The combined organic layer was dried over anhydrous Na_2SO_4 and concentrated under reduced pressure. The resulting residue was purified by column chromatography (silica gel, 100-200 mesh size) using hexanes/ethyl acetate as eluent to afford the desired product **31** and **34**.

5-(4-Methoxyphenyl)naphtho[1',2':4,5]imidazo[1,2-*a*]pyridine-6-carbaldehyde (31aa).

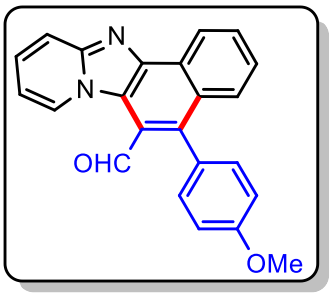

Purification by column chromatography on silica gel (eluent: EtOAc/hexanes, 3:7 *v/v*); Yellow solid; 69 mg (76%); mp = 263-265 °C; FT-IR ν_{max} (neat)/cm^{-1}: 1674, 1604, 1435, 1288, 1242, 1026, 756, 555; ^{1}H NMR (400 MHz, $CDCl_3$) δ = 10.07 (s, 1H), 9.84 (d, J = 7.2 Hz, 1H), 8.98 (d, J = 8.4 Hz, 1H), 7.88 (d, J = 9.2 Hz, 1H), 7.84 – 7.80 (m, 1H), 7.71 (d, J = 8.4 Hz, 1H), 7.58 – 7.54 (m, 1H), 7.50 – 7.46 (m, 1H), 7.40 (d, J = 8.8 Hz, 2H), 7.12 (d, J = 8.4 Hz, 2H), 6.95 – 6.91 (m, 1H), 3.96 (s, 3H); ^{13}C{^{1}H} NMR (100 MHz, $CDCl_3$) δ = 193.6, 159.8, 148.8, 144.1, 142.2, 132.7, 131.3, 131.0, 129.5, 129.4, 128.3, 128.3, 128.2, 126.7, 123.4, 120.8, 117.5, 113.8, 110.9, 55.5; HRMS (ESI) *m/z*: $[M + H]^+$ Calcd for $C_{23}H_{17}N_2O_2^+$ 353.1285; Found 353.1281.

5-(4-Methoxyphenyl)-3-methylnaphtho[1',2':4,5]imidazo[1,2-*a*]pyridine-6-carbaldehyde (31ba).

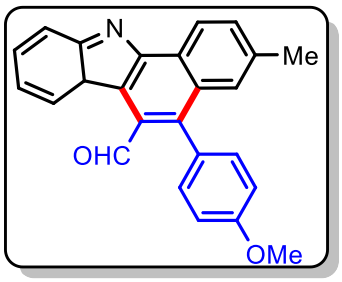

Purification by column chromatography on silica gel (eluent: EtOAc/hexanes, 1:4 *v/v*); Yellow solid; 68 mg (71%); mp = 268-270 °C; FT-IR ν_{max} (neat)/cm^{-1}: 1674, 1604, 1435, 1288, 1242, 1026, 756, 555; ^{1}H NMR (400 MHz, $CDCl_3$) δ = 10.01 (s, 1H), 9.81 (d, J = 7.2 Hz, 1H), 8.85 (d, J = 8.4 Hz, 1H), 7.85 (d, J = 9.2 Hz, 1H), 7.65 – 7.63 (m, 1H), 7.46 – 7.42 (m, 2H), 7.36 (d, J = 8.8 Hz, 2H), 7.09 (d, J = 8.8 Hz, 2H), 6.91 – 6.87 (m, 1H), 3.94 (s, 3H), 2.45 (s, 3H); ^{13}C{^{1}H} NMR (100 MHz, $CDCl_3$) δ = 193.7, 159.7, 148.7, 143.7, 142.1, 136.7, 132.7, 131.6, 131.3, 131.2, 128.5, 128.2, 127.5, 127.3, 123.5, 123.3, 120.5, 117.4, 113.8, 110.9, 55.4, 22.0; HRMS (ESI) *m/z*: $[M + H]^+$ Calcd for $C_{24}H_{19}N_2O_2^+$ 367.1441; Found 367.1439.

3-Methoxy-5-(4-methoxyphenyl)naphtho[1',2':4,5]imidazo[1,2-*a*]pyridine-6-carbaldehyde (31ca).

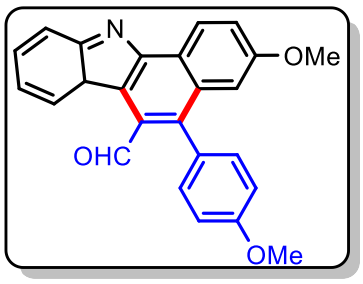

Purification by column chromatography on silica gel (eluent: EtOAc/hexanes, 1:3 *v/v*); Yellow solid ;72 mg (73%); mp = 219-221 °C; FT-IR ν_{max} (neat)/cm^{-1}: 1658, 1504, 1458, 1373, 1242, 1165, 1026, 748, 694, 524; ^{1}H NMR (400 MHz, $CDCl_3$) δ = 10.05 (s, 1H), 9.83 (d, J = 7.2 Hz, 1H), 8.90 (d, J = 8.9 Hz, 1H), 7.87 (d, J = 9.1 Hz, 1H), 7.49 – 7.45 (m, 2H), 7.42 – 7.39 (m, 2H), 7.13 – 7.11 (m, 2H), 7.04 (d, J = 2.5 Hz, 1H), 6.93 – 6.89 (m, 1H), 3.97 (s, 3H), 3.78 (s, 3H); ^{13}C{^{1}H} NMR (100 MHz, $CDCl_3$) δ = 193.8, 159.7, 158.4, 148.9, 142.9, 132.6, 132.5, 131.2, 129.8, 128.5, 128.2,

125.0, 124.1, 123.8, 120.3, 117.3, 114.4, 113.9, 110.8, 108.3, 55.4, 55.3; HRMS (ESI) *m/z*: $[M + H]^+$ Calcd for $C_{24}H_{19}N_2O_3^+$ 383.1390; Found 383.1393.

3-Chloro-5-(4-methoxyphenyl)naphtho[1',2':4,5]imidazo[1,2-*a*]pyridine-6-carbaldehyde

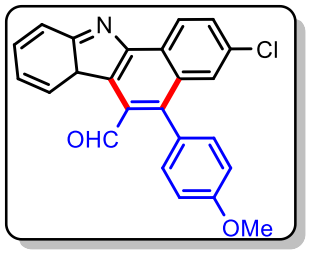

(31da). Purification by column chromatography on silica gel (eluent: EtOAc/hexanes, 1:3 *v/v*); Yellow solid; 69 mg (69%); mp = 295-297 °C; FT-IR ν_{max} (neat)/cm^{-1}: 1674, 1550, 1512, 1458, 1242, 1103, 1033, 833, 748, 532; ^1H NMR (400 MHz, $CDCl_3$) δ = 10.05 (s, 1H), 9.81 – 9.77 (m, 1H), 8.92 (d, *J* = 8.7 Hz, 1H), 7.89 – 7.86 (m, 1H), 7.76 (dd, *J* = 8.7, 2.1 Hz, 1H), 7.67 (d, *J* = 2.0 Hz, 1H), 7.53 – 7.49 (m, 1H), 7.39 (d, *J* = 8.6 Hz, 2H), 7.13 (d, *J* = 8.6 Hz, 2H), 6.97 – 6.93 (m, 1H), 3.98 (s, 3H); $^{13}C\{^1H\}$ NMR (100 MHz, $CDCl_3$) δ = 193.5, 160.0, 149.1, 142.5, 142.0, 133.0, 132.7, 132.0, 131.2, 130.0, 128.6, 127.52, 127.47, 127.1, 125.1, 124.3, 120.9, 117.5, 114.1, 111.2, 55.5; HRMS (ESI) *m/z*: $[M + H]^+$ Calcd for $C_{23}H_{16}ClN_2O_2^+$ 387.0895; Found 387.0899.

3-Bromo-5-(4-methoxyphenyl)naphtho[1′,2′:4,5]imidazo[1,2-*a*]pyridine-6-carbaldehyde

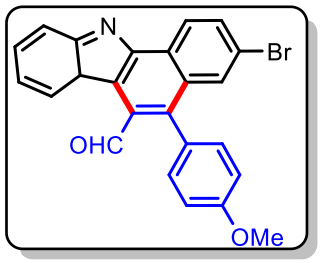

(31ea). Purification by column chromatography on silica gel (eluent: EtOAc/hexanes, 1:4 *v/v*) Green solid; 78 mg (70%); mp = 256−258 °C; FT-IR ν_{max} (neat)/cm^{-1}: 1658, 1504, 1458, 1373, 1242, 1165, 1026, 748, 694, 524; ^1H NMR (400 MHz, $CDCl_3$) δ = 10.04 (s, 1H), 9.80 (d, *J* = 7.2 Hz, 1H), 8.86 (d, *J* = 8.8 Hz, 1H), 7.92−7.85 (m, 2H), 7.52 (t, *J* = 7.6 Hz, 1H), 7.39 (d, *J* = 8.4 Hz, 2H), 7.14 (d, *J* = 8.4 Hz, 2H), 6.96 (t, *J* = 6.8 Hz, 1H), 3.98 (s, 3H); $^{13}C\{^1H\}$ NMR (100 MHz, $CDCl_3$) δ = 193.5, 159.6, 149.0, 132.7, 132.5, 132.4, 131.2, 130.3, 130.0, 128.7, 127.7, 127.4, 127.1, 125.2, 124.2, 121.2, 117.5, 114.1, 111.3, 55.5 HRMS (ESI) *m/z*: $[M + H]^+$ Calcd for $C_{23}H_{16}BrN_2O_2^+$ $[M + H]^+$ 431.0390; Found 431.0384.

6-Formyl-5-(4-methoxyphenyl)naphtho[1',2':4,5]imidazo[1,2-*a*]pyridine-3-carbonitrile

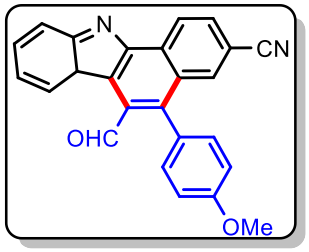

(31fa). Purification by column chromatography on silica gel (eluent: EtOAc/hexanes, 1:3 *v/v*); Yellow solid; 59 mg (60%); mp = 221-223 °C; FT-IR ν_{max} (neat)/cm^{-1}: 1681, 1604, 1512, 1489, 1242, 1026, 756, 694, 524; ^1H NMR (400 MHz, $CDCl_3$) δ = 10.05 (s, 1H), 9.80 (d, *J* = 7.2 Hz, 1H), 8.92 (d, *J* = 8.4 Hz, 1H), 7.88 (d, *J* = 9.2 Hz, 1H), 7.77 (dd,

J = 8.8, 2.0 Hz, 1H), 7.67 (d, *J* = 2.0 Hz, 1H), 7.53 – 7.49 (m, 1H), 7.39 (d, *J* = 8.8 Hz, 2H), 7.14 (d, *J* = 8.8 Hz, 2H), 6.97 – 6.94 (m, 1H), 3.98 (s, 3H); $^{13}C\{^{1}H\}$ NMR (100 MHz, $CDCl_3$) δ = 193.5, 160.0, 149.0, 142.5, 142.0, 133.0, 132.7, 132.0, 131.2, 130.0, 128.6, 127.52, 127.47, 127.3, 127.1, 125.1, 124.2, 120.9, 117.5, 114.1, 111.2, 55.5; HRMS (ESI) *m/z*: $[M + H]^+$ Calcd for $C_{24}H_{16}N_3O_2^+$ 378.1237; Found 378.1231.

5-(4-Methoxyphenyl)-3-(trifluoromethyl)naphtho[1',2':4,5]imidazo[1,2-*a*]pyridine-6-carbaldehyde (31ga). Purification by column chromatography on silica gel (eluent: EtOAc/hexanes, 3:7 *v/v*); Yellow solid; 67 mg (61%); mp = 256-258 °C; FT-IR ν_{max} (neat)/cm^{-1}: 1681, 1512, 1357, 1242, 1026, 840, 756, 532; ^{1}H NMR (400 MHz, $CDCl_3$) δ = 10.08 (s, 1H), 9.76 (d, *J* = 7.2 Hz, 1H), 9.03 (d, *J* = 8.5 Hz, 1H), 8.06 (s, 1H), 7.99 – 7.92 (m, 1H), 7.89 (d, *J* = 9.1 Hz, 1H), 7.58 – 7.52 (m, 1H), 7.40 (d, *J* = 8.5 Hz, 2H), 7.16 (d, *J* = 8.5 Hz, 2H), 6.99 (t, *J* = 6.6 Hz, 1H), 4.00 (s, 3H); $^{13}C\{^{1}H\}$ NMR (100 MHz, $CDCl_3$) δ = 193.1, 160.3, 149.3, 142.9, 141.5, 133.9, 132.7, 131.2, 130.8, 130.3, 129.9, 129.2, 126.6, 124.6 (d, *J* = 2.6 Hz), 122.3, 119.0, 117.7, 114.3, 111.7, 110.2, 55.6; HRMS (ESI) *m/z*: $[M + H]^+$ Calcd for $C_{24}H_{16}F_3N_2O_2^+$ 421.1158; Found 421.1155.

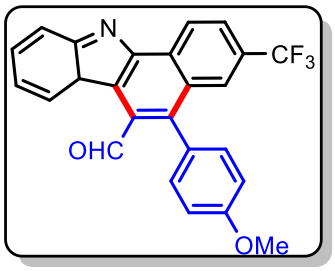

5-(4-Methoxyphenyl)-3-nitronaphtho[1',2':4,5]imidazo[1,2-*a*]pyridine-6-carbaldehyde (31ha). Purification by column chromatography on silica gel (eluent: EtOAc/hexanes, 1:4 *v/v*); Yellow solid; 58 mg (56%); mp = 205-207 °C; FT-IR ν_{max} (neat)/cm^{-1}: 1674, 1612, 1519, 1242, 1180, 1026, 833, 756, 709, 578; ^{1}H NMR (400 MHz, $CDCl_3$ + DMSO-d_6) δ = 10.09 (s, 1H), 9.79 (d, *J* = 6.6 Hz, 1H), 9.14 (d, *J* = 8.8 Hz, 1H), 8.70 (s, 1H), 8.60 (d, *J* = 8.8 Hz, 1H), 7.93 (d, *J* = 9.2 Hz, 1H), 7.58 (t, *J* = 7.0 Hz, 1H), 7.43 (d, *J* = 8.0 Hz, 2H), 7.18 (d, *J* = 8.1 Hz, 2H), 7.02 (t, *J* = 7.0 Hz, 1H), 4.01 (s, 3H); $^{13}C\{^{1}H\}$ NMR (100 MHz, $CDCl_3$ + DMSO-d_6) δ = 193.1, 160.3, 149.5, 145.4, 143.8, 132.7, 131.2, 130.2, 129.3, 129.1, 126.5, 125.1, 125.0, 124.5, 124.3, 122.6, 117.8, 115.4, 114.3, 111.8, 55.5; HRMS (ESI) *m/z*: $[M + H]^+$ Calcd for $C_{23}H_{16}N_3O_4^+$ 398.1135; Found 398.1136.

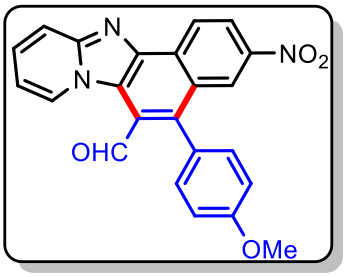

5-(4-Methoxyphenyl)-2-nitronaphtho[1',2':4,5]imidazo[1,2-*a*]pyridine-6-carbaldehyde

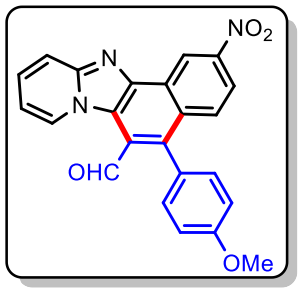

(31ia). Purification by column chromatography on silica gel (eluent: EtOAc/hexanes, 35:65 *v/v*); Yellow solid; 53 mg (51%); mp = 216-218 °C; FT-IR ν_{max} (neat)/cm^{-1}: 1681, 1504, 1442, 1249, 1026, 910, 825, 748, 532; ^{1}H NMR (400 MHz, $CDCl_3$) δ = 10.10 (s, 1H), 9.85 (d, J = 2.6 Hz, 1H), 9.74 (d, J = 7.3 Hz, 1H), 8.27 (dd, J = 9.2, 2.4 Hz, 1H), 7.96 (d, J = 9.1 Hz, 1H), 7.88 (d, J = 9.2 Hz, 1H), 7.60 – 7.53 (m, 1H), 7.42 (d, J = 8.1 Hz, 2H), 7.16 (d, J = 8.1 Hz, 2H), 7.02 (t, J = 7.0 Hz, 1H), 3.99 (s, 3H); ^{13}C{^{1}H} NMR (100 MHz, $CDCl_3$) δ = 193.3, 160.2, 149.4, 147.3, 142.9, 141.8, 133.9, 132.7, 131.1, 130.0, 129.8, 129.4, 128.4, 127.1, 125.8, 121.5, 120.0, 119.8, 117.8, 114.4, 114.3, 111.8, 55.5; HRMS (ESI) *m/z*: $[M + H]^+$ Calcd for $C_{23}H_{16}N_3O_4^+$ 398.1135; Found 398.1136.

5-(4-Methoxyphenyl)-1-methylnaphtho[1',2':4,5]imidazo[1,2-*a*]pyridine-6-carbaldehyde

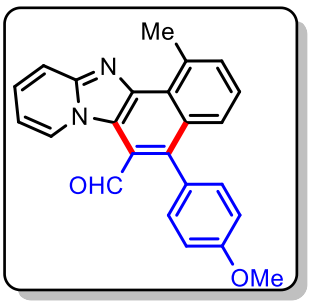

(31ja). Purification by column chromatography on silica gel (eluent: EtOAc/hexanes, 1:3 *v/v*); Yellow solid; 74 mg (78%); mp = 223-225 °C; FT-IR ν_{max} (neat)/cm^{-1}: 1674, 1604, 1504, 1342, 1242, 1172, 1041, 833, 756, 532; ^{1}H NMR (400 MHz, $CDCl_3$) δ = 10.06 (s, 1H), 9.73 (d, J = 7.2 Hz, 1H), 7.89 (d, J = 9.1 Hz, 1H), 7.62 (d, J = 7.1 Hz, 1H), 7.57 (d, J = 8.4 Hz, 1H), 7.47 – 7.42 (m, 2H), 7.40 – 7.37 (m, 2H), 7.12 – 7.10 (m, 2H), 7.00 – 6.86 (m, 1H), 3.97 (s, 3H), 3.44 (s, 3H); ^{13}C{^{1}H} NMR (100 MHz, $CDCl_3$) δ = 193.7, 159.7, 147.5, 144.3, 143.3, 136.8, 132.6, 132.2, 131.9, 130.7, 129.1, 128.6, 127.4, 126.5, 125.9, 123.2, 121.5, 117.9, 113.8, 110.8, 55.5, 24.6; HRMS (ESI) *m/z*: $[M + H]^+$ Calcd for $C_{24}H_{19}N_2O_2^+$ 367.1441; Found 367.1445.

5-(4-Methoxyphenyl)-11-methylnaphtho[1',2':4,5]imidazo[1,2-*a*]pyridine-6-carbaldehyde

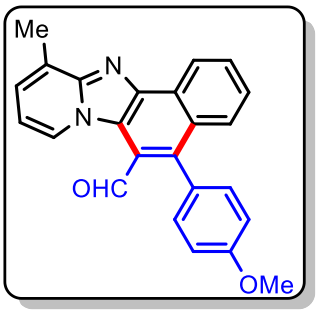

(31la). Purification by column chromatography on silica gel (eluent: EtOAc/hexanes, 1:4 *v/v*); Yellow solid; 68 mg (72%); mp = 223-225 °C; FT-IR ν_{max} (neat)/cm^{-1}: 1674, 1512, 1435, 1242, 1172, 1033, 833, 748, 532; ^{1}H NMR (400 MHz, $CDCl_3$) δ = 10.08 (s, 1H), 9.69 (d, J = 7.2 Hz, 1H), 9.08 (d, J = 8.2 Hz, 1H), 7.83 (t, J = 7.6 Hz, 1H), 7.71 (d, J = 8.4 Hz, 1H), 7.56 (t, J = 7.6 Hz, 1H), 7.41 (d, J = 8.3 Hz, 2H), 7.29 (d, J = 6.3 Hz, 1H), 7.12 (d, J = 8.3 Hz, 2H), 6.86 (t, J = 7.0 Hz, 1H), 3.97 (s, 3H), 2.86 (s, 3H);

$^{13}C\{^{1}H\}$ NMR (100 MHz, $CDCl_3$) δ = 193.7, 159.7, 146.24, 146.17, 143.8, 132.7, 130.9, 129.3, 128.9, 128.5, 128.4, 128.2, 127.2, 126.8, 126.6, 123.7, 123.5, 121.3, 113.8, 110.9, 55.4, 17.7; HRMS (ESI) *m/z*: $[M + H]^+$ Calcd for $C_{24}H_{19}N_2O_2^+$ 367.1441; Found 367.1439.

5-(4-Methoxyphenyl)-9-methylnaphtho[1′,2′:4,5]imidazo[1,2-*a*]pyridine-6-carbaldehyde (31ma). Purification by column chromatography on silica gel (eluent: EtOAc/hexanes, 15:85 *v/v*); Yellow solid; 73 mg (77%); mp = 211−213 °C; FT-IR ν_{max} (neat)/cm^{-1}: 1674, 1512, 1435, 1242, 1172, 1033, 833, 748, 532; ^{1}H NMR (400 MHz, $CDCl_3$) δ = 10.07 (s, 1H), 9.74 (d, *J* = 7.6 Hz, 1H), 8.96 (d, *J* = 7.6 Hz, 1H), 7.82 (t, *J* = 7.6 Hz, 1H), 7.70 (d, *J* = 8.4 Hz, 1H), 7.64 (s, 1H), 7.57−7.53 (m, 1H), 7.40 (d, *J* = 8.8 Hz, 2H), 7.11 (d, *J* = 8.8 Hz, 2H), 6.77 (dd, *J* = 7.6, 1.6 Hz, 1H), 3.97 (s, 3H), 2.53 (s, 3H); $^{13}C\{^{1}H\}$ NMR (100 MHz, $CDCl_3$) δ = 193.8, 159.7, 149.4, 143.4, 142.3, 139.6, 132.7, 130.9, 130.3, 129.3, 129.3, 128.4, 128.3, 126.6, 123.4, 123.3, 120.7, 115.7, 113.8, 113.7, 55.5, 21.6; HRMS (ESI) m/z: $[M + H]^+$ Calcd for $C_{24}H_{19}N_2O_2^+$ 367.1441; found 367.1438.

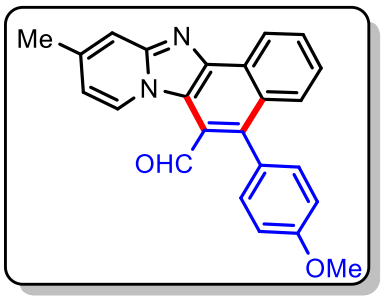

5-(4-Methoxyphenyl)-3,10-dimethylnaphtho[1',2':4,5]imidazo[1,2-*a*]pyridine-6-carbaldehyde (31na). Purification by column chromatography on silica gel (eluent: EtOAc/hexanes, 15:85 *v/v*); Yellow solid; 75 mg (76%); mp = 263-265 °C; FT-IR ν_{max} (neat)/cm^{-1}: 1666, 1604, 1504, 1435, 1342, 1280, 1242, 1026, 833, 748, 578; ^{1}H NMR (400 MHz, $CDCl_3$) δ = 10.02 (s, 1H), 9.71 (d, *J* = 7.3 Hz, 1H), 8.84 (d, *J* = 8.3 Hz, 1H), 7.66 – 7.62 (m, 2H), 7.44 – 7.37 (m, 3H), 7.12 – 7.10 (m, 2H), 6.74 (dd, *J* = 7.4, 1.9 Hz, 1H), 3.97 (s, 3H), 2.51 (s, 3H), 2.47 (s, 3H); $^{13}C\{^{1}H\}$ NMR (100 MHz, $CDCl_3$) δ = 193.8, 159.6, 149.3, 143.0, 142.2, 139.5, 136.4, 132.7, 131.4, 131.1, 130.3, 128.6, 127.4, 127.3, 123.32, 123.30, 120.3, 115.5, 113.8, 113.6, 55.4, 22.0, 21.6; HRMS (ESI) *m/z*: $[M + H]^+$ Calcd for $C_{25}H_{21}N_2O_2^+$ 381.1598; Found 381.1595.

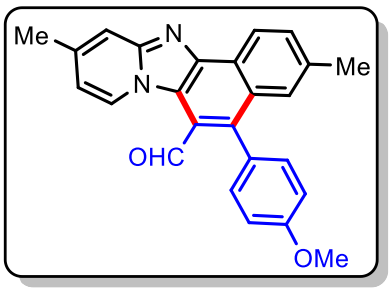

3-Methoxy-5-(4-methoxyphenyl)-10-methylnaphtho[1',2':4,5]imidazo[1,2-*a*]pyridine-6-carbaldehyde (31oa). Purification by column chromatography on silica gel (eluent: EtOAc/hexanes, 1:4 *v/v*); Yellow solid; 79 mg (77%); mp = 222-224 °C; FT-IR ν_{max} (neat)/cm^{-1}: 1681, 1612, 1540, 1249, 1033, 833, 748, 532; ^{1}H NMR (400 MHz, $CDCl_3$) δ = 10.02 (s, 1H), 9.70 (d, J = 7.4 Hz, 1H), 8.86 (d, J = 8.7 Hz, 1H), 7.61 (s, 1H), 7.45 (d, J = 6.8 Hz, 1H), 7.39 (d, J = 8.1 Hz, 2H), 7.11 (d, J = 8.1 Hz, 2H), 7.01 (d, J = 2.3 Hz, 1H), 6.74 (d, J = 7.3 Hz, 1H), 3.96 (s, 3H), 3.76 (s, 3H), 2.51 (s, 3H); ^{13}C{^{1}H} NMR (100 MHz, $CDCl_3$) δ = 193.8, 159.7, 158.3, 142.2, 139.7, 132.6, 132.4, 130.3, 128.6, 125.0, 124.0, 123.6, 120.3, 115.4, 113.9, 113.6, 108.2, 55.4, 55.3, 21.6; HRMS (ESI) *m/z*: [M + H]$^+$ Calcd for $C_{25}H_{21}N_2O_3^+$ 397.1547; Found 397.1551.

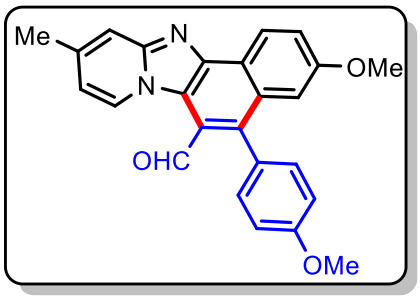

7-(4-Methoxyphenyl)anthra[1',2':4,5]imidazo[1,2-*a*]pyridine-6-carbaldehyde (31pa). Purification by column chromatography on silica gel (eluent: EtOAc/hexanes, 15:85 *v/v*); Yellow solid; 86 mg (80%); mp = 226-228°C; FT-IR ν_{max} (neat)/cm^{-1}: 1681, 1612, 1540, 1249, 1033, 833, 748, 532; ^{1}H NMR (400 MHz, $CDCl_3$) δ = 10.07 (s, 1H), 9.79 – 9.77 (m, 1H), 9.48 (s, 1H), 8.24 (s, 1H), 8.20 (d, J = 8.4 Hz, 1H), 7.93 – 7.90 (m, 2H), 7.62 (t, J = 7.5 Hz, 1H), 7.53 – 7.46 (m, 4H), 7.17 (d, J = 8.6 Hz, 2H), 6.96 (t, J = 6.8 Hz, 1H), 4.01 (s, 3H); ^{13}C{^{1}H} NMR (100 MHz, $CDCl_3$) δ = 193.5, 159.9, 148.4, 145.8, 133.5, 132.8, 131.8, 131.1, 130.0, 129.14, 129.13, 128.3, 128.2, 127.6, 127.5, 126.7, 126.0, 124.2, 122.1, 119.4, 117.4, 114.0, 111.4, 55.5; HRMS (ESI) *m/z*: [M + H]$^+$ Calcd for $C_{27}H_{19}N_2O_2^+$ 403.1441; Found 403.1443.

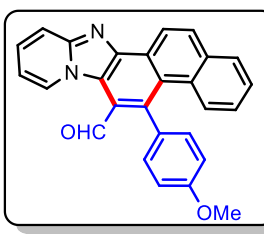

4-(4-Methoxyphenyl)thieno[2'',3'':5',6']benzo[1',2':4,5]imidazo[1,2-*a*]pyridine-5-carbaldehyde (31qa). Purification by column chromatography on silica gel; (eluent: EtOAc/hexanes, 1:4 *v/v*); Yellow solid; 54 mg (60%); mp = 256-258 °C; FT-IR ν_{max} (neat)/cm^{-1}: 1681, 1512, 1450, 1357, 1249, 1172, 1064, 833, 748; H NMR (400 MHz, $CDCl_3$) δ = 10.10 (s, 1H), 8.22 (d, J = 5.4 Hz, 1H), 7.89 – 7.81 (m, 2H), 7.54 – 7.47 (m, 4H), 7.13 – 7.10 (m, 1H), 6.94 (t, J = 6.8 Hz, 1H), 3.96 (s, 3H); ^{13}C{^{1}H} NMR (100 MHz, $CDCl_3$) δ = 192.6, 160.2, 149.2, 140.5, 140.1, 139.4, 135.4, 133.0, 132.1, 131.93, 131.86, 129.2, 129.1, 123.3, 122.9, 120.2, 117.4,

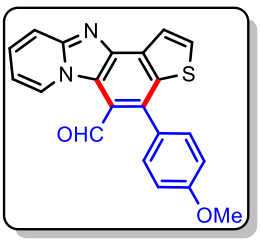

114.2, 114.0, 110.7, 55.5; HRMS (ESI) *m/z*: $[M + H]^+$ Calcd for $C_{21}H_{15}N_2O_2S^+$ 359.0849; Found 359.0846.

5-Phenylnaphtho[1',2':4,5]imidazo[1,2-*a*]pyridine-6-carbaldehyde (31ab). Purification by column chromatography on silica gel (eluent: EtOAc/hexanes, 1:3 *v/v*); Yellow solid; 59 mg (70%); mp = 232-234 °C; FT-IR ν_{max} (neat)/cm^{-1}: 1674, 1635, 1496, 1257, 1149, 1033, 748, 725, 555; ^1H NMR (400 MHz, $CDCl_3$) δ = 10.05 (s, 1H), 9.85 (d, J = 7.2 Hz, 1H), 8.98 (d, J = 8.2 Hz, 1H), 7.89 – 7.80 (m, 2H), 7.64 – 7.46 (m, 8H), 6.95 – 6.91 (m, 1H); $^{13}C\{^1H\}$ NMR (100 MHz, $CDCl_3$) δ = 193.4, 148.8, 144.3, 142.3, 136.5, 131.5, 131.3, 130.7, 129.5, 129.4, 128.43, 128.35, 128.31, 128.28, 126.8, 123.4, 123.1, 120.8, 117.5, 111.0; HRMS (ESI) *m/z*: $[M + H]^+$ Calcd for $C_{22}H_{15}N_2O^+$ 323.1179; Found 323.1182.

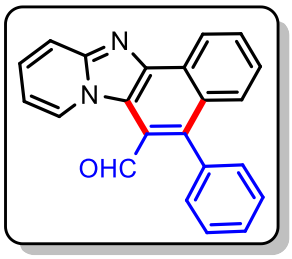

3-Methyl-5-phenylnaphtho[1',2':4,5]imidazo[1,2-*a*]pyridine-6-carbaldehyde (31bb). Purification by column chromatography on silica gel (eluent: EtOAc/hexanes, 3:7 *v/v*); Yellow solid; 62 mg (68%); mp = 256-258 °C; FT-IR ν_{max} (neat)/cm^{-1}: 1666, 1566, 1450, 1350, 1265, 1226, 740, 648; ^1H NMR (400 MHz, $CDCl_3$) δ = 10.04 (s, 1H), 9.84 (d, J = 7.2 Hz, 1H), 8.90 (d, J = 9.2 Hz, 1H), 7.86 (d, J = 9.2 Hz, 1H), 7.61 – 7.57 (m, 3H), 7.51 – 7.46 (m, 4H), 6.95 (d, J = 2.4 Hz, 1H), 6.92 (td, J = 7.0, 1.1 Hz, 1H), 3.75 (s, 3H); $^{13}C\{^1H\}$ NMR (100 MHz, $CDCl_3$) δ = 193.6, 158.4, 148.9, 143.1, 142.5, 136.6, 132.2, 131.4, 131.3, 128.4, 128.2, 125.0, 124.2, 123.4, 120.4, 119.8, 117.3, 110.8, 108.3, 55.2; HRMS (ESI) *m/z*: $[M + H]^+$ Calcd for $C_{23}H_{17}N_2O^+$ 337.1335; Found 337.1331.

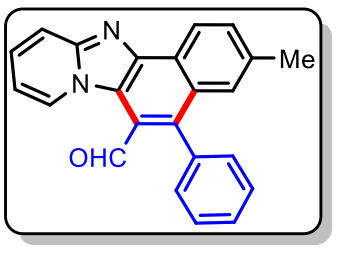

3-Methoxy-5-phenylnaphtho[1',2':4,5]imidazo[1,2-*a*]pyridine-6-carbaldehyde (31cb). Purification by column chromatography on silica gel (eluent: EtOAc/hexanes, 1:4 *v/v*); Yellow solid; 58 mg (64%); mp = 271-273 °C; FT-IR ν_{max} (neat)/cm^{-1}: 1674, 1620, 1566, 1450, 1265, 1033, 740, 586, 570; ^1H NMR (400 MHz, $CDCl_3$) δ = 10.04 (s, 1H), 9.85– 9.83 (m, 1H), 8.90 (d, J = 8.9 Hz, 1H), 7.88 – 7.84 (m, 1H), 7.61 – 7.57 (m, 3H), 7.52 – 7.46 (m, 4H), 6.95 (d, J = 2.6 Hz, 1H), 6.94 – 6.90 (m, 1H), 3.75 (s, 3H); $^{13}C\{^1H\}$ NMR (100 MHz, $CDCl_3$) δ = 193.6, 158.4, 148.9, 143.1, 142.6, 136.7, 132.2, 131.4,

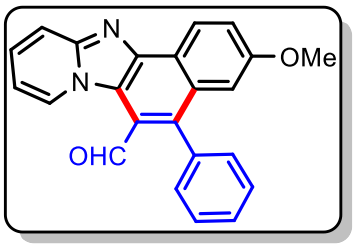

131.3, 128.5, 128.2, 125.0, 124.2, 123.4, 120.4, 119.9, 117.3, 110.8, 108.3, 55.2; HRMS (ESI) *m/z*: $[M + H]^+$ Calcd for $C_{23}H_{17}N_2O_2^+$ 353.1285; Found 353.1280.

5-(4-Nitrophenyl)naphtho[1',2':4,5]imidazo[1,2-*a*]pyridine-6-carbaldehyde (31ac).

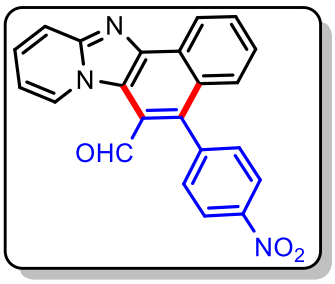

Purification by column chromatography on silica gel (eluent: EtOAc/hexanes, 15:85 *v/v*); Yellow solid; 51 mg (54 %); mp = 290-292 °C; FT-IR ν_{max} (neat)/cm^{-1}: 1681, 1597, 1342, 1280, 1103, 848,748, 671; ^1H NMR (400 MHz, $CDCl_3$) δ = 10.04 (s, 1H), 9.83 (d, J = 7.2 Hz, 1H), 9.04 (d, J = 8.2 Hz, 1H), 8.49 (d, J = 8.5 Hz, 2H), 7.95 – 7.86 (m, 2H), 7.73 (d, J = 8.5 Hz, 2H), 7.63 – 7.53 (m, 2H), 7.49 (d, J = 8.5 Hz, 1H), 7.09 – 6.94 (m, 1H); $^{13}C\{^1H\}$ NMR (100 MHz, $CDCl_3$) δ = 193.4, 148.8, 144.3, 142.3, 136.5, 131.5, 131.3, 130.7, 129.5, 129.4, 128.43, 128.35, 128.31, 128.28, 126.8, 123.4, 123.1, 120.8, 117.5, 111.0; HRMS (ESI) *m/z*: $[M + H]^+$ Calcd for $C_{22}H_{14}N_3O_3^+$ 368.1030; Found 368.1032.

5-(4-Methoxyphenyl)benzo[*d*]naphtho[1',2':4,5]imidazo[2,1-*b*]thiazole-6-carbaldehyde (34).

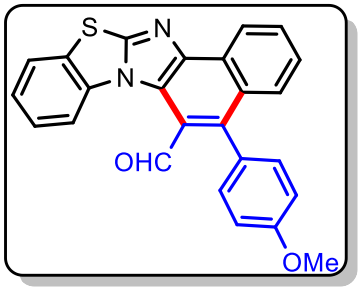

Purification by column chromatography on silica gel (eluent: EtOAc/hexanes, 1:4 *v/v*); Yellow solid; 58 mg (55%); mp = 223-225 °C; FT-IR ν_{max} (neat)/cm^{-1}: 1681, 1604, 1512, 1489, 1242, 1026, 756, 694, 524; ^1H NMR (400 MHz, $CDCl_3$) δ = 10.22 (s, 1H), 8.83 (d, J = 8.1 Hz, 1H), 8.82 – 7.73 (m, 3H), 7.55 – 7.45 (m, 5H), 7.43 – 7.38 (m, 1H), 7.15 – 7.13 (m, 2H), 3.98 (s, 3H); $^{13}C\{^1H\}$ NMR (100 MHz, $CDCl_3$) δ = 193.2, 159.8, 155.6, 144.7, 141.6, 134.6, 132.7, 131.5, 130.1, 129.5, 129.4, 129.0, 128.2, 127.8, 126.1, 125.7, 124.6, 123.8, 123.1, 122.7, 118.6, 113.8, 55.5; HRMS (ESI) *m/z*: $[M + H]^+$ Calcd for $C_{25}H_{17}N_2O_2S^+$ 409.1005; Found 409.1008.

3.4.3. General Procedure for Pd(II)-Catalysed Annulation Reaction.

An oven dried 10 mL pressure tube was charged with **1** (0.26 mmol, 1 equiv.), arylacrylaldehyde **30** (0.39 mmol, 1.5 equiv.), $Pd(OAc)_2$ (3 mg, 5 mol %), $Cu(OAc)_2{\cdot}H_2O$ (104 mg, 0.52 mmol, 2 equiv.), K_2CO_3 (72 mg, 0.52 mmol, 2 equiv.), XPhos (37 mg, 30 mol %) and DMF (2 mL). The reaction vial was capped and stirred at 140 °C for 24 h in an oil bath. After completion of reaction, reaction mixture was cooled to room temperature and diluted with cold water (10 mL). The mixture was extracted with EtOAc (3 × 3 mL). The combined organic layer was dried over anhydrous

Na_2SO_4 and concentrated under reduced pressure. The resulting residue was purified by column chromatography (hexanes/ethyl acetate as eluent) on silica gel (100-200 mesh size) column to afford the desired product **32**.

6-(4-Methoxyphenyl)naphtho[1',2':4,5]imidazo[1,2-*a*]pyridine-5-carbaldehyde (32aa).

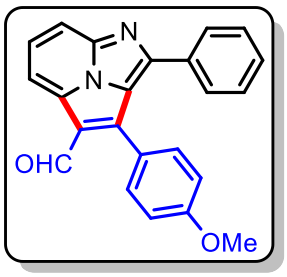

Purification by column chromatography on silica gel (eluent: EtOAc/hexanes, 1:4 *v/v*); Yellow solid; 64 mg (71%); mp = 208-210 °C FT-IR ν_{max} (neat)/cm^{-1}: 1705, 1604, 1496, 1249, 1033, 956, 748, 516; ^{1}H NMR (400 MHz, $CDCl_3$) δ = 10.17 (s, 1H), 8.42 (d, J = 7.4 Hz, 1H), 8.12 – 8.04 (m, 2H), 7.89 (d, J = 7.4 Hz, 2H), 7.57 (d, J = 8.5 Hz, 2H), 7.43 (t, J = 7.2 Hz, 1H), 7.36 (t, J = 7.4 Hz, 2H), 7.07 (d, J = 8.5 Hz, 2H), 3.95 (s, 3H); ^{13}C{^{1}H} NMR (100 MHz, $CDCl_3$) δ = 188.3, 160.9, 155.4, 140.5, 140.4, 132.75, 132.70, 130.45, 130.36, 130.1, 129.6, 128.6, 124.0, 123.8, 123.6, 115.1, 114.3, 112.2, 55.5; HRMS (ESI) *m/z*: $[M + H]^+$ Calcd for $C_{23}H_{17}N_2O_2^+$ 353.1285; Found, 353.1286.

7-(4-Methoxyphenyl)-1-(*p*-tolyl)imidazo[5,1,2-*cd*]indolizine-6-carbaldehyde (32ba).

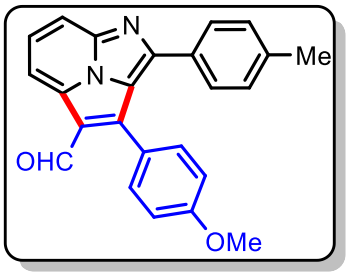

Purification by column chromatography on silica gel (eluent: EtOAc/hexanes, 15:85 *v/v*); Yellow solid; 58 mg (66%); mp = 170-172 °C; FT-IR ν_{max} (neat)/cm^{-1}: 1720, 1651, 1604, 1489, 1249, 1026, 972, 756; ^{1}H NMR (400 MHz, $CDCl_3$) δ = 10.16 (s, 1H), 8.42 (d, J = 7.5 Hz, 1H), 8.12 – 8.03 (m, 2H), 7.81 (d, J = 7.7 Hz, 2H), 7.59 (d, J = 8.7 Hz, 2H), 7.18 (d, J = 7.3 Hz, 2H), 7.09 (d, J = 8.7 Hz, 2H), 3.97 (s, 3H), 2.42 (s, 3H); ^{13}C{^{1}H} NMR (100 MHz, $CDCl_3$) δ = 188.4, 160.9, 140.8, 140.5, 132.7, 130.4, 130.05, 129.99, 129.98, 129.6, 123.9, 123.7, 115.0, 114.3, 111.9, 55.5, 21.5; HRMS (ESI) *m/z*: $[M + H]^+$ Calcd for $C_{24}H_{19}N_2O_2^+$ 367.1441; Found 367.1425.

1,7-Bis(4-methoxyphenyl)imidazo[5,1,2-*cd*]indolizine-6-carbaldehyde (32ca). Purification by column chromatography on silica gel (eluent: EtOAc/hexanes, 3:7 *v/v*); Yellow solid; 59 mg (69%); mp = 189-191 °C; FT-IR ν_{max} (neat)/cm^{-1}: 1658, 1519, 1489, 1249, 1026, 779, 756, 524; ^{1}H NMR (400 MHz, $CDCl_3$) δ = 10.14 (s, 1H), 8.39 (d, J = 7.7 Hz, 1H), 8.08 (t, J = 8.0 Hz, 1H), 7.99 (d, J = 8.0 Hz, 1H), 7.86 (d, J = 8.8 Hz, 2H), 7.59 (d, J = 8.6 Hz, 2H), 7.09 (d, J = 8.6 Hz, 2H),

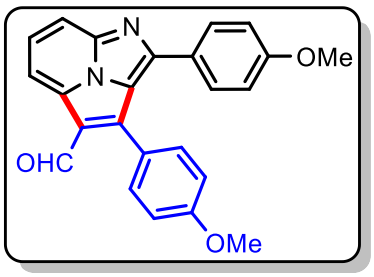

6.87 (d, J = 8.7 Hz, 2H), 3.96 (s, 3H), 3.88 (s, 3H); $^{13}C\{^1H\}$ NMR (100 MHz, $CDCl_3$) δ = 188.3, 161.6, 160.8, 155.5, 140.6, 140.2, 132.6, 131.2, 130.3, 130.1, 125.4, 123.79, 123.75, 123.6, 114.7, 114.3, 114.1, 111.5, 55.5, 55.4; HRMS (ESI) *m/z*: $[M + H]^+$ Calcd for $C_{24}H_{19}N_2O_3^+$ 383.1390; Found 383.1393.

1-(4-Chlorophenyl)-7-(4-methoxyphenyl)imidazo[5,1,2-*cd*]indolizine-6-carbaldehyde (32da). 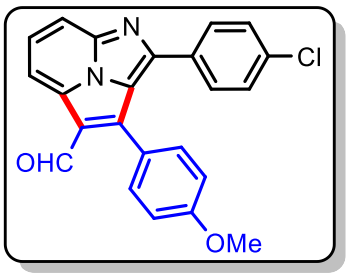

Purification by column chromatography on silica gel (eluent: EtOAc/hexanes, 1:9 *v/v*); Green solid; 56 mg (67%); mp = 216-218 °C; FT-IR ν_{max} (neat)/cm^{-1}: 1658, 1512, 1489, 1249, 1026, 756, 516; ^1H NMR (400 MHz, $CDCl_3$) δ = 10.16 (s, 1H), 8.45 (d, J = 7.5 Hz, 1H), 8.14 – 8.05 (m, 2H), 7.83 (d, J = 8.4 Hz, 2H), 7.57 (d, J = 8.6 Hz, 2H), 7.34 (d, J = 8.5 Hz, 2H), 7.09 (d, J = 8.7 Hz, 2H), 3.97 (s, 3H); $^{13}C\{^1H\}$ NMR (100 MHz, $CDCl_3$) δ = 188.2, 161.0, 140.4, 140.3, 136.5, 132.6, 131.3, 130.8, 130.5, 130.3, 128.9, 124.2, 123.4, 115.4, 114.4, 112.4, 55.5; HRMS (ESI) *m/z*: $[M + H]^+$ Calcd for $C_{23}H_{16}ClN_2O_2^+$ 387.0895; Found 387.0892.

4-(6-Formyl-7-(4-methoxyphenyl)imidazo[5,1,2-*cd*]indolizin-1-yl)benzonitrile (32fa). 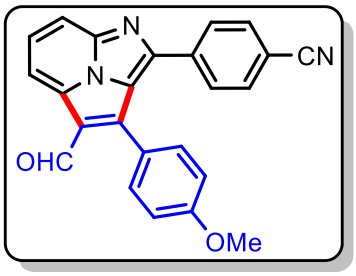

Purification by column chromatography on silica gel (eluent: EtOAc/hexanes, 1:9 *v/v*); Green solid; 56 mg (65%); mp = 181-183 °C; FT-IR ν_{max} (neat)/cm^{-1}: 1674, 1597, 1450, 1249, 1087, 1033, 756, 509; ^1H NMR (400 MHz, $CDCl_3$) δ = 10.19 (s, 1H), 8.50 (d, J = 7.2 Hz, 1H), 8.19 – 8.13 (m, 2H), 8.00 (d, J = 8.4 Hz, 2H), 7.66 (d, J = 8.5 Hz, 2H), 7.56 (d, J = 8.6 Hz, 2H), 7.10 (d, J = 8.6 Hz, 2H), 3.98 (s, 3H); $^{13}C\{^1H\}$ NMR (100 MHz, $CDCl_3$) δ = 188.2, 161.2, 152.3, 140.6, 140.2, 137.1, 132.6, 132.3, 130.7, 130.6, 130.0, 124.7, 123.1, 118.5, 116.1, 114.6, 113.5, 113.2, 55.6; HRMS (ESI) *m/z*: $[M + H]^+$ Calcd for $C_{24}H_{16}N_3O_2^+$ 378.1237; Found 378.1235.

7-(4-Methoxyphenyl)-1-(4-(trifluoromethyl)phenyl)imidazo[5,1,2-*cd*]indolizine-6-carbaldehyde (36ga). 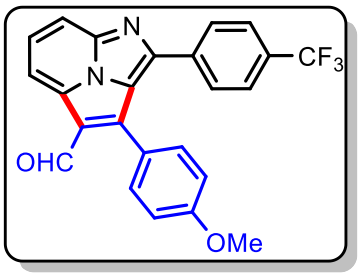

Purification by column chromatography on silica gel (eluent: EtOAc/hexanes, 1:4 *v/v*); Yellow solid; 49 mg (61%); mp = 188-190 °C; FT-IR ν_{max} (neat)/cm^{-1}: 1658, 1489, 1319, 1249, 1018, 848, 717, 524; ^1H NMR (400 MHz, $CDCl_3$) δ = 10.19 (s, 1H), 8.51 (t, J = 4.0 Hz, 1H), 8.20 (d, J = 4.0 Hz, 2H), 8.05 (d, J

= 7.2 Hz, 2H), 7.64 (d, J = 7.6 Hz, 2H), 7.57 (d, J = 8.8 Hz, 2H), 7.10 (d, J = 8.4 Hz, 2H), 3.98 (s, 3H); $^{13}C\{^1H\}$ NMR (100 MHz, $CDCl_3$) δ = 188.2, 161.2, 153.1, 140.7, 140.2, 136.1, 132.6, 131.8 (q, $^2J_{C\text{-}F}$ = 32.3 Hz), 130.6, 130.4, 130.0, 129.8, 126.6 (q, $^1J_{C\text{-}F}$ = 270.6 Hz), 125.5 (q, $^3J_{C\text{-}F}$ = 3.7 Hz), 124.5, 124.0, 123.2, 115.8, 114.5, 114.4, 112.9, 55.6; HRMS (ESI) *m/z*: $[M + H]^+$ Calcd for $C_{24}H_{16}F_3N_2O_2^+$ 421.1158; Found 421.1155.

7-(4-Methoxyphenyl)-1-(3-nitrophenyl)imidazo[5,1,2-*cd*]indolizine-6-carbaldehyde (32ia).

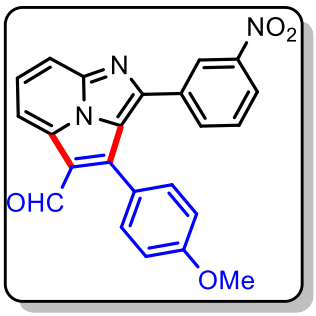

Purification by column chromatography on silica gel (eluent: EtOAc/hexanes, 2:3 *v/v*); Yellow solid (47 mg, 56%); mp = 193-195 °C; FT-IR ν_{max} (neat)/cm^{-1}: 1650, 1592, 1481, 1242, 1033, 775, 509; ^1H NMR (400 MHz, $CDCl_3$) δ = 10.21 (s, 1H), 8.64 (s, 1H), 8.53 – 8.51 (m, 1H), 8.40 (s, 1H), 8.29 (d, J = 8.0 Hz, 1H), 8.20 (d, J = 3.6 Hz, 2H), 7.62 (d, J = 7.2 Hz, 1H), 7.58 (d, J = 8.8 Hz, 2H), 7.11 (d, J = 8.4 Hz, 2H), 3.96 (s, 3H); $^{13}C\{^1H\}$ NMR (100 MHz, $CDCl_3$) δ = 188.0, 161.5, 151.7, 148.5, 143.6, 141.3, 135.0, 132.3, 131.6, 131.0, 130.8, 129.9, 129.4, 125.2, 124.9, 124.5, 122.6, 116.4, 114.9, 113.0, 55.7; HRMS (ESI) *m/z*: $[M + H]^+$ Calcd for $C_{23}H_{16}N_3O_4^+$ 398.1135; Found 398.1134.

7-(4-Methoxyphenyl)-3-methyl-1-phenylimidazo[5,1,2-*cd*]indolizine-6-carbaldehyde (32la).

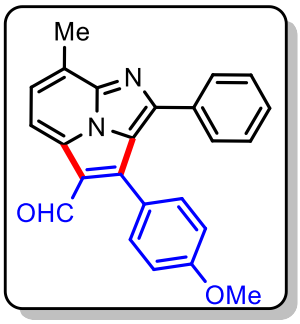

Purification by column chromatography on silica gel (eluent: EtOAc/hexanes, 15:85 *v/v*); Orange solid; 60 mg (70%); mp = 174-176 °C; FT-IR ν_{max} (neat)/cm^{-1}: 1643, 1604, 1496, 1249, 1033, 979, 702; ^1H NMR (400 MHz, $CDCl_3$) δ = 10.15 (s, 1H), 8.31 (d, J = 8.0 Hz, 1H), 7.90 – 7.87 (m, 3H), 7.56 (d, J = 8.8 Hz, 2H), 7.44 – 7.40 (m, 1H), 7.38 – 7.34 (m, 2H), 7.05 (d, J = 8.7 Hz, 2H), 3.95 (s, 3H), 3.03 (s, 3H); $^{13}C\{^1H\}$ NMR (100 MHz, $CDCl_3$) δ = 188.4, 160.8, 154.1, 139.9, 139.7, 133.0, 132.7, 131.2, 130.1, 129.6, 128.7, 128.5, 124.1, 123.98, 123.89, 123.8, 115.2, 114.2, 55.5, 16.0; HRMS (ESI) *m/z*: $[M + H]^+$ Calcd for $C_{24}H_{19}N_2O_2^+$ 367.1441; Found 367.1445.

7-(4-Methoxyphenyl)-4-methyl-1-phenylimidazo[5,1,2-*cd*]indolizine-6-carbaldehyde

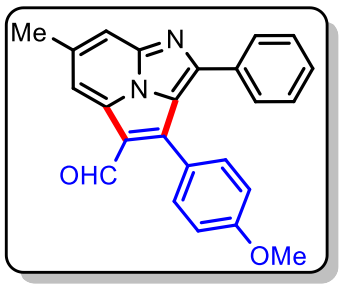

(32ma). Purification by column chromatography on silica gel (eluent: EtOAc/hexanes, 1:9 *v/v*); Green solid; 62 mg (71%); mp = 188−190 °C; ^{1}H NMR (400 MHz, $CDCl_3$) δ = 10.13 (s, 1H), 8.28 (s, 1H), 7.89−7.85 (m, 3H), 7.59−7.55 (m, 2H), 7.45−7.40 (m, 1H), 7.39−7.34 (m, 2H), 7.08− 7.04 (m, 2H), 3.95 (s, 3H), 2.86 (s, 3H); ^{13}C{^{1}H} NMR (100 MHz, $CDCl_3$) δ = 188.4, 160.9, 155.6, 142.2, 140.6, 140. 3, 132.8, 132.7, 130.3, 129.9, 129.6, 128.6, 123.7, 123.5, 123.3, 116.1, 114.3, 112.8, 55.5, 22.9; HRMS (ESI) *m/z*: $[M + H]^+$ Calcd for $C_{24}H_{19}N_2O_{2+}$ 367.1441; Found 367.1445.

7-(4-Methoxyphenyl)-4-methyl-1-(*p*-tolyl)imidazo[5,1,2-*cd*]indolizine-6-carbaldehyde

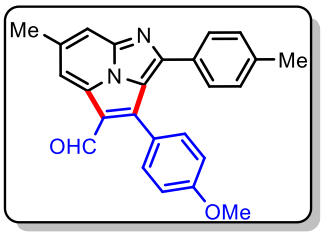

(32na). Purification by column chromatography on silica gel (eluent: EtOAc/hexanes, 1:9 *v/v*); Green solid; 62 mg (73%); mp = 200-202 °C; FT-IR ν_{max} (neat)/cm^{-1}: 1627, 1481, 1365, 1249, 1026, 794; ^{1}H NMR (400 MHz, $CDCl_3$) δ = 10.11 (s, 1H), 8.26 (s, 1H), 7.83 (s, 1H), 7.78 (d, J = 8.4 Hz, 2H), 7.57 (d, J = 8.4 Hz, 2H), 7.17 (d, J = 8.0 Hz, 2H), 7.07 (d, J = 8.4 Hz, 2H), 3.96 (s, 3H), 2.85 (s, 3H), 2.41 (s, 3H); ^{13}C{^{1}H} NMR (100 MHz, $CDCl_3$) δ = 188.4, 160.8, 155.8, 142.1, 140.7, 140.5, 140.4, 132.6, 130.0, 129.8, 129.5, 129.3, 123.8, 123.4, 123.3, 115.9, 114.2, 112.5, 55.5, 22.9, 21.5; HRMS (ESI) *m/z*: $[M + H]^+$ Calcd for $C_{25}H_{21}N_2O_2^+$ 381.1598; Found 381.1594.

1,7-Bis(4-methoxyphenyl)-4-methylimidazo[5,1,2-*cd*]indolizine-6-carbaldehyde (32oa).

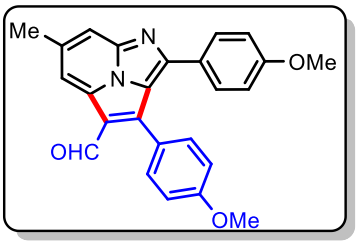

Purification by column chromatography on silica gel (eluent: EtOAc/hexanes, 1:4 *v/v*); Yellow solid (52 mg, 62%); mp = 160-162 °C; FT-IR ν_{max} (neat)/cm^{-1}: 1643, 1604, 1435, 1249, 1026, 979, 779, 524; ^{1}H NMR (400 MHz, $CDCl_3$) δ 10.10 (s, 1H), 8.23 (s, 1H), 7.84 (d, J = 8.7 Hz, 2H), 7.79 (s, 1H), 7.58 (d, J = 8.6 Hz, 2H), 7.09 – 7.06 (m, 2H), 6.89 – 6.85 (m, 2H), 3.96 (s, 3H), 3.87 (s, 3H), 2.84 (s, 3H); ^{13}C{^{1}H} NMR (100 MHz, $CDCl_3$) δ = 188.4, 161.5, 160.8, 155.6, 142.1, 140.4, 140.2, 132.6, 131.2, 129.8, 125.4, 123.9, 123.2, 123.1, 114.2, 114.0, 112.1, 55.5, 55.4, 22.9; HRMS (ESI) *m/z*: $[M + H]^+$ Calcd for $C_{25}H_{21}N_2O_3^+$ 397.1547; Found 397.1549.

7-(4-Methoxyphenyl)-1-(naphthalen-2-yl)imidazo[5,1,2-*cd*]indolizine-6-carbaldehyde

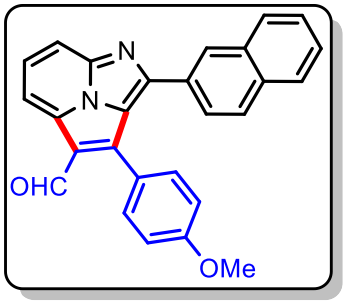

(32pa). Purification by column chromatography on silica gel (eluent: EtOAc/hexanes, 1:9 *v/v*); Orange solid; 53 mg (65%); mp = 186-188 °C; FT-IR ν_{max} (neat)/cm^{-1}: 1651, 1519, 1481, 1234, 1026, 972, 763, 509; ^{1}H NMR (400 MHz, $CDCl_3$) δ = 10.20 (s, 1H), 8.46 (d, J = 7.2 Hz, 1H), 8.26 (s, 1H), 8.16 – 8.09 (m, 3H), 7.87 (d, J = 8.4 Hz, 2H), 7.64 (d, J = 8.8 Hz, 2H), 7.56 – 7.46 (m, 3H), 7.10 (d, J = 8.8 Hz, 2H), 3.97 (s, 3H); ^{13}C{^{1}H} NMR (100 MHz, $CDCl_3$) δ = 188.3, 161.0, 155.4, 140.5, 134.3, 133.0, 132.8, 130.41, 130.37, 130.2, 130.0, 128.7, 128.4, 127.8, 127.4, 126.5, 126.0, 124.3, 124.2, 123.8, 115.3, 114.5, 113.7, 112.2, 55.6; HRMS (ESI) *m/z*: $[M + H]^+$ Calcd for $C_{27}H_{19}N_2O_2^+$ 403.1441; Found 403.1446.

7-(4-Methoxyphenyl)-1-(thiophen-3-yl)imidazo[5,1,2-*cd*]indolizine-6-carbaldehyde (32qa).

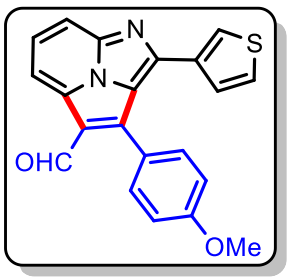

Purification by column chromatography on silica gel (eluent: EtOAc/hexanes, 1:4 *v/v*); Yellow solid; 47 mg (53%); mp = 199-201 °C; FT-IR ν_{max} (neat)/cm^{-1}: 1666, 1597, 1442, 1249, 1303, 1026, 972, 763, 509; ^{1}H NMR (400 MHz, $CDCl_3$) δ = 10.13 (s, 1H), 8.41 (d, J = 7.2 Hz, 1H), 8.16 – 7.97 (m, 2H), 7.66 (d, J = 8.1 Hz, 2H), 7.55 – 7.53 (m, 2H), 7.15 (d, J = 8.0 Hz, 2H), 7.03 (s, 1H), 3.99 (s, 3H); ^{13}C{^{1}H} NMR (100 MHz, $CDCl_3$) δ = 188.1, 169.4, 161.0, 152.8, 132.3, 130.39, 130.36, 130.2, 130.0, 128.4, 128.3, 125.6, 123.4, 118.0, 115.2, 114.4, 114.2, 111.8, 55.5; HRMS (ESI) *m/z*: $[M + H]^+$ Calcd for $C_{21}H_{15}N_2O_2S^+$ 359.0849; Found 359.0852.

6-(4-1,7-Diphenylimidazo[5,1,2-cd]indolizine-6-carbaldehyde (36ab). Purification by column

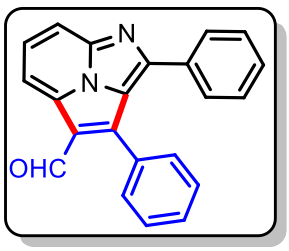

chromatography on silica gel (eluent: EtOAc/hexanes, 15:85 *v/v*); Yellow solid; 53 mg (64%); mp = 147-149 °C; FT-IR ν_{max} (neat)/cm^{-1}: 1658, 1489, 1219, 1026, 972, 748, 547; ^{1}H NMR (400 MHz, $CDCl_3$) δ = 10.17 (s, 1H), 8.49 (d, J = 7.4 Hz, 1H), 8.19 – 8.07 (m, 2H), 7.87 (d, J = 5.8 Hz, 2H), 7.69 – 7.62 (m, 2H), 7.62 – 7.53 (m, 3H), 7.43 (t, J = 7.1 Hz, 1H), 7.37 – 7.30 (m, 2H); ^{13}C{^{1}H} NMR (100 MHz, $CDCl_3$) δ = 188.2, 150.5, 146.6, 144.7, 131.5, 131.2, 130.5, 130.2, 129.7, 129.6, 128.8, 128.6, 124.3, 122.8, 115.5, 112.4, 112.0; HRMS (ESI) *m/z*: Calcd for $C_{22}H_{15}N_2O^+$ $[M + H]^+$ 323.1179; Found 323.1177.

3.4.4. Experimental Procedure for Synthesis of 35. A 10 mL round bottom flask containing MeOH (1 mL) was charged with **32aa** (25 mg, 0.07 mmol, 1 equiv.) and cooled to 0 °C for 15-20 min. $NaBH_4$ (8 mg, 0.21 mmol, 3.0 equiv.) was added portion-wise to the mixture with vigorous stirring. After addition, the reaction mixture was allowed to attain room temperature with continuous stirring till the completion of reaction (monitored by TLC). The solvent was then evaporated, and the crude reaction mixture was diluted with EtOAc (3 mL) and washed with water (3 × 5 mL). The aqueous layer was again extracted with EtOAc (2 × 2 mL). The combined organic layer was dried over anhydrous Na_2SO_4 and concentrated under reduced pressure. The resulting residue was purified by column chromatography (silica gen, 100-200 mesh size) using hexanes/ethyl acetate as eluent to afford **35**.

(7-(4-Methoxyphenyl)-1-phenylimidazo[5,1,2-*cd*]indolizin-6-yl)methanol (35). Purification

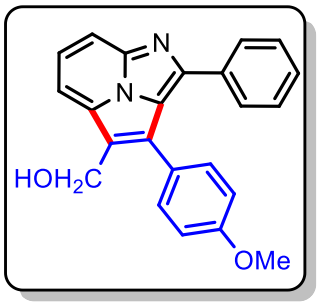

by column chromatography on silica gel (eluent: EtOAc/hexanes, 1:9 *v/v*); Green solid; 21.5 mg (86%); mp = 152-154 °C; FT-IR ν_{max} (neat)/cm^{-1}: 2839, 1681, 1489, 1242, 1026, 779, 740; ^1H NMR (400 MHz, $CDCl_3$) δ = 7.95 (t, J = 8.2 Hz, 2H), 7.88 (t, J = 7.7 Hz, 1H), 7.78 (d, J = 7.8 Hz, 2H), 7.56 – 7.48 (m, 2H), 7.13 (d, J = 7.8 Hz, 2H), 7.02 (d, J = 8.5 Hz, 2H), 5.07 (s, 2H), 3.93 (s, 3H), 2.39 (s, 3H); $^{13}C\{^1H\}$ NMR (100 MHz, $CDCl_3$) δ = 159.9, 151.0, 139.7, 133.8, 132.0, 131.9, 130.6, 129.5, 129.2, 126.6, 125.6, 125.3, 123.3, 114.0, 111.7, 110.6, 56.8, 55.4, 21.4; HRMS (ESI) *m/z*: $[M+H]^+$ Calcd for $C_{24}H_{21}N_2O_2^+$ $[M+H]^+$ 369.1598; Found 369.1595.

3.4.5. Experimental Procedure for Synthesis of 36. An oven dried 10 mL pressure tube was charged with **1b** (50 mg, 0.26 mmol, 1 equiv.), (*E*)-3-(4-methoxyphenyl)acrylaldehyde **30a** (63 mg, 0.39 mmol, 1.5 equiv.), $Pd(OAc)_2$ (3 mg, 5 mol %), $Cu(OAc)_2{\cdot}H_2O$ (104 mg, 0.52 mmol, 2 equiv.), K_2CO_3 (72 mg, 0.52 mmol, 2 equiv.), XPhos (37 mg, 30 mol %) and DMF (2 mL). The reaction vial was capped and stirred at 140 °C for 10 h in an oil bath. Next, the reaction mixture was cooled to room temperature, diluted by EtOAc (5 mL) and washed with chilled water (3 × 10 mL). The aqueous layer was again extracted with EtOAc (2 × 3 mL). The combined organic layer was dried over anhydrous Na_2SO_4 and concentrated under reduced pressure. The resulting residue was purified by column chromatography on a silica gel (100-200 mesh size) column using hexanes/ethyl acetate as eluent.

3-(4-Methoxyphenyl)-3-(2-(*p*-tolyl)imidazo[1,2-*a*]pyridin-3-yl)acrylaldehyde (36).

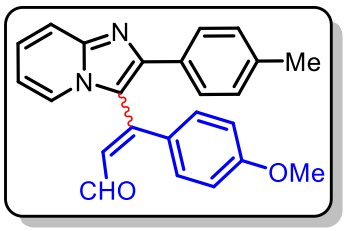

Purification by column chromatography on silica gel obtained as the mixture of *E/Z* isomers in 10:3.5 ratio; (eluent: EtOAc/hexanes, 2:3 *v/v*); Yellow semi-solid; 57 mg (57%), ^{1}H NMR (400 MHz, $CDCl_3$) δ = 9.79 (d, *J* = 7.9 Hz, 0.35H), 9.35 (d, *J* = 7.9 Hz, 1H), 7.80 (d, *J* = 8.9 Hz, 1.35H), 7.73 (d, *J* = 7.6 Hz, 2H), 7.61 (d, *J* = 6.8 Hz, 1.35H), 7.56 (d, *J* = 6.8 Hz, 1.35H), 7.44 (d, *J* = 8.3 Hz, 2H), 7.38 (d, *J* = 8.1 Hz, 1H), 7.31 (d, *J* = 7.6 Hz, 1H), 7.17 – 7.14 (m, 3H), 6.95 (d, *J* = 8.0 Hz, 3H), 6.77 – 6.72 (m, 3H), 6.36 (d, *J* = 7.7 Hz, 0.35H), 3.86 (s, 5H), 2.34 (s, 5H); ^{13}C{^{1}H} NMR (100 MHz, $CDCl_3$) δ = 192.6, 192.1, 162.5, 161.9, 148.8, 148.0, 146.8, 146.4, 145.9, 138.5, 138.4, 132.1, 130.3, 130.0, 129.6, 129.33, 129.27, 129.2, 128.8, 128.7, 128.0, 127.9, 127.1, 126.5, 126.1, 124.8, 124.5, 119.8, 117.7, 117.5, 115.2, 114.7, 114.3, 113.3, 55.5, 21.3; HRMS (ESI) *m/z*: $[M+H]^+$ Calcd for $C_{24}H_{21}N_2O_2^+$ 369.1598; Found 369.1604.

Ethyl (*E*)-3-(2-(Imidazo[1,2-*a*]pyridin-2-yl)phenyl)acrylate (38aa).

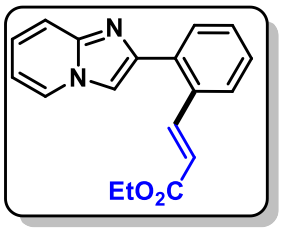

Purification by column chromatography on silica gel (eluent: EtOAc/hexanes, 1:4 *v/v*); Brown oil; 45 mg (60%); ^{1}H NMR (400 MHz, $CDCl_3$) δ = 8.25 (d, *J* = 15.8 Hz, 1H), 8.16 (d, *J* = 5.2 Hz, 1H), 7.93 (d, *J* = 6.6 Hz, 1H), 7.72−7.62 (m, 3H), 7.54−7.36 (m, 2H), 7.22 (t, *J* = 6.7 Hz, 1H), 6.82 (t, *J* = 6.5 Hz, 1H), 6.47 (d, *J* = 15.8 Hz, 1H), 4.27 (q, *J* = 7.6 Hz, 2H), 1.34 (t, *J* = 6.8 Hz, 3H); ^{13}C{^{1}H} NMR (100 MHz, $CDCl_3$) δ = 167.1, 145.3, 144.3, 143.8, 134.4, 133.0, 130.2, 129.9, 128.1, 127.1, 125.7, 125.0, 119.8, 117.8, 112.6, 112.0, 60.5, 14.4; HRMS (ESI) *m/z*: $[M+H]^+$ Calcd for $C_{18}H_{17}N_2O_2^+$ 293.1285; Found 293.1288.

Methyl (*E*)-3-(2-Phenylimidazo[1,2-*a*]pyridin-3-yl)acrylate (39aa). Purification by column chromatography on silica gel (eluent: EtOAc/hexanes, 1:4 *v/v*); Green solid; 39 mg (55%); mp = 148−150 °C; ^{1}H NMR (400 MHz, $CDCl_3$) δ = 8.50−8.48 (m, 1H), 8.07 (d, *J* = 16.4 Hz, 1H), 7.80−7.75 (m, 3H), 7.56−7.51 (m, 2H), 7.50−7.45 (m, 1H), 7.42−7.37 (m, 1H), 7.06−7.02 (m, 1H), 6.39 (d, *J* = 16.4 Hz, 1H), 3.83 (s, 3H); ^{13}C{^{1}H} NMR (100 MHz, $CDCl_3$) δ = 167.9, 151.2, 147.3, 133.7, 130.8, 129.5, 128.9, 128.8, 126.7, 125.3, 118.3, 117.2, 114.0, 113.2, 51.8; HRMS (ESI) *m/z*: $[M+H]^+$ Calcd for $C_{17}H_{15}N_2O_2^+$ 279.1128; Found 279.1134.

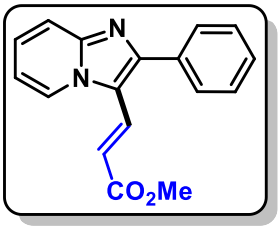

3.4.6. Sample Preparation and Crystal Measurement of 31aa and 32ca: Single crystals of **31aa** [$C_{23}H_{16}N_2O_2$] and **32ca** [$C_{24}H_{18}N_2O_3$] were grown from slow evaporation of dichloromethane solution. A suitable crystal was selected and mounted on a XtaLAB AFC12 (RINC): Kappa dual home/near diffractometer. The crystal was kept at 93(2) K during data collection. Using Olex2[58], the structure was solved with the ShelXT[59] structure solution program using Intrinsic phasing and refined with the ShelXL[60] refinement package using least squares minimisation.

Table 3.4. Crystal data for **31aa and 32ca.**

Identification code	**31aa**	**32ca**
Empirical formula	$C_{23}H_{16}N_2O_2$	$C_{24}H_{18}N_2O_3$
Formula weight	352.38	382.40
Temperature/K	93(2)	93(2)
Crystal system	triclinic	triclinic
Space group	P-1	P-1
a/Å	6.4215(3)	9.4640(2)
b/Å	11.0446(5)	10.5043(4)
c/Å	12.4667(6)	10.8802(3)
α/°	79.816(4)	62.617(4)
β/°	78.678(4)	77.363(2)
γ/°	83.107(4)	79.392(3)
Volume/Å^3	849.97(7)	932.81(6)
Z	2	2
ρ_{calc}g/cm^3	1.377	1.361
μ/mm^{-1}	0.713	0.735
F(000)	368.0	400.0
Crystal size/mm^3	0.15 × 0.1 × 0.06	0.12 × 0.1 × 0.04
Radiation	Cu Kα (λ = 1.54184)	Cu Kα (λ = 1.54184)
2Θ range for data collection/°	7.324 to 159.388	9.264 to 158.828
Index ranges	-8 ≤ h ≤ 7, -13 ≤ k ≤ 14, -15 ≤ l ≤ 12	-9 ≤ h ≤ 12, -13 ≤ k ≤ 13, -13 ≤ l ≤ 13
Reflections collected	8699	10135

Independent reflections	3535 [R_{int} = 0.0343, R_{sigma} = 0.0456]	3914 [R_{int} = 0.0352, R_{sigma} = 0.0429]
Data/restraints/parameters	3535/0/245	3914/0/264
Goodness-of-fit on F^2	1.108	1.057
Final R indexes [I>=2σ (I)]	R_1 = 0.0460, wR_2 = 0.1280	R_1 = 0.0632, wR_2 = 0.1920
Final R indexes [all data]	R_1 = 0.0507, wR_2 = 0.1318	R_1 = 0.0681, wR_2 = 0.2008
Largest diff. peak/hole / e $Å^{-3}$	0.24/-0.21	2.00/-0.31

3.5 REFERENCES

1. Langer, S.; Arbilla, S.; Benavides, J.; Scatton, B., *Advances in Biochemical Psychopharmacology* **1990**, *46*, 61-72.
2. Sanger, D., *Behavioural Pharmacology* **1995**, *6*, 116-126.
3. Kitamura, N.; Shiraiwa, H.; Inomata, H.; Nozaki, T.; Ikumi, N.; Sugiyama, K.; Nagasawa, Y.; Karasawa, H.; Iwata, M.; Matsukawa, Y., *International Journal of Rheumatic Diseases* **2018**, *21*, 813-820.
4. Mizushige, K.; Ueda, T.; Yukiiri, K.; Suzuki, H., *Cardiovascular Drug Reviews* **2002**, *20*, 163-174.
5. Jenkinson, S.; Thomson, M.; McCoy, D.; Edelstein, M.; Danehower, S.; Lawrence, W.; Wheelan, P.; Spaltenstein, A.; Gudmundsson, K., *Antimicrobial Agents and Chemotherapy* **2010**, *54*, 817-824.
6. Devi, N.; Singh, D.; K Rawal, R.; Bariwal, J.; Singh, V., *Current Topics in Medicinal Chemistry* **2016**, *16*, 2963-2994.
7. Goel, R.; Luxami, V.; Paul, K., *Current Topics in Medicinal Chemistry* **2016**, *16*, 3590-3616.
8. Bagdi, A. K.; Santra, S.; Monir, K.; Hajra, A., *Chemical Communications* **2015**, *51*, 1555-1575.
9. Haruhiko, T.; Takafumi, H.; Shojiro, S.; Toshiki, M.; Koji, A., *Bulletin of the Chemical Society of Japan* **1999**, *72*, 1327-1334.
10. Kielesiński, Ł.; Tasior, M.; Gryko, D. T., *Organic Chemistry Frontiers* **2015**, *2*, 21-28.

11. Firmansyah, D.; Banasiewicz, M.; Deperasińska, I.; Makarewicz, A.; Kozankiewicz, B.; Gryko, D. T., *Chemistry – An Asian Journal* **2014**, *9*, 2483-2493.
12. Pericherla, K.; Kaswan, P.; Pandey, K.; Kumar, A., *Synthesis* **2015**, *47*, 887-912.
13. Bagdi, A. K.; Santra, S.; Monir, K.; Hajra, A., *Chemical Communications* **2015**, *51*, 1555-1575.
14. Reen, G. K.; Kumar, A.; Sharma, P., *Beilstein Journal of Organic Chemistry* **2019**, *15*, 1612-1704.
15. Patel, O. P. S.; Nandwana, N. K.; Legoabe, L. J.; Das, B. C.; Kumar, A., *Advanced Synthesis & Catalysis* **2020**, *362*, 4226-4255.
16. Tashrifi, Z.; Mohammadi-Khanaposhtani, M.; Larijani, B.; Mahdavi, M., *European Journal of Organic Chemistry* **2020**, *2020*, 269-284.
17. Konwar, D.Bora, U., *ChemistrySelect* **2021**, *6*, 2716-2744.
18. Sharma, M.Prasher, P., *Synthetic Communications* **2022**, DOI: https://doi.org/10.1080/00397911.2022.2079091.
19. Shi, L.; Li, T.; Mei, G.-J., *Green Synthesis and Catalysis* **2022**, *3*, 227-242.
20. Zhang, Z.; Han, H.; Wang, L.; Bu, Z.; Xie, Y.; Wang, Q., *Organic & Biomolecular Chemistry* **2021**, *19*, 3960-3982.
21. Hagui, W.; Doucet, H.; Soulé, J.-F., *Chem* **2019**, *5*, 2006-2078.
22. Sun, C.-L.; Li, B.-J.; Shi, Z.-J., *Chemical reviews* **2011**, *111*, 1293-1314.
23. Yamaguchi, J.; Yamaguchi, A. D.; Itami, K., *Angewandte Chemie International Edition* **2012**, *51*, 8960-9009.
24. Docherty, J. H.; Lister, T. M.; Mcarthur, G.; Findlay, M. T.; Domingo-Legarda, P.; Kenyon, J.; Choudhary, S.; Larrosa, I., *Chemical Reviews* **2023**.
25. Davies, H. M.Morton, D., *Journal*, 2016, **81**, 343-350.
26. Bag, S.; Patra, T.; Modak, A.; Deb, A.; Maity, S.; Dutta, U.; Dey, A.; Kancherla, R.; Maji, A.; Hazra, A., *Journal of the American Chemical Society* **2015**, *137*, 11888-11891.
27. Samanta, S.; Mondal, S.; Santra, S.; Kibriya, G.; Hajra, A., *The Journal of Organic Chemistry* **2016**, *81*, 10088-10093.
28. Dutta, B.; Sharma, V.; Sassu, N.; Dang, Y.; Weerakkody, C.; Macharia, J.; Miao, R.; Howell, A. R.; Suib, S. L., *Green Chemistry* **2017**, *19*, 5350-5355.

29. Shaw, M. H.; Twilton, J.; MacMillan, D. W., *The Journal of Organic Chemistry* **2016**, *81*, 6898-6926.
30. Vanda, D.; Zajdel, P.; Soural, M., *European Journal of Medicinal Chemistry* **2019**, *181*, 111569.
31. Cao, H.; Lei, S.; Liao, J.; Huang, J.; Qiu, H.; Chen, Q.; Qiu, S.; Chen, Y., *RSC Advances* **2014**, *4*, 50137-50140.
32. Liu, S.; Jiang, H.; Liu, W.; Zhu, X.; Hao, X.-Q.; Song, M.-P., *The Journal of Organic Chemistry* **2020**, *85*, 15167-15182.
33. Zhang, Q.; Huang, X.; Gui, Y.; He, Y.; Liao, S.; Huang, G.; Liang, T.; Zhang, Z., *Organic Letters* **2023**, *25*, 1447-1452.
34. Shinde, V. N.; Rangan, K.; Kumar, A., *The Journal of Organic Chemistry* **2022**.
35. Zhu, Y.; Dai, R.; Huang, C.; Zhou, W.; Zhang, X.; Yang, K.; Wen, H.; Li, W.; Liu, J., *The Journal of Organic Chemistry* **2022**, *87*, 11722-11734.
36. Qi, Z.; Yu, S.; Li, X., *The Journal of Organic Chemistry* **2015**, *80*, 3471-3479.
37. Ghosh, M.; Naskar, A.; Mishra, S.; Hajra, A., *Tetrahedron Letters* **2015**, *56*, 4101-4104.
38. Li, P.; Zhang, X.; Fan, X., *The Journal of Organic Chemistry* **2015**, *80*, 7508-7518.
39. Peng, H.; Yu, J.-T.; Jiang, Y.; Wang, L.; Cheng, J., *Organic & Biomolecular Chemistry* **2015**, *13*, 5354-5357.
40. Wang, W.; Niu, J.-L.; Liu, W.-B.; Shi, T.-H.; Hao, X.-Q.; Song, M.-P., *Tetrahedron* **2015**, *71*, 8200-8207.
41. Zheng, G.; Tian, M.; Xu, Y.; Chen, X.; Li, X., *Organic Chemistry Frontiers* **2018**, *5*, 998-1002.
42. Reddy, K. N.; Chary, D. Y.; Sridhar, B.; Reddy, B. V. S., *Organic Letters* **2019**, *21*, 8548-8552.
43. Ghosh, K.; Nishii, Y.; Miura, M., *Organic Letters* **2020**, *22*, 3547-3550.
44. Li, P.; Zhang, X.; Fan, X., *The Journal of Organic Chemistry* **2015**, *80*, 7508-7518.
45. Ghosh, S. K.; Kuo, B. C.; Chen, H. Y.; Li, J. Y.; Liu, S. D.; Lee, H. M., *European Journal of Organic Chemistry* **2015**, *2015*, 4131-4142.
46. Ghosh, M.; Naskar, A.; Mishra, S.; Hajra, A., *Tetrahedron Letters* **2015**, *56*, 4101-4104.
47. Qi, Z.; Yu, S.; Li, X., *The Journal of Organic Chemistry* **2015**, *80*, 3471-3479.
48. Mu, B.; Li, J.; Zou, D.; Wu, Y.; Chang, J.; Wu, Y., *Organic Letters* **2016**, *18*, 5260-5263.

49. Zheng, G.; Tian, M.; Xu, Y.; Chen, X.; Li, X., *Organic Chemistry Frontiers* **2018**, *5*, 998-1002.
50. Reddy, K. N.; Chary, D. Y.; Sridhar, B.; Reddy, B. S., *Organic Letters* **2019**, *21*, 8548-8552.
51. Xue, C.; Han, J.; Zhao, M.; Wang, L., *Organic Letters* **2019**, *21*, 4402-4406.
52. Shinde, V. N.; Kanchan Roy, T.; Jaspal, S.; Nipate, D. S.; Meena, N.; Rangan, K.; Kumar, D.; Kumar, A., *Advanced Synthesis & Catalysis* **2020**, *362*, 5751-5764.
53. Li, Y.; Wang, F.; Yu, S.; Li, X., *Advanced Synthesis & Catalysis* **2016**, *358*, 880-886.
54. Battula, S.; Bukya, H.; Chandra Shekar, K.; Nayani, K., *The Journal of Organic Chemistry* **2023**, *88*, 10986-10995.
55. Kotla, S. K. R.; Choudhary, D.; Tiwari, R. K.; Verma, A. K., *Tetrahedron Letters* **2015**, *56*, 4706-4710.
56. Zhang, Q.; Huang, X.; Gui, Y.; He, Y.; Liao, S.; Huang, G.; Liang, T.; Zhang, Z., *Organic Letters* **2023**, *25*, 1447-1452.
57. Pericherla, K.; Kaswan, P.; Khedar, P.; Khungar, B.; Parang, K.; Kumar, A., *RSC Advances* **2013**, *3*, 18923-18930.
58. Dolomanov, O. V.; Bourhis, L. J.; Gildea, R. J.; Howard, J. A. K.; Puschmann, H., *Journal of Applied Crystallography* **2009**, *42*, 339-341.
59. Sheldrick, G., *Acta Crystallographica Section A* **2015**, *71*, 3-8.
60. Sheldrick, G., *Acta Crystallographica Section C* **2015**, *71*, 3-8.

Chapter 4A

Design and Synthesis of Selenium Coordinated Pd(II)-Complex: Catalyst for Site Selective Annulation of 2-arylimidazo[1,2-*a*]pyridines

4.4A.1 INTRODUCTION

Transition metal-catalyzed C-H functionalization has emerged as one of the promising and efficient methods for synthesis of diverse functional molecules with easily available and inexpensive starting material. Transition metal complexes containing Ru, Rh, Ir, and Pd have been extensively used as catalysts in C-H functionalization reactions.[1-6] Among of them Pd catalysis can achieve the desired results in various transformations.[7] By using rational design and careful ligand selection, high turnover numbers and low catalyst loading can be achieved. Ligands play a crucial role in stabilizing the metal center and controlling the selectivity of chemical transformations.[8-10] In this regard molecular rotor frameworks are attractive ligands because they are stable in air and moisture, and they can adjust the catalytic activity of metal atoms. Molecular rotor ligands offer a remarkable balance between reactivity and stability in their metal complexes, effectively shielding the metal within a protective environment.

In past few decades, there has been a great deal of interest in the design and synthesis of new molecular devices. One of the most prominent classes of such molecular devices is molecular rotor. Generally, a molecular rotor consists of a rotating unit called a rotator, which rotates around a stationary part of the molecule, distinct as a stator. Moreover, the axle of rotation around the molecular rotor rotates can be either parallel (known as an altitudinal rotor) or perpendicular (known as an azimuthal rotor) to the surface (**Figure 4.4A.1)**.[11-13] The dynamical behavior of a molecular rotor is affected by both the energy states of the system (including the stator) and the environmental temperature. Higher temperature generally promote easier reorientation of the rotor by providing more thermal energy to overcome potential energy barriers, while lower temperatures restrict the rotor's motion due to reduced thermal energy.[14-17]

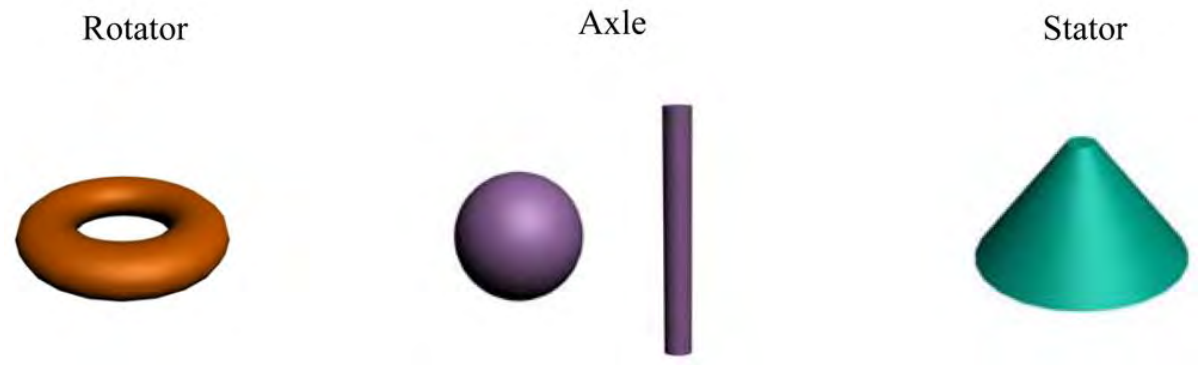

Figure 4.4A.1: The components of the molecular rotor[18]

Over the past few years, numerous research groups have contributed to this field, reporting molecular rotors with functional anchors, bulky stators, and cage-encased rotors. The development of molecular rotors with functional anchors was one of the notable studies by Kaleta and Michl.[19] These anchors played a crucial role in facilitating the rotation of the rotor within the crystal structure. On the other hand, Garcia-Garibay and other researchers have studied molecular rotors with bulky stators. In order to influence and control the rotational behavior of the rotor, these stators were designed. As reported by Gladysz,[20-24] Garcia-Garibay,[25-28] and other researchers, rotors encased by cages were another significant advancement in molecular rotors. As part of this approach, the rotor was enclosed in a protective cage that not only provided stability, but also influenced the dynamics of the rotor. In particular study, the researchers investigated how crystal properties are modulated by the rotational dynamics of the molecular rotor. The birefringence of the crystal changed with temperature, as the rotor switched between static and dynamic states. Moreover, the researchers explored the impact of molecular rotor rotation on crystal structures.[29, 30] For instance, they studied a phenylene bridged macrocage crystal and observed inflation, which was caused by the rotational motion of the rotor embedded within it.[31-33] Additionally, the dielectric relaxation of a powdered molecular dipolar rotor was also investigated, revealing valuable insights into its behavior.[34] These recent studies on molecular rotors have provided a deeper understanding of their properties and behavior in different environments. In the past few years, the emphasis has been on developing unidirectional molecular rotors based on the ratchet mechanism and molecular rotors with random rotations induced thermally.[35-38] The rotation in the latter class of molecules is non-directional, and their use as a gyroscope is conceivable. However, by incorporating a dipole moment in the rotor unit, these molecules can be transformed into unidirectional rotors. The rotation of unidirectional molecular rotors is typically controlled through chemical or physical stimuli.[35, 39] Recently in 2016, the Nobel Prize in Chemistry was awarded to Jean-Pierre Sauvage, Sir J. Fraser Stoddart, and Bernard L. Feringa for their pioneering work in designing and synthesizing molecular machines.[40, 41] They have developed molecules with controllable movements to perform a task with added energy. The ability of molecular rotors to exhibit rotational motion within crystalline structures holds great potential for various applications in the field of molecular machines and nanotechnology[25, 42-44] energy storage,[45, 46] and catalysis[47] (**Figure 4.4A.2)**.

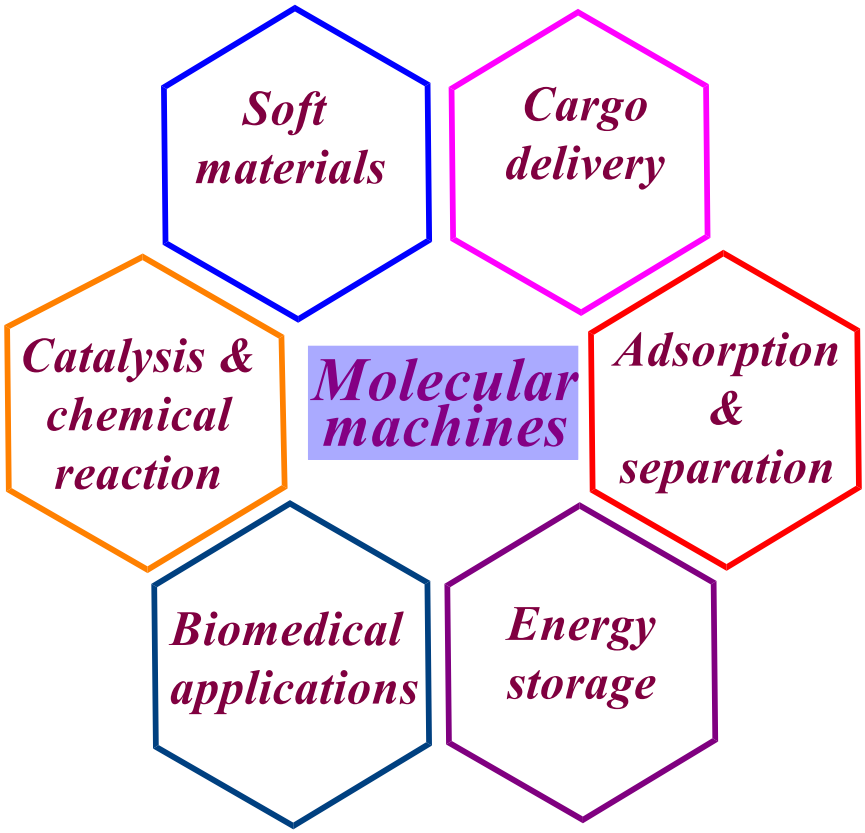

Figure 4.4A.2: Applications of molecular machines

For instance, the Garcia-Garibay and Setaka groups[48-52] independently synthesized molecular rotors with organic rotor units and investigated their rotational properties. Garcia-Garibay and colleagues, have established a novel binuclear emissive crystalline rotor with a pyrazine rotator (**3**) connected to Cu or Au metal through an NHC carbene stator (**1**) **(Scheme 4.4A.1)**.[53] The π-accepting ability of the molecular rotor influenced the rotation barrier, and the length of the rotational axle connected to Cu or Au played a critical role in controlling it. The Cu(I) rotor complex exhibits higher rotational energy and electronic delocalization than the Au rotor. This difference was attributed to a more significant steric interaction in the Cu(I) complex, resulting in a red-shifted emission in the solid state. Although this system's specific application has not been reported, the physical properties of amphidynamic crystals, including those described, offer potential for utilization in pharmaceuticals, sensors, and adsorption/desorption processes.

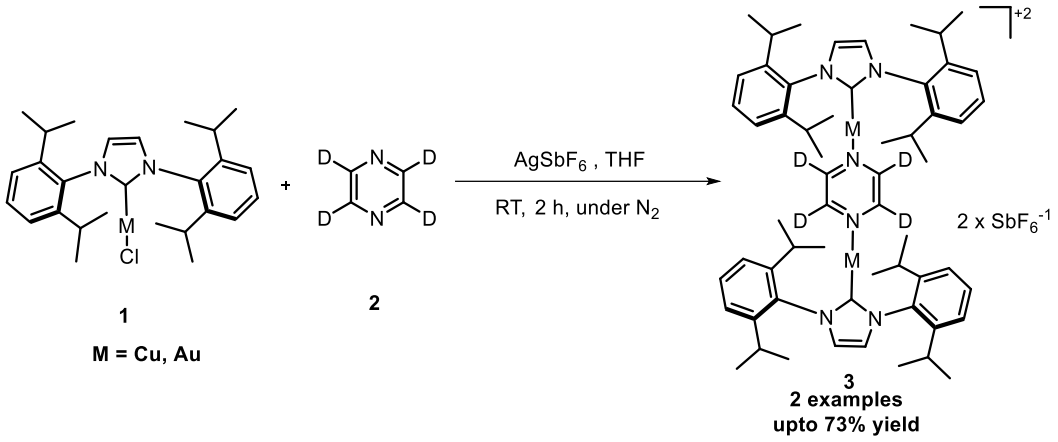

Scheme 4.4A.1: Synthesis of *N*-heterocyclic carbene-based binuclear transition metal complex of Cu(I) as a molecular rotor

Very recently, Setaka *et al.* reported the synthesis of dimethylfluorenene-diyl fluorophores containing molecular gyrotops (**5**) using 2,7-dibromo-9,9-dimethyl-9*H*-fluorene (**4)** by substitution and metathesis reaction. Two examples of such macrocage derivatives were synthesized encorporating C18 and C22 units of CH_2 as a side chain of the cage. The structure of both macrocage derivatives, was characterized by NMR spectroscopy and crystal data. The crystal data indicates that the cage of C22 should larger void space as compared to C18. These dimethyl fluorene moieties displayed no flipping motions in the solid state, also confirmed by the solid-state ^{2}H NMR and comparison of their fluorescence properties in solution and solid form (**Scheme 4.4A.2)**.[54]

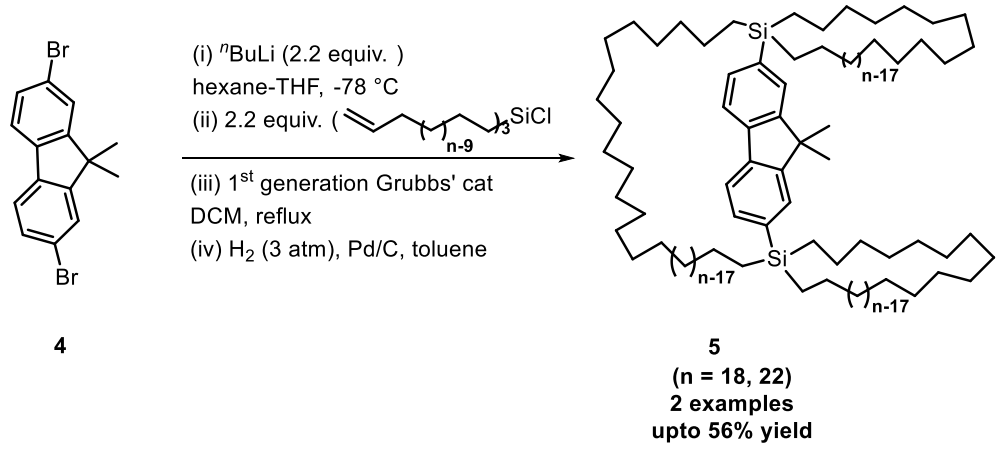

Scheme 4.4A.2: Synthesis of molecular gyrotops based on dimethyl fluorene-diyl type bridge

The same group reported the thienothiophene-dioxide-bridged based macrocage compounds (**7**) following the same process in the presence of thieno[3,2-*b*]thiophene (**6**). Cages such as C14TTO2, C18TTO2, and C22TTO2, were successfully synthesized and demonstrated solid-state fluorescence and dielectric relaxation. The fluorophore was encapsulated within these molecular structures, allowing rotational movement even in the crystalline state. The rotational behavior of the fluorophore in its crystalline form was examined using temperature-dependent dielectric relaxation. The results showed that the fluorophore in C14TTO2 remained static, whereas constrained and facile rotation was observed in C18TTO2 and C22TTO2, respectively. The solid-state fluorescence quantum yield was decreased as the alkyl chain length increased. This drop in fluorescence intensity suggests that the fluorophore's internal dynamics inside the macrocage structure substantially impact it (**Scheme 4.4A.3**).[55]

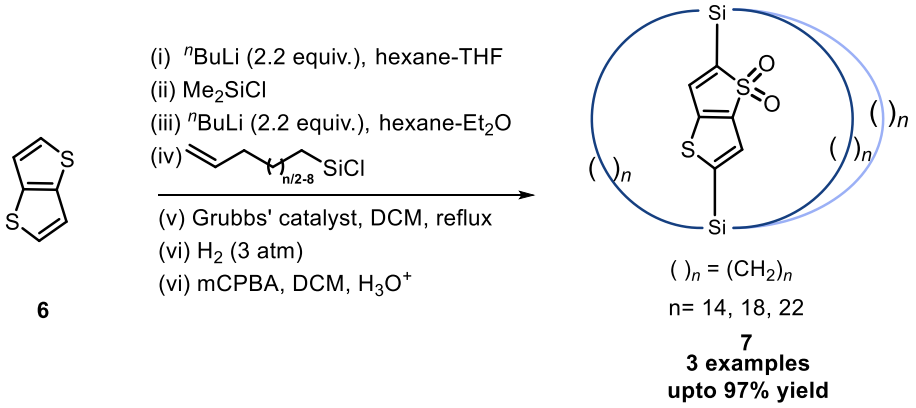

Scheme 4.4A.3: Synthesis of thieno[3,2-*b*]thiophene-dioxide-diyl based bridged molecular gyrotops

Subsequently, Kurimoto *et al.* developed a novel class of molecular rotors (**10**) that can spin around a 1,4-napthylene bridge. These structures consist of bridging the 1,4-diaminonaphthalene unit (**8**) with two elongated alkyl chains. The primary objective was to explore the influence of the frame size on the rotational behavior. To accomplish this, they synthesized framed rotors labelled as CnNp (where 'n' represents the length of a side chain). The synthesis involved synthesizing four compounds: C12Np, C14Np, and C16Np. They achieved this by directly cyclizing 1,4-napthalenediamine (**8**) with *α,ω*-dihaloalkane (**9**) in the presence of Na_2CO_3 as a base. Upon analyzing the behavior of the naphthylene rotor in solution, they observed that the rotation was effectively inhibited in C12Np, C14Np, and C16Np. However, in the case of C18Np, the rotor

demonstrated rotational movement. This was verified by the temperature-dependent coalescence of the NMR signals originating from the α-CH_2 groups (**Scheme 4.4A.4**).[56]

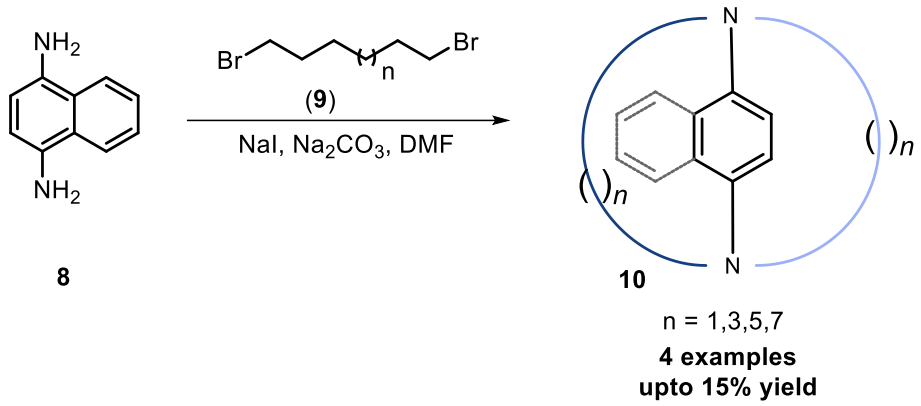

Scheme 4.4A.4: Synthesis of 1,4-naphthylene bridged diazamacrocycles

Gladysz's group has made significant contributions for the design and synthesis of various molecular gyroscopes with an inorganic rotor unit in the molecule and an understanding of their rotational behavior. In 2015 Gladysz and co-workers described the chloride-substitution reactions of *trans*-[Rh(CO)(Cl){P{$(CH_2)_{14}$}$_3$$P^2$(Rh–$P^2$)}] (**11**) with $ZnPh_2$, or MeLi lead to the formation of the respective products: *trans*-[Rh(CO)(Ph){P{$(CH_2)_{14}$}$_3$$P^2$(Rh–$P^2$)}] (**12**), and *trans*-[Rh(CO)(Me){P{$(CH_2)_{14}$}$_3$$P^2$(Rh–$P^2$)}] (**13**) with a yield of 89%, and 94% respectively (**Scheme 4.4A.5**). Additionally, dibridgehead diphosphine P[$(CH_2)_{14}$]$_3$P is formed with a yield of 58%. Complex **14** acts as a catalyst precursor for the hydroformylation of 1-octene (**15**) under neat conditions or in the presence of THF (tetrahydrofuran) at 60 °C and 75 psig pressure with a 1:1 ratio of CO to H_2 (**Scheme 4.4A.6**).[57]

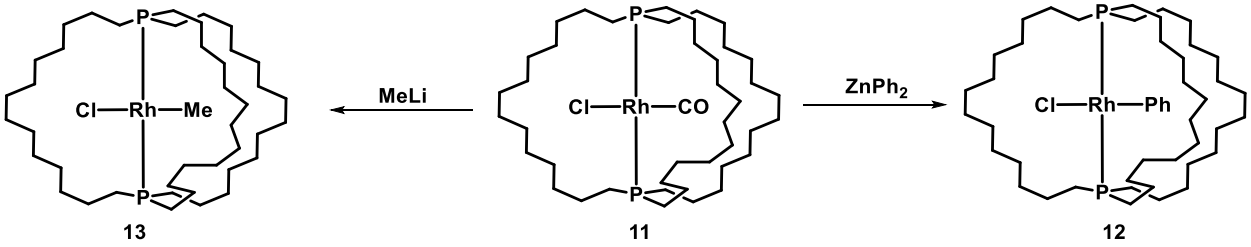

Scheme 4.4A.5: Synthesis of dibridgehead-diphosphines based Rh(I)-complex

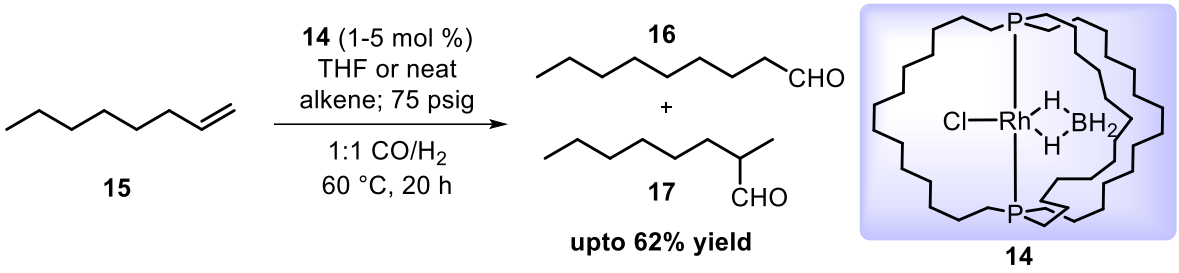

Scheme 4.4A.6: Hydroformylation of alkene *via* Rh(I)-complex

Recently, Gladysz's and colleagues demonstrated the synthesis of square planar *trans*-Rh(CO)(Cl)[P($(CH_2)_{14})_3$P] (**19**) gyroscope-like complex from *trans*-Rh(CO)(Cl)[P($(CH_2)_6CH=CH_2)_3]_2$ (**18**) *via* a C=C metathesis/hydrogenation approach. The gyroscope-like complex has cage-like *trans*-aliphatic dibridgehead diphosphine as a stators unit and Rh(CO)(X) or $Rh(CO)_2$(I) as a rotor. The dimensions of the rotators and the diphosphine cages' void spaces were calculated using crystal data. Eyring plot calculations and variable-temperature NMR studies have been used to study the rotor's dynamic properties (**Scheme 4.4A.7**).[23]

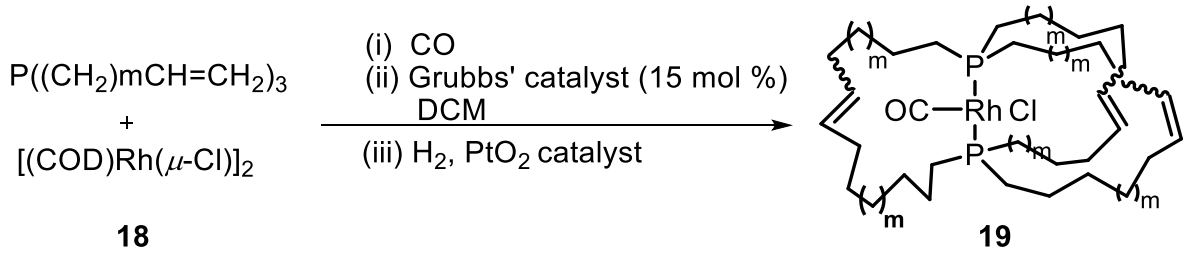

Scheme 4.4A.7: Synthesis of gyroscope-based Rh(I)-complex

In 2020 Goswami *et al.* demonstrated a simple and efficient method for the preparation of multi-component devices such as $[Cu(A)(B)]^{2+}$ and $[Cu(A)_2]^{4+}$, both molecular rotors (**23**), undergo domino rotation with fluxional axles. Subseuently, the molecular rotors were tested as a catalyst for the click reaction of azide (**20**) and acetylene (**21**) due to the presence of Cu(I) in the molecular rotor (**Scheme 4.4A.8**).[47]

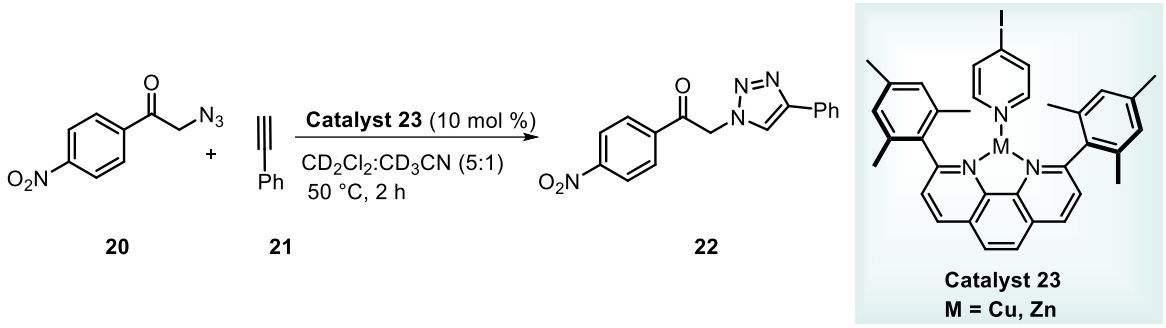

Scheme 4.4A.8: Azide-Alkyne Huisgen cycloaddition catalysis *via* molecular rotor

Fekl and colleagues created a low rotational barrier molecular rotor with an H-Pt-H rotor (**24**) unit attached to a P-Pt-P spin axis. In addition, they studied solid-state ^{2}H and phosphorus (^{195}P) NMR spectroscopy with variable temperatures to calculate rotational barriers using the Eyring plot. An NMR study revealed that *trans*-H(Cl)-Pt-$(PBu_3)_2$ **(25)** does not rotate at room temperature, whereas *trans*-H_2-Pt-$(PBu_3)_2$ (**24)** rotates at temperatures as low as 75 k. Moreover, the barrier to rotation of the *trans*-H_2-Pt-$(PBu_3)_2$ complex has estimated to be closer to 3 kcal mol^{-1} (**Scheme 4.4A.9).**

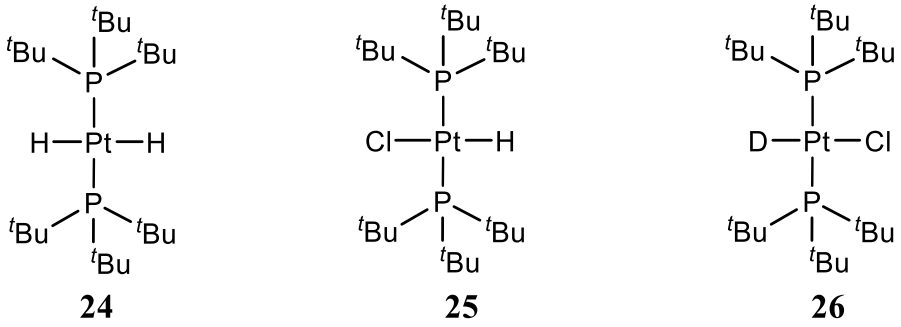

Scheme 4.4A.9: Structure of molecular rotor [*trans*-$H_2Pt(P^tBu_3)_2$], [*trans*-H(Cl)$Pt(P^tBu_3)_2$], and [*trans*-D(Cl)$Pt(P^tBu_3)_2$]

The design and synthesis of new molecular devices have attracted great interest. Inorganic molecular rotors are distinct in design, with a bulky stator unit protecting the metal center and the metal center in a sterically confined space. This feature can be used in the catalysis of organic reactions where product selectivity is an issue, as the steric bulk on the metal center will force incoming reagents to approach the metal center from a specific direction, assisting in introducing selectivity in product formation. Despite this, molecular rotors are underutilized as catalysts. Gladysz and colleagues reported hydroformylation of 1-octene using a molecular gyroscope containing rhodium metal. Schmittle group used a molecular rotor with double rotor units on a fluxional axle as a catalyst for the Huisgen azide-alkyne cycloaddition reaction. Inspired by the

applications of macroscopic gyroscope in the field of organic catalysis, we have design and synthesized air stable molecular rotor with Cl−Pd−Cl rotor spoke attached to a Se−Pd−Se axle. Bulky stator ligand (**28**) was synthesized by the reaction of 1-benzyloxy-2-(chloromethyl)benzene (**27**) with selenium powder in the presence of $NaBH_4$. In the next step, **28** was reacted with 0.5 equiv. of $PdCl_2(CH_3CN)_2$ to give the molecular rotor **29** (**Scheme 4.4A.10**).

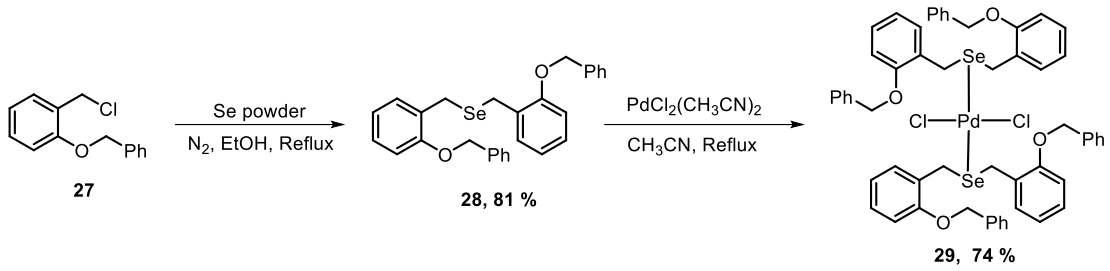

Scheme 4.4A.10: Syntheses of the molecular rotor **29**

4.4A.2 RESULTS AND DISCUSSIONS

The sterically bulky stator ligand was specifically designed to provide protection to Cl−Pd−Cl rotator through the bulky air-stable selenium ligand. The new ligand and palladium complex were characterized with the help of ^1H (Figure 4.4A.3), $^{13}C\{^1H\}$ (Figure 4.4A.4), NMR, IR, and HRMS. Two singlets were observed at 3.87 and 5.10 ppm for $SeCH_2$ and OCH_2, respectively in the ^1H NMR spectrum of ligand **28**. Upon coordination of **28** with palladium, the $SeCH_2$ protons became diastereotopic due to intramolecular SeCH...Cl secondary interactions and showed two doublets at 4.56 and 4.13 ppm (**Figure 4.4A.3**). In ^{13}C NMR the $SeCH_2$ carbon appears at 30.7 and OCH2 carbon appears at 69.9 ppm. Peak at *m/z* 475.1129 and 475.1181 corresponding to $[M + H]^+$ and $[M – PdCl_2 + H]^+$ ions were observed in HRMS analysis of **28** and **29**, respectively.

Further, the structure and bonding of molecular rotor **29** were also authenticated with the help of a single crystal X-ray (**Figure 4.4A.5**). The Cl-Pd-Cl rotor possesses *trans*-geometry with respect to bulky stator ligand **28**. The two selenium orient themselves in *anti*-position with respect to each other. The Se–Se distance of the stator unit in the molecule is 4.878 Å whereas Cl–Cl distance of rotor unit is 4.574 Å. The Pd–Se and Pd–Cl distance in the molecule are 2.4391 and 2.2869 Å, respectively. The molecule possesses intramolecular SeCH…Cl interactions of 2.880 Å in between the stator ligand and rotor unit (**Figure 4.4A.5**). These secondary interactions block the rotation of molecule at room temperature.

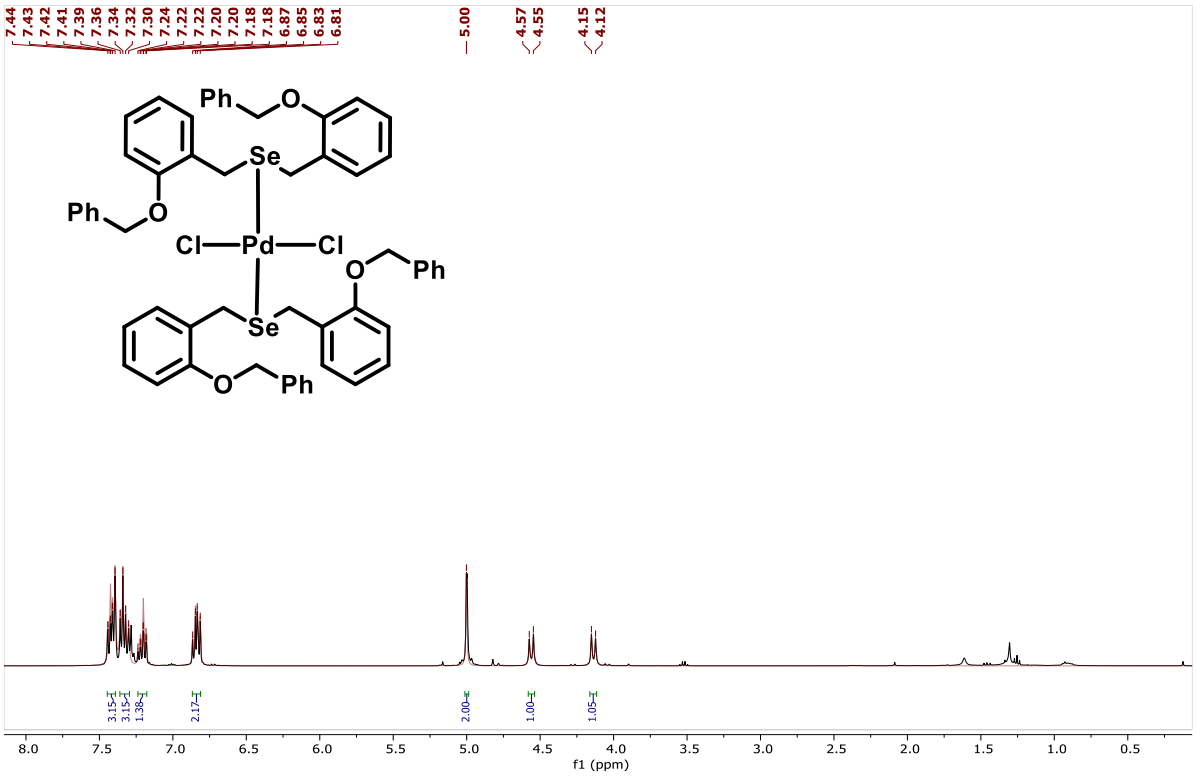

Figure 4.4A.3: ^{1}H NMR spectrum of **29** recorded in $CDCl_3$

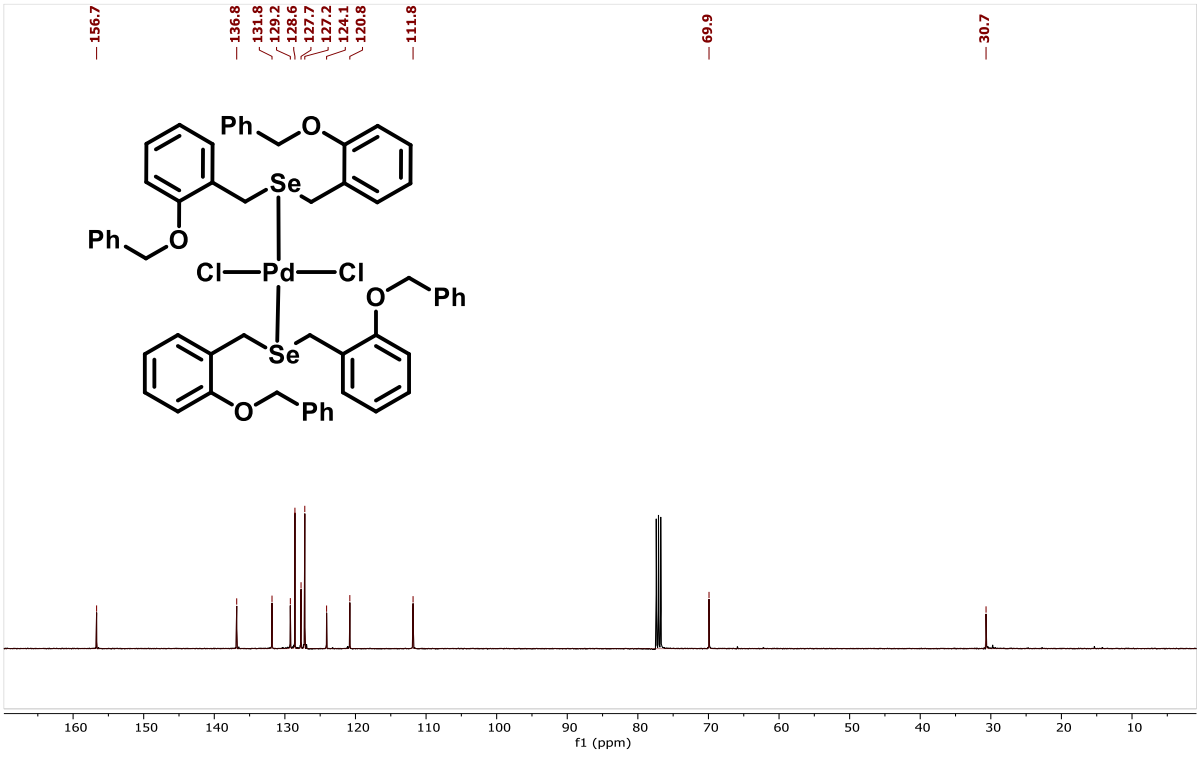

Figure 4.4A.4: $^{13}C\{^{1}H\}$ NMR spectrum of **29** recorded in $CDCl_3$

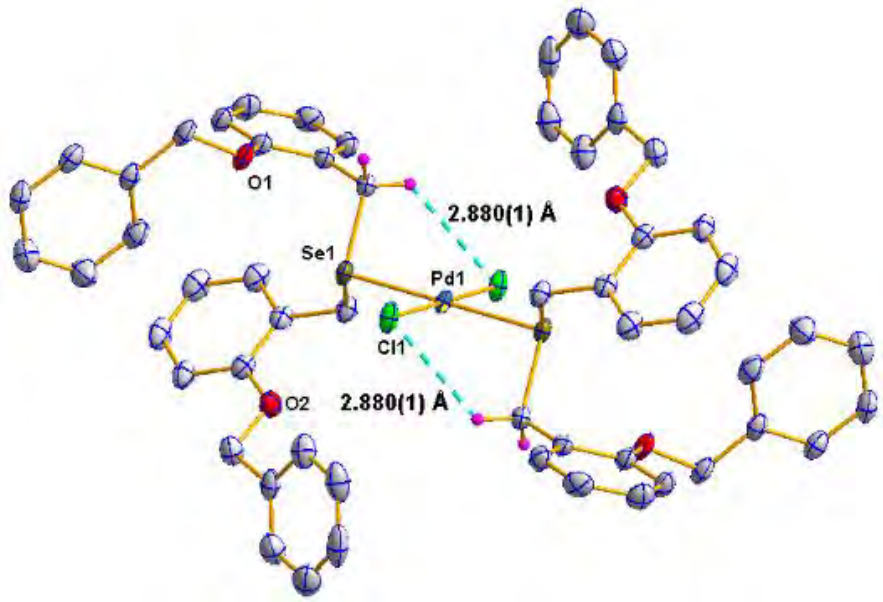

Figure 4.4A.5: Thermal ellipsoid plots (50% probability) of molecular rotor **29** showing intramolecular SeCH---Cl interactions

4.4A.2.1 Dynamic Process in Molecular Rotor 29

It was assumed that the rotation is blocked at room temperature due to intramolecular SeCH…Cl interactions which is also supported by the presence of two peaks for diastereotopic $SeCH_2$ protons in the ^1H NMR of **29** at room temperature (**Figure 4.4A.5**). The metal complexes of *trans*-$[MX_2(SeR_2)_2]$ are known to show a pyramidal inversion of selenium atom at elevated temperatures.[58] The detailed studies for pyramidal inversion of *trans*-$[PdCl_2(SeEt_2)_2]$ showed a rotational barrier of 16.2 kcal/mol.[58] The molecular rotor **29**, have possibility of showing pyramidal inversion at elevated temperature.

The thermal response of the molecular rotor **29** was studied with the help of variable temperature (VT) NMR which shows pyramidal inversion at the selenium atom. The rotation of chlorine through Cl-Pd-Cl in the **29** was studied with the help of a relaxed potential energy scan and indicated a rotational barrier of ~15.5 kcal/mol. As shown in **Figure 4.4A.6 (left),** when the DMSO-d_6 solution of **29** was warmed, the two diastereotopic proton signals of $SeCH_2$ in the ^1H NMR started to coalesce. In molecular rotor **29**, the diastereotopic proton signals show coalescence around 40-50 °C, which is closely related to earlier reported *trans*-$[PdCl_2(SeEt_2)_2]$ complex.[58]This suggests that the coalescing phenomenon is due to the inversion of the selenium atom and rotation around $SeCH_2$ bond (**Scheme 4.4A.11**).[58] The line shapes of the coalescing signals in **Figure**

4.4A.6 (right) were simulated using gNMR, and the rate constants were determined at each temperature. An Eyring plot utilizing these rate constants afforded $\Delta H^{\ddagger}$, $\Delta S^{\ddagger}$, and $\Delta G^{\ddagger}_{298K}$ values of 7.1 kcal/mol, −5.8 eu, and 15.5 kcal/mol for the process rendering the diastereotopic proton signals equivalent.

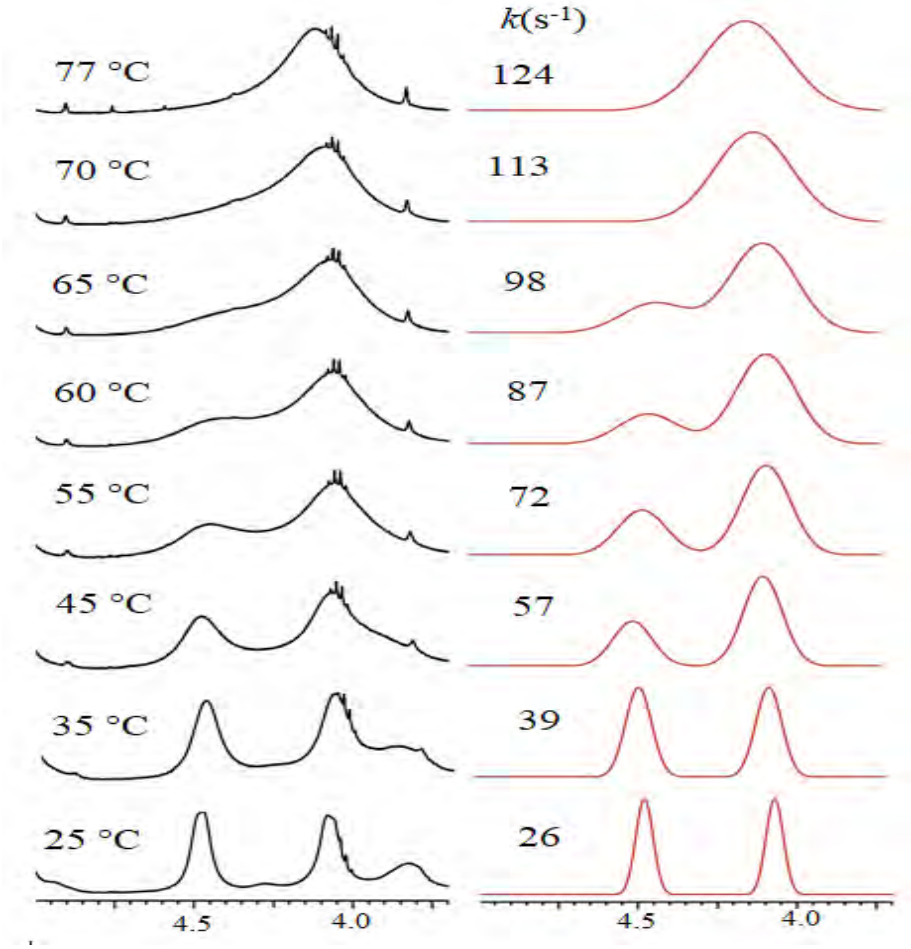

Figure 4.4A.6: Partial ^{1}H NMR spectra of **29** (DMSO-d_6) as a function of temperature. Each spectrum (left) is paired with simulated line shapes (right) for the signals of interest

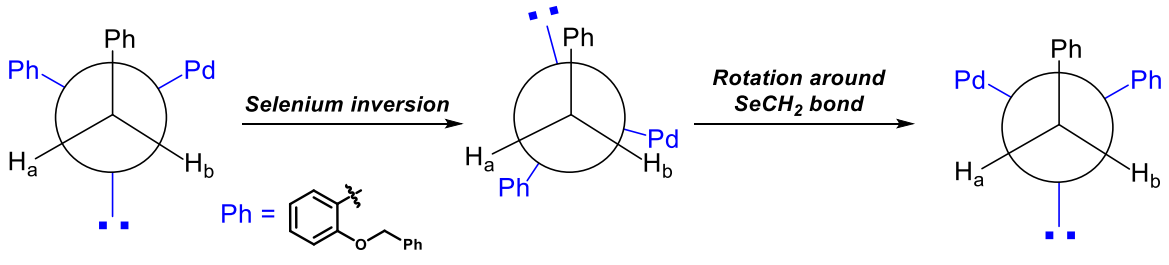

Scheme 4.4A.11: Newman projections representing selenium inversion and rotation around -$SeCH_2$ bond in **29**

4.4A.2.2 A Selenium-Coordinated Palladium(II) *trans*-dichloride Molecular Rotor (29) Catalyzed Oxidative Annulation of Imidazo[1,2-*a*]pyridine

Initially, a reaction of 2-phenylimidazo[1,2-*a*]pyridine (**30a**) and diphenylacetylene (**31a**) in the presence of catalyst **29** (1.0 mol %), $Cu(OAc)_2{\cdot}H_2O$ (2 equiv.), and DMAc (3 mL) afforded exclusively 2,3,4-triphenylimidazo[5,1,2-*cd*]indolizine (**33a**) in 31% yield (**Table 4.4A.1**, entry 1). Further, yield of **33a** improved to 58%, when **30a** and **31a** were reacted in the presence of K_2CO_3 under otherwise identical conditions (**Table 4.4A.1**, entry 2). Encouraged with these results, several bases like KO^{t}Bu, K_3PO_4, Na_2CO_3, and DIPEA were screened (**Table 4.4A.1**, entries 3-6), and highest yield of **33a** (67%) was obtained by using KO^{t}Bu (**Table 4.4A.1**, entry 3). When K_3PO_4 was used as base under the standard conditions, the other regioisomer, 5,6-diphenylnaphtho[1',2':4,5]imidazo[1,2-*a*]pyridine (**32a**), was also isolated in 32% yield (**Table 4A.1**, entry 4).

Further, various oxidants like $Cu(OAc)_2{\cdot}H_2O$, $AgNO_3$, AgOAc, Ag_2CO_3, IBD, and TBHP were tested for the model reaction (**Table 4.4A.1**, entries 3, 7-11), and among them $Cu(OAc)_2{\cdot}H_2O$ was found the best. In case of IBD, the product **32a** was also observed in 27% yield. Reaction didn't work when TBHP was used as oxidant (**Table 4.4A.1**, entry 11). Different solvents like DMAc, DMF, DMSO, and xylene were then screened, and DMAc was found the best among all (**Table 4.4A.1**, entries 3, 12-14). The choice of catalyst loading was subsequently screened (**Table 4.4A.1**, entries 15, and 16). When 1.5 mol % of **29** was used under standard reaction conditions (**Table 4.4A.1**, entry 3), the yield of **33a** increased to 74% (**Table 4.4A.1**, entry 15). Upon increasing the catalyst loading to 2.0 mol %, **33a** was isolated in 63% along with other regioisomer **32a** (13%, **Table 4.4A.1**, entry 16). Upon decreasing reaction temperature and time, the yield of **33a** was lowered (**Table 4.4A.1**, entries 17 and 18). Reactions in the absence of catalyst or oxidant did not result in the formation of **33a** (**Table 4.4A.1**, entries 19 and 20).

With the optimal reaction conditions in hand, the scope and generality of the reaction was studied for structurally divergent 2-arylimidazo[1,2-*a*]pyridines (**30a-k**) and results are summarized in **Table 4.4A.2.** It is worth noticing that reaction went smoothly to give good yield of annulated products **33a-n** with excellent tolerance towards different functional groups. Substituents like Br and Cl which are prone to palladium catalyzed coupling reactions also showed excellent tolerance

and no byproducts were observed during the reactions. Imidazo[1,2-*a*]pyridines with electron releasing groups (**33e, 33i,** and **33j**) afforded better yields of annulated products.

Table 4.4A.1: Optimization of reaction conditions for cycloaromatization of 2-arylimidazo[1,2-*a*]pyridines (**30a**) with diphenylacetylene (**31a**)[a].

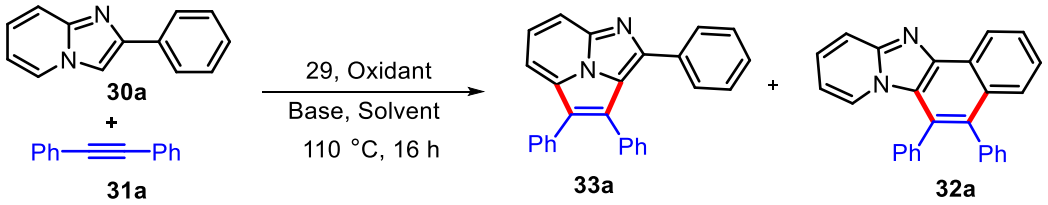

Entry no.	Catalyst (mol%)	Oxidant	Base	Solvent	Yield% (33a)[b]	Yield% (32a)[b]
1	**29** (1 mol %)	$Cu(OAc)_2{\cdot}H_2O$	—	DMAc	31	nd
2	**29** (1 mol %)	$Cu(OAc)_2{\cdot}H_2O$	K_2CO_3	DMAc	58	nd
3	**29** (1 mol %)	$Cu(OAc)_2{\cdot}H_2O$	KO^{t}Bu	DMAc	67	nd
4	**29** (1 mol %)	$Cu(OAc)_2{\cdot}H_2O$	K_3PO_4	DMAc	22	32
5	**29** (1 mol %)	$Cu(OAc)_2{\cdot}H_2O$	Na_2CO_3	DMAc	11	nd
6	**29** (1 mol %)	$Cu(OAc)_2{\cdot}H_2O$	DIPEA	DMAc	03	nd
7	**29** (1 mol %)	$AgNO_3$	KO^{t}Bu	DMAc	22	nd
8	**29** (1 mol %)	AgOAc	KO^{t}Bu	DMAc	52	nd
9	**29** (1 mol %)	Ag_2CO_3	KO^{t}Bu	DMAc	26	nd
10	**29** (1 mol %)	IBD	KO^{t}Bu	DMAc	21	27
11	**29** (1 mol %)	TBHP	KO^{t}Bu	DMAc	nr	nr
12	**29** (1 mol%)	$Cu(OAc)_2{\cdot}H_2O$	KO^{t}Bu	DMF	36	23
13	**29** (1 mol %)	$Cu(OAc)_2{\cdot}H_2O$	KO^{t}Bu	DMSO	54	19
14	**29** (1 mol %)	$Cu(OAc)_2{\cdot}H_2O$	KO^{t}Bu	Xylene	08	nd
15	**29** (1.5 mol %)	$Cu(OAc)_2{\cdot}H_2O$	KO^{t}Bu	DMAc	74	nd
16	**29** (2.0 mol %)	$Cu(OAc)_2{\cdot}H_2O$	KO^{t}Bu	DMAc	63	13
17[c]	**29** (1.5 mol %)	$Cu(OAc)_2{\cdot}H_2O$	KO^{t}Bu	DMAc	52	nd
18[d]	**29** (1.5 mol %)	$Cu(OAc)_2{\cdot}H_2O$	KO^{t}Bu	DMAc	55	nd
19	**29** (1 mol %)	—	KO^{t}Bu	DMAc	nd	nd
20	—	$Cu(OAc)_2{\cdot}H_2O$	KO^{t}Bu	DMAc	nd	nd
21[e]	**29** (1.5 mol %)	$Cu(OAc)_2{\cdot}H_2O$	KO^{t}Bu	DMAc	13	nd

[a]Reaction conditions unless specified otherwise: **30a** (0.250 mmol), **31a** (1.1 equiv), oxidant (2 equiv), base (2 equiv), solvent (3 mL). nd = not determined, nr = no reaction. [b]Isolated yield. [c]at 90 °C. [d]at 10 h. [e]$Cu(OAc)_2{\cdot}H_2O$ (10 mol %).

Annulation of 2-(thiophen-2-yl)imidazo[1,2-*a*]pyridine (**30k**) with **31a** also yielded corresponding annulated product **33k** in 67% yield. The reaction of unsymmetrical alkyne, prop-1-yn-1-ylbenzene (**31b**) with **30a** gave 3-methyl-2,4-diphenylimidazo[5,1,2-*cd*]indolizine (**33l**) in 63% yield. A similar regioselectivity was observed in Pd(II) catalyzed annulation of unsymmetrical alkyne with 2-arylimidazo[1,2-*a*]pyridines. The reaction of symmetrically substituted alkyne (**31c**) resulted in 78% yield of annulated product **33m**. Aliphatic alkyene, diethyl but-2-ynedioate (**31d**) was also reacted with **30a** to give annulated product **33n** in 31% yield. It is worth mentioning that reaction of 5-methyl-2-phenylimidazo[1,2-*a*]pyridine (**30o**) with **31a** gave 8-methyl-5,6-diphenylnaphtho[1',2':4,5]imidazo[1,2-*a*]pyridine (**32o**) in 62% yield under these conditions.

Table 4.4A.2: Substrate scope for synthesis of imidazo[5,1,2-*cd*]indolizines.

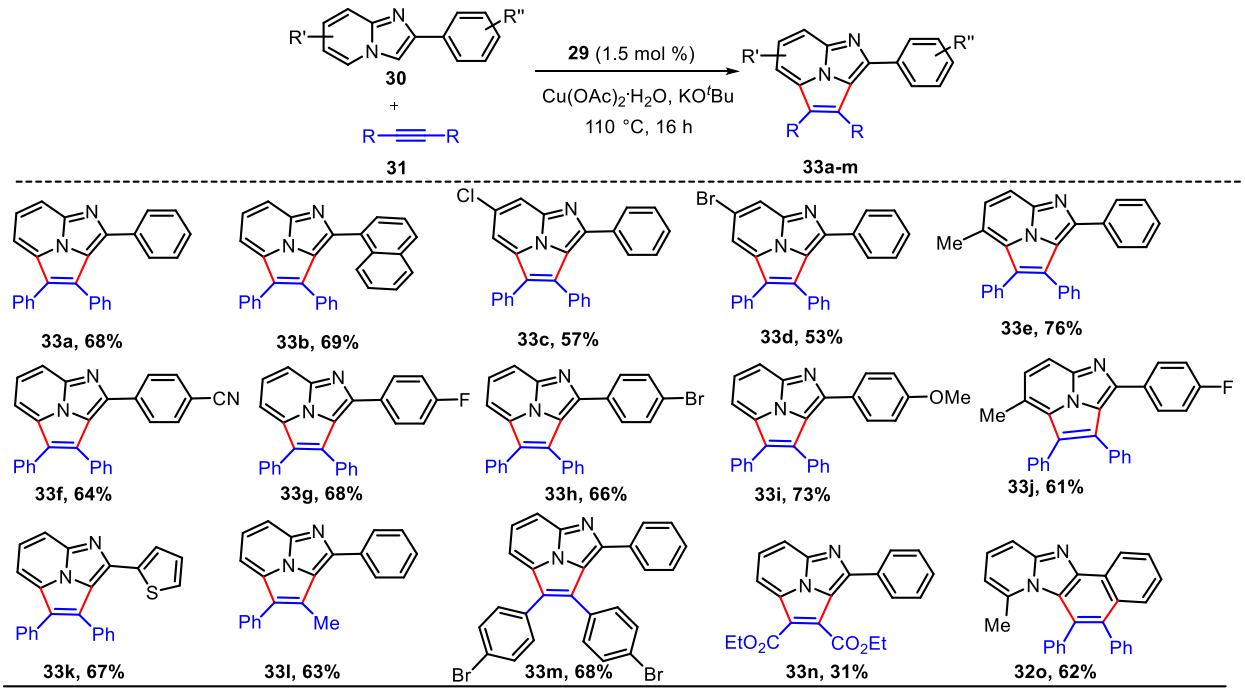

[a]Reaction conditions unless specified otherwise: **30** (0.250 mmol), **31** (1.1 equiv), $Cu(OAc)_2 \cdot H_2O$ (2 equiv.), KO^{t}Bu (2 equiv.), DMAc (3 mL), 110 °C, 16 h.

Based on the experimental results, theoretical calculations, and previous reports,[59-61] plausible mechanism of the reaction is proposed in **Scheme 4.4A.13**. intermediate A by electrophilic aromatic palladation on C3-position, which was also supported by the deuterium exchange experiments. DFT geometry optimization by QUICKSTEP module[62] of CP2k package[63] using Perdew, Burke, and Ernzerhof (PBE) exchange–correlation functional and Goedecker-Teter-Hutter pseudopotential[64] (GTH-PBE) with MOLOPT type DZVP basis set[65] (except for Se and Pd

were short range – DZVP-MOLOPT-SR-GTH) indicated that the trans-isomer of A is favored by 14.77 kcal/mol over cis-isomer due to stabilization through CH-π interactions[66, 67] between aryl group of 2-arylimidazo[1,2-*a*]pyridine and π-cloud of ligand phenyl ring (**Figure 4.4A.7**).

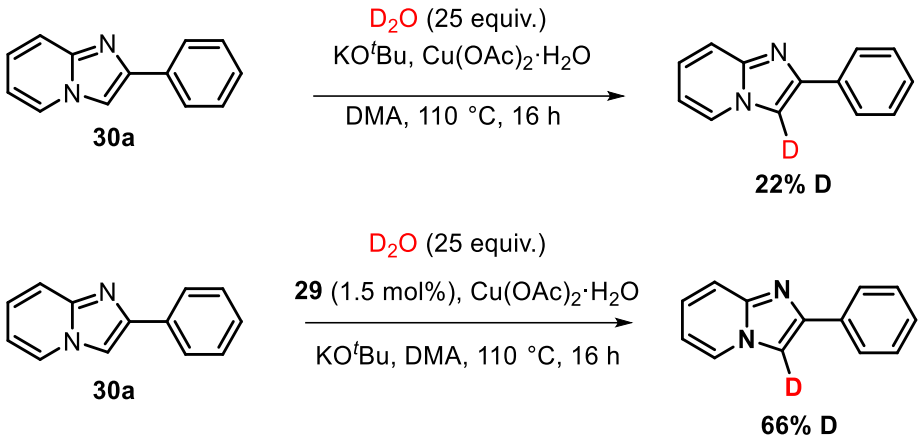

Scheme 4.4A.12: Deuterium exchange experiment catalysed by **29**

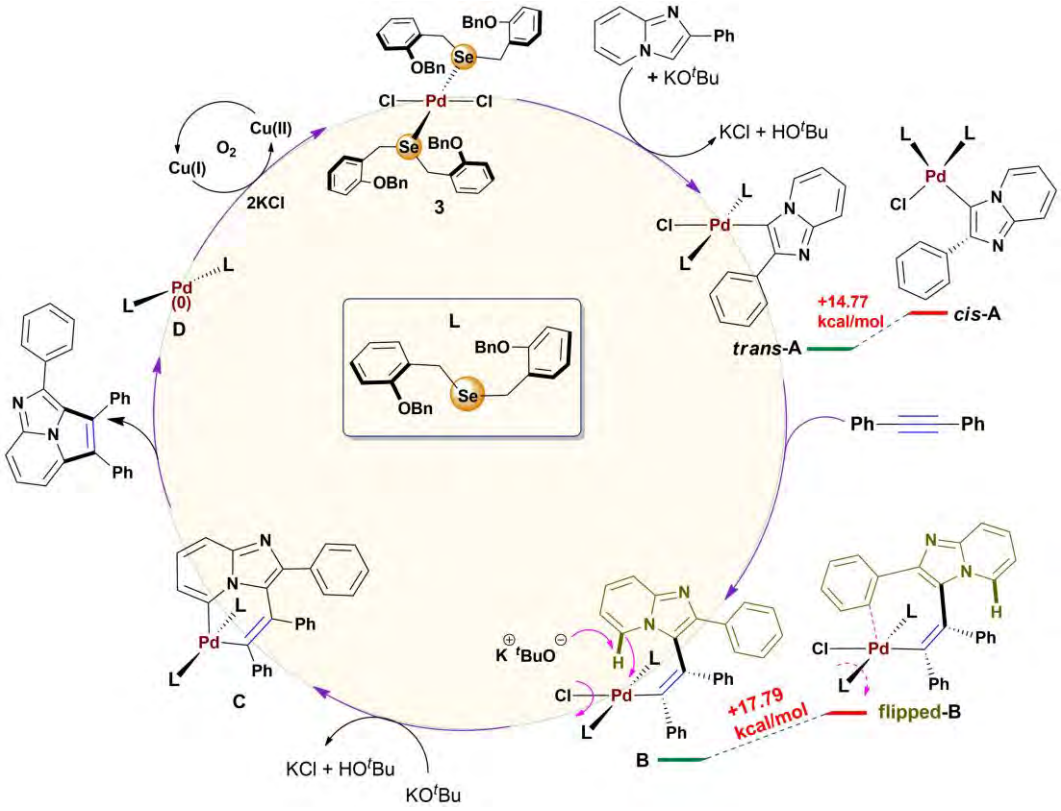

Scheme 4.4A.13: Plausible mechanism for formation of **33a** (Relative energies (kcal/mol) cis- & trans- isomers of A; B & its 2-arylimidazo[1,2-*a*]pyridine flipped-B computed by DFT)

In second step, the C−C triple bond of **31** inserts into the Pd−C bond of A to give intermediate B. The relative energy of B and geometry optimization of flipped-2-arylimidazo[1,2-*a*]pyridine of B (flipped-B) from DFT study give rise to less favored (+17.8 kcal/mol) seven membered configuration and cleavage of Pd-L bond (**Figure 4.4A.8**). This stabilization of 2-arylimidazo[1,2-*a*]pyridine orient C-H of pyridine ring toward chlorine of catalyst **29** (B), which justify the observed regioselectivity in the reaction. In third step, the cleavage of C5−H bond in B affords a six membered palladacycle intermediate C. Finally, reductive elimination occurs with C to generate **33a** together with ligand stabilized Pd(0) (D), which is re-oxidized into the Pd(II) species (**29**) by $Cu(OAc)_2{\cdot}H_2O/O_2$, KCl.

4.4A.3 CONCLUSIONS

We have successfully synthesized a low barrier secondary interaction (SeCH---Cl) controlled molecular rotor. Variable temperature NMR data established ΔG‡298K value of 15.5 kcal/mol for the dynamic process. The molecular rotor showed excellent catalytic activity at low catalyst loading (1.5 mol %) with reverse regioselectivity for annulation of 2-arylimidazo[1,2-*a*] pyridines.

4.4A.4 EXPERIMENTAL SECTION

4.4A.4.1 General Information. The ligand and complex were synthesized using standard Schlenk techniques. The catalysis reactions were carried out in pressure tube under open air conditions. HPLC grade DMF, CH_2Cl_2, EtOH, EtOAc, hexane, CH_3CN, DMAc, DMSO and xylene were used directly as received. Salicylaldehyde (Sigma Aldrich), benzyl bromide (Spectrochem), K_2CO_3 (Spectrochem), selenium powder (Sigma Aldrich), $NaBH_4$ (Spectrochem), Na_2SO_4 (Spectrochem), $CDCl_3$ (Sigma Aldrich), and $PdCl_2$ (Alfa Aesar, 99.9%) were used as purchased. All other reagents for catalysis reaction were purchased from local commercial sources and used as it is. NMR spectrum were recorded on a Bruker NMRs 400 MHz instrument at ambient probe temperatures and referenced as follows (δ, ppm): ^1H, residual internal $CHCl_3$ (7.26); $^{13}C\{^1H\}$, internal $CDCl_3$ (77.00). IR spectrums of new ligand and complex were taken on a Nicolet Protége 460 FT-IR spectrometer on KBr pellets. Melting points of new complexes were recorded in an open capillary. HRMS measurements were carried out by electrospray ionization (ESI) method on an Agilent Q-TOF LCMS spectrometer.

4.4A.4.2 Synthesis of Bis(2-(benzyloxy)benzyl)selane (28). A three necked round bottom flask was charged with selenium powder (4.00 mmol, 0.316 g) in 40 mL ethanol, and fitted with

condenser under N_2 atmosphere. The mixture was refluxed and solid $NaBH_4$ (0.310 g, 8.2 mmol) was added in small portions until the mixture turned into colorless solution. A solution of 1-(benzyloxy)-2-(chloromethyl)benzene (1, 0.465 g, 2.00 mmol) in C_2H_5OH (5 mL) was added drop wise with stirring. After 12 h mixture was cooled to room temperature, solvent was reduced (~2 mL) by using rotary evaporated. The residue was placed at the top of a silica column (3 × 14 cm), which was eluted with hexanes (150 mL) and then hexanes/EtOAc (90:10 v/v). The solvent was evaporated from the product containing fractions (assayed by TLC) by rotary evaporation to give **28** as a yellow oil (0.768 g, 1.622 mmol, 81%). Anal. Calcd for $C_{28}H_{26}O_2Se$ (473.47): C, 71.03; H, 5.54. Found: C, 70.92; H, 5.47.

NMR ($CDCl_3$, δ/ppm): ^1H (400 MHz) 7.47-7.45 (m, 2H), 7.38-7.31 (m, 3H), 7.19-7.15 (m, 2H), 6.91-6.83 (m, 2H), 5.01 (s, 2H, OCH_2), 3.87 (s, 2H, $SeCH_2$); $^{13}C\{^1H\}$ (100 MHz) 156.2, 137.2, 130.2, 128.9, 128.5, 127.8, 127.7, 127.2, 120.6, 111.9, 69.9 (s, OCH_2), 22.3 (s, $SeCH_2$); IR (cm^{-1}, powder film): 3216 (w), 3050 (w), 2875 (w), 1597, 1489, 1450, 1242, 694; HRMS (ESI) *m/z*: $[M+H]^+$ Calcd for $C_{28}H_{27}O_2Se$ 475.1176, Found 475.1129.

4.4A.4.3 Palladium Complex of Bis(2-(benzyloxy)benzyl)selane (29). A round bottom flask was charged with **28** (0.473 g, 1.00 mmol), $PdCl_2(CH_3CN)_2$ (0.130 g, 0.50 mmol), acetonitrile (15 mL), and fitted with a condenser. The mixture was stirred (2h) while refluxing. The mixture was then cooled, passed through a short pad of silica gel (18 cm) and washed with CH_3CN (25 mL). The solvent was removed by rotary evaporation and residue was washed with cold n-pentane to give **29** as a yellow solid (0.417 g, 0.371 mmol, 74%); m.p: 296-298 ˚C; Anal. Calcd for $C_{56}H_{52}Cl_2O_4PdSe_2$ (1124.25): C, 59.83; H, 4.66. Found: C, 59.91; H, 4.58.

NMR ($CDCl_3$, δ/ppm): ^1H (400 MHz) 7.44-7.39 (m, 3H), 7.36-7.28 (m, 3H), 7.24-7.18 (m, 1H), 6.86-6.81 (m, 2H), 5.00 (s, 2H, OCH_2), 4.56 (d, 2H, J = 11.2 Hz, SeCH2), 4.14 (d, 2H, J = 11.2 Hz, $SeCH_2$); $^{13}C\{^1H\}$ (100 MHz) 156.6, 136.8, 131.7, 129.2, 128.5, 127.6, 127.1, 124.0, 120.7, 111.8, 69.8 (s, OCH_2), 30.6 (s, $SeCH_2$); IR (cm^{-1}, powder film): 3192 (m), 2914 (w), 2211 (m), 1645, 1527, 1210, 1032, 755; HRMS (ESI) *m/z*: $[M–PdCl_2 + H]^+$: Calcd for $C_{28}H_{27}O_2Se$ 475.1176, Found 475.1118.

4.4A.4.4 Procedure for Oxidative Annulation Reaction: A pressure tube was charged with 2-aryl imidazo[1,2-*a*]pyridine (0.250 mmol), 1,2-diarylethyne (1.1 equiv.), oxidant (2 equiv.), base (2 equiv.), and **29** (1.5 mol %) in 3 mL solvent. After that, the reaction mixture was refluxed at

110 °C for 16 h. The progress of reaction was monitored by TLC and reaction was quenched with aq. NH_4Cl. The reaction mixture was extracted with ethyl acetate (15 mL × 3). The crude product was purified by chromatography on silica-gel to afford annulated products **33a-33n** and **32o**.

2,3,4-Triphenylimidazo[5,1,2-*cd*]indolizine (33a). Purification by column chromatography on silica gel (eluent: EtOAc/hexanes, 1:9 *v/v*); Yellow solid; 65 mg (68%); mp = 208-210 ˚C; ^{1}H NMR (400 MHz, $CDCl_3$) δ 8.09 – 8.02 (m, 1H), 8.01 – 7.95 (m, 2H), 7.83 (d, *J* = 7.3 Hz, 2H), 7.47 (d, *J* = 7.3 Hz, 2H), 7.45 – 7.39 (m, 4H), 7.39 – 7.31 (m, 5H), 7.29 (d, *J* = 7.7 Hz, 2H); ^{13}C{^{1}H} NMR (100 MHz, $CDCl_3$) δ 149.7, 139.1, 133.6, 133.6, 132.6, 132.1, 132.0, 131.0, 130.2, 129.8, 129.8, 128.7, 128.6, 128.5, 128.4, 127.8, 127.3, 124.0, 113.2, 111.3; HRMS (ESI) *m/z*: $[M+H]^+$ Calcd for $C_{27}H_{19}N_2$ 371.1548, Found 371.1594.

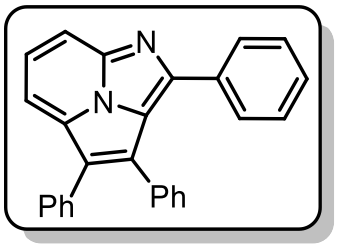

2-(Naphthalen-1-yl)-3,4-diphenylimidazo[5,1,2-*cd*]indolizine (33b). Purification by column chromatography on silica gel (eluent: EtOAc/hexanes, 1:9 *v/v*); Yellow solid; 60 mg (69%); mp = 223-225 ˚C; ^{1}H NMR (400 MHz, $CDCl_3$) δ 8.20 (dd, *J* = 8.6, 1.7 Hz, 1H), 8.15 (s, 1H), 8.11 (dd, *J* = 6.6, 1.9 Hz, 1H), 8.06 – 8.00 (m, 2H), 7.86 – 7.81 (m, 2H), 7.56 – 7.47 (m, 6H), 7.47 – 7.38 (m, 6H), 7.38 – 7.32 (m, 1H); ^{13}C{^{1}H} NMR (100 MHz, $CDCl_3$) δ 151.0, 140.2, 134.4, 133.9, 133.9, 133.1, 131.6, 131.1, 130.9, 130.2, 130.0, 128.7, 128.7, 128.7, 128.3, 128.0, 127.7, 127.5, 127.1, 127.1, 126.8, 126.4, 126.2, 124.7, 112.9, 111.4. (one carbon is not visible due to overlapping peaks)

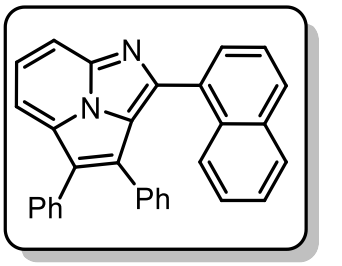

6-Chloro-2,3,4-triphenylimidazo[5,1,2-*cd*]indolizine (33c). Purification by column chromatography on silica gel (eluent: EtOAc/hexanes, 1:9 *v/v*); Brown solid; 47 mg (57%); mp = 222-224 ˚C; ^{1}H NMR (400 MHz, $CDCl_3$) δ 8.18 (s, 1H), 7.94 (d, *J* = 7.3 Hz, 3H), 7.84 (s, 1H), 7.59 (d, *J* = 9.5 Hz, 2H), 7.45 (t, *J* = 7.6 Hz, 4H), 7.37 – 7.29 (m, 4H).7.15 (d, *J* = 9.4 Hz, 2H); ^{13}C{^{1}H} NMR (100 MHz, $CDCl_3$) δ 149.5, 139.9, 133.9, 133.7, 132.6, 131.8, 131.5, 131.0, 130.9, 130.1, 128.7, 128.3, 127.7, 127.2, 127.1, 124.3, 123.8, 113.0, 111.6.

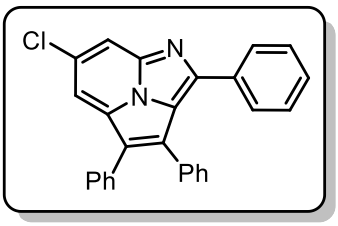

6-Bromo-2,3,4-triphenylimidazo[5,1,2-*cd*]indolizine (33d). Purification by column chromatography on silica gel (eluent: EtOAc/hexanes, 1:9 *v/v*); Light brown solid; 44 mg (53%);

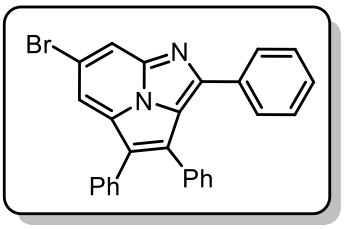

mp = 235-237 ˚C; ^{1}H NMR (400 MHz, $CDCl_3$) 8.11 – 8.06 (m, 1H), 8.04 – 8.00 (m, 2H), 7.71 (d, *J* = 8.5 Hz, 2H), 7.53 – 7.47 (m, 3H), 7.47 – 7.38 (m, 8H), 7.38 – 7.32 (m, 1H); ^{13}C{^{1}H} NMR (100 MHz, $CDCl_3$) δ 149.8, 140.2, 134.2, 134.0, 132.9, 132.1, 131.9, 131.8, 131.3, 131.2, 130.4, 129.0, 128.7, 128.0, 127.6, 127.5, 124.1, 113.3, 111.9.

5-Methyl-2,3,4-triphenylimidazo[5,1,2-*cd*]indolizine (33e). Purification by column

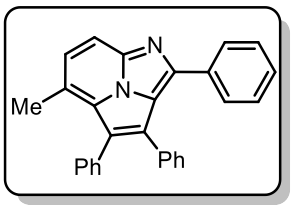

chromatography on silica gel (eluent: EtOAc/hexanes, 1:9 *v/v*); Yellow solid; 70 mg (76%); mp = 184-186 ˚C; ^{1}H NMR (400 MHz, $CDCl_3$) δ δ 7.92 – 7.76 (m, 4H), 7.51 – 7.26 (m, 13H), 2.85 (s, 3H); ^{13}C{^{1}H} NMR (100 MHz, $CDCl_3$) δ 150.8, 139.9, 138.6, 134.1, 134.1, 133.7, 131.8, 131.3, 131.0, 130.2, 129.6, 129.3, 128.6, 128.5, 128.3, 127.0, 126.7, 123.9, 113.8, 111.9, 22.9.

4-(3,4-Diphenylimidazo[5,1,2-*cd*]indolizin-2-yl)benzonitrile (33f). Purification by column

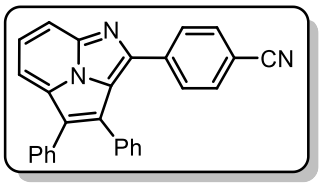

chromatography on silica gel (eluent: EtOAc/hexanes, 1:9 *v/v*); Orange solid; 70 mg (74%); mp = 238-240 ˚C; ^{1}H NMR (400 MHz, $CDCl_3$) δ 8.14 – 8.09 (m, 1H), 8.04 (d, *J* = 4.3 Hz, 2H), 7.90 (d, *J* = 8.1 Hz, 2H), 7.55 (d, *J* = 8.1 Hz, 2H), 7.50 – 7.31 (m, 10H); ^{13}C{^{1}H} NMR (100 MHz, $CDCl_3$) δ 147.5, 139.6, 137.7, 133.4, 133.1, 131.8, 131.8, 131.2, 130.5, 129.8, 129.6, 128.5, 128.4, 128.3, 128.2, 127.3, 127.1, 124.6, 118.5, 113.4, 112.2, 112.1.

2-(4-Fluorophenyl)-3,4-diphenylimidazo[5,1,2-*cd*]indolizine (33g). Purification by column

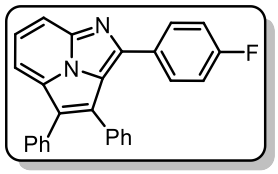

chromatography on silica gel (eluent: EtOAc/hexanes, 15:85 *v/v*); Yellow solid; 62 mg (68%); mp = 203-205 ˚C; ^{1}H NMR (400 MHz, $CDCl_3$) δ 8.14 (d, *J* = 6.6 Hz, 1H), 8.08 – 8.00 (m, 2H), 7.84 (q, *J* = 8.6, 5.5 Hz, 2H), 7.51 – 7.33 (m, 10H), 7.00 (t, *J* = 8.6 Hz, 2H); ^{13}C{^{1}H} NMR (100 MHz, $CDCl_3$) δ 163.8 (d, J_{C-F} = 258.8 Hz), 149.0, 139., 133.8 , 133.6 (d, J_{C-F} = 17.7 Hz), 131.9, 131.8, 131.7 (d, J_{C-F} = 8.4 Hz), 130.9, 130.1, 128.7, 128.6, 128.4, 127.6, 127.2, 115.5 (d, J_{C-F} = 21.6 Hz), 113.1, 111.2.

2-(4-Bromophenyl)-3,4-diphenylimidazo[5,1,2-*cd*]indolizine (33h). Purification by column chromatography on silica gel (eluent: EtOAc/hexanes, 1:9 *v/v*); Yellow solid; 54 mg (66%); mp = 221-223 ˚C; ^{1}H NMR (400 MHz, $CDCl_3$) δ 8.08 – 8.03 (m, 1H), 8.02 – 7.97 (m, 2H), 7.69 (d, *J* = 8.5 Hz, 2H), 7.50 – 7.29 (m, 12H); ^{13}C{^{1}H} NMR (100 MHz, $CDCl_3$) δ 149.5, 140.0, 133.9, 133.7, 132.6, 131.8, 131.6, 131.0, 130.9, 130.1, 128.7, 128.4, 127.7, 127.2, 127.2, 123.8, 113.0, 111.6.

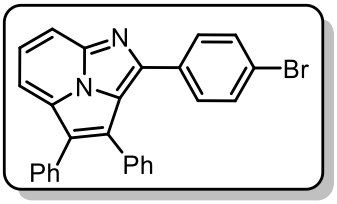

2-(4-Methoxyphenyl)-3,4-diphenylimidazo[5,1,2-*cd*]indolizine (33i). Purification by column chromatography on silica gel (eluent: EtOAc/hexanes, 1:9 *v/v*); Pale Yellow solid; 65 mg (73%); mp = 198-200 ˚C; ^{1}H NMR (400 MHz, $CDCl_3$) δ 8.16 (d, *J* = 7.4 Hz, 1H), 8.09 – 7.97 (m, 2H), 7.84 (d, *J* = 8.5 Hz, 2H), 7.52 – 7.34 (m, 10H), 6.85 (d, *J* = 8.4 Hz, 2H), 3.86 (s, 3H); ^{13}C{^{1}H} NMR (100 MHz, $CDCl_3$) δ 160.8, 147.6, 140.2, 134.2, 134.1, 131.5, 131.4, 131.1, 131.0, 130.2, 128.6, 128.5, 128.1, 126.9, 126.8, 126.3, 113.8, 112.4, 110.6, 55.3.

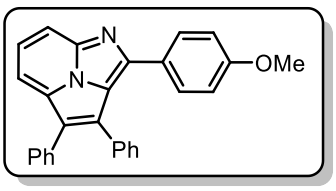

2-(4-Fluorophenyl)-5-methyl-3,4-diphenylimidazo[5,1,2-*cd*]indolizine (33j). Purification by column chromatography on silica gel (eluent: EtOAc/hexanes, 5:95 *v/v*); Light brown solid; 54 mg (61%); mp = 184-186 ˚C; ^{1}H NMR (400 MHz, $CDCl_3$) δ 7.98 (d, *J* = 8.1 Hz, 1H), 7.82 (dd, *J* = 8.6, 5.5 Hz, 2H), 7.74 (d, *J* = 8.1 Hz, 1H), 7.48 – 7.22 (m, 10H), 6.99 (t, *J* = 8.7 Hz, 2H), 2.56 (s, 3H); ^{13}C{^{1}H} NMR (100 MHz, $CDCl_3$) δ 163.6 (d, $J_{C\text{-}F}$ = 247.9 Hz), 148.1, 138.2, 134.1, 133.6, 131.9, 131.5 (d, $J_{C\text{-}F}$ = 7.4 Hz), 131.4, 131.1, 130.0 (d, $J_{C\text{-}F}$ = 7.0 Hz), 129.9, 128.2, 128.0, 127.9, 127.5, 125.6, 123.5, 115.4 (d, $J_{C\text{-}F}$ = 21.5 Hz), 111.0, 17.8.

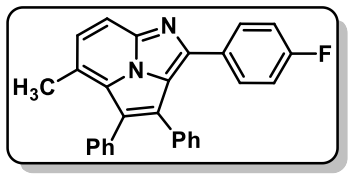

3,4-Diphenyl-2-(thiophen-2-yl)imidazo[5,1,2-*cd*]indolizine (33k). Purification by column chromatography on silica gel (eluent: EtOAc/hexanes, 1:9 *v/v*); Brown solid; 63 mg (67%); mp = 209-211 ˚C; ^{1}H NMR (400 MHz, $CDCl_3$) δ 8.03 – 7.95 (m, 3H), 7.56 – 7.51 (m, 2H), 7.50 – 7.45 (m, 5H), 7.44 – 7.31 (m, 4H), 7.00 (dd, *J* = 3.7, 0.9 Hz, 1H), 6.96 – 6.92 (m, 1H); ^{13}C{^{1}H} NMR (100 MHz, $CDCl_3$) *δ* 144.9, 140.0, 137.7, 134.1, 133.8, 131.5, 131.1, 130.8, 130.0, 129.1, 128.7, 128.6, 128.5, 128.4, 128.0, 127.5, 127.2, 127.0, 123.4, 112.8, 111.0.

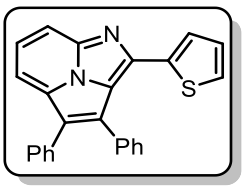

3-Methyl-2,4-diphenylimidazo[5,1,2-*cd*]indolizine (33l). Purification by column chromatography on silica gel (eluent: EtOAc/hexanes, 1:9 *v/v*); Yellow solid; 50 mg (63%); mp = 115-117 ˚C; ^{1}H NMR (400 MHz, $CDCl_3$) δ 8.33 – 8.28 (m, 2H), 7.98 (d, *J* = 8.0 Hz, 1H), 7.91 (t, *J* = 7.6 Hz, 1H), 7.84 (d, *J* = 7.6 Hz, 1H), 7.69 – 7.64 (m, 2H), 7.62 – 7.55 (m, 4H), 7.52 – 7.42 (m, 2H), 2.93 (s, 3H); ^{13}C{^{1}H} NMR (100 MHz, $CDCl_3$) δ 150.3, 139.8, 134.4, 134.1, 132.0, 130.0, 129.4, 129.1, 128.9, 128.9, 128.6, 127.5, 127.2, 126.7, 111.3, 110.6, 14.0.

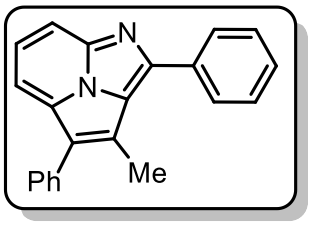

3,4-Bis(4-bromophenyl)-2-phenylimidazo[5,1,2-*cd*]indolizine (33m). Purification by column chromatography on silica gel (eluent: EtOAc/hexanes, 1:9 *v/v*); Yellow solid; 93 mg (68%); mp = 200-202 ˚C; ^{1}H NMR (400 MHz, $CDCl_3$) δ 8.09 (d, *J* = 7.7 Hz, 1H), 8.03 – 7.92 (m, 2H), 7.83 (d, *J* = 7.4 Hz, 2H), 7.59 – 7.48 (m, 4H), 7.44 – 7.25 (m, 7H); ^{13}C{^{1}H} NMR (100 MHz, $CDCl_3$) δ 151.5, 140.1, 133.4, 132.6, 132.6, 132.1, 131.9, 131.7, 131.3, 130.1, 129.7, 129.7, 128.5, 127.3, 126.0, 123.8, 122.8, 121.6, 112.7, 111.8.

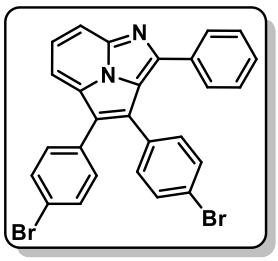

Diethyl 2-phenylimidazo[5,1,2-*cd*]indolizine-3,4-dicarboxylate (33n). Purification by column chromatography on silica gel (eluent: EtOAc/hexanes, 5:95 *v/v*); Yellow solid; 29 mg (31%); mp = 119-121 ˚C; ^{1}H NMR (400 MHz, $CDCl_3$) δ 8.42 – 8.35 (m, 1H), 8.26 (d, *J* = 7.8 Hz, 2H), 8.16 – 8.09 (m, 2H), 7.63 – 7.50 (m, 3H), 4.60 (q, *J* = 7.1 Hz, 2H), 4.53 (q, *J* = 7.1 Hz, 2H), 1.51 (t, *J* = 7.1 Hz, 3H), 1.45 (t, *J* = 7.1 Hz, 3H); ^{13}C{^{1}H} NMR (100 MHz, $CDCl_3$) δ 165.6, 163.3, 154.6, 140.9, 132.9, 130.8, 130.1, 129.4, 129.1, 129.1, 116.4, 116.2, 112.7, 62.7, 61.1, 14.4, 14.1.

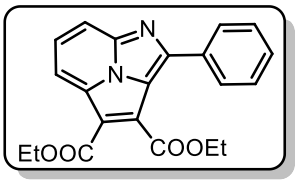

8-Methyl-5,6-diphenylnaphtho[1',2':4,5]imidazo[1,2-*a*]pyridine (32o). Purification by column chromatography on silica gel (eluent: EtOAc/hexanes, 15:85 *v/v*); Yellow solid; 57 mg (62%); mp = 271-273 ˚C; ^{1}H NMR (400 MHz, $CDCl_3$) δ 8.10 (d, *J* = 8.0 Hz, 1H), 8.02 (d, *J* = 8.0 Hz, 2H), 7.77 (s, 3H), 7.64 – 7.51 (m, 3H), 7.47 (t, *J* = 7.7 Hz, 4H), 7.41 – 7.31 (m, 3H), 6.74 (d, *J* = 7.7 Hz, 1H), 2.67 (s, 3H); ^{13}C{^{1}H} NMR (100 MHz, $CDCl_3$) δ 139.6, 137.9, 134.0, 131.6, 131.6, 131.0, 130.2, 129.6, 129.1, 129.1, 128.6, 128.5, 128.1, 127.0, 126.9, 123.3, 120.8, 114.8, 112.6, 112.2, 111.0, 29.7.

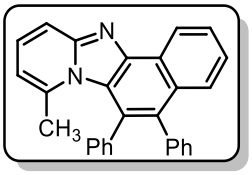

4.4A.4.5 Computational Studies

Initial geometry was taken from crystal structure **29** and optimized using QUICKSTEP module[62] of CP2k program package.[68] We used Perdew, Burke, and Ernzerhof (PBE) exchange–correlation functional (PBE XC functionals) and Goedecker-Teter-Hutter (GTH) pseudopotential[64] with MOLOPT type DZVP basis set[65] with an energy cut-off of 280 Ry. One of Cl-atom of optimized geometry **29** was further substituted as expected intermediate **A** to optimize *cis*- and *trans*-isomers. A visual inspection/representation was obtained using visual molecular dynamics program (VMD 1.9.2)[69] and the distances between particular atom/ring and centre of mass of aromatic ring was drawn using Tcl scripting language embedded in VMD.

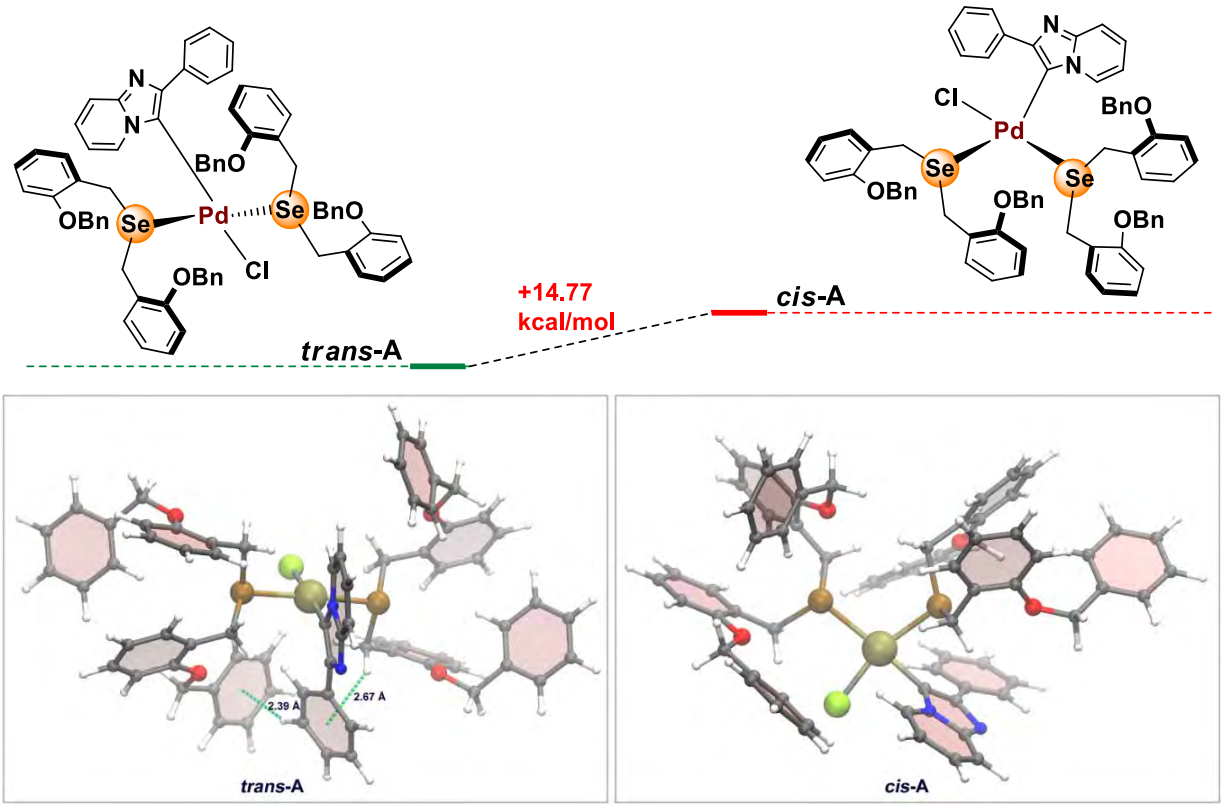

Figure 4.4A.7: Geometry optimized structure of *trans*-**A** (CH-π distances 2.39 Å and 2.67 Å) and *cis*-**A** isomer. [Color scheme: Pd-Tan (CPK), Se-Ochre (CPK), Cl-Lime (CPK), C-Gray, H-White, N-Blue (Licorice); aromatic rings- Glass1 (Paperchain)]

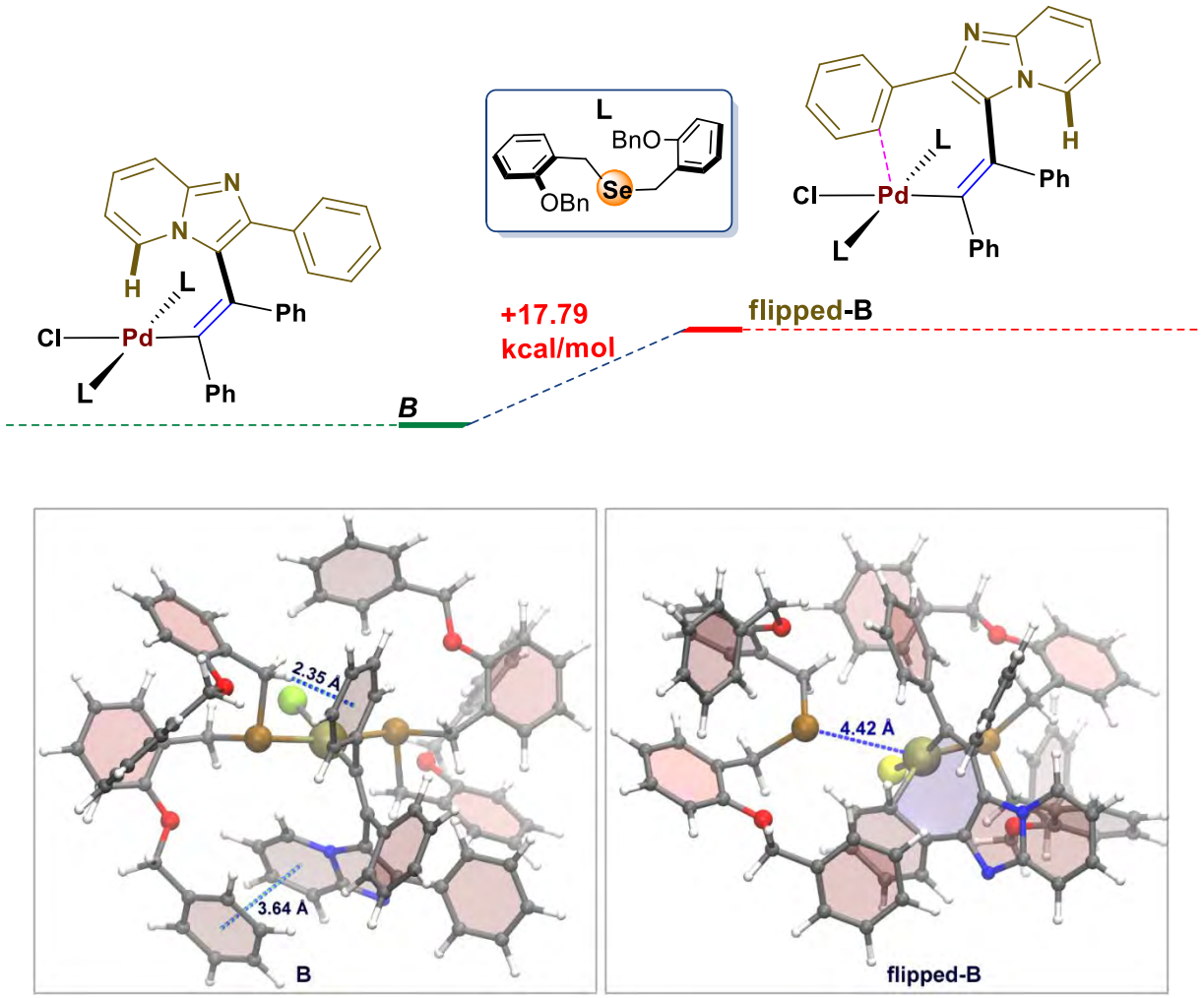

Figure 4.4A.8: Geometry optimized structure of **B** (CH-π distance 2.35 Å and π-π distance 3.64 Å) and flipped-2-arylimidazo[1,2-*a*]pyridines of **B** (flipped-**B**). [Color scheme: Pd-Tan (CPK), Se-Ochre (CPK), Cl-Lime (CPK), C-Gray, H-White, N-Blue (Licorice); aromatic rings- Glass1 (Paperchain)]

In case of optimized structure of configuration **B**, CH-π interactions at distance 2.35 Å and π-π interactions at distance 3.64 Å are observed. Whereas, flipped-2-arylimidazo[1,2-*a*]pyridines of **B** optimization leads to 7 membered ring formation with breaking of Pd-Se bond having a distance of 4.42 Å. CH-π interactions and π-π interactions are not seen in between 2-arylimidazo[1,2-*a*]pyridines and **L** in **flipped-B** configuration of the complex and less favored with relatively higher energy *i.e.* 17.79 kcal/mol compared to configuration **B**.

4.4A.4.6 Sample Preparation & Crystal Measurement of 29: A CH_3CN solution of **29** (5 mL) was slowly concentrated over a period of 14 days to afford suitable colorless plate like crystals.

The data was collected and reported in **Table 4A.3**. Cell parameters were obtained from 60 data frames using a 1° scan and refined with 11864 reflections. APEX2 was used to collect the integrated intensity information of each reflection by reducing the data frames. Lorentz and polarization corrections were applied. The absorption correction program SADABS[70] was employed to correct the data for absorption effects. The space group was determined from systematic reflection conditions and statistical tests. The structure was refined (weighted least squares refinement on F^2) to convergence.[71] Olex2[72] was employed for the final data presentation and structure plots. Non-hydrogen atoms were refined with anisotropic thermal parameters. Hydrogen atoms were fixed in idealized positions using a riding model. The absence of additional symmetry or voids was confirmed using PLATON (ADDSYM).[73] Molecule possess an inversion symmetry and symmetry generated atoms are not labeled in the **Figure 4.4A.5**.

Table 4.4A.3: Crystal Data for **29**.

	29
Empirical formula	$C_{56}H_{52}Cl_2O_4PdSe_2$
Formula weight	1124.19
Temperature [K]	110.0
Diffractometer	Bruker Apex 2
Wavelength [Å]	0.71073
Crystal system	Triclinic
Space group	P-1
Unit cell dimensions:	
a [Å]	8.2319(4)
b [Å]	10.9599(5)
c [Å]	14.1131(8)
α [°]	101.73(2)
β [°]	100.17(2)
γ [°]	97.03(2)
V [Å^3]	1210.44(11)
Z	1
ρ_{calc} [Mg/m^3]	1.542

μ [mm^{-1}]	2.044
F(000)	568
Crystal size [mm^3]	0.10× 0.08 × 0.01
Θ limit [°]	2.548 to 25.000
Index range (h, k, l)	–9, 9, –13, 12, –16, 16
Reflections collected	11864
Independent reflections	4210
R(int)	0.0273
Completeness to θ	98.8
Max. and min. transmission	0.3334 and 0.2686
Data/restraints/parameters	4210/0/295
Goodness-of-fit on F^2	1.060
R indices (final) [I> 2σ(I)]	
R_1	0.0253
wR_1	0.0491
R indices (all data)	
R_1	0.0352
wR_2	0.0547
Largest diff. peak and hole [eÅ^{-3}]	0.471 and –0.363

4.4A.5 REFERENCES

1. Lyons, T. W.Sanford, M. S., *Chemical Reviews* **2010**, *110*, 1147-1169.
2. Ackermann, L., *Chemical Reviews* **2011**, *111*, 1315-1345.
3. Hu, F.; Xia, Y.; Ma, C.; Zhang, Y.; Wang, J., *Chemical Communications* **2015**, *51*, 7986-7995.
4. Chen, X.; Engle, K. M.; Wang, D. H.; Yu, J. Q., *Angewandte Chemie International Edition* **2009**, *48*, 5094-5115.
5. Monsigny, L.; Doche, F.; Besset, T., *Beilstein Journal of Organic Chemistry* **2023**, *19*, 448-473.

6. Docherty, J. H.; Lister, T. M.; Mcarthur, G.; Findlay, M. T.; Domingo-Legarda, P.; Kenyon, J.; Choudhary, S.; Larrosa, I., *Chemical Reviews* **2023**.
7. Horbaczewskyj, C. S.Fairlamb, I. J., *Organic Process Research & Development* **2022**, *26*, 2240-2269.
8. Zhang, Y.; Yang, J.; Ge, R.; Zhang, J.; Cairney, J. M.; Li, Y.; Zhu, M.; Li, S.; Li, W., *Coordination Chemistry Reviews* **2022**, *461*, 214493.
9. Wang, C.; Wang, Z.; Mao, S.; Chen, Z.; Wang, Y., *Chinese Journal of Catalysis* **2022**, *43*, 928-955.
10. Heuer-Jungemann, A.; Feliu, N.; Bakaimi, I.; Hamaly, M.; Alkilany, A.; Chakraborty, I.; Masood, A.; Casula, M. F.; Kostopoulou, A.; Oh, E.; Susumu, K.; Stewart, M. H.; Medintz, I. L.; Stratakis, E.; Parak, W. J.; Kanaras, A. G., *Chemical Reviews* **2019**, *119*, 4819-4880.
11. Kottas, G. S.; Clarke, L. I.; Horinek, D.; Michl, J., *Chemical Reviews* **2005**, *105*, 1281-1376.
12. Erbas-Cakmak, S.; Leigh, D. A.; McTernan, C. T.; Nussbaumer, A. L., *Chemical Reviews* **2015**, *115*, 10081-10206.
13. Roy, I.Stoddart, J. F., *Trends in Chemistry* **2019**, *1*, 627-629.
14. Jiang, X.; Duan, H.-B.; Jellen, M. J.; Chen, Y.; Chung, T. S.; Liang, Y.; Garcia-Garibay, M. A., *Journal of the American Chemical Society* **2019**, *141*, 16802-16809.
15. Kay, E. R.; Leigh, D. A.; Zerbetto, F., *Angewandte Chemie International Edition* **2007**, *46*, 72-191.
16. Ehnbom, A.Gladysz, J. A., *Chemical Reviews* **2021**, *121*, 3701-3750.
17. Simonov, S.; Zorina, L.; Wzietek, P.; Rodríguez-Fortea, A.; Canadell, E.; Mézière, C.; Bastien, G.; Lemouchi, C.; Garcia-Garibay, M. A.; Batail, P., *Nano Letters* **2018**, *18*, 3780-3784.
18. Xue, M.Wang, K. L., *Sensors* **2012**, *12*, 11612-11637.
19. Kaleta, J.; Chen, J.; Bastien, G.; Dracinsky, M.; Mašát, M.; Rogers, C. T.; Feringa, B. L.; Michl, J., *Journal of the American Chemical Society* **2017**, *139*, 10486-10498.
20. Zhu, Y.; Stollenz, M.; Zarcone, S. R.; Kharel, S.; Joshi, H.; Bhuvanesh, N.; Reibenspies, J. H.; Gladysz, J. A., *Chemical Science* **2022**, *13*, 13368-13386.
21. Estrada, A. L.; Wang, L.; Hess, G.; Hampel, F.; Gladysz, J. A., *Inorganic Chemistry* **2022**, *61*, 17012-17025.

22. Leong, T. X.; Collins, B. K.; Dey Baksi, S.; Mackin, R. T.; Sribnyi, A.; Burin, A. L.; Gladysz, J. A.; Rubtsov, I. V., *The Journal of Physical Chemistry A* **2022**, *126*, 4915-4930.
23. Estrada, A. L.; Wang, L.; Bhuvanesh, N.; Hampel, F.; Gladysz, J. A., *Organometallics* **2022**, *41*, 733-749.
24. Zhu, Y.; Ehnbom, A.; Fiedler, T.; Shu, Y.; Bhuvanesh, N.; Hall, M. B.; Gladysz, J. A., *Dalton Transactions* **2021**, *50*, 12457-12477.
25. Garcia-Garibay, M. A., *Proceedings of the National Academy of Sciences* **2005**, *102*, 10771-10776.
26. Jiang, X.; Duan, H.-B.; Jellen, M. J.; Chen, Y.; Chung, T. S.; Liang, Y.; Garcia-Garibay, M. A., *Journal of the American Chemical Society* **2019**, *141*, 16802-16809.
27. Howe, M. E.Garcia-Garibay, M. A., *The Journal of Organic Chemistry* **2019**, *84*, 9570-9576.
28. Howe, M. E.Garcia-Garibay, M. A., *The Journal of Organic Chemistry* **2019**, *84*, 9835-9849.
29. Naumov, P.; Karothu, D. P.; Ahmed, E.; Catalano, L.; Commins, P.; Mahmoud Halabi, J.; Al-Handawi, M. B.; Li, L., *Journal of the American Chemical Society* **2020**, *142*, 13256-13272.
30. Comotti, A.; Bracco, S.; Yamamoto, A.; Beretta, M.; Hirukawa, T.; Tohnai, N.; Miyata, M.; Sozzani, P., *Journal of the American Chemical Society* **2014**, *136*, 618-621.
31. Setaka, W.Yamaguchi, K., *Journal of the American Chemical Society* **2012**, *134*, 12458-12461.
32. Setaka, W.; Kajiyama, K.; Inagaki, Y., *The Journal of Organic Chemistry* **2022**, *87*, 10869-10875.
33. Kurimoto, T.; Inagaki, Y.; Ohara, K.; Yamaguchi, K.; Setaka, W., *Organic & Biomolecular Chemistry* **2022**, *20*, 8465-8470.
34. Bhowal, R.; Balaraman, A. A.; Ghosh, M.; Dutta, S.; Dey, K. K.; Chopra, D., *Journal of the American Chemical Society* **2021**, *143*, 1024-1037.
35. Michl, J.Sykes, E. C. H., *ACS nano* **2009**, *3*, 1042-1048.
36. Li, H.-M.; Zhong, G.-M.; Wu, S.-Q.; Sato, O.; Zheng, X.-Y.; Yao, Z.-S.; Tao, J., *Inorganic Chemistry* **2021**, *60*, 8042-8048.

37. Chen, K.-Y.; Ivashenko, O.; Carroll, G. T.; Robertus, J.; Kistemaker, J. C. M.; London, G.; Browne, W. R.; Rudolf, P.; Feringa, B. L., *Journal of the American Chemical Society* **2014**, *136*, 3219-3224.
38. Kobr, L.; Zhao, K.; Shen, Y.; Shoemaker, R. K.; Rogers, C. T.; Michl, J., *Crystal Growth & Design* **2014**, *14*, 559-568.
39. Schied, M.; Prezzi, D.; Liu, D.; Kowarik, S.; Jacobson, P. A.; Corni, S.; Tour, J. M.; Grill, L., *ACS nano* **2023**, *17*, 3958-3965.
40. Barnes, J. C.Mirkin, C. A., *Proceedings of the National Academy of Sciences* **2017**, *114*, 620-625.
41. Sammut, D., *Chemistry in Australia* **2016**, 28-31.
42. Vogelsberg, C. S.Garcia-Garibay, M. A., *Chemical Society Reviews* **2012**, *41*, 1892-1910.
43. Abendroth, J. M.; Bushuyev, O. S.; Weiss, P. S.; Barrett, C. J., *ACS nano* **2015**, *9*, 7746-7768.
44. Ariga, K., *Chemical Science* **2020**, *11*, 10594-10604.
45. Aprahamian, I., *ACS Central Science* **2020**, *6*, 347-358.
46. Abe, J. O.; Popoola, A.; Ajenifuja, E.; Popoola, O. M., *International journal of hydrogen energy* **2019**, *44*, 15072-15086.
47. Goswami, A.Schmittel, M., *Angewandte Chemie International Edition* **2020**, *59*, 12362-12366.
48. Yoshizawa, R.; Inagaki, Y.; Momma, H.; Kwon, E.; Ohara, K.; Yamaguchi, K.; Setaka, W., *New Journal of Chemistry* **2023**, *47*, 5946-5952.
49. Hayashi, D.; Inagaki, Y.; Setaka, W., *Journal of Materials Chemistry C* **2021**, *9*, 8220-8225.
50. Nobuhara, K.; Inagaki, Y.; Setaka, W., *Organic & Biomolecular Chemistry* **2021**, *19*, 6328-6333.
51. Tsuchiya, T.; Inagaki, Y.; Yamaguchi, K.; Setaka, W., *The Journal of Organic Chemistry* **2021**, *86*, 2423-2430.
52. Inagaki, Y.; Ueda, S.; Yamaguchi, K.; Setaka, W., *Chemistry Letters* **2020**, *49*, 1291-1293.
53. Jin, M.; Ando, R.; Jellen, M. J.; Garcia-Garibay, M. A.; Ito, H., *Journal of the American Chemical Society* **2020**, *143*, 1144-1153.
54. Yoshizawa, R.; Inagaki, Y.; Momma, H.; Kwon, E.; Ohara, K.; Yamaguchi, K.; Setaka, W., *New Journal of Chemistry* **2023**, *47*, 5946-5952.

55. Hayashi, D.; Inagaki, Y.; Setaka, W., *Journal of Materials Chemistry C* **2021**, *9*, 8220-8225.
56. Kurimoto, T.; Inagaki, Y.; Ohara, K.; Yamaguchi, K.; Setaka, W., *Organic & Biomolecular Chemistry* **2022**, *20*, 8465-8470.
57. Estrada, A. L.; Jia, T.; Bhuvanesh, N.; Blümel, J.; Gladysz, J. A., *European Journal of Inorganic Chemistry* **2015**, *2015*, 5318-5321.
58. Cross, R. J.; Green, T. H.; Keat, R., *Journal of the Chemical Society, Dalton Transactions* **1976**, DOI: 10.1039/DT9760001150, 1150-1152.
59. Li, P.; Zhang, X.; Fan, X., *The Journal of Organic Chemistry* **2015**, *80*, 7508-7518.
60. Hu, H.; Li, G.; Hu, W.; Liu, Y.; Wang, X.; Kan, Y.; Ji, M., *Organic Letters* **2015**, *17*, 1114-1117.
61. Qi, Z.; Yu, S.; Li, X., *The Journal of Organic Chemistry* **2015**, *80*, 3471-3479.
62. VandeVondele, J.; Krack, M.; Mohamed, F.; Parrinello, M.; Chassaing, T.; Hutter, J., *Computer Physics Communications* **2005**, *167*, 103-128.
63. Hutter, J.; Iannuzzi, M.; Schiffmann, F.; VandeVondele, J., *WIREs Computational Molecular Science* **2014**, *4*, 15-25.
64. Goedecker, S.; Teter, M.; Hutter, J., *Physical Review B* **1996**, *54*, 1703-1710.
65. VandeVondele, J.Hutter, J., *The Journal of Chemical Physics* **2007**, *127*, 114105.
66. Tsuzuki, S.; Honda, K.; Uchimaru, T.; Mikami, M.; Tanabe, K., *Journal of the American Chemical Society* **2000**, *122*, 3746-3753.
67. Plevin, M. J.; Bryce, D. L.; Boisbouvier, J., *Nature Chemistry* **2010**, *2*, 466-471.
68. Hutter, J.; Iannuzzi, M.; Schiffmann, F.; VandeVondele, J., *Rev.: Comput. Mol. Sci* **2014**, *4*, 15-25.
69. Humphrey, W.; Dalke, A.; Schulten, K., *Journal of Molecular Graphics* **1996**, *14*, 33-38.
70. Sheldrick, G.SADABS, V., *Inc., Madison, WI, USA* **2001**.
71. Sheldrick, G., *Acta Crystallographica Section A* **2008**, *64*, 112-122.
72. Dolomanov, O. V.; Bourhis, L. J.; Gildea, R. J.; Howard, J. A. K.; Puschmann, H., *Journal of Applied Crystallography* **2009**, *42*, 339-341.
73. Spek, A., *Journal of Applied Crystallography* **2003**, *36*, 7-13.

Chapter 4B

Design and Synthesis of Selenium Coordinated Pd(II)*trans*-dichloride Complex: Catalyst for Decarboxylative Arylation of Coumarin-3-carboxylic Acids

4.4B.1 INTRODUCTION

Coumarins and its derivatives are essential in natural products and synthetic organic compounds due to their diverse pharmacological properties such as antifungal,[1] antidiabetic,[2] anti-Alzheimer,[3] antitumor,[4] anticancer,[5, 6] anticoagulant,[7] antimicrobial,[8] anti-inflammatory,[8] and antiviral activities **Figure 4.4B.1**.[9-13] When an organic moiety is fused with coumarin, the resulting target moiety not only amplified the biological properties of the compound but also exhibits interesting photophysical properties.[14-17] Additionally, coumarins are effective fluorophores that exhibit outstanding photophysical properties with good quantum yields.[18] However, one of the current challenges lies in increasing the band intensity of coumarin derivatives, and the most effective approach to achieving this is by extending the π-conjugation within the molecular structure.[19-21] Over the years, numerous endeavors have been made to synthesize coumarin derivatives with extended π-conjugation.[22] By elongating the conjugated system within the molecule, researchers strive to improve the absorption and emission properties, leading to enhanced fluorescence and a more intense band.

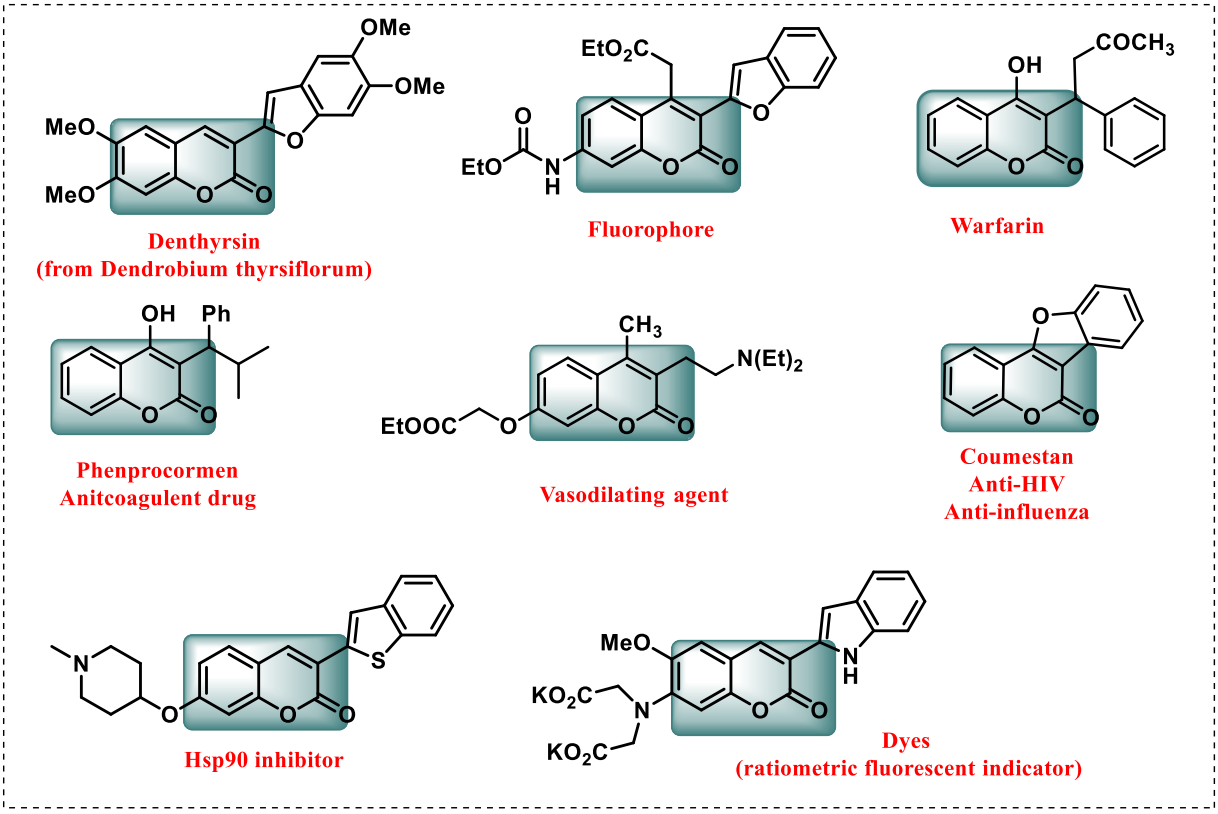

Figure 4.4B.1: Selective examples of naturally occurring and biologically active coumarins

Carboxylic acids are versatile and affordable compounds that can be easily synthesized, making them highly attractive for organic synthesis.[23] They can be easily obtained through various established methods and possess favorable characteristics such as stability to air and moisture, ease of storage, and convenient handling. They have remarkable decarboxylation properties,[24] which means the C-COOH bond undergoes a cleavage of the C-C bond and releases CO_2.[25] This process also creates an active carbon species, such as a carbon radical or a carbon-metal species. These species can react with other molecules and form new C-C bonds. Some metals, such as Pd,[26, 27] Cu,[28] Ag,[29] Au,[30] and Rh,[31] can catalyze the decarboxylation of benzoic acids and produce aryl-metal species. Some of them have been isolated and characterized. Carboxylic acids have gained recognition as promising alternatives to organic halides and organometallic reagents for C-C bond formation **Figure 4.4B.2**.

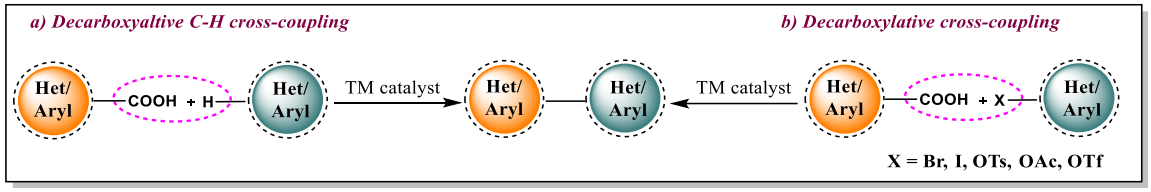

Figure 4.4B.2: A general overview of transition metal-catalyzed decarboxylative reaction

Consequently, many synthetic chemists have been exploring the application of in-situ-generated aryl-metal species derived from decarboxylation in C-H bond functionalization. This strategy combines C-H bond activation and decarboxylation benefits to develop a new synthetic methodology, such as a decarboxylative C-H bond cross-coupling reactions. Mechanistically, two modes of decarboxylation in carboxylic acids have been established for decarboxylative C-H bond functionalization reactions **Figure 4.4B.3**. One is redox-neutral decarboxylation, which generates nucleophilic organometallic intermediates without changing the oxidation state of the metal ions involved in the decarboxylation process.

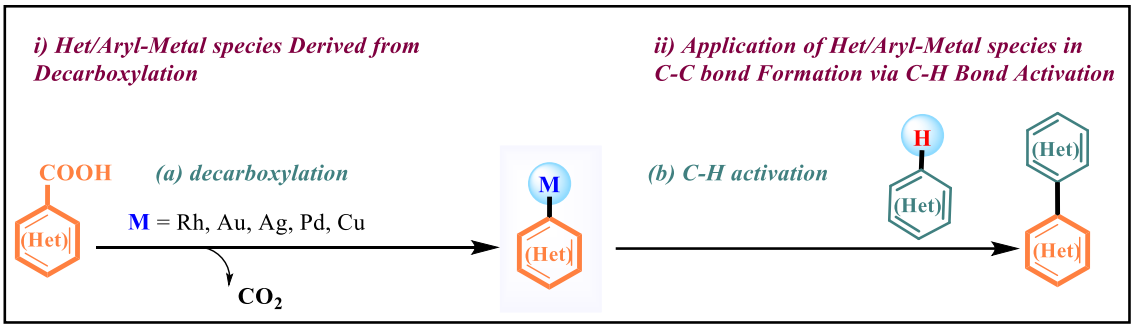

Figure 4.4B.3: A general mechanistic pathway for decarboxylation reaction *via* transition metal-catalyst

The other is oxidative decarboxylation, which produces radical intermediates and changes the metal oxidation state. In recent years, there has been significant progress in transition metal-catalyzed decarboxylative C-C bond formation. Palladium complexes are the key players in the oxidative coupling of two heteroarenes in catalytic systems. However, one of the main challenges is to functionalize one C-H bond in a molecule selectively. To overcome this challenge, several methods have been developed, and one famous way uses directing groups on the substrate. These directing groups bind to the metal center, allowing the catalyst to target the closest C-H bond and achieve high regioselectivity. However, this method is mainly limited to *ortho*-C-H activation, restricting the range of substrates and requiring the prior attachment of directing groups.

Ortho-olefination and *ortho*-arylation of coumarin derivatives are essential building blocks in organic chemistry, with applications in natural products, polymers, advanced materials, ligands, pharmaceuticals, and medicinal chemistry. They also act as chromophores in various drugs, such as antifungal, anticancer, antibiotics, and anti-hypertensive agents. Synthetic chemists have been working hard to develop better and more practical ways to form carbon-carbon bonds in coumarin with high selectivity under mild conditions. Traditional methods have some benefits, but they also face some difficulties, such as *ortho*-olefination or *ortho*-arylation, which uses a heterocyclic halide with an organometallic heterocyclic compound *via* palladium catalysis. However, this method needs to prepare and use specific amounts of organometallic compounds like $HetArB(OR)_2$, HetArMgX, $HetArSnR_3$, or HetArZnX. Unfortunately, these methods were impractical because the C-M bond in these organometallic derivatives can be unstable. To solve these difficulties, the scientific community has explored transition metal-catalyzed reactions as a new way to create C-C bonds. These novel methods provide easy and efficient access to *ortho*-functionalized heterocyclic compounds.

On the other hand, non-directed dual C-H activation, which does not depend on directing groups, is an ideal, effective, and simple method for synthesizing *ortho*-functionalized compounds. This method offers more flexibility and broadens the range of substrates, making it a valuable tool in organic synthesis. This progress includes various reactions involving C-H bond functionalization. Many research groups have developed new methods and highly efficient catalysts for decarboxylation.

For instance, Schiedel *et al*. introduced the substituents on the C3-position of coumarin through Pd(II)-catalyzed cross-coupling reactions. They have utilized Suzuki, Sonogashira, and Heck-type coupling for the C-C bond formation with various coupling partners such as phenylboronic acid, alkynes, and alkenes (**Scheme 4.4B.1**).[18] This chapter mainly focuses on the *ortho*-olefination and *ortho*-arylation of coumarin derivatives, which are common in natural products, pharmaceuticals, and functional materials. Among transition metal-catalyzed synthesis methods, palladium-catalyzed C-H functionalization is a powerful strategy because of the high reactivity of palladium ions and the easy formation of Pd-C bonds from C-H bonds.

Scheme 4.4B.1: Pd(II)-catalyzed cross-coupling reaction with 3-vinyl-2*H*-chromen-2-one and arylhalide

In 2013, Alami and co-workers described the synthesis of 4-substituted 3-(hetero)arylquinolin-2(1*H*)-ones *via* a Pd(II)-catalyzed decarboxylative cross-coupling reactions of various 4-substituted quinolin-2(1*H*)-one-3-carboxylic acids **(4)** with heteroaryl halides **(2)** (**Scheme 4.4B.2**).[32]

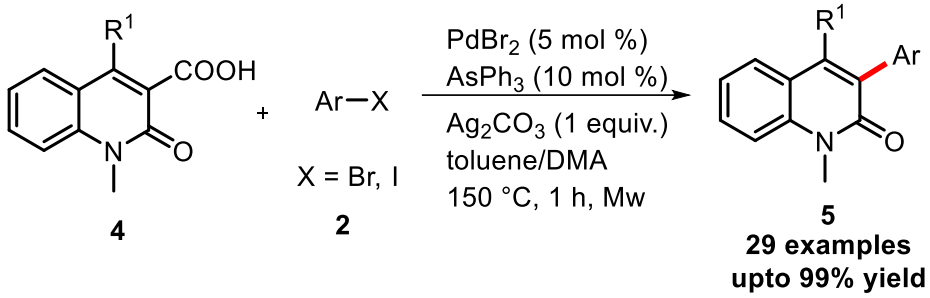

Scheme 4.4B.2: Synthesis of 4-substituted 3-(hetero)arylquinolin-2(1*H*)-ones *via* Pd(II)

Likewise, Hong and the group reported the direct C-H olefination of coumarins through a Pd(II)-catalyzed oxidative heck reaction. Subsequently, this approach was used to develop a variety of 3-vinyl and 3-styryl coumarin scaffolds **(3)**, which are privileged structures and prevalent motifs in many biologically active compounds and fluorophores (**Scheme 4.4B.3**).[33]

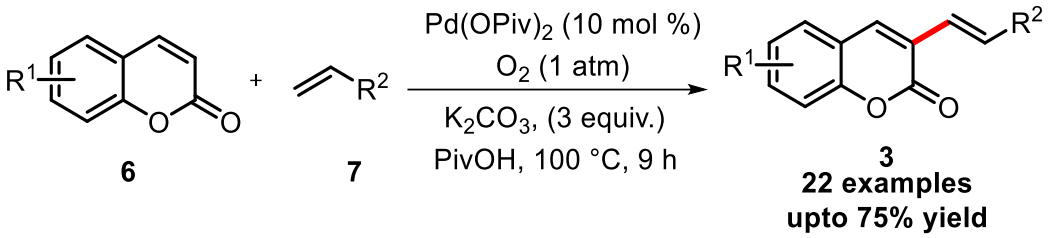

Scheme 4.4B.3: Pd(II)-catalyzed C3-olefination of coumarin

In the same year, Jafarpour *et al.* investigated a ligand-free Pd(II)-catalyzed decarboxylative, arylation, and alkenylation of coumarin-3-carboxylic acid **(8)**. The developed protocol allowed for constructing a wide range of biologically essential coumarin derivatives using various electron-donating and electron-withdrawing substituents at coumarin-3-carboxylic acid (**Scheme 4.4B.4**).[34]

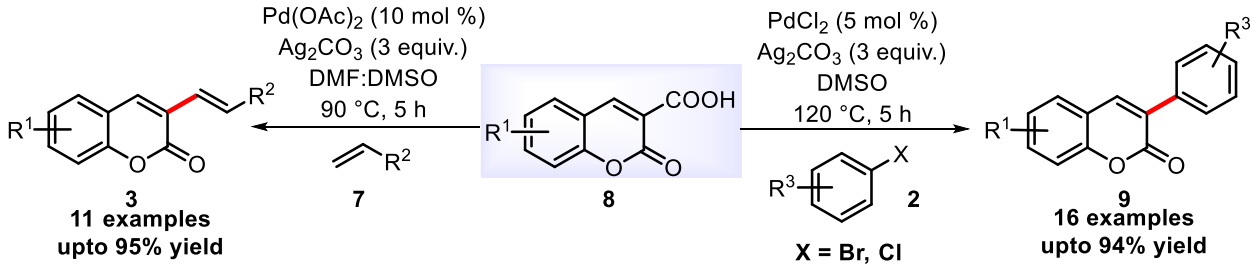

Scheme 4.4B.4: Pd(II)-catalyzed decarboxylative arylation and alkenylation of coumarin-3-carboxylic acids

Huang and colleagues established an efficient approach to access 3-styrylcoumarins **(3)** from coumarins **(10)** and cinnamic acid **(11)** *via* a Pd(II)-catalyzed decarboxylative cross-coupling reaction. The developed protocol delivered 3-styrylcoumarins derivatives in moderate to good yield. The synthesizing products of coumarins showed a high quantum yield (**Scheme 4.4B.5**).[35]

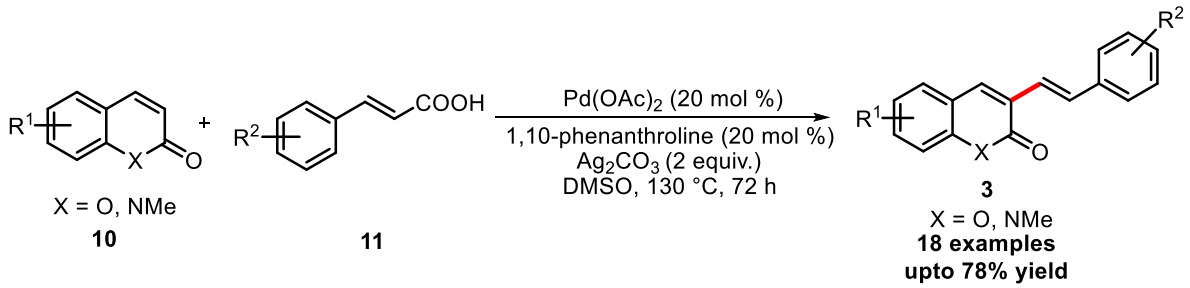

Scheme 4.4B.5: Pd(II)-catalyzed synthesis of 3-styryl-coumarins from cinnamic acid derivatives

Alami and the group demonstrated an efficient method to synthesize biheterocylces *via* Pd(II)-catalyzed decarboxylative coupling of heterocyclic carboxylic acids **(8, 12, 13)** with heterocyclic halides **(14)**. Initially, extrusion of CO_2 from the salt of carboxylic acid in the presence of silver

salt, then oxidative addition followed by reductive elimination delivers biheterocycles in moderate to good yields (**Scheme 4.4B.6**).[36]

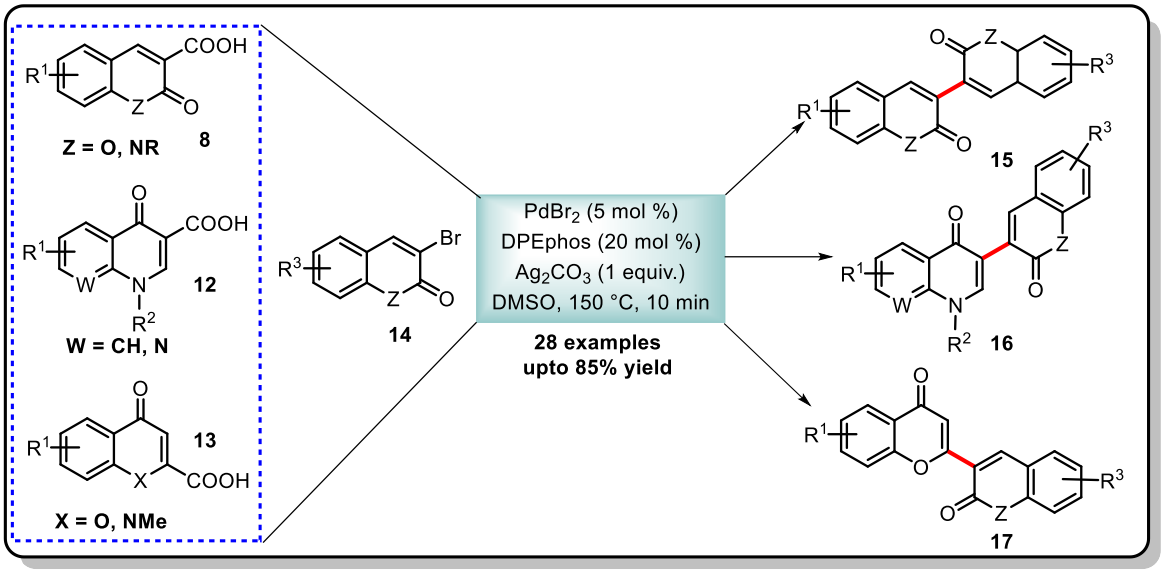

Scheme 4.4B.6: Synthesis of biheterocycles *via* Pd(II)-catalyzed decarboxylative coupling

Chen and co-workers have successfully developed a C-C bond forming reaction utilizing Pd-catalysis. This innovative process involves the deaminative/decarboxylative cross-coupling organoammonium salts **(18)** with carboxylic acids **(19).** Under the reaction conditions, polyfluoroaromatic carboxylic acids, propiolic acids, and α-cyano benzyl carboxylic acid reacted smoothly with benzyl ammonium salts to produce the corresponding C-C coupling products in good-to-excellent yields (**Scheme 4.4B.7**).[37]

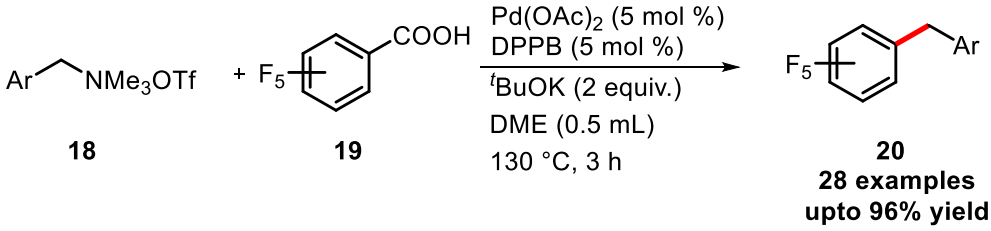

Scheme 4.4B.7: Pd(II)-catalyzed cross-coupling reaction of carboxylic acids with ammonium salts

Li *et al*. demonstrated a novel copper-catalyzed decarboxylative oxyalkylation of alkynyl carboxylic acids **(21)** with ketones **(22)** and alkyl nitriles **(24)** *via* direct C(sp^3)−H bond functionalization to construct new C−C bonds and C−O double bonds has been developed (**Scheme 4.4B.8**).[38] This transformation was featured by broad functional group compatibility and

readily available reagents, thus affording a general approach to γ-diketones **(23)** and γ-keto nitriles **(25)**. The mechanistic study suggested that the reaction proceeds through a radical pathway, and water is involved in the transformation as an oxygen donor.

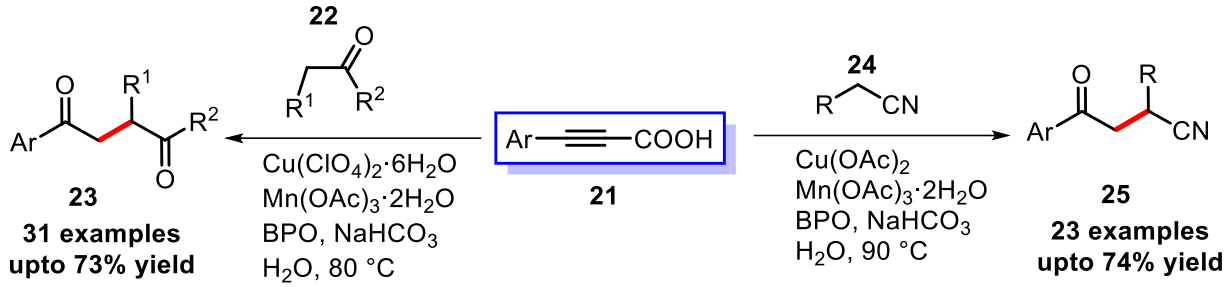

Scheme 4.4B.8: Decarboxylative oxyalkylation of alkynyl carboxylic acids with ketones/alkylnitriles

Li *et al.,* have developed a cobalt-catalyzed decarboxylative cross-coupling reaction of (hetero)aryl carboxylic acids **(27)** with azoles **(26)** in the presence of $CoBr_2$/IPr.HCl (**Scheme 4.4B.9**).[39] This transformation offers a convenient pathway for the synthesis of diverse fused aryl(hetero)aryl and unsymmetrical bi(hetero)aryl **(28)** based structural frameworks. Similarly, Yang *et al*., have developed an efficient decarboxylative cross-coupling of azoles **(26)** and heteroaromatic acids **(29)** through Ni(II)-catalyst (**Scheme 4.4B.10**).[40]

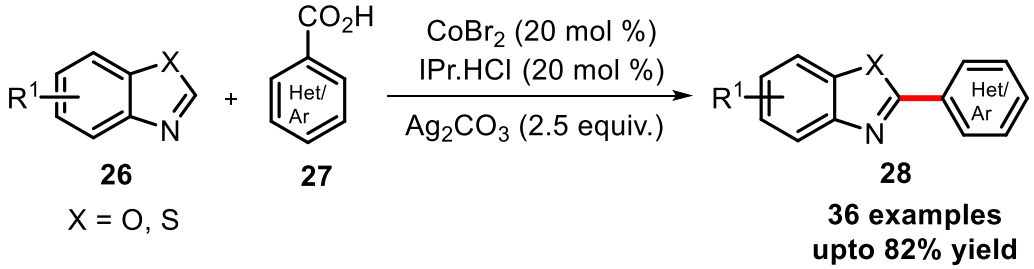

Scheme 4.4B.9: Co(II)-catalyzed decarboxylative C-H (hetero)arylation

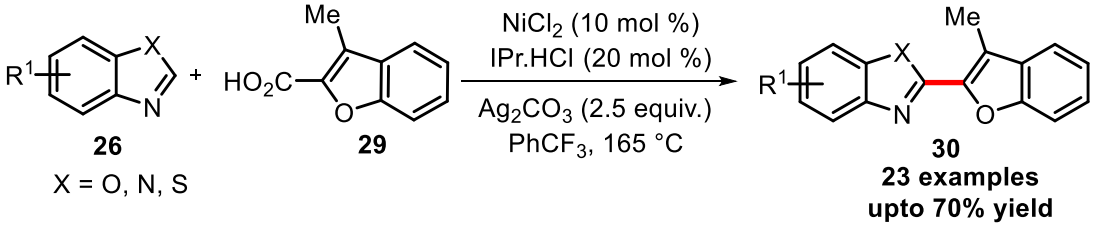

Scheme 4.4B.10: Ni(II)-catalyzed decarboxylative C-H (hetero)arylation

McMillan and colleagues have revealed a novel approach to synthesize arylboronic esters using copper catalysis, capitalizing on the phenomenon of photoinduced ligand-to-metal charge transfer (LMCT) (**Scheme 4.4B.11**).[41] This innovative method transforms (hetero)aryl acids **(31)** into aryl

radicals that can readily undergo borylation at ambient temperatures. This near-UV mediated procedure operates smoothly under mild conditions and eliminates the need for prefunctionalization of the native acids. Importantly, it demonstrates remarkable versatility across a wide range of substrates, including aryls, heteroaryls, and pharmaceutical compounds. Furthermore, the researchers have introduced a one-pot protocol for decarboxylative cross-coupling, merging the catalytic LMCT-driven borylation with palladium-catalyzed Suzuki−Miyaura reactions involving arylation, vinylation, or alkylation using organobromides. This combined approach enables the synthesis of a diverse array of value-added products. A significant application of these protocols lies in the development of a heteroselective double-decarboxylative C(sp^2)−C(sp^2) coupling sequence.

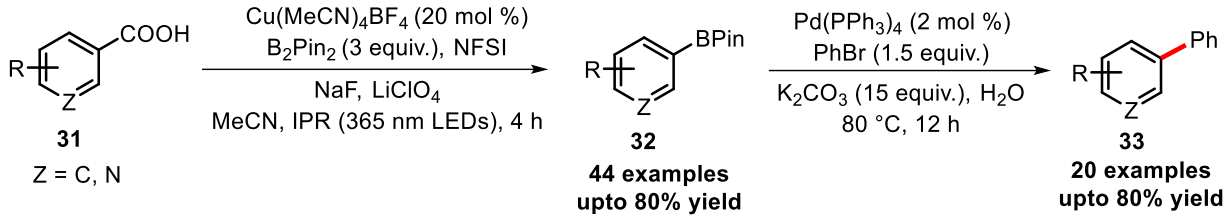

Scheme 4.4B.11: Cu(II)-catalyzed decarboxylative borylation of (hetero)aryl acids

Recently, our group also synthesized a pincer-based palladium complex. They were found to be very effective catalysts for decarboxylative C-H bond activation reaction of heteroarenes **(35)** (**Scheme 4.4B.12)**. A wide range of heteroarenes can be activated using this protocol. The regioselectivity of the product can be controlled based on the position of acid group on one of the coupling partners. Among mono and bi-metallic complexes, the bimetallic palladium pincer complex showed high efficiency for the decarboxylative C-H bond activation reaction.

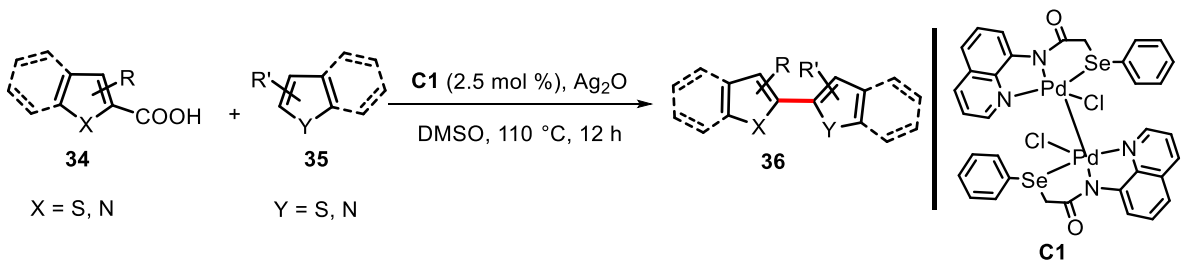

Scheme 4.4B.12: Bimetallic Pd(II)-catalyzed decarboxylative direct C–H heteroarylation of (hetero)arenes

The decarboxylative transformations have gained impressive performance and versatility in recent years. A new decarboxylative transformation that gives access to another interesting substrate class starting from readily available carboxylic acids has been disclosed. Still, several

challenges must be met to establish decarboxylative couplings as standard tools in organic synthesis. Lowering the reaction temperature required for the decarboxylation step is of high priority. New, more effective catalyst generations are thus needed. Another critical development will be to extend the substrate scope, particularly of monometallic Pd- and Rh-catalyzed decarboxylative couplings. One strategy is to incorporate new co-catalysts, and another is to design new ligand systems for cross-coupling catalysts that facilitate their decarboxylation activity. Even though considerable efforts have been made to develop the protocols to synthesize extended π-conjugation bearing coumarins, most of the developed protocols require high loading of metal catalysts, which are sensitive to oxygen and moisture and require the use of costly additives such as silver salt or phosphine ligands. So in this chapter, we have utilize molecular rotors **C1-C3** as catalysts to develop a simple and efficient method for preparing coumarins with extended π-conjugation through a decarboxylative Heck coupling reaction.

4.4B.2 RESULTS AND DISCUSSIONS

We have reported syntheses of three new *trans*-palladium dichloride complexes (**C1-C3**) having dibenzylselane (**L1**), bis(naphthalen-1-ylmethyl)selane (**L2**), and bis(2-(benzyloxy)-3,5-di-*tert*-butylbenzyl)selane (**L3**) as stator ligand units encased with Cl–Pd–Cl rotor spoke onto a Se–Pd–Se axle. The thermal response of these molecules was studied with the help of variable temperature (VT) NMR which shows pyramidal inversion at the selenium atom. The rotation of chlorine through Cl-Pd-Cl in the **C2** was studied with the help of a relaxed potential energy scan and indicated a rotational barrier of ~12.5 kcal/mol. The catalytic potential of these molecular rotors was investigated for the silver-free decarboxylative coupling of coumarin-3-carboxylic acids with styrene, aryl bromides and arylboronic acids (**Scheme 4.4B.13**). The mechanism of the catalytic transformation has been validated with the help of experimental and computational studies.

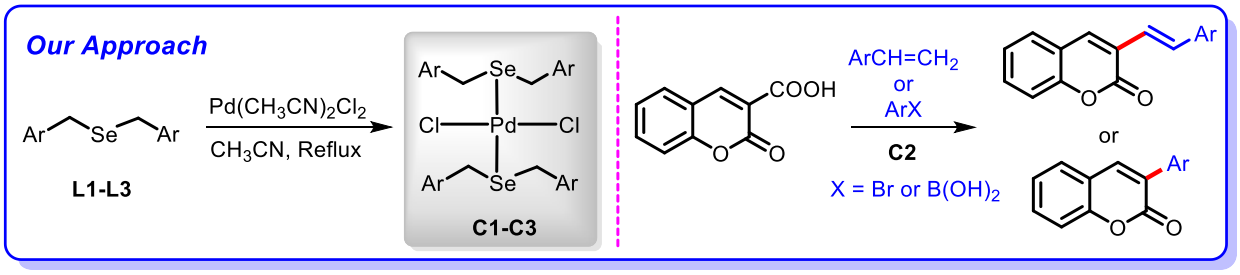

Scheme 4.4B.13: *Trans*-palladium dichloride complex catalyzed decarboxylative coupling of coumarin-3-carboxylic acids with styrenes, aryl bromides and arylboronic acids

4.4B.2.1 Syntheses and Characterization of Ligands L1-L3 and *trans*-Palladium Dichloride Complexes C1-C3. The ligands dibenzylselane (**L1**),[42] bis(naphthalen-1-ylmethyl)selane (**L2**), and bis(2-(benzyloxy)-3,5-di-*tert*-butylbenzyl)selane (**L3**) were synthesized by the reaction of selenium powder in the presence of solid $NaBH_4$ (2.2 equiv.) with benzyl chloride (**37**), 1-(chloromethyl)naphthalene (**38**), and 2-(benzyloxy)-1,5-di-*tert*-butyl-3-(chloromethyl)benzene (**39**), respectively (**Scheme 4.4B.14**). The new ligands were completely characterized with the help of ^1H, $^{13}C\{^1H\}$ NMR, UV-Vis., IR, HRMS, and elemental analysis.

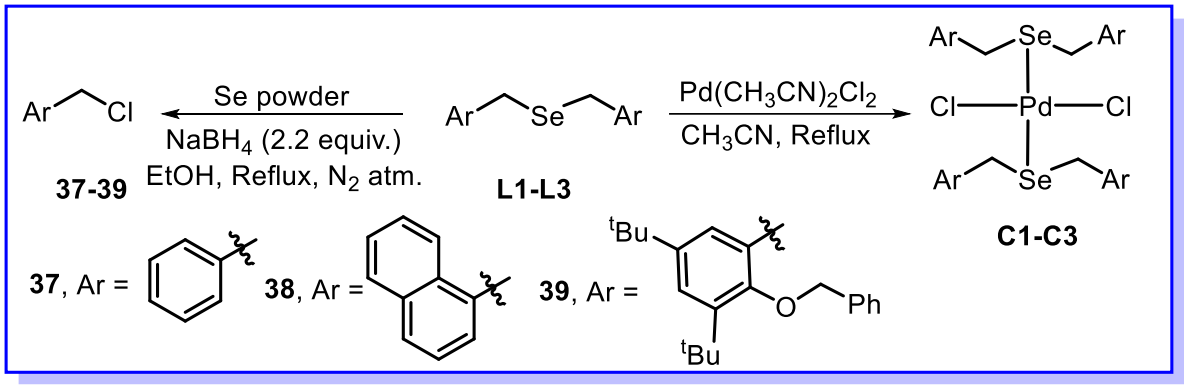

Scheme 4.4B.14: Syntheses of molecular rotors **C1-C3**

The ligands **L1-L3** showed characteristic Se*CH*$_2$ singlet in the range of δ 4.72-3.77 ppm in ^1H NMR which is shielded with respect to their chloro precursors due to less electronegativity of the selenium as compared to chlorine. Further, the palladium complexes **C1-C3** were synthesized by refluxing a mixture of ligands **L1-L3** and $Pd(CH_3CN)_2Cl_2$ (0.5 equiv.) in acetonitrile (**Scheme 4.4B.14**). The complexes **C1-C3** were also characterized with the help of ^1H, $^{13}C\{^1H\}$ NMR, UV-Vis., IR, HRMS, and elemental analysis. The UV-visible spectrum of ligands (**L1-L3**) and complexes (**C1-C3**) were measured in DCM solution (1.0×10^{-5} M) at 25 °C. The UV-visible spectra of ligands show two absorption peaks around 230 and 280 nm. Whereas, in the UV-visible spectra of complexes **C1-C3**, along with ligand peaks an additional peak appeared around 345-355 nm which indicated coordination of ligands with palladium (**Figure 4.4B.4**). The palladium complexes **C1-C3** are referred as molecular rotors. In these molecules, the bulky selenium ligand is acting as a stator unit which is providing protection to the Cl−Pd−Cl rotator unit. The palladium precursor when coordinates with **L1** and **L2**, the Se*CH*$_2$ protons becomes diastereotopic as indicated by the presence of two doublets at δ 4.51, and 3.95 ppm (for **C1, Figure 4.4B.5**) and at δ 5.21, and 4.38 ppm (for **C2**, **Figure 4.4B.7**) in the ^1H NMR as against the singlet for corresponding protons in the respective ligands. Similarly, four doublets at δ 4.94, 4.77, 4.55, and

4.24 ppm were observed in the ^{1}H NMR of **C3** as against two singlets in the ^{1}H NMR of **L3** at δ 5.10 and 3.95 ppm due to OC***H***$_2$ and SeC***H***$_2$, respectively **Figure 4.4B.4b**. The appearance of four doublets is due to diastereotopic nature of both OCH_2 and $SeCH_2$ protons. The HRMS analysis of **C1**, **C2** and **C3** showed peaks at *m/z* 700.8973, 922.9579 and 699.3571 corresponding to $[M + H]^+$, $[M + Na]^+$ and $[M + H - PdCl_2]^+$ ions, respectively. The *trans*-palladium dichloride complexes **C1-C3** are air and moisture insensitive and can be stored in open air at room temperature for more than two months. The palladium complexes **C1-C3** showed good solubility in solvents like CH_3CN, $CHCl_3$, CH_2Cl_2, DMSO, DMF, and are insoluble in non-polar solvents like diethyl ether, pentane, and hexane.

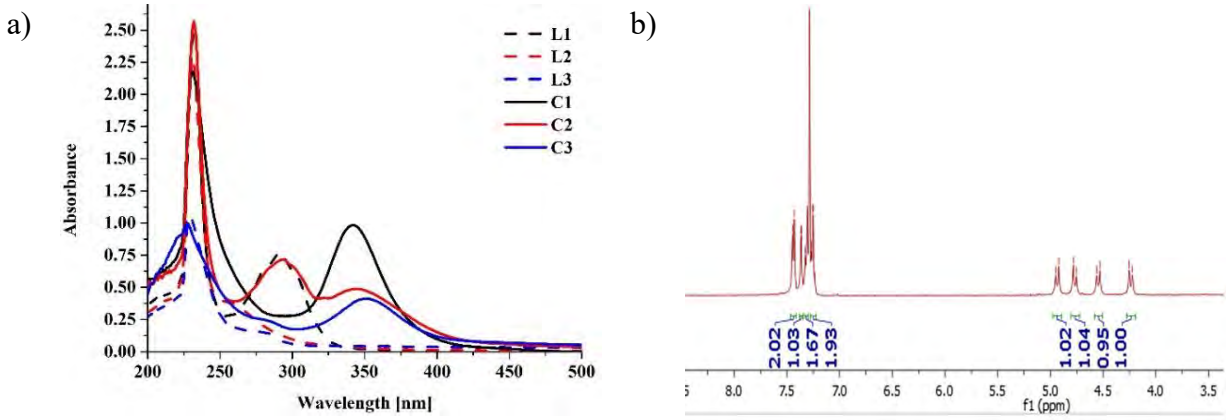

Figure 4.4B.4: a) UV-Vis absorption spectrums of **L1-L3** and **C1-C3**; b) ^{1}H NMR spectrum of **C3** showing four doublets due to dual intramolecular OCH---Cl and SeCH---Cl interactions

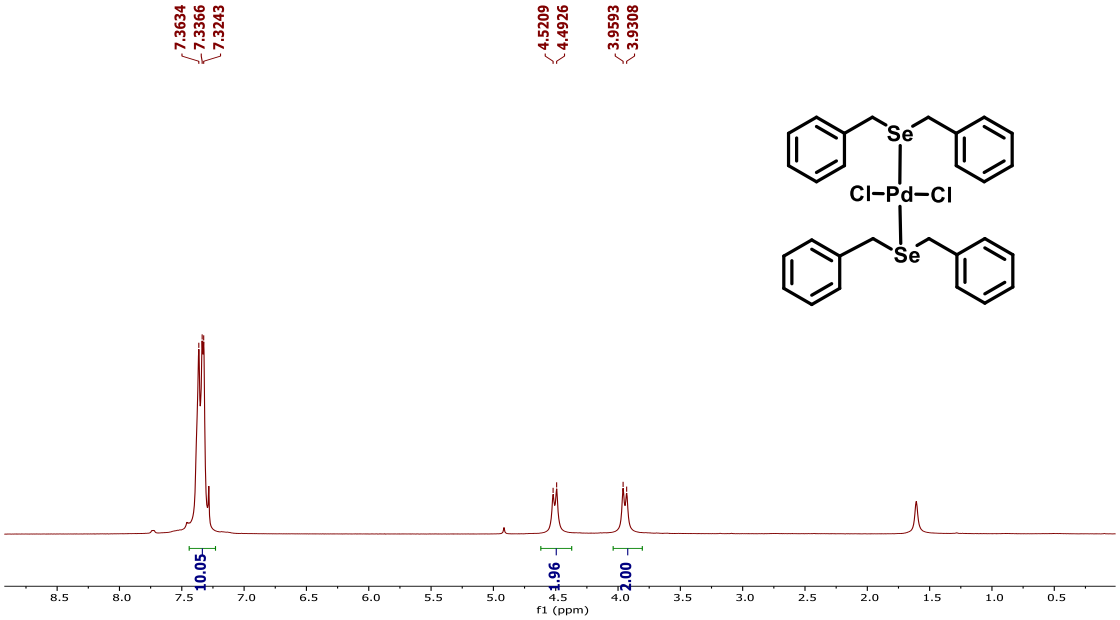

Figure 4.4B.5: ^{1}H NMR spectrum of **C1** recorded in $CDCl_3$

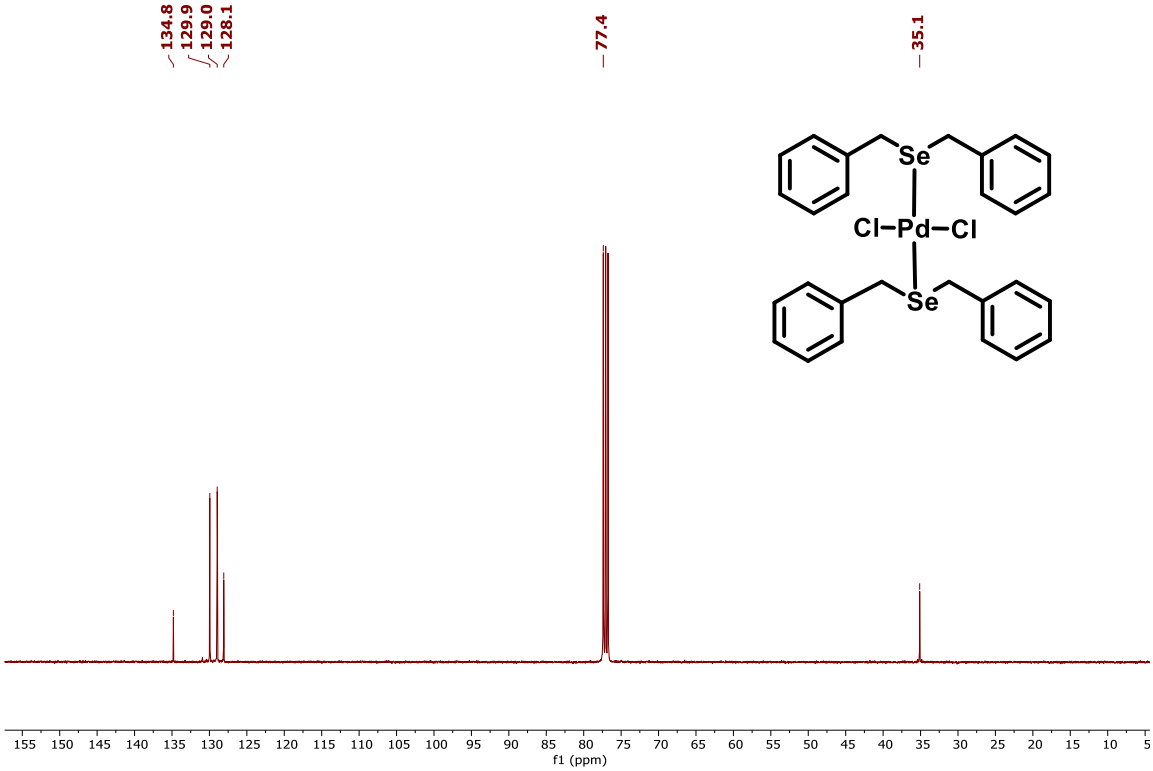

Figure 4.4B.6: $^{13}C\{^{1}H\}$ NMR spectrum of **C1** recorded in $CDCl_3$

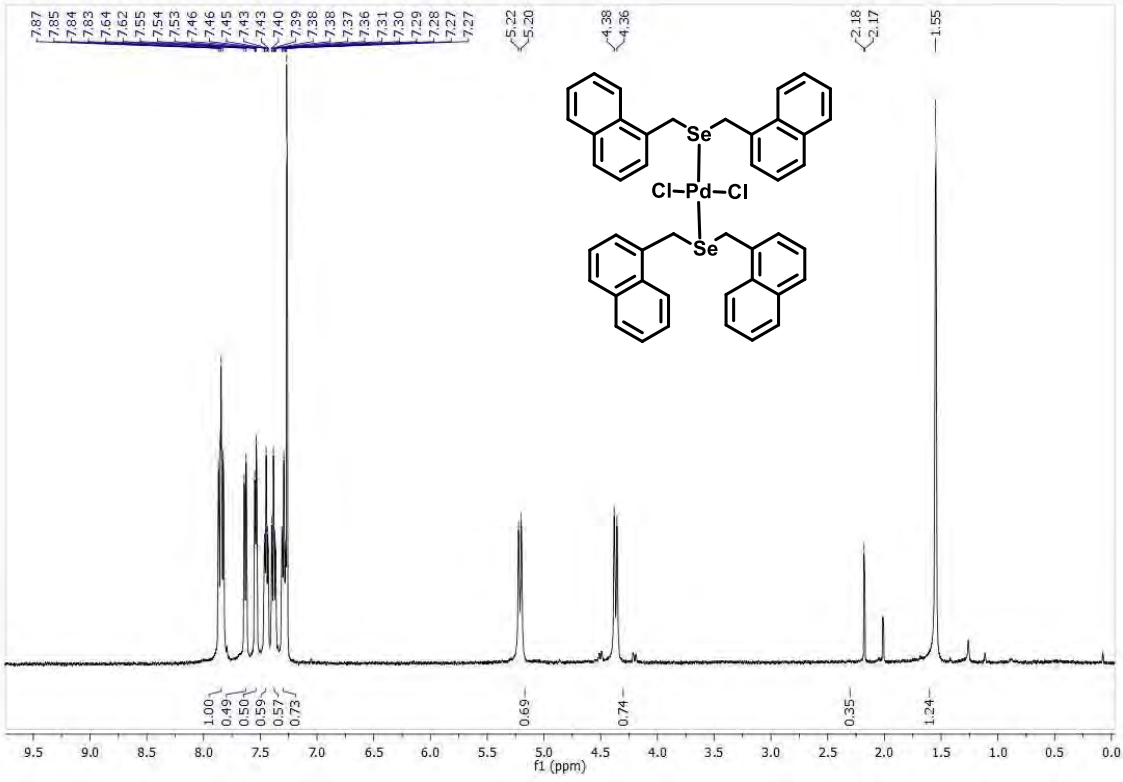

Figure 4.4B.7: ^{1}H NMR spectrum of **C2** recorded in $CDCl_3$

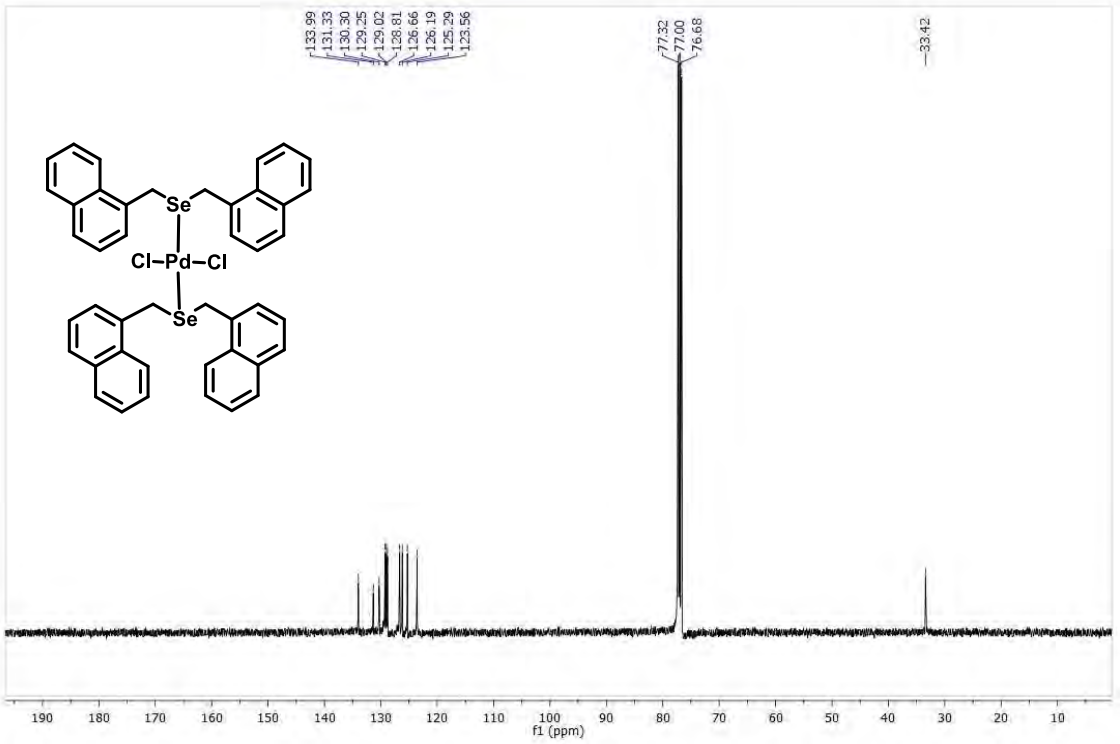

Figure 4.4B.8: $^{13}C\{^{1}H\}$ NMR spectrum of **C2** recorded in $CDCl_3$

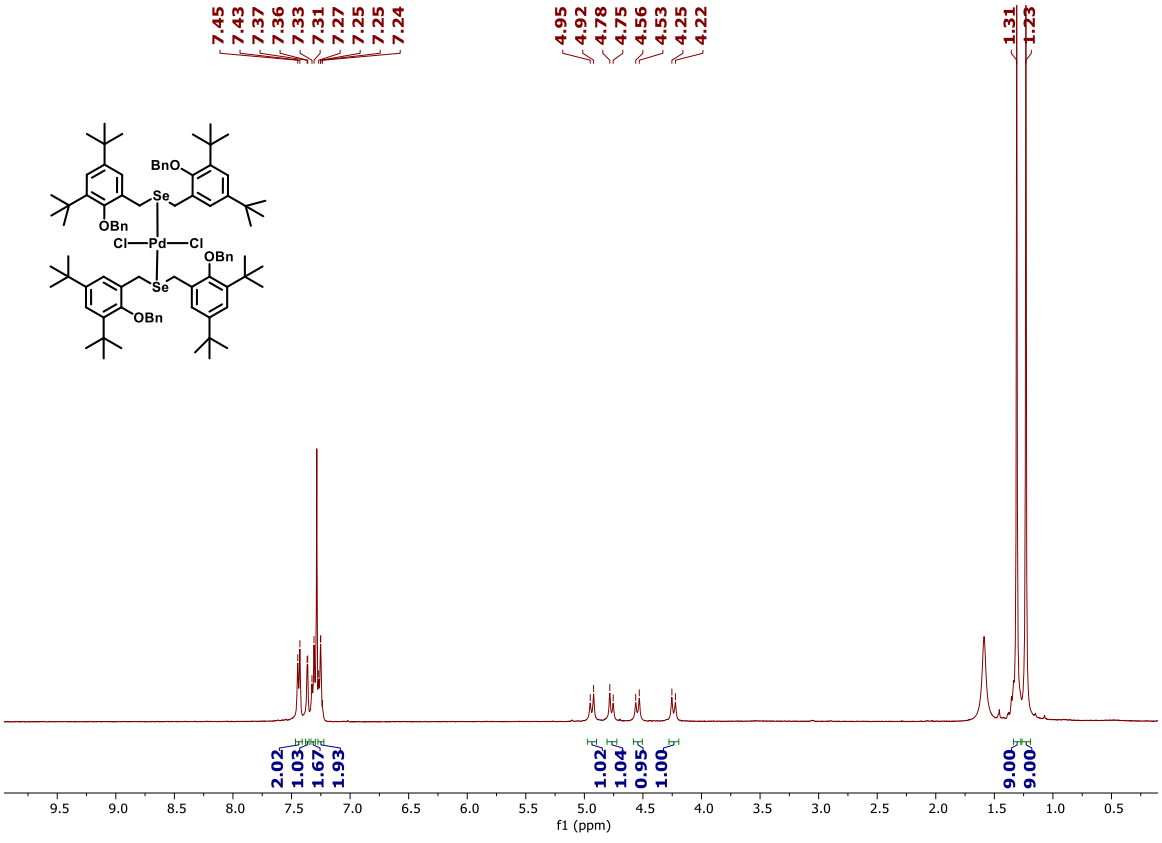

Figure 4.4B.9: ^{1}H NMR spectrum of **C3** recorded in $CDCl_3$

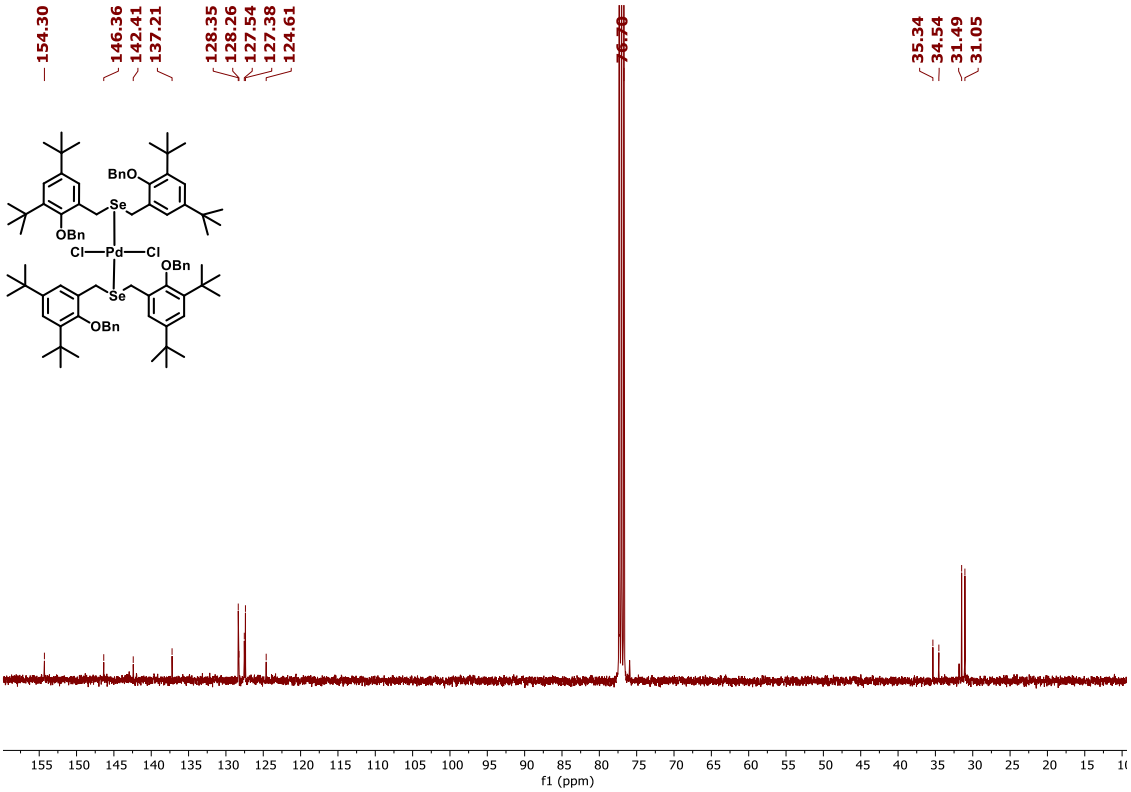

Figure 4.4B.10: $^{13}C\{^{1}H\}$ NMR spectrum of **C3** recorded in $CDCl_3$

4.4B.2.2 Crystal Structure. The structure of *trans*-palladium dichloride complex (**C2**) and bonding modes of palladium with ligand was authenticated with the help of single crystal X-ray (**Figure 4.4B.11**). The crystals of molecular rotor **C2** were obtained by slow evaporation of its CH_3CN solution. The attempts to crystalize complexes **C1** and **C3** were unsuccessful. The complex **C2** showed distorted square planar geometry around palladium center. Elongated thermal ellipsoid on Cl1 along with nearby residual electron density peak suggested disorder which was modeled between two positions with an occupancy ratio of 0.74:0.26. The crystallographic parameters along with selected bond angles and bond lengths are given in **Table 4.4B.4.** The Cl-Pd-Cl rotor unit orient itself in *trans* geometry with respect to bulky stator ligand **L2**. The two selenium atoms of stator unit orient themselves in *anti*-position with respect to each other and the distance between them is 4.845 Å, whereas the distance between two chlorines of rotor unit is 4.641 Å. The Pd–Cl and Pd–Se distance in the molecule is 2.320 and 2.423 Å, respectively. The molecule possesses intramolecular SeCH---Cl interactions of 2.654 Å (**Figure 4.4B.11**, left) in between the rotor unit and stator ligand, which is shorter than earlier reported benzyl protected molecular rotor's distance of 2.880 Å. The unit cell of molecule possesses nine molecules in it (**Figure 4.4B.11**, right).

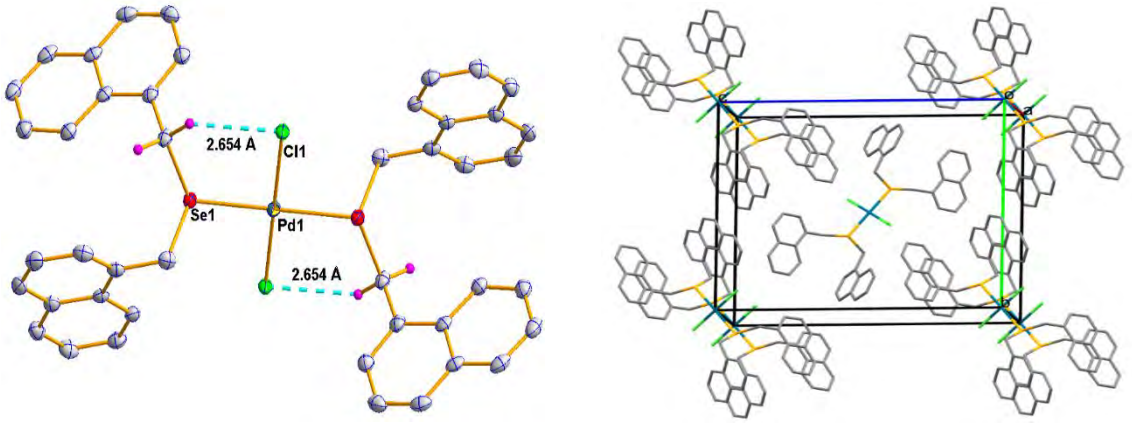

Figure 4.4B.11: Thermal ellipsoid plots (50% probability) of **C2** showing intramolecular SeCH---Cl interactions (left), Unit Cell diagram of **C2** (right)

4.4B.2.3 Dynamic Process in Molecular Rotors C1-C3. The metal complexes of *trans*-$[MX_2(SeR_2)_2]$ are known to show pyramidal inversion of selenium atom at elevated temperatures.[43] The detailed studies for pyramidal inversion of *trans*-$[PdCl_2(SeEt_2)_2]$ showed a rotational barrier of 16.2 kcal/mol.[43] The molecular rotors **C1-C3**, have possibility of showing pyramidal inversion at elevated temperature. Accordingly, when rotors **C1** and **C2** were taken in DMSO-d_6 and heated to observe the coalescence phenomena in the ^{1}H NMR spectrum of these complexes. The results presented in **Figure 4.4B.12** and **Figure 4.4B.13** shows when the molecular rotors **C1** and **C2** were warmed, the two diastereotopic proton of $SeCH_2$ started to coalesce with increasing temperature.

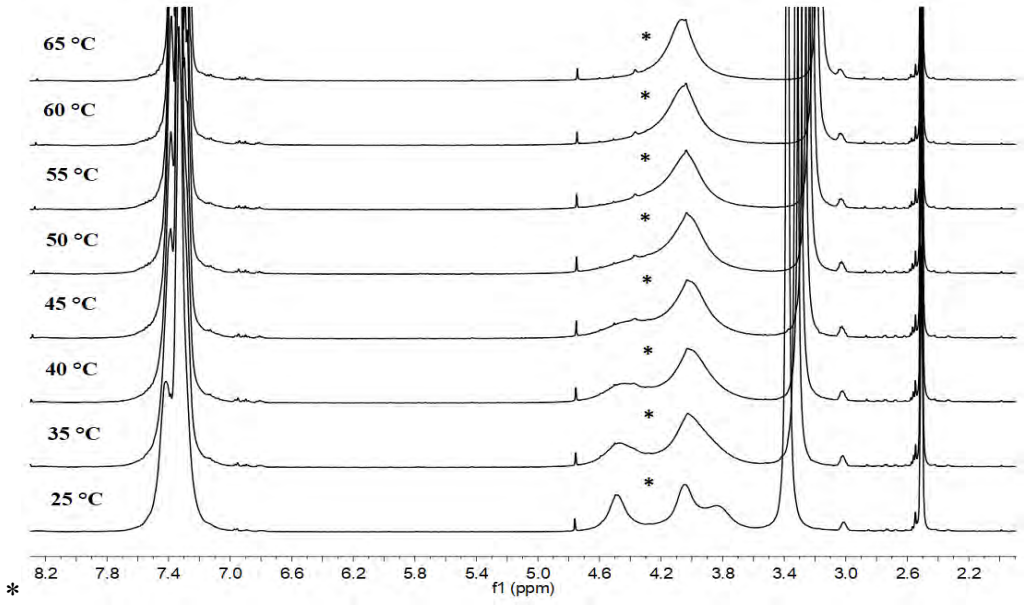

Figure 4.4B.12: ^{1}H NMR spectra of **C1** (DMSO-d_6) as a function of temperature. Coalescing signals are denoted with a *

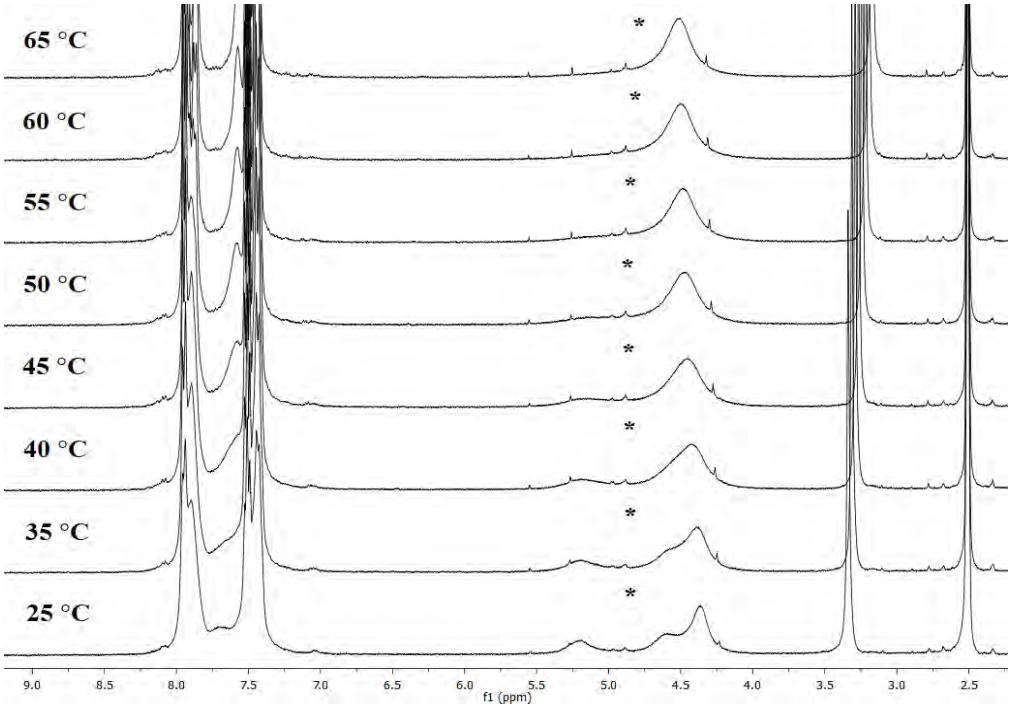

Figure 4.4B.13: ^{1}H NMR spectra of **C2** (DMSO-d_6) as a function of temperature. Coalescing signals are denoted with a*

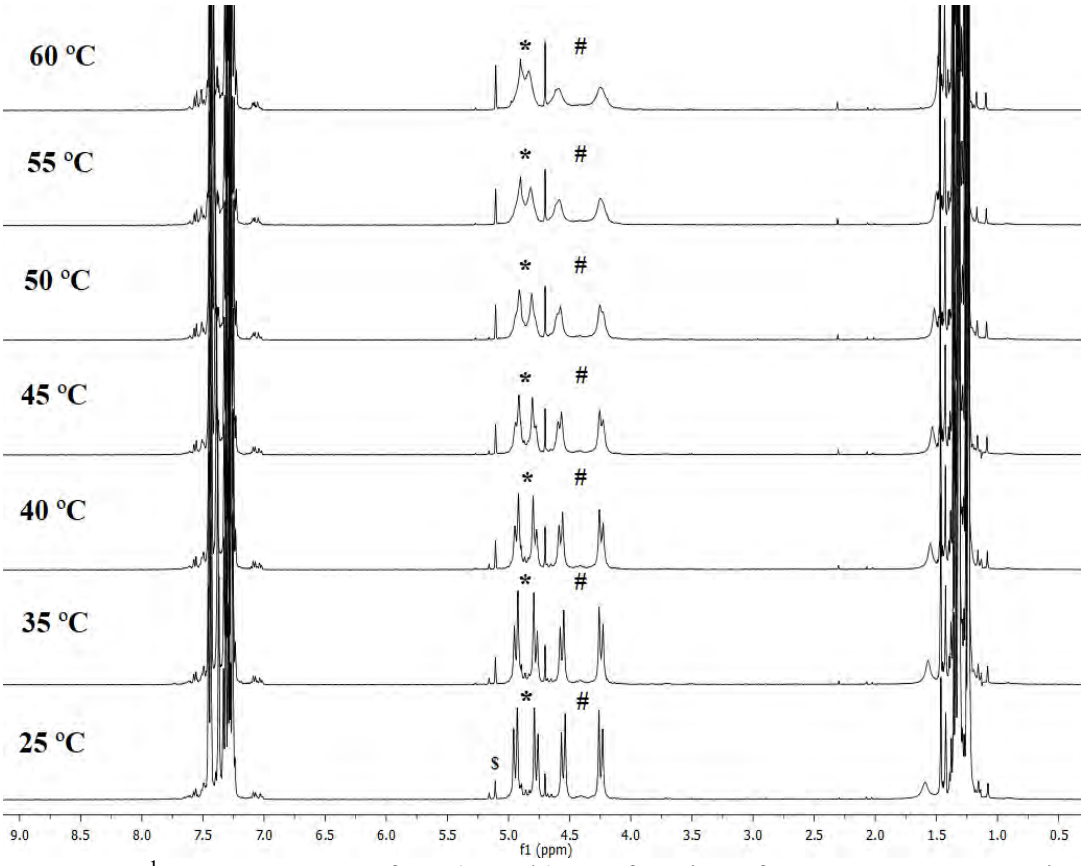

Figure 4.4B.14: ^{1}H NMR spectra of **C3** ($CDCl_3$) as a function of temperature. Target signal for monitoring the coalescence are denoted with * and #. $ represents solvent impurity

In both the complexes **C1** and **C2**, the diastereotopic proton signals show coalescence around 40-50 °C, which is closely related to earlier reported *trans*-[$PdCl_2(SeEt_2)_2$] complex.[43] This suggests that the coalescing phenomenon is due to the inversion of selenium atom and rotation around $SeCH_2$ bond (**Figure 4.4B.12**).[43] It has also been reported that the inversion barriers are lowered when one of the three substituents of a pyramidal heteroatom is a transition metal (**Figure 4.4B.15**).[43-45]

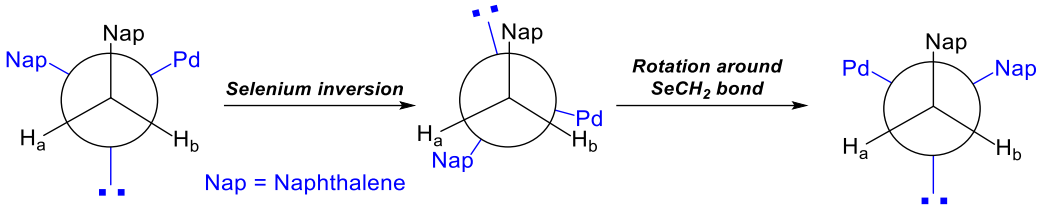

Figure 4.4B.15: Newman projections representing selenium inversion and rotation around - $SeCH_2$ bond

Next, the complex **C3** was taken in $CDCl_3$ and heated on elevated temperatures to observe the coalescence phenomena in the ^1H NMR spectrum (**Figure 4.4B.14**). It is observed that no coalescence was seen in the molecule **C3** even at 60 °C, the slight shifting in the peaks was observed due to elevated temperature. This suggests that the selenium of molecular rotor **C3** do not show pyramidal inversion at 60 °C, and higher temperature might be required for the inversion to be observed in such molecules. The four doublets in the proton NMR spectrum (**Figure 4.4B.14**) of **C3** indicate that there may be intramolecular OCH---Cl and SeCH---Cl interactions with bulky stator ligands (**Figure 4.4B.16**).

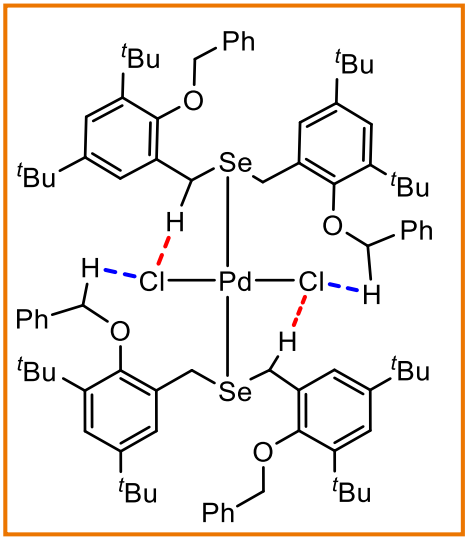

Figure 4.4B.16: Intramolecular OCH---Cl and SeCH---Cl interactions in **C3**

4.4B.2.4 Chlorine Rotation in Molecular Rotor C2. It is observed in the *.cif* file of **C2**, that the chlorines in the complex are distorted in the crystal structure (**Figure 4.4B.17**).

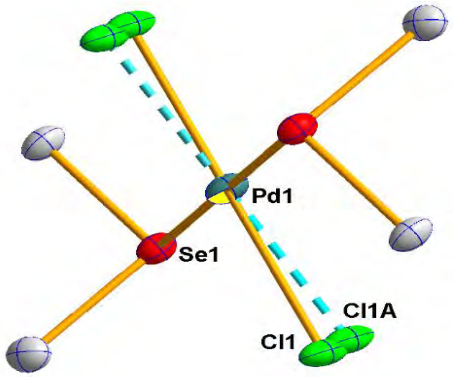

Figure 4.4B.17: Distortion observed in the Cl atoms of **C2** (the naphthalene ligand and hydrogens were omitted for clarity)

This gives an indication for the rotation of the Cl-Pd-Cl rotor. To understand the rotation of chlorine through the Cl-Pd-Cl rotor, the potential energy surface (PES) of **C2** along the Cl-Pd-Cl rotational coordinate was studied and results are given in **Figure 4.4B.18**. The geometry of **C2** is taken from the crystal structure. We have performed a relaxed energy scan by changing the torsional angle Cl84-Pd1-Se2-C3 from its initial value (105 degree) to 465 degrees with an increment of 5 degree. The torsional angle Cl85-Pd1-Se2-Cl84 is fixed to 180 degrees during the partial optimizations. During the partial optimization only the coordinates of chlorine and hydrogen atoms are allowed to varied to mimic the crystal environment.

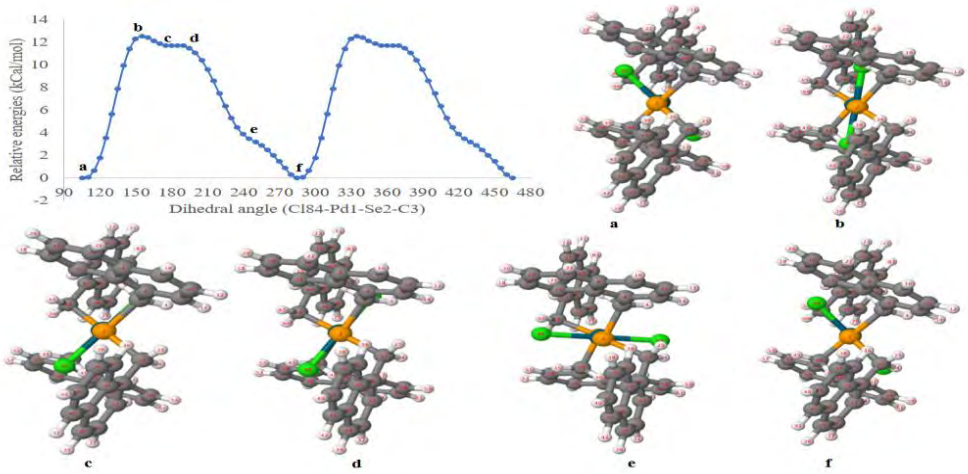

Figure 4.4B.18: Relaxed potential energy scan of the torsional angle Cl84-Pd1-Se2-C3 from 105 degrees to 465 degrees

The PES from 105 to 285 degrees and 285 to 465 degrees are similar due to the symmetry in the structure **C2**. For brevity, we discuss the PES between 105 to 285 degrees. The PES exhibit two global minima (***a*** and ***f***), one local minimum (***c***) and two maxima (***b*** and ***d***). The structures ***a*** and ***f*** correspond to secondary hydrogen bonding interactions between chlorine-hydrogen pairs (Cl84-H24, Cl85-H65), and (C84-H65, Cl85-H24) respectively and are global minima. The maxima ***b*** and ***d*** correspond to repulsive interactions between the chlorine and hydrogen pairs (C84-H46 and Cl85-H5) and (Cl84-H45 and Cl85-H6), respectively. The local minimum ***c*** corresponds to attractive interactions between H5-Cl85-H6 and H45-Cl84-H46. The geometry ***e*** corresponds to the attractive interactions between H45-Cl84-65 and H4-Cl85-H24. The separation between the minimum (***a***) and the maximum (**b**) is 12.5 kcal/mol. This activation energy is needed to unlock the dynamical rotational process. To substantiate our claim, we compare the activation energy of current rotational process with literature. The activation energies ranging from 0.8 kcal/mol to 16.1 kcal/mol are reported depending on the bulky nature of the stator units.[46, 47]

We embarked on the investigation with a reaction of coumarin-3-carboxylic acid (2-oxo-2*H*-chromene-3-carboxylic acid, **8a**) and styrene (**7a**) using molecular rotor **C1-C3** as catalysts (**Table 4.4B.1**). To our satisfaction, the desired product (*E*)-3-styryl-2*H*-chromen-2-one (**11aa**) was obtained in 32% yield on heating a mixture of **8a** (1.0 mmol) and **7a** (1.0 mmol) in DMF (3 mL) at 100 °C using **C2** (2.5 mol %) as the catalyst and Ag_2CO_3 as a base (**Table 4.4B.1**, entry 1). Notably, no product formation was observed either in the absence of base or in the absence of catalyst (**Table 4.4B.1**, entries 2-3). Next, we screened various bases such as NaOAc, CsOAc, AgOAc, Ag_2O, K_2CO_3 and Cs_2CO_3 under similar reaction conditions as entry 1 (**Table 4.4B.1**, entries 4-9). Among all bases screened, Cs_2CO_3 was found to be the most suitable affording **11aa** in 58% yield (**Table 4.4B.1**, entry 9). It is worth mentioning that no byproduct was formed under these conditions and 38% of unreacted **8a** was isolated. This protocol showed high degree of regioselectivity towards the decarboxylative C3-coupling.

To further improve the yield of **11aa**, we screened different solvents such as xylene, toluene, DMA, DMSO, NMP and HFIP (**Table 4.4B.1**, 10-15). However, no improvement in the yield of **11aa** was observed and thus we selected DMF as the solvent of choice for further investigation. Subsequently, we evaluated effect of different catalysts and catalyst loading (**Table 4.4B.1**, entries 16-18). On using **C1** and **C3** as catalyst under standard conditions as entry 9, **11aa** was obtained in 36% and 39% yields, respectively (**Table 4.4B.1**, entries 16 and 17). A reaction using $Pd(OAc)_2$ (2.5 mol %) as catalyst gave only 21% yield of **11aa** under standard reaction

conditions (**Table 4.4B.1**, entry 18), indicating that strong sigma electron donating selenium ligand enhances catalytic efficiency of the palladium complex. Upon increasing **C2** catalyst loading from 2.5 mol % to 5.0 mol %, only slight increase in the yield (60%) of **11aa** was observed (**Table 4.4B.1**, entry 19) while decreasing it to 2.0 mol % led to a significant decrease in the yield (34%) of **11aa** (**Table 4.4B.1**, entry 20).

Table 4.4B.1: Optimization of reaction conditions for decarboxylative Heck coupling.[a]

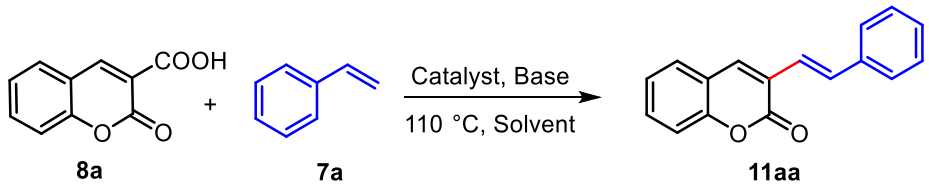

8a **7a** **11aa**

S. No.	Catalyst	Base	Solvent	Yield[b] (%)
1	**C2**	Ag_2CO_3	DMF	32
2	**C2**	-	DMF	nr
3	**-**	Ag_2CO_3	DMF	nr
4	**C2**	NaOAc	DMF	43
5	**C2**	CsOAc	DMF	24
6	**C2**	AgOAc	DMF	trace
7	**C2**	Ag_2O	DMF	31
8	**C2**	K_2CO_3	DMF	37
9	**C2**	**Cs_2CO_3**	**DMF**	**58**
10	**C2**	Cs_2CO_3	Xylene	trace
11	**C2**	Cs_2CO_3	Toluene	nr
12	**C2**	Cs_2CO_3	DMA	43
13	**C2**	Cs_2CO_3	DMSO	52
14	**C2**	Cs_2CO_3	NMP	32
15	**C2**	Cs_2CO_3	HFIP	26
16	**C1**	Cs_2CO_3	DMF	36
17	**C3**	Cs_2CO_3	DMF	39
18	**$Pd(OAc)_2$**	Cs_2CO_3	DMF	21
19	**C2**	Cs_2CO_3	DMF	60[c]
20	**C2**	Cs_2CO_3	DMF	34[d]
21	**C2**	Cs_2CO_3	DMF	45[e]
22	**C2**	Cs_2CO_3	DMF	48[f]

[a]Reaction conditions: **8a** (1.00 mmol), **7a** (1.00 mmol), catalyst (2.5 mol %), base (1.0 equiv), solvent (3 mL), 10 h. [b]Isolated yield. [c]Using 5 mol % of **C2**. [d]Using 5 mol % of **C2**. [e]Reaction at 80 °C. [f]Recation at 130 °C. nr = no reaction.

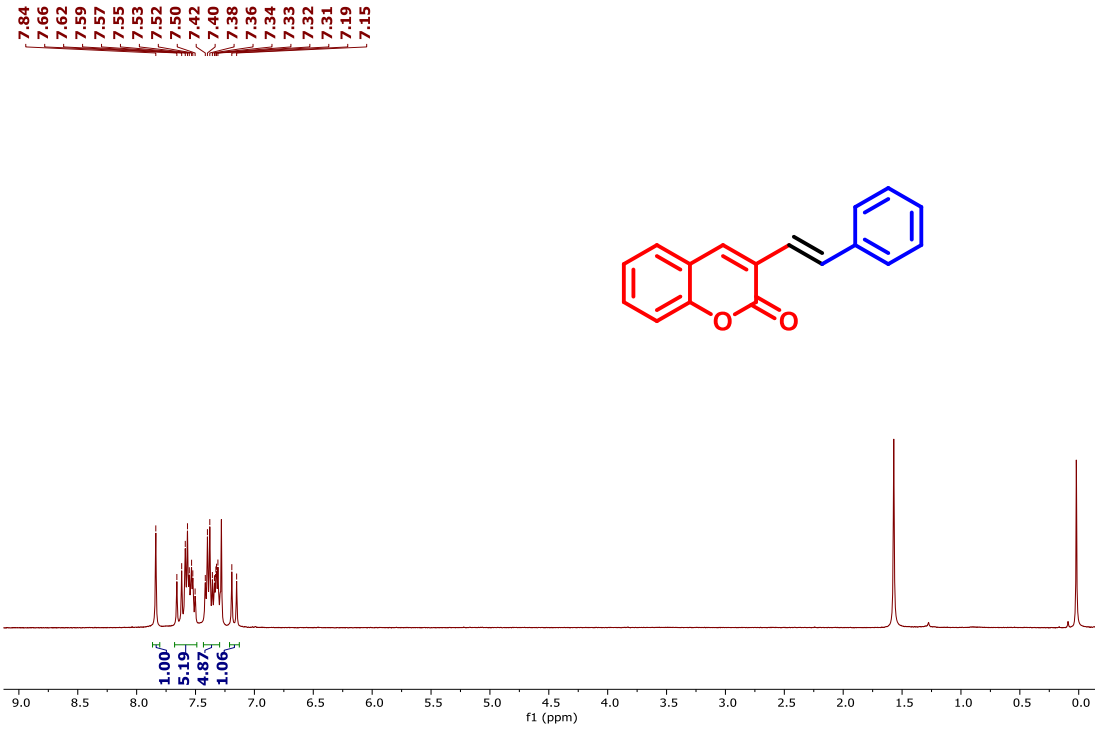

Figure 4.4B.19: ^{1}H-NMR spectrum of (*E*)-3-Styryl-2*H*-chromen-2-one (**11aa**) recorded in $CDCl_3$

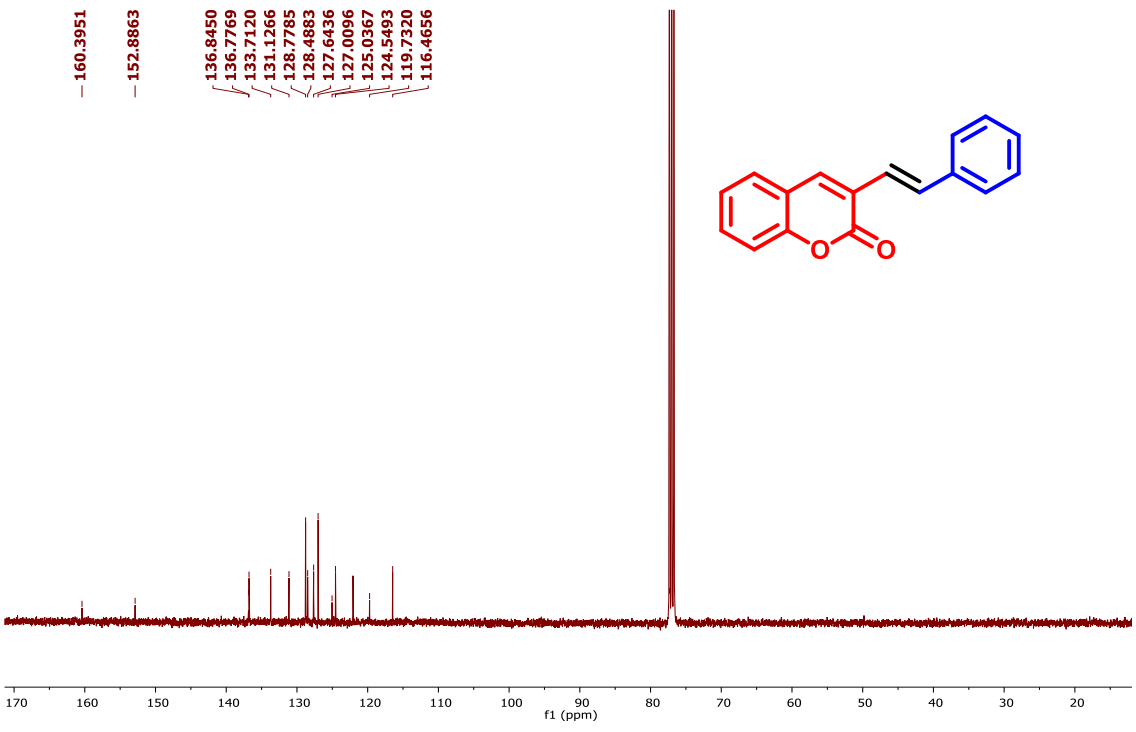

Figure 4.4B.20: ^{13}C-NMR spectrum of (*E*)-3-Styryl-2*H*-chromen-2-one (**11aa**) recorded in $CDCl_3$

Finally, effect of reaction temperature was evaluated and decreasing or increasing the reaction temperature to 80 °C or 130 °C could not improve the yield of **11aa** (**Table 4.4B.1**, entries 21 and 22). The rate of reaction was studied by monitoring progress of reaction at different time intervals (Figure 9). Initially for first five hours the reaction was very slow and only 11% coupled product **11aa** was observed during this time. The NMR and HRMS studies of reaction mixture suggests a slow decarboxylation reaction for first few hours. The rate of product formation increases after first five hours till ten hours. The progress of reaction after 6, 8, and 10 hours shows 27, 48, and 58% yields of **11aa**. The monitoring of reaction after 13 h shows no progress and **11aa** was isolated in 58% yield.

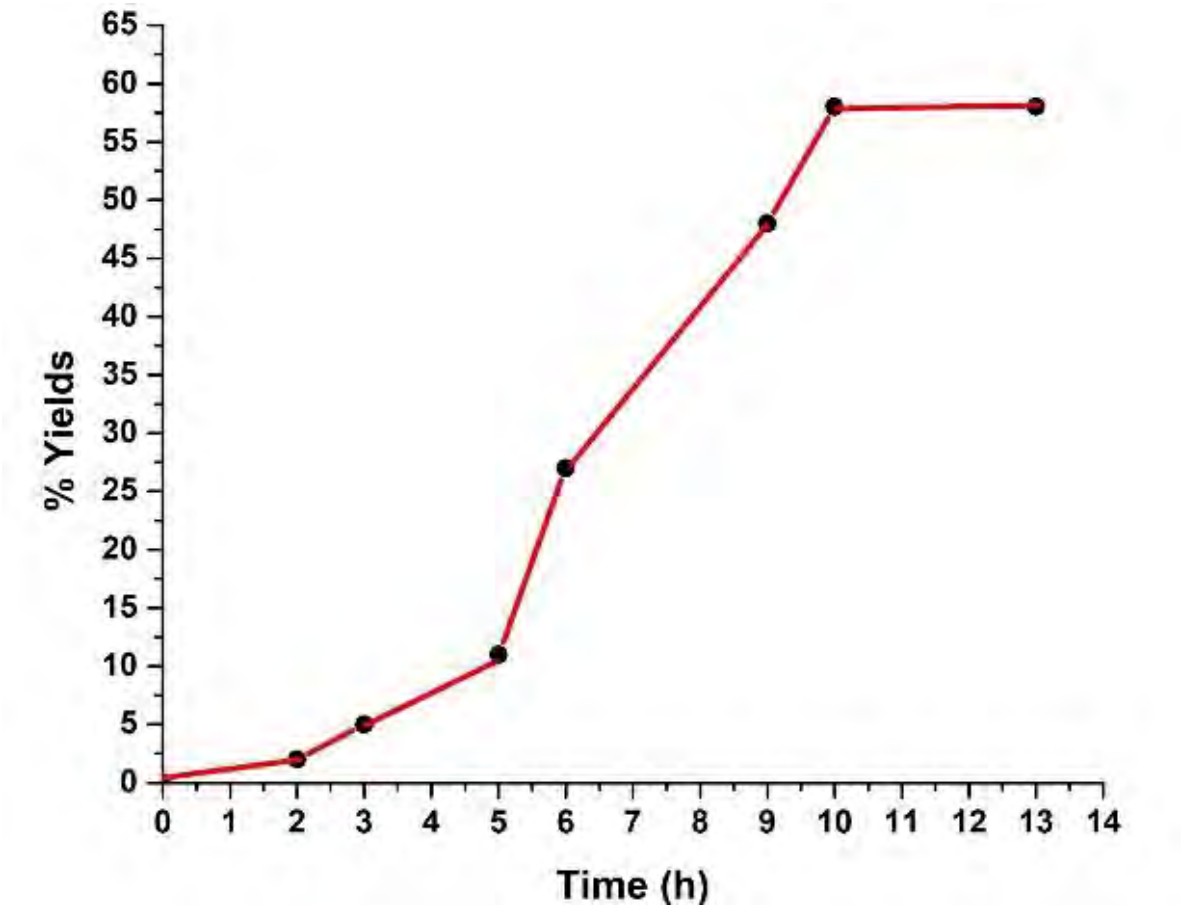

Figure 4.4B.21: Time profile of the catalytic decarboxylative coupling of coumarins with styrene using **C2** as catalyst

Next, with the best screened reaction conditions in hand, the scope and generality of protocol was examined for the coupling of coumarin-3-carboxylic acids (**8a-d**) with styrene derivatives (**7a-o**) and results are presented in **Table 4.4B.2**.

Table 4.4B.2: Substrate scope for the **C2**-catalyzed decarboxylative Heck coupling.[a]

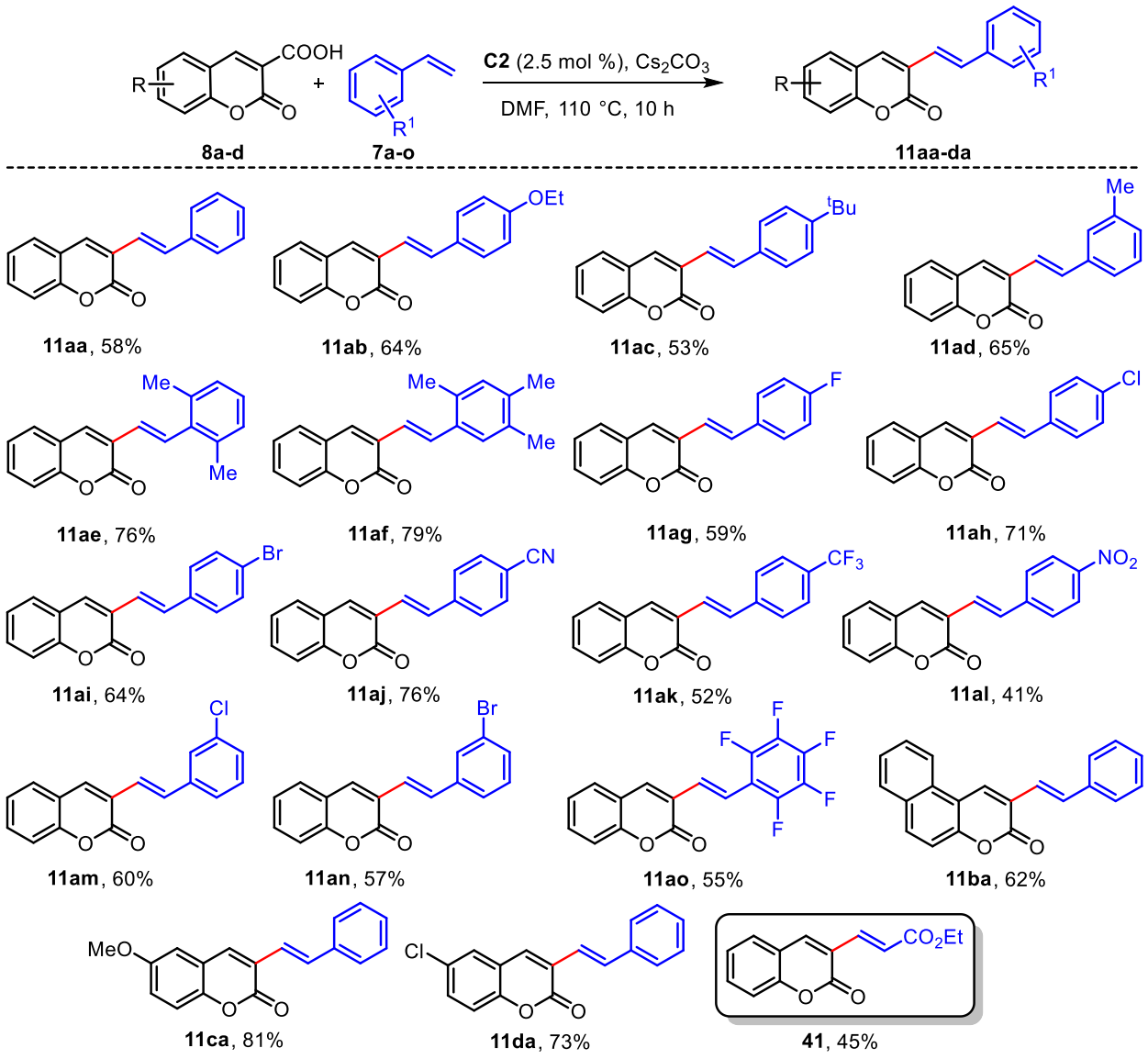

[a]Reaction conditions: **8** (1.00 mmol), **7** (1.00 mmol), **C2** (2.5 mol %), Cs_2CO_3 (1.0 equiv.), DMF (3 mL), 10 h. [b]Isolated yield.

To our delight, the reaction with all structurally divergent substrates went smoothly to give moderate to good yields of regioselective decarboxylative coupled products **11aa-da**. Various functional groups such as -Br, -Cl, -NO_2, and -CN, which are sensitive toward palladium catalysis were well tolerated under these conditions. Further, it is important to mention that styrenes substituted at *ortho*-, *meta*- and *para*-positions with both electron donating and electron withdrawing groups reacted smoothly to afford corresponding decarboxylative Heck products in good yields. Slightly lower yields of Heck products were obtained from deactivated styrenes.

Interestingly, 1,2,3,4,5-pentafluoro-6-vinylbenzene could be effectively coupled with **8a** to result corresponding Heck product **11ao** in 55% yield. Similarly, substituted coumarins (**8b-d**) also reacted smoothly with **7a** to afford corresponding Heck coupled products **11ba-da** in good to high yields (62-81%). Finally, **8a** was reacted with ethyl acrylate (**40**) under standard reaction conditions and corresponding Heck coupled product **41** was obtained in 45% yield indicating that the developed protocol can be extended for decarboxylative coupling of coumarin-3-carboxylic acids with other alkenes.

Intrigued with the results of regioselective decarboxylative Heck coupling reaction, we wondered if the protocol can be extended to other coupling reactions. First, we tested the efficiency of molecular rotor **C2** for decarboxylative direct arylation reaction of **8a** with aryl bromides (**2a-d**) under standard reaction conditions obtained from **Table 4.4B.1**. To our satisfaction, moderate yields of 3-arylcoumarins (**9a-d**) were obtained for the direct arylation reactions (**Table 4.4B.3**). With the success of direct arylation reaction, we examined decarboxylative Suzuki-Miyaura coupling reaction of **8a** with different arylboronic acids (**42a-d**) using **C2** catalyst. Interestingly, 3-arylcoumarins (**9a-d**) were obtained in moderate (32-56%) yields under these conditions. The results of decarboxylative direct arylation and Suzuki-Miyaura coupling indicate that **C2** can be a potential catalyst for different decarboxylative coupling reactions. The yields of these reactions can be further improved with optimization of the reaction conditions.

Table 4.4B.3: C2-catalyzed decarboxylative arylation and Suzuki-Miyaura coupling reaction of Coumarin **8a**.

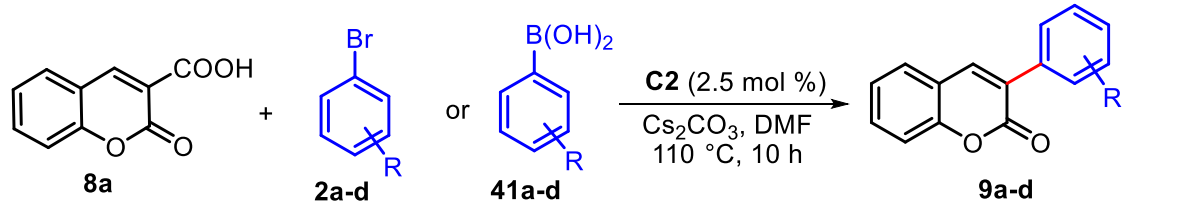

[a]Yields in parentheses are for Suzuki reaction

The substituted coumarin derivatives with delocalized π-electron system are known to show an enhanced fluorescence.[12] Synthetic utility of the developed protocol is demonstrated by

synthesizing a coumarin derivative with extended π-conjugation from the decarboxylative Heck product **11ai** (**Scheme 4.4B.9**). Interestingly, the Suzuki-Miyaura coupling reaction of **11ai** with (4-methoxyphenyl)boronic acid (**41b**) gave 48% yield of coupled product **42** in 24 h.

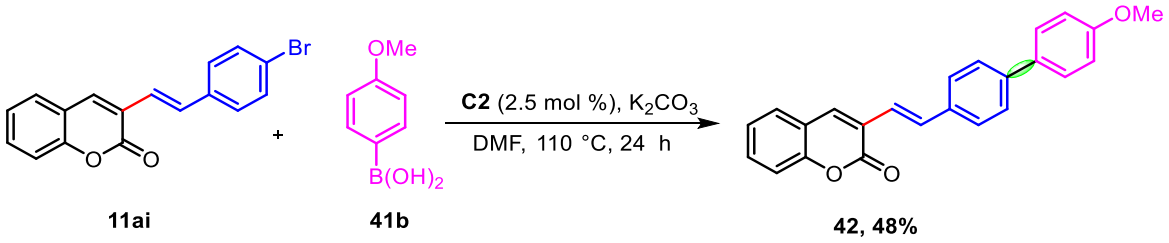

Scheme 4.4B.15: Scope for **C2**-catalyzed decarboxylative Suzuki-Miyaura coupling reaction

4.4B.2.5 Mechanistic Studies of Silver-free Regioselective Decarboxylative Heck Coupling of Coumarin-3-carboxylic Acids. To better understand the reaction mechanism, first we performed a deuterium exchange experiment (**Scheme 4.4B.16**). Reaction of **8a** with D_2O (25 equiv.) under standard reaction conditions in the absence of the catalyst **C2** resulted in formation of coumarin (**6**) with incorporation of 54% deuterium at the C3-position. This indicates the decarboxylation of coumarin as initiation step of the reaction. Further to confirm this, we performed reaction of **8a** and **7a** under standard reaction conditions (**Table 4.4B.1, entry 9**) and monitored the progress of reaction through mass spectrometry after one hour it shows a peak at *m/z* 147.0449 which corresponds to decarboxylated coumarin $[M - CO_2 + H]^+$ ion.

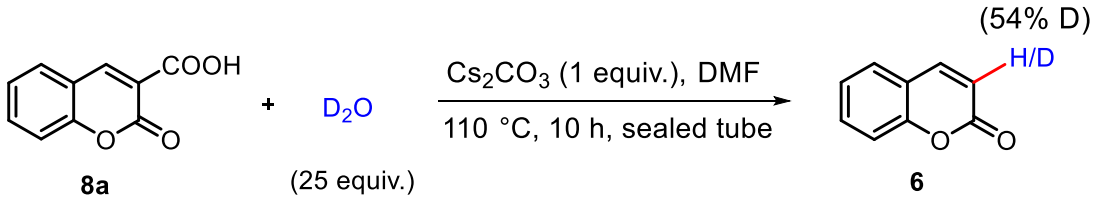

Scheme 4.4B.16: Deuterium exchange experiment

Based on the above results, previous reports,[33-35, 48-50] and computational studies (**Figure 4.4B.22**) a plausible mechanism of the reaction was proposed in **Scheme 4.4B.17**. Initially 2-oxo-2*H*-chromene-3-carboxylic acid upon reaction with Cs_2CO_3 gives decarboxylated coumarin, which further reacts with cesium and from (2-oxo-2*H*-chromen-3-yl)cesium. This was also confirmed by HRMS of reaction mixture after 1.5 hour. A peak appeared at m/z 300.9224 which corresponds to (2-oxo-2*H*-chromen-3-yl)cesium $[M–CS + Na]^+$. In the next step, molecular rotor catalyst **C2** react with (2-oxo-2*H*-chromen-3-yl)cesium and gives intermediate *trans*-**A** followed by removal of CsCl. At B3LYP7Lanl2DZ/6-31g (d, p) level of theory, *trans-**A*** stabilized by an energy of 6.55 kcal/mol than *cis-**A*** due to the presence of steric interactions. Further, the styrene

reacts with *trans*-**A** to form the π_1-complex intermediate by removal of one ligand to minimize the steric repulsion. The styrene then undergoes the classical Heck type insertion reaction into palladium complex resulting palladium σ-intermediate by assessing transition state (TS_1). The computed energies of the relevant species in the Heck reaction (π_1-complex, palladium σ-intermediate, π_2-complex, TS_1 and TS_2) are shown in Figure 10. The activation energy required for the alkyl chain migration found to be 18.37 kcal/mol. The palladium σ-intermediate further undergoes *β*-H elimination reaction to form another π_2-complex intermediate having palladium hydride bond through the transition state (TS_2) at energy 21.8 kcal/mol. Finally, this π_2-complex intermediate upon reductive elimination reaction gives the desired C3-substituted coumarins and regenerate the complex through reaction with earlier eliminated ligand and CsCl.

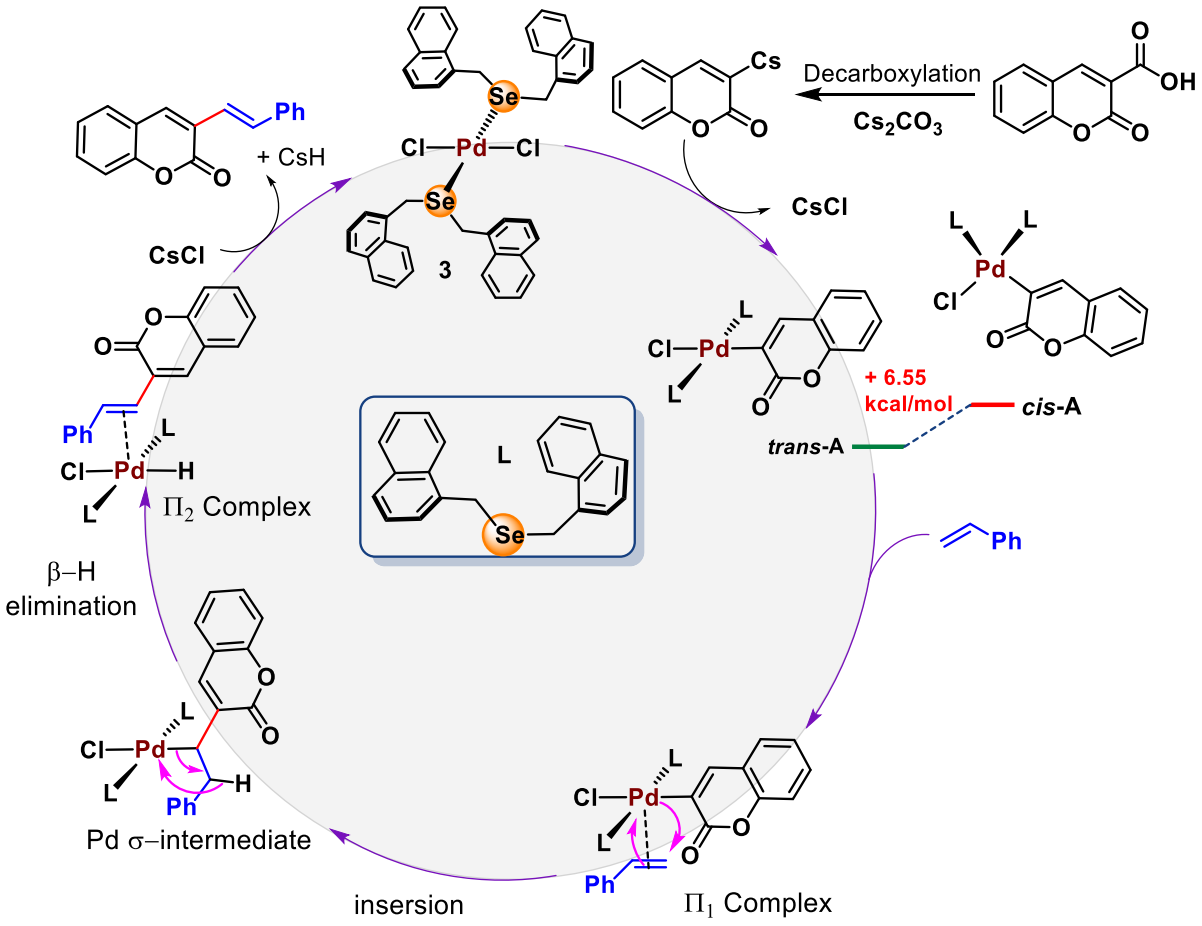

Scheme 4.4B.17: Plausible mechanism for formation of **11aa**

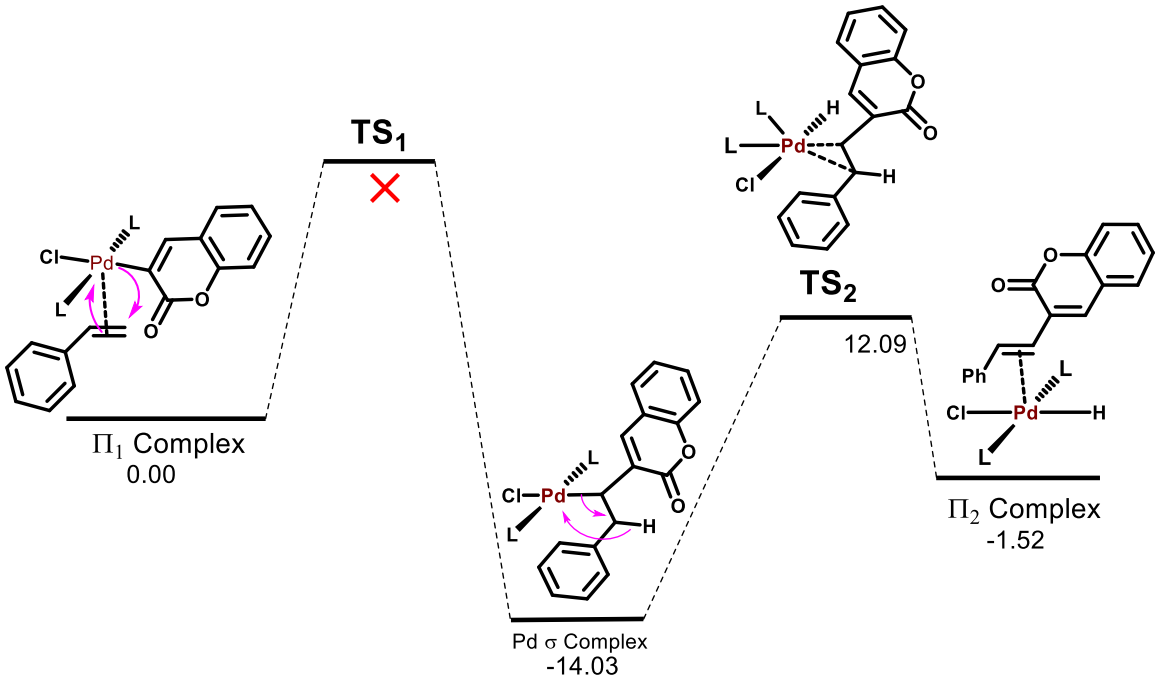

Figure 4.4B.22: The PES along the reaction coordinate calculated at B3LYP7Lanl2DZ/6-31g(d, p)

4.4B.3 CONCLUSION

We have synthesized three new *trans*-palladium dichloride complexes. The complexes were characterized with the help of NMR, HRMS, UV Vis., IR, and elemental analysis. The structure of *trans*-palladium dichloride complex **C2** was authenticated with the help of single crystal X-ray. The rotor possesses a square planer geometry with two chlorine and two ligands are *trans* to each other. The chlorine of rotor unit possesses intramolecular secondary interactions with CH_2 of stator ligand. The VT NMR data shows coalescence of diastereotopic protons, which indicates pyramidal inversion of selenium atom in the complexes **C1** and **C2** at elevated temperature. The complex **C3** do not show pyramidal inversion of selenium at 60 ˚C. The relaxed PES suggests a barrier of 12.5 kcal/mol for rotation of chlorine through Cl-Pd-Cl in the **C2**. The *trans*-palladium dichloride complexes **C1**-**C3** were tested as catalyst for silver-free regioselective decarboxylative Heck coupling of coumarin-3-carboxylic acids with styrene derivatives. Among the three *trans*-palladium dichloride complexes, **C2** was found to be the most suitable to achieve high yields of coupled product in less time, mild reaction conditions, broad substrate scope, large functional group tolerance with only 2.5 mol % catalyst loading. Importantly, the reaction works under silver-free conditions which reduces the overall cost of protocol. The protocols also worked well for decarboxylative direct arylation and decarboxylative Suzuki-Miyaura coupling reactions with

moderate yields. The tentative mechanism of reaction was also proposed with the help of experimental and computational studies, which shows a classical Heck-type mechanism of the reaction after decarboxylation step.

4.4B.4 EXPERIMENTAL SECTION

4.4B.4.1 General Information

The ligand precursors, ligands and molecular rotor complexes were synthesized using standard Schlenk line techniques. The decarboxylative heck coupling reaction was carried out using pressure tubes under open air conditions. HPLC grade solvents like DMSO, DMF, DMA, MeOH, CH_2Cl_2, EtOH, Hexane, EtOAc, CH_3CN, HFIP, toluene, and xylene were used directly without further purification. Benzyl bromide (Spectrochem), 1-naphthaldehyde (Sigma Aldrich), 3,5-di-*tert*-butyl-2-hydroxybenzaldehyde (Sigma Aldrich), $NaBH_4$ (Spectrochem), $SOCl_2$ (Spectrochem), selenium powder (Sigma Aldrich), K_2CO_3 (Spectrochem), Ag_2CO_3 (Sigma Aldrich), NaOAc (Sigma Aldrich), CsOAc (Sigma Aldrich), AgOAc (Sigma Aldrich), Ag_2O (Sigma Aldrich), $K_2S_2O_8$ (Sigma Aldrich), IBD (Sigma Aldrich), Cs_2CO_3 (Sigma Aldrich), $PdCl_2$ (Alfa Aesar, 99.9%), and Na_2SO_4 (Spectrochem) were used as purchased. All other reagents for catalysis reaction were purchased from local commercial sources and used as it is. ^1H and $^{13}C\{^1H\}$ NMR spectra of all compounds were recorded on a Bruker NMRs 400 MHz instruments at ambient probe temperatures and referenced as follows (δ, ppm): ^1H, residual internal $CHCl_3$ (7.26); $^{13}C\{^1H\}$, internal $CDCl_3$ (77.00). The variable temperature NMRs were recorded in DMSO-d_6. IR spectrums of new ligand and complex were taken on a Nicolet Protége 460 FT-IR spectrometer on KBr pellets. Melting points of new complexes were recorded in an open capillary. HRMS measurements were carried out by electrospray ionization (ESI) method on an Agilent Q-TOF LCMS spectrometer. The absorption spectrums were measured on a JASCO, V-650 UV-Visible spectrophotometer. Elemental analyses were carried out with a Perkin–Elmer 2400 Series-II C, H, N analyzer.

4.4B.4.2 Synthesis of Ligand Precursor 2-(benzyloxy)-3,5-di-*tert*-butylbenzaldehyde (A). A 100 mL round bottom flask was charged with 3,5-di-*tert*-butyl-2-hydroxybenzaldehyde (1.172 g, 5.00 mmol), benzyl bromide (0.855 g, 5.00 mmol), K_2CO_3 (0.760 g, 5.50 mmol), and DMF (20 mL). The mixture was fitted with condenser at 90 °C and stirred overnight. The resulting mixture was then cooled to room temperature and extracted with ethyl acetate (20 mL × 3). The solvent of extract was removed using rotary evaporator to give ligand precursor **A** as colorless liquid (1.074,

3.31 mmol, 66%).

NMR ($CDCl_3$, δ/ppm): **^{1}H** (400 MHz) 10.38 (s, 1H), 7.79 (d, *J* = 2.6 Hz, 1H), 7.70 (d, *J* = 2.6 Hz, 1H), 7.53 (d, *J* = 7.2 Hz, 2H), 7.48 – 7.43 (m, 2H), 7.42 – 7.39 (m, 1H), 5.08 (s, 2H), 1.49 (s, 9H), 1.38 (s, 9H); **^{13}C{^{1}H}** (100 MHz) 190.8, 159.7, 146.7, 143.1, 136.6, 131.0, 129.4, 128.7, 128.2, 127.0, 124.1, 80.4, 35.4, 34.8, 31.3, 31.0 .

4.4B.4.3 Synthesis of Ligand Precursor (2-(benzyloxy)-3,5-di-*tert*-butylphenyl)methanol. A 100 mL round bottom flask was charged with ligand precursor **A** (0.649 g, 2.00 mmol) in 20 mL MeOH. Solid $NaBH_4$ (0.113 g, 3.00 mmol) was added slowly in portions to the reaction mixture by stirring at the room temperature. The progress of reaction was monitored by TLC until the maximum conversion of desired product occurred then the solvent was extracted from the reaction mixture by using a rotatory evaporator. The residue was then extracted using chloroform (2 * 25 mL). The solvent of extract was removed using rotary evaporator to give ligand precursor (2-(benzyloxy)-3,5-di-*tert*-butylphenyl)methanol as colorless liquid (0.572 g, 1.75 mmol, 87%).

NMR ($CDCl_3$, δ/ppm): **^{1}H** (400 MHz) 7.54 (d, *J* = 7.5 Hz, 2H), 7.45 (t, *J* = 7.4 Hz, 2H), 7.41 – 7.37 (m, 2H), 7.35 (d, *J* = 2.5 Hz, 1H), 5.03 (s, 2H), 4.81 (s, 2H), 1.47 (s, 9H), 1.37 (s, 9H); **^{13}C{^{1}H}** (100 MHz) 153.9, 146.4, 142.2, 137.7, 133.8, 128.6, 127.7, 126.9, 124.9, 124.3, 75.9, 61.8, 35.5, 34.6, 31.5, 31.3.

4.4B.4.4 Synthesis of Ligand Precursor 2-(benzyloxy)-1,5-di-*tert*-butyl-3-(chloromethyl)benzene (B). A 100 mL round bottom flask was charged with ligand precursor (2-(benzyloxy)-3,5-di-*tert*-butylphenyl)methanol (0.572 g, 1.75 mmol) in 15 mL dry dichloromethane. The mixture was placed in an ice bath and freshly distilled $SOCl_2$ (0.238 g, 2.00 mmol) was added drop wise to the reaction mixture by stirring. After complete addition of $SOCl_2$, the ice bath was removed, and mixture was allowed to stir at room temperature. The progress of reaction was monitored by TLC until the maximum conversion of desired product occurred then the reaction was neutralized using $NaHCO_3$. The solvent was extracted from the reaction mixture by using a rotatory evaporator. The residue was then extracted using chloroform (2×25 mL). The solvent of extract was removed using rotary evaporator to give ligand precursor **B** as yellow liquid (0.517 g, 1.50 mmol, 85%).

NMR ($CDCl_3$, δ/ppm): **^{1}H** (400 MHz) 7.59 (d, *J* = 7.4 Hz, 2H), 7.47 (t, *J* = 7.4 Hz, 2H), 7.43 (d, *J* = 2.5 Hz, 1H), 7.41 – 7.39 (m, 2H), 5.13 (s, 2H), 4.72 (s, 2H), 1.49 (s, 9H), 1.38 (s, 9H); **^{13}C{^{1}H}** (100 MHz) 154.2, 146.6, 142.5, 137.7, 130.7, 128.6, 127.8, 126.8, 125.3, 76.1, 42.3, 35.6, 34.6, 31.5, 31.3.

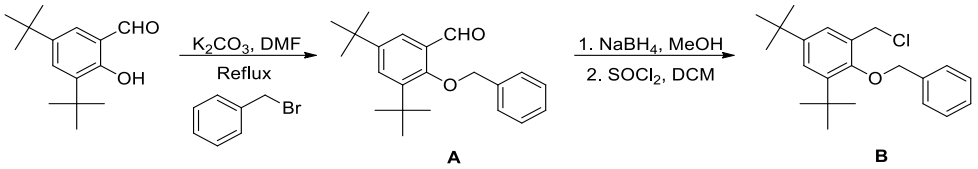

Scheme 4.4B.18: Synthesis of ligand precursors **A** and **B**.

4.4B.4.5 Synthesis of Dibenzylselane (L1). The ligand was synthesized by a modified procedure reported earlier.[8] Selenium powder (0.158 g, 2.00 mmol) and ethanol (30 ml) was added to a two necked round bottom flask fitted with condenser under N_2 atmosphere. In the mixture $NaBH_4$ (0.159 g, 4.2 mmol) was added in small portions and allowed to stir till the mixture became colorless. An ethanolic solution of benzyl chloride (**1**, 0.506 g, 4.00 mmol) was added dropwise to the reaction mixture and the mixture was allowed to stir at reflux for 8 h under N_2 atmosphere. The mixture was then cooled to room temperature and solvent was reduced (~2.5 mL) by using rotary evaporator. The residue was purified by using silica column (3 × 14 cm) with hexanes/EtOAc (95:05 *v/v*) as eluent. The solvent was evaporated from the product containing fractions (assayed by TLC) by rotary evaporation to give **L1** as brown solid (0.371 g, 1.421 mmol, 72%). The ^{1}H NMR data of **L1** were in agreement with literature reported data.[8]

NMR ($CDCl_3$, δ/ppm): **^{1}H** (400 MHz) δ 7.38 – 7.22 (m, 5H, Ph ring), 3.77 (s, 2H, SeCH_2).

4.4B.4.6 Synthesis of Bis(naphthalen-1-ylmethyl)selane (L2). Synthesis of **L2** was achieved by the reaction of selenium powder (0.158 g, 2.00 mmol and 2-(chloromethyl)naphthalene (**2**, 0.707 g, 4.00 mmol) in the presence of $NaBH_4$ (0.159 g, 4.2 mmol), in ethanol (30 mL) using same procedure as for **L1**. Purification of crude mixture gave **L2** as brown solid (0.478 g, 1.32 mmol, 66%). m.p: 90-92 °C; Anal. Calcd for $C_{22}H_{18}Se$ (361.338): C, 73.13; H, 5.02. Found: C, 73.02; H, 4.97.

NMR ($CDCl_3$, δ/ppm): **^{1}H** (400 MHz) 7.89 (d, *J* = 6.8 Hz, 1H), 7.85 (d, *J* = 6.8 Hz, 1H), 7.76 (d, *J* = 6.0 Hz 1H), 7.48-7.35 (m, 3H), 4.24 (s, 2H, SeCH_2); **^{13}C{^{1}H}** (100 MHz) 134.5, 134.0, 131.3, 128.7, 127.8, 126.9, 125.9, 125.8, 125.1, 124.0, 25.9 (s, Se*C*H_2); **IR** (cm^{-1}, powder film): 3001, 1701, 1261, 1068, 794, 783, 578, 524; HRMS (ESI) calcd for $C_{22}H_{18}SeNa$ $[M + Na]^+$ 385.0471; Found 385.0477.

4.4B.4.7 Synthesis of Bis(2-(benzyloxy)-3,5-di-*tert*-butylbenzyl)selane (L3): Synthesis of **L3** was achieved by the reaction of selenium powder (0.059 g, 0.75 mmol), 2-(benzyloxy)-1,5-di-*tert*-butyl-3-(chloro methyl)benzene (**3**, 0.517 g, 1.50 mmol) and $NaBH_4$ (0.064 g, 1.7 mmol) using same procedure as for **L1**. Purification of crude mixture gave **L3** as yellow solid (0.642 g, 0.92

mmol, 61%); m.p: 96-99 °C. Anal. Calcd for $C_{44}H_{58}O_2Se$ (697.8901): C, 75.72; H, 8.38. Found: C, 75.76; H, 8.29.

NMR ($CDCl_3$, δ/ppm): **^{1}H** (400 MHz) 7.50 (d, *J* = 7.0 Hz, 2H), 7.43 – 7.38 (m, 2H), 7.37 – 7.33 (m, 1H), 7.30 (d, *J* = 2.5 Hz, 1H), 7.26 (d, *J* = 2.5 Hz, 1H), 5.10 (s, 2H), 3.95 (s, 2H, SeC*H*$_2$), 1.46 (s, 9H), 1.33 (s, 9H); **^{13}C{^{1}H}** (100 MHz) 154.0, 146.5, 142.2, 138.1, 131.8, 128.5, 127.5, 126.8, 126.6, 123.3, 75.1, 35.5, 34.5, 31.5, 31.3, 24.1; **IR** (cm^{-1}, powder film): 2962, 1438, 1361, 1219, 1203, 996, 883, 795, 694; HRMS (ESI) calcd for $C_{44}H_{59}O_2Se$ $[M + H]^+$ 699.3675; Found 699.3571.

4.4B.4.8 Palladium Complex of Dibenzylselane (C1). A round bottom flask was charged with **L1** (0.131 g, 0.50 mmol) and $Pd(CH_3CN)_2Cl_2$ (0.065 g, 0.25 mmol) in acetonitrile (10 mL) and refluxed for 4 h. The mixture was then cooled to room temperature and passed through a short pad of silica gel (15 cm). The solvent was removed by rotary evaporation and residue was washed with cold hexane to give **C1** as a yellow solid (0.101 g, 0.144 mmol, 57%); m.p: 186-188 ˚C; Anal. Calcd for $C_{28}H_{28}Cl_2PdSe_2$ (699.7679): C, 48.06; H, 4.03. Found: C, 48.11; H, 4.08.

NMR ($CDCl_3$, δ/ppm): **^{1}H** (400 MHz) 7.44 – 7.23 (m, 10H), 4.51 (d, *J* = 11.3 Hz, 2H, SeC*H*$_2$), 3.95 (d, *J* = 11.3 Hz, 2H, SeC*H*$_2$); **^{13}C{^{1}H}** (100 MHz) 134.8, 129.9, 129.0, 128.1, 35.1; **IR** (cm^{-1}, powder film): 1492, 1197, 1028, 754; HRMS (ESI) calcd for $C_{28}H_{29}Cl_2PdSe_2$ $[M + H]^+$ 700.9006; Found 700.8973.

4.4B.4.9 Palladium Complex of Bis(naphthalen-1-ylmethyl)selane (C2). The complex **C2** was synthesized by the reaction of **L2** (0.181 g, 0.50 mmol), $Pd(CH_3CN)_2Cl_2$ (0.065 g, 0.25 mmol), and acetonitrile (10 mL) using same procedure as for **C1**. An identical workup gave **C2** as yellow solid (0.145 g, 0.161 mmol, 64%); m.p: 170-172 °C; Anal. Calcd for $C_{44}H_{36}Cl_2PdSe_2$ (900.0026): C, 58.72; H, 4.03. Found: C, 58.83; H, 4.12.

NMR ($CDCl_3$, δ/ppm): **^{1}H** (400 MHz) 7.85 (dd, *J* = 20 Hz, 2H), 7.63 (d, *J* = 10 Hz, 2H), 7.54 (m, 3H), 7.45 (m, 2H), 7.38 (td, *J* = 20 Hz, 2H), 7.30 (m, 3H), 5.21 (d, *J* = 10 Hz, 2H, SeC*H*$_2$), 4.38 (d, *J* = 10 Hz, 2H, SeC*H*$_2$); **^{13}C{^{1}H}** (100 MHz) 134.0, 131.3, 130.3, 129.2, 129.0, 128.8, 126.7, 126.2, 125.3, 123.6, 33.4; **IR** (cm^{-1}, powder film): 3005, 1693, 1508, 1396, 1176, 1014, 875, 574; HRMS (ESI) calcd for $C_{44}H_{36}Cl_2PdSe_2Na$ $[M + Na]^+$ 922.9452; Found 922.9579.

4.4B.4.10 Palladium Complex of Bis(2-(benzyloxy)-3,5-di-*tert*-butylbenzyl)selane (C3). The complex **C3** was synthesized by the reaction of **L3** (0.349 g, 0.50 mmol), $Pd(CH_3CN)_2Cl_2$ (0.065 g, 0.25 mmol), and acetonitrile (10 mL) using same procedure as for **C1**. An identical workup gave **C3** as yellow solid (0.248 g, 0.158 mmol, 63%). m.p: 198-200 °C. Anal. Calcd for

$C_{88}H_{116}Cl_2O_4PdSe_2$ (1573.1062): C, 67.19; H, 7.43. Found: C, 67.12; H, 7.38.

NMR ($CDCl_3$, δ/ppm): **^{1}H** (400 MHz) 7.44 (d, *J* = 7.2 Hz, 2H), 7.36 (d, *J* = 2.0 Hz, 1H), 7.33 – 7.30 (m, 2H), 7.27 – 7.22 (m, 2H), 4.94 (d, *J* = 11.4 Hz, 1H), 4.77 (d, *J* = 11.5 Hz, 1H), 4.55 (d, *J* = 12.2 Hz, 1H), 4.24 (d, *J* = 12.1 Hz, 1H), 1.31 (s, 9H), 1.23 (s, 9H); **^{13}C{^{1}H}** (100 MHz) 154.3, 146.4, 142.4, 137.2, 128.3, 128.3, 127.5, 127.4, 124.6, 76.7, 35.3, 34.5, 31.5, 31.0; **IR** (cm^{-1}, powder film): 3263, 1651, 1049, 922, 825, 763; HRMS (ESI) calcd for $C_{44}H_{59}O_2Se$ [M + H – $PdCl_2$]$^+$: 699.3680; Found: 699.3571.

4.4B.4.11 Procedure for Decarboxylative Heck Coupling of Coumarins. A pressure tube was charged with coumarin-carboxylic acid **4** (1.0 mmol), styrene **5** (1.0 mmol), K_2CO_3 (1.0 mmol), **C2** (2.5 mol %), and DMF (3 mL). The reaction mixture was stirred at 110 °C and progress of reaction was monitored by TLC until the maximum conversion of desired product is achieved. After 10 h the reaction mixture was cooled to room temperature and diluted with ice cold water and EtOAc (15 mL). The organic layer was extracted and dried over anhydrous Na_2SO_4. The solvent of filtrate was concentrated using rotary evaporator and residue was purified by chromatography on silica-gel (hexane/EtOAc gradient, 5-10%) to afford coupled products **11aa-11da.**

4.4B.4.12 General Procedure for Decarboxylative Suzuki-Miyaura Coupling and C-H Activation Reactions: A pressure tube was charged with coumarin-3-carboxylic acid (1 equiv.), phenylboronic acid derivatives (1 equiv.) or bromobenzene derivatives (1 equiv.), Cs_2CO_3 (1 equiv.), C2 (2.5 mol %), and DMF (3 mL). The mixture was stirred at 110 °C for 10 h. The reaction mixture was then cooled to room temperature, quenched with water (5 mL) and diluted with EtOAc (15 mL). The layers were separated, and the aqueous layer was extracted with (3 x 10 mL) of EtOAc. The organic layer was dried over Na_2SO_4, filtered, and concentrated on reduced pressure. The residue was purified by chromatography on silica-gel (hexane/EtOAc gradient, 5-10%) to afford coupled products **11a**-**11d**.

4.4B.4.13 Deuterium Exchange Experiment.

A pressure tube was charged with coumarin-3-carboxylic acid (1 equiv.), D_2O (25 equiv.), Cs_2CO_3 (1 equiv.), and DMF (3 mL). The mixture was stirred at 110 °C for 10 h. The reaction mixture was then cooled to room temperature, quenched with water (5 mL) and diluted with EtOAc (15 mL). The layers were separated, and the aqueous layer was extracted with (3 x 10 mL) of EtOAc. The organic layer was dried over Na_2SO_4, filtered, and concentrated on reduced pressure. The residue was purified by washing with cold pentane and ether. The dry product was than analyzed with ^{1}H

NMR spectroscopy.

(*E*)-3-Styryl-2*H*-chromen-2-one (11aa). Purification by column chromatography on silica gel (eluent: EtOAc/hexanes, 3:7 *v/v*); Pale yellow solid; 38 mg (58%); mp = 164-166 °C; ^{1}H NMR (400 MHz, $CDCl_3$) δ 7.84 (s, 1H), 7.68 – 7.49 (m, 5H), 7.43 – 7.30 (m, 5H), 7.17 (d, *J* = 16.3 Hz, 1H); $^{13}C\{^{1}H\}$ NMR (100 MHz, $CDCl_3$) δ 160.4, 152.9, 136.8, 136.8, 133.7, 131.2, 128.8, 128.5, 127.6, 127.0, 125.0, 124.5, 122.1, 119.7, 116.5.

(*E*)-3-(4-Ethoxystyryl)-2*H*-chromen-2-one (11ab). Purification by column chromatography on silica gel (eluent: EtOAc/hexanes, 3:7 *v/v*); Yellow solid; 49 mg (64%); mp = 160-162 °C; ^{1}H NMR (400 MHz, $CDCl_3$) δ 7.78 (s, 1H), 7.60 – 7.47 (m, 5H), 7.37 – 7.26 (m, 2H), 7.04 (d, *J* = 16.3 Hz, 1H), 6.93 (d, 2H), 4.09 (q, *J* = 7.0 Hz, 2H), 1.45 (t, *J* = 7.0 Hz, 3H); $^{13}C\{^{1}H\}$ NMR (100 MHz, $CDCl_3$) δ 160.6, 159.4, 152.7, 135.7, 133.3, 130.8, 129.5, 128.4, 127.5, 125.4, 124.5, 119.9, 119.7, 116.4, 114.8, 63.5, 14.8.

(*E*)-3-(4-(Tert-Butyl)styryl)-2*H*-chromen-2-one (11ac). Purification by column chromatography on silica gel (eluent: EtOAc/hexanes, 3:7 *v/v*); Yellow solid; 42 mg (53%); mp = 184-186 °C; ^{1}H NMR (400 MHz, $CDCl_3$) δ 7.82 (s, 1H), 7.61 (d, *J* = 16.3 Hz, 1H), 7.55 – 7.48 (m, 4H), 7.42 (d, *J* = 8.4 Hz, 2H), 7.36 (d, *J* = 8.3 Hz, 1H), 7.31 (dd, *J* = 7.5, 1.0 Hz, 1H), 7.14 (d, *J* = 16.4 Hz, 1H), 1.36 (s, 9H); $^{13}C\{^{1}H\}$ NMR (100 MHz, $CDCl_3$) δ 160.5, 152.8, 151.8, 136.3, 134.1, 133.5, 131.0, 127.6, 126.8, 125.7, 125.2, 124.5, 121.2, 119.8, 116.4, 34.7, 31.3.

(*E*)-3-(3-Methylstyryl)-2*H*-chromen-2-one (11ad). Purification by column chromatography on silica gel (eluent: EtOAc/hexanes, 3:7 *v/v*); Pale yellow solid; 44 mg (65%); mp = 132-134 °C; ^{1}H NMR (400 MHz, $CDCl_3$) δ 7.83 (s, 1H), 7.59 (d, *J* = 16.4 Hz, 1H), 7.56 – 7.49 (m, 2H), 7.41 (s, 1H), 7.37 (dd, *J* = 7.7, 5.1 Hz, 2H), 7.33 – 7.26 (m, 2H), 7.20 – 7.12 (m, 2H), 2.40 (s, 3H); $^{13}C\{^{1}H\}$ NMR (100 MHz, $CDCl_3$) δ 160.5, 152.9, 138.4, 136.8, 136.5, 133.8, 131.0, 129.3, 128.7, 127.6, 125.1, 124.5, 124.3, 121.8,

119.8, 116.4, 21.4.

(*E*)-3-(2,6-Dimethylstyryl)-2*H*-chromen-2-one (11ae). Purification by column chromatography on silica gel (eluent: EtOAc/hexanes, 3:7 *v/v*); Orange solid; 55 mg (76%); mp = 144-146 °C; ^{1}H NMR (400 MHz, $CDCl_3$) δ 7.88 – 7.80 (m, 2H), 7.57 – 7.45 (m, 3H), 7.39 – 7.28 (m, 2H), 7.13 – 7.03 (m, 3H), 2.44 (s, 3H), 2.37 (s, 3H); ^{13}C{^{1}H} NMR (100 MHz, $CDCl_3$) δ 136.6, 135.6, 135.6, 133.4, 131.6, 131.0, 130.5, 129.2, 127.6, 126.1, 125.4, 124.5, 122.9, 119.8, 116.4, 21.0, 19.4.

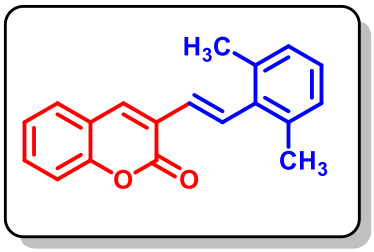

(*E*)-3-(2,4,5-Trimethylstyryl)-2*H*-chromen-2-one (11af). Purification by column chromatography on silica gel (eluent: EtOAc/hexanes, 3:7 *v/v*); Yellow solid; 60 mg (79%); mp = 120-122 °C; ^{1}H NMR (400 MHz, $CDCl_3$) *δ* 7.77 (s, 1H), 7.65 (d, *J* = 16.6 Hz, 1H), 7.57 – 7.49 (m, 2H), 7.37 (d, *J* = 8.2 Hz, 1H), 7.31 (td, *J* = 7.6, 1.1 Hz, 1H), 6.93 (s, 2H), 6.67 (d, *J* = 16.6 Hz, 1H), 2.39 (s, 6H), 2.32 (s, 3H); ^{13}C{^{1}H} NMR (100 MHz, $CDCl_3$) δ 160.4, 152.9, 136.9, 136.5, 136.2, 133.5, 132.5, 131.0, 128.9, 127.6, 127.2, 125.3, 124.5, 119.7, 116.4, 21.1, 21.0.

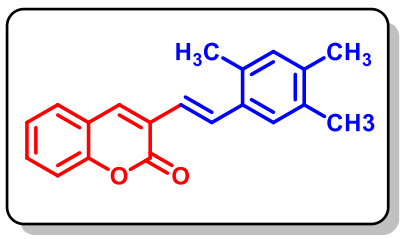

(*E*)-3-(4-Fluorostyryl)-2*H*-chromen-2-one (11ag). Purification by column chromatography on silica gel (eluent: EtOAc/hexanes, 3:7 *v/v*); Pale yellow solid; 41 mg (59%); mp = 185-187 °C; ^{1}H NMR (400 MHz, $CDCl_3$) δ 7.81 (s, 1H), 7.61 (d, *J* = 16.3 Hz, 1H), 7.57 – 7.50 (m, 4H), 7.36 (d, *J* = 8.1 Hz, 1H), 7.31 (td, *J* = 7.5, 1.1 Hz, 1H), 7.12 – 7.03 (m, 3H); ^{13}C{^{1}H} NMR (100 MHz, $CDCl_3$) δ 164.1, 161.6, 160.3, 152.8, 136.9, 133.1, 133.06, 132.5, 131.2, 128.6, 128.5, 124.8, 124.6, 121.9, 121.9, 119.7, 116.5, 115.9, 115.7; HRMS (ESI) *m/z*: $[M+H]^+$ Calcd for $C_{17}H_{12}FO_2$ 267.0816, Found 267.0813.

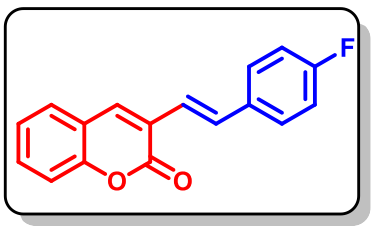

(*E*)-3-(4-Chlorostyryl)-2*H*-chromen-2-one (11ah). Purification by column chromatography on silica gel (eluent: EtOAc/hexanes, 3:7 *v/v*); Pale yellow solid; 53 mg (71%); mp = 159-161 °C; ^{1}H NMR (400 MHz, $CDCl_3$) δ 7.82 (s, 1H), 7.61 (d, *J* = 16.3 Hz, 1H), 7.56 – 7.46 (m, 4H), 7.40 – 7.27 (m, 4H), 7.11 (d, *J* = 16.3 Hz, 1H); ^{13}C{^{1}H} NMR (100 MHz, $CDCl_3$) δ 160.3, 152.9, 137.3, 135.4, 134.1, 132.4, 131.3,

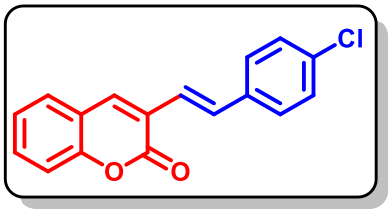

129.0, 128.1, 127.7, 124.7, 124.6, 122.7, 119.6, 116.5; HRMS (ESI) *m/z*: $[M+H]^+$ Calcd for $C_{17}H_{12}ClO_2$ 283.0520, Found 283.0516.

(*E*)-3-(4-Bromostyryl)-2*H*-chromen-2-one (11ai). Purification by column chromatography on silica gel (eluent: EtOAc/hexanes, 3:7 *v/v*); Yellow solid; 55 mg (64%); mp = 204-206 °C; ^{1}H NMR (400 MHz, $CDCl_3$) δ 7.83 (s, 1H), 7.60 (d, *J* = 16.3 Hz, 1H), 7.53 (dd, *J* = 10.3, 8.2 Hz, 4H), 7.43 (d, *J* = 8.4 Hz, 2H), 7.36 (d, *J* = 8.3 Hz, 1H), 7.31 (t, *J* = 7.5 Hz, 1H), 7.13 (d, *J* = 16.3 Hz, 1H); ^{13}C{^{1}H} NMR (100 MHz, $CDCl_3$) δ 160.2, 152.9, 137.4, 135.8, 132.5, 131.9, 131.3, 128.4, 127.7, 124.7, 124.6, 122.8, 122.4, 119.6, 116.5.

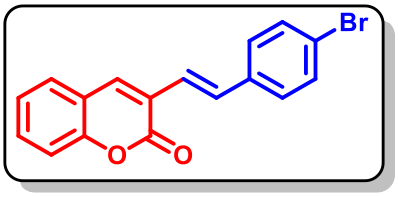

(*E*)-4-(2-(2-Oxo-2*H*-chromen-3-yl)vinyl)benzonitrile (11aj). Purification by column chromatography on silica gel (eluent: EtOAc/hexanes, 3:7 *v/v*); White solid; 55 mg (76%); mp = 179-181 °C; ^{1}H NMR (400 MHz, $CDCl_3$) δ 7.74 (s, 1H), 7.66 (d, *J* = 16.3 Hz, 1H), 7.58 (d, *J* = 7.3 Hz, 2H), 7.52 (d, *J* = 2.4 Hz, 1H), 7.46 (dd, *J* = 8.8, 2.4 Hz, 1H), 7.41 (t, *J* = 7.4 Hz, 2H), 7.35 (dt, *J* = 8.5, 1.8 Hz, 1H), 7.30 (d, *J* = 8.8 Hz, 1H), 7.14 (d, *J* = 16.4 Hz, 1H); ^{13}C{^{1}H} NMR (100 MHz, $CDCl_3$) δ 159.8, 151.8, 136.6, 135.2, 134.7, 130.9, 129.8, 128.8, 128.76, 127.1, 126.7, 126.1, 121.6, 120.8, 117.8.

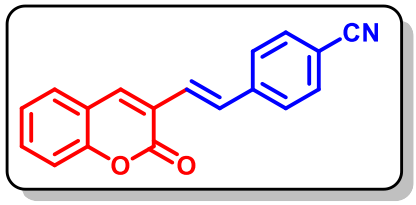

(*E*)-3-(4-(Trifluoromethyl)styryl)-2*H*-chromen-2-one (11ak). Purification by column chromatography on silica gel (eluent: EtOAc/hexanes, 3:7 *v/v*); Yellow solid; 43 mg (52%); mp = 199-201°C; ^{1}H NMR (400 MHz, $CDCl_3$) δ 7.87 (s, 1H), 7.71 (d, *J* = 16.3 Hz, 1H), 7.68 – 7.63 (m, 4H), 7.58 – 7.53 (m, 2H), 7.40 – 7.36 (m, 1H), 7.36 – 7.31 (m, 1H), 7.22 (d, *J* = 16.3 Hz, 1H); ^{13}C{^{1}H} NMR (100 MHz, $CDCl_3$) δ 160.1, 153.0, 140.3, 138.3, 132.2, 131.6, 127.8, 127.1, 125.7 (q, *J* = 3.8 Hz), 124.7, 124.7, 124.3, 119.5, 116.5.

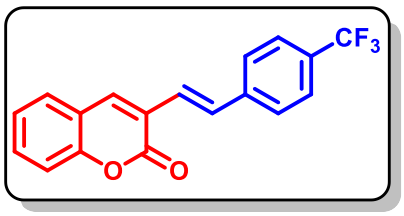

(*E*)-3-(4-Nitrostyryl)-2*H*-chromen-2-one (11al). Purification by column chromatography on silica gel (eluent: EtOAc/hexanes, 3:7 *v/v*); Yellow solid; 32 mg (41%); mp = 197-199 °C; ^{1}H NMR (400 MHz, $CDCl_3$) *δ* 8.25 (d, *J* = 8.8 Hz, 2H), 7.90 (s, 1H), 7.78 (d, *J* = 16.3 Hz, 1H), 7.70 (d, *J* = 8.7 Hz, 2H), 7.61 – 7.54 (m, 2H), 7.41 – 7.31

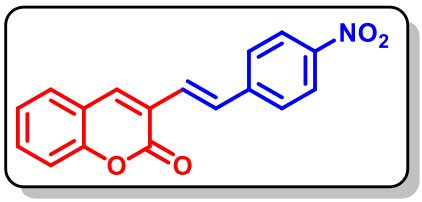

(m, 2H), 7.24 (s, 1H); $^{13}C\{^{1}H\}$ NMR (100 MHz, $CDCl_3$) δ 159.9, 153.1, 143.3, 139.4, 132.0, 131.4, 128.0, 127.4, 126.7, 124.8, 124.4, 124.2, 123.9, 119.4, 116.6.

(*E*)-3-(3-Chlorostyryl)-2*H*-chromen-2-one (11am). Purification by column chromatography on silica gel (eluent: EtOAc/hexanes, 3:7 *v/v*); Pale yellow solid; 45 mg (60%); mp = 166-168 °C; ^{1}H NMR (400 MHz, $CDCl_3$) δ 7.83 (s, 1H), 7.61 (d, *J* = 16.3 Hz, 1H), 7.57 – 7.50 (m, 3H), 7.43 (dt, *J* = 7.3, 1.2 Hz, 1H), 7.39 – 7.31 (m, 2H), 7.31 – 7.26 (m, 2H), 7.13 (d, *J* = 16.3 Hz, 1H); $^{13}C\{^{1}H\}$ NMR (100 MHz, $CDCl_3$) δ 160.1, 153.0, 138.8, 137.8, 134.8, 132.3, 131.4, 130.0, 128.3, 127.8, 126.7, 125.2, 124.6, 124.5, 123.6, 119.6, 116.5.

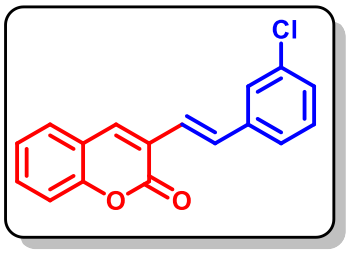

(*E*)-3-(3-Bromostyryl)-2*H*-chromen-2-one (11an). Purification by column chromatography on silica gel (eluent: EtOAc/hexanes, 3:7 *v/v*); Yellow solid; 49 mg (57%); mp = 172-174 °C; ^{1}H NMR (400 MHz, $CDCl_3$) δ 7.82 (s, 1H), 7.71 (s, 1H), 7.63 – 7.49 (m, 3H), 7.49 – 7.40 (m, 2H), 7.39 – 7.22 (m, 3H), 7.11 (d, *J* = 16.3 Hz, 1H); $^{13}C\{^{1}H\}$ NMR (100 MHz, $CDCl_3$) δ 160.2, 152.9, 139.0, 137.8, 132.2, 131.5, 131.2, 130.3, 129.6, 127.8, 125.7, 124.6, 124.5, 123.6, 123.0, 119.6, 116.5.

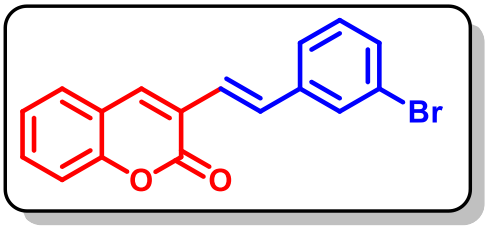

(*E*)-3-(2-(Perfluorophenyl)vinyl)-2*H*-chromen-2-one (11ao). Purification by column chromatography on silica gel (eluent: EtOAc/hexanes, 3:7 *v/v*); Pale yellow solid; 49 mg (55%); mp = 205-208 °C; ^{1}H NMR (400 MHz, $CDCl_3$) δ 7.86 (s, 1H), 7.68 (d, *J* = 16.7 Hz, 1H), 7.60 – 7.55 (m, 2H), 7.44 – 7.37 (m, 2H), 7.34 (td, *J* = 7.7, 1.0 Hz, 1H); $^{13}C\{^{1}H\}$ NMR (100 MHz, $CDCl_3$) δ 159.6, 153.2, 146.3, 143.8, 140.0, 136.5, 132.1, 130.8 (td, *J* = 8.7, 2.4 Hz), 129.1, 128.1, 124.8, 124.0, 119.3, 118.3, 118.3, 118.2, 116.6, 112.1.

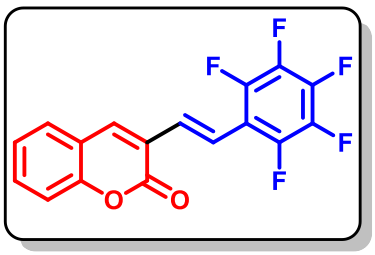

(*E*)-2-Styryl-3H-benzo[*f*]chromen-3-one (11ba). Purification by column chromatography on silica gel (eluent: EtOAc/hexanes, 3:7 *v/v*); White solid; 38 mg (62%); mp = 161-163 °C; ^{1}H NMR

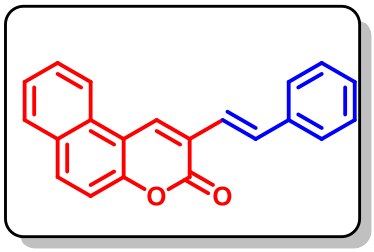

(400 MHz, $CDCl_3$) δ 8.53 (d, *J* = 9.8 Hz, 1H), 8.26 (d, *J* = 8.4 Hz, 1H), 8.02 (d, *J* = 9.0 Hz, 1H), 7.95 (d, *J* = 8.1 Hz, 1H), 7.82 – 7.68 (m, 3H), 7.61 (t, *J* = 7.3 Hz, 1H), 7.50 (d, *J* = 9.0 Hz, 1H), 7.45 (t, *J* = 7.1 Hz, 1H), 7.35 (t, *J* = 7.5 Hz, 1H), 7.20 (d, *J* = 2.0 Hz, 1H), 7.14 (dd, *J* = 8.8, 2.4 Hz, 1H), 6.62 (d, *J* = 9.7 Hz, 1H); ^{13}C{^{1}H} NMR (100 MHz, $CDCl_3$) δ 161.1, 153.9, 153.5, 139.2, 133.2, 130.3, 129.8, 129.0, 128.3, 127.8, 126.5, 126.7, 126.1, 123.5, 121.4, 117.8, 117.1, 115.7, 109.5.

(*E*)-6-Methoxy-3-styryl-2*H*-chromen-2-one (11ca). Purification by column chromatography on

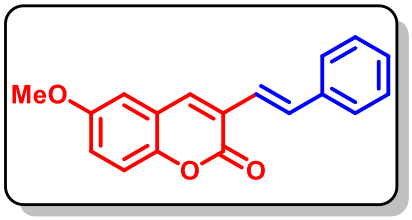

silica gel (eluent: EtOAc/hexanes, 3:7 *v/v*); Yellow solid; 51mg (81%); mp = 188-190 °C; ^{1}H NMR (400 MHz, $CDCl_3$) δ 7.79 (s, 1H), 7.68 – 7.53 (m, 3H), 7.40 (t, *J* = 7.4 Hz, 2H), 7.35 – 7.29 (m, 2H), 7.17 (d, *J* = 16.3 Hz, 1H), 7.10 (dd, *J* = 9.0, 2.7 Hz, 1H), 6.97 (d, *J* = 2.6 Hz, 1H), 3.89 (s, 3H); ^{13}C{^{1}H} NMR (100 MHz, $CDCl_3$) δ 160.5, 156.2, 147.4, 136.7, 136.6, 133.7, 128.8, 128.5, 127.0, 125.3, 122.1, 120.1, 118.9, 117.5, 109.7, 55.8.

(*E*)-6-Chloro-3-styryl-2*H*-chromen-2-one (11da). Purification by column chromatography on

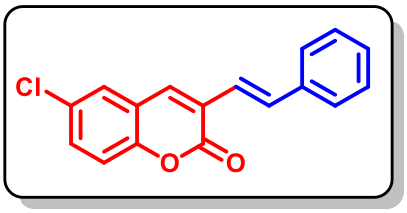

silica gel (eluent: EtOAc/hexanes, 3:7 *v/v*); Yellow solid; 46 mg (73%); mp = 148-150 °C; ^{1}H NMR (400 MHz, $CDCl_3$) δ 7.74 (s, 1H), 7.66 (d, *J* = 16.3 Hz, 1H), 7.58 (d, *J* = 7.3 Hz, 2H), 7.52 (d, *J* = 2.4 Hz, 1H), 7.49 – 7.38 (m, 3H), 7.37 – 7.29 (m, 2H), 7.14 (d, *J* = 16.4 Hz, 1H); ^{13}C{^{1}H} NMR (100 MHz, $CDCl_3$) δ 159.8, 151.2, 136.6, 135.2, 134.7, 130.9, 129.8, 128.8, 128.76, 127.1, 126.7, 126.1, 121.6, 120.8, 117.9.

Ethyl (*E*)-3-(2-oxo-2*H*-chromen-3-yl)acrylate (41). Purification by column chromatography on silica gel (eluent: EtOAc/hexanes, 3:7 *v/v*); White solid; 29 mg (45%); mp = 122-124 ˚C; ^{1}H NMR (400 MHz, $CDCl_3$) δ 7.90 (s, 1H), 7.64 – 7.54 (m, 3H), 7.41 – 7.31 (m, 2H), 7.12 (d, *J* = 15.9 Hz, 1H), 4.29 (q, *J* = 7.1 Hz, 2H), 1.36 (t, *J* = 7.1 Hz, 3H); ^{13}C{^{1}H} NMR (100 MHz, $CDCl_3$) δ 166.9, 159.1, 153.6, 143.4, 137.8, 132.9, 128.5, 124.8, 123.8, 122.5, 119.0, 116.7, 60.8, 14.3.

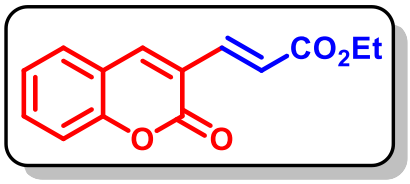

3-Phenyl-2H-chromen-2-one (9a). Purification by column chromatography on silica gel (eluent: EtOAc/hexanes, 3:7 *v/v*); White solid; 27 mg (47%); mp = 138-140 °C; ^{1}H NMR (400 MHz, $CDCl_3$) δ 7.85 (s, 1H), 7.73 (dd, *J* = 8.1, 1.4 Hz, 2H), 7.60 – 7.53 (m, 2H), 7.51 – 7.38 (m, 4H), 7.33 (td, *J* = 7.5, 1.0 Hz, 1H); ^{13}C{^{1}H} NMR (100 MHz, $CDCl_3$) δ 160.6, 153.6, 139.9, 134.7, 131.4, 128.9, 128.6, 128.5, 128.4, 127.9, 124.5, 119.7, 116.5.

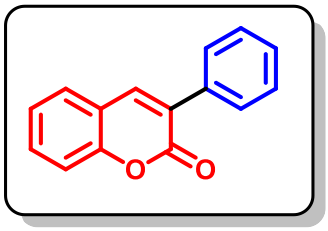

3-(4-Methoxyphenyl)-2*H*-chromen-2-one (9b). Purification by column chromatography on silica gel (eluent: EtOAc/hexanes, 3:7 *v/v*); Pale yellow solid; 34 mg (52%); mp = 140-142 °C; ^{1}H NMR (400 MHz, $CDCl_3$) δ 7.79 (s, 1H), 7.71 (d, *J* = 8.8 Hz, 2H), 7.58 – 7.50 (m, 2H), 7.38 (d, *J* = 8.2 Hz, 1H), 7.31 (t, *J* = 7.6 Hz, 1H), 7.00 (d, *J* = 8.8 Hz, 2H), 3.88 (s, 3H); ^{13}C{^{1}H} NMR (100 MHz, $CDCl_3$) δ 160.8, 160.2, 153.3, 138.5, 131.0, 129.9, 127.9, 127.7, 127.1, 124.4, 119.9, 116.4, 113.9, 55.4.

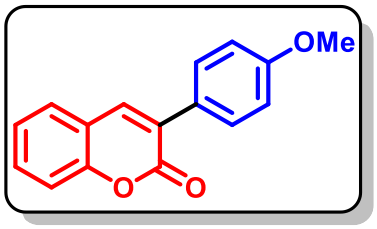

3-(4-Nitrophenyl)-2*H*-chromen-2-one (9c). Purification by column chromatography on silica gel (eluent: EtOAc/hexanes, 3:7 *v/v*); Yellow solid; 24 mg (34%); mp = 240-243 °C;^{1}H NMR (400 MHz, $CDCl_3$) δ 8.62 (s, 1H), 8.38 (d, *J* = 8.7 Hz, 1H), 8.33 (d, *J* = 8.8 Hz, 1H), 7.99 – 7.92 (m, 1H), 7.81 (d, *J* = 8.7 Hz, 1H), 7.66 – 7.57 (m, 2H), 7.45 – 7.33 (m, 2H); ^{13}C{^{1}H} NMR (100 MHz, $CDCl_3$) δ 160.1, 153.4, 143.7, 132.6, 132.4, 129.5, 128.9, 124.8, 124., 123.7, 120.1, 119.1, 116.4.

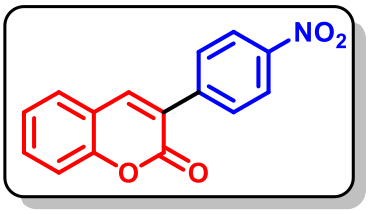

3-(2-Nitrophenyl)-2H-chromen-2-one (9d). Purification by column chromatography on silica gel (eluent: EtOAc/hexanes, 3:7 *v/v*); White solid; 23 mg (33%); mp = 156-158 °C; ^{1}H NMR (400 MHz, $CDCl_3$) δ 8.63 (s, 1H), 7.70 – 7.54 (m, 4H), 7.44 – 7.32 (m, 4H); ^{13}C{^{1}H} NMR (100 MHz, $CDCl_3$) δ 147.0, 138.8, 136.8, 135.4, 129.6, 127.1, 126.7, 124.3, 123.7, 123.0, 121.9, 120.1, 111.5, 108.6.

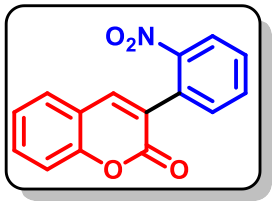

(*E*)-3-(2-(4'-methoxy-[1,1'-biphenyl]-4-yl)vinyl)-2*H*-chromen-2-one (42). Purification by column chromatography on silica gel (eluent: EtOAc/hexanes, 3:7 *v/v*); Yellow solid; 26 mg (48%); mp = 240-243 °C; ^{1}H NMR (400 MHz, $CDCl_3$) δ 7.85 (s, 1H), 7.70 – 7.57 (m, 7H), 7.57 – 7.50 (m, 2H), 7.37 (d, *J* = 8.1 Hz, 1H), 7.32 (t, *J* = 7.6 Hz, 1H), 7.20 (d, *J* = 16.3 Hz, 1H), 7.01 (d, *J* = 8.7 Hz, 2H), 3.89 (s, 3H); ^{13}C{^{1}H} NMR (100 MHz, $CDCl_3$) δ 152.8, 140.8, 136.6, 135.3, 133.3, 131.1, 128.0, 127.6, 127.5, 126.9, 125.1, 124.6, 121.7, 116.5, 114.3, 55.4.

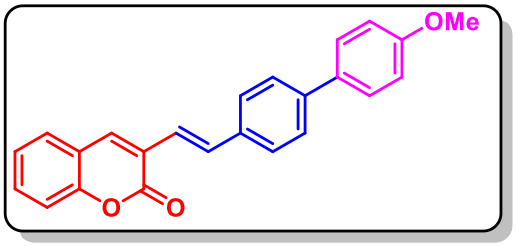

4.4B.4.14 Sample Preparation & Crystal Measurement of C2.

A CH_3CN solution of **C2** (4 mL) was slowly concentrated over a period of 17 days to afford suitable colorless needle like crystals. The data was collected and reported in **Table 4.4B.4.** Cell parameters were obtained from 45 data frames using a 1° scan and refined with 33403 reflections. APEX3 was used to collect the integrated intensity information of each reflection by reducing the data frames.[s1] Lorentz and polarization corrections were applied. The absorption correction program SADABS[s2] was employed to correct the data for absorption effects. The space group was determined from systematic reflection conditions and statistical tests. The structure was refined (weighted least squares refinement on F^2) to convergence.[s3] Olex2[s4] was employed for the final data presentation and structure plots. Non-hydrogen atoms were refined with anisotropic thermal parameters. Hydrogen atoms were fixed in idealized positions using a riding model. The absence of additional symmetry or voids was confirmed using PLATON (ADDSYM).[s5] Molecule possess an inversion symmetry and symmetry generated atoms are not labeled in **Figure 4.4B.11**. Elongated thermal ellipsoid on Cl1 along with nearby residual electron density peak suggested disorder which was modeled between two positions with an occupancy ratio of 0.74:0.26. Appropriate restraints and constraints were added to keep the bond distances, and thermal ellipsoids meaningful.

Table 4.4B.4. Crystal Data for **C2**.

Identification Code	**C2**
Empirical formula	$C_{44}H_{36}Cl_2PdSe_2$
Formula weight	899.95
Temperature [K]	110.0

Diffractometer	BRUKER Venture
Wavelength [Å]	1.54178
Crystal system	Monoclinic
Space group	P 121/n 1
Unit cell dimensions:	
a [Å]	5.3522 (3)
b [Å]	17.6203 (10)
c [Å]	19.1005 (11)
α [°]	90
β [°]	97.9290 (10)
γ [°]	90
V [Å^3]	1784.10(18)
Z	2
ρ_{calc} [Mg/m^3]	1.675
μ [mm^{-1}]	8.145
F (000)	896
Crystal size [mm^3]	0.204× 0.019 × 0.016
Θ limit [°]	3.428 to 70.205
Index range (*h*, *k*, *l*)	–6, 5, –21, 21, –23, 23
Reflections collected	33403
Independent reflections	3396
R(int)	0.0279
Completeness to θ	99.8
Max. and min. transmission	0.4684 and 0.2912
Data/restraints/parameters	3396/1/227
Goodness-of-fit on F^2	1.076
R indices (final)[$I>2\sigma(I)$]	
R_1	0.0193
wR_1	0.0531
R indices (all data)	
R_1	0.0200
wR_2	0.0540
Largest diff. peak and hole [eÅ^{-3}]	0.520 and –0.506

4.4B.5 RFERENCES

1. Jia, C.; Zhang, J.; Yu, L.; Wang, C.; Yang, Y.; Rong, X.; Xu, K.; Chu, M., *Frontiers in Cellular and Infection Microbiology* **2019**, *8*, 445.
2. Li, H.; Yao, Y.; Li, L., *Journal of Pharmacy and Pharmacology* **2017**, *69*, 1253-1264.

3. Ali, M. Y.; Jannat, S.; Jung, H. A.; Choi, R. J.; Roy, A.; Choi, J. S., *Asian Pacific journal of tropical medicine* **2016**, *9*, 103-111.
4. Wu, Y.; Xu, J.; Liu, Y.; Zeng, Y.; Wu, G., *Frontiers in Oncology* **2020**, *10*, 592853.
5. Al-Wahaibi, L. H.; Abu-Melha, H. M.; Ibrahim, D. A., *Journal of Chemistry* **2018**, *2018*.
6. Thakur, A.; Singla, R.; Jaitak, V., *European Journal of Medicinal Chemistry* **2015**, *101*, 476-495.
7. HAZIRI, A.; MAZREKU, I.; RUDHANI, I., *Malaysian Applied Biology* **2022**, *51*, 107-109.
8. Singh, L. R.; Avula, S. R.; Raj, S.; Srivastava, A.; Palnati, G. R.; Tripathi, C.; Pasupuleti, M.; Sashidhara, K. V., *The Journal of Antibiotics* **2017**, *70*, 954-961.
9. Flores-Morales, V.; Villasana-Ruíz, A. P.; Garza-Veloz, I.; González-Delgado, S.; Martinez-Fierro, M. L., *Molecules* **2023**, *28*, 2413.
10. Emami, S.Dadashpour, S., *European Journal of Medicinal Chemistry* **2015**, *102*, 611-630.
11. Sandhu, S.; Bansal, Y.; Silakari, O.; Bansal, G., *Bioorganic & medicinal chemistry* **2014**, *22*, 3806-3814.
12. Carneiro, A.; Matos, M. J.; Uriarte, E.; Santana, L., *Molecules* **2021**, *26*, 501.
13. Qin, H.-L.; Zhang, Z.-W.; Ravindar, L.; Rakesh, K., *European Journal of Medicinal Chemistry* **2020**, *207*, 112832.
14. Sarmah, M.; Chutia, K.; Dutta, D.; Gogoi, P., *Organic & Biomolecular Chemistry* **2022**, *20*, 55-72.
15. Patra, P.Kar, G. K., *New Journal of Chemistry* **2021**, *45*, 2879-2934.
16. Salehian, F.; Nadri, H.; Jalili-Baleh, L.; Youseftabar-Miri, L.; Bukhari, S. N. A.; Foroumadi, A.; Küçükkilinç, T. T.; Sharifzadeh, M.; Khoobi, M., *European Journal of Medicinal Chemistry* **2021**, *212*, 113034.
17. Wang, C.; Wu, C.; Zhu, J.; Miller, R. H.; Wang, Y., *Journal of medicinal chemistry* **2011**, *54*, 2331-2340.
18. Gordo, J.; Avo, J.; Parola, A. J.; Lima, J. C.; Pereira, A.; Branco, P. S., *Organic letters* **2011**, *13*, 5112-5115.
19. Christie, R. M.Lui, C.-H., *Dyes and Pigments* **2000**, *47*, 79-89.
20. Elangovan, A.; Lin, J.-H.; Yang, S.-W.; Hsu, H.-Y.; Ho, T.-I., *The Journal of Organic Chemistry* **2004**, *69*, 8086-8092.
21. Turki, H.; Abid, S.; El Gharbi, R.; Fery-Forgues, S., *Comptes Rendus Chimie* **2006**, *9*,

1252-1259.

22. Hirano, T.; Hiromoto, K.; Kagechika, H., *Organic Letters* **2007**, *9*, 1315-1318.
23. Hegedus, L.Wade, L., *Journal*, 1977, **3**, 8-32.
24. Gooßen, L. J.; Rodríguez, N.; Gooßen, K., *Angewandte Chemie International Edition* **2008**, *47*, 3100-3120.
25. Rodríguez, N.Goossen, L. J., *Chemical Society Reviews* **2011**, *40*, 5030-5048.
26. Myers, A. G.; Tanaka, D.; Mannion, M. R., *Journal of the American Chemical Society* **2002**, *124*, 11250-11251.
27. Tanaka, D.; Romeril, S. P.; Myers, A. G., *Journal of the American Chemical Society* **2005**, *127*, 10323-10333.
28. Goossen, L. J.; Deng, G.; Levy, L. M., *Science* **2006**, *313*, 662-664.
29. Gooßen, L. J.; Linder, C.; Rodríguez, N.; Lange, P. P.; Fromm, A., *Chemical Communications* **2009**, 7173-7175.
30. Dupuy, S.; Lazreg, F.; Slawin, A. M.; Cazin, C. S.; Nolan, S. P., *Chemical Communications* **2011**, *47*, 5455-5457.
31. Sun, Z. M.Zhao, P., *Angewandte Chemie International Edition* **2009**, *48*, 6726-6730.
32. Carrer, A.; Brion, J. D.; Messaoudi, S.; Alami, M., *Advanced Synthesis & Catalysis* **2013**, *355*, 2044-2054.
33. Min, M.; Kim, Y.; Hong, S., *Chemical Communications* **2013**, *49*, 196-198.
34. Jafarpour, F.; Zarei, S.; Barzegar Amiri Olia, M.; Jalalimanesh, N.; Rahiminejadan, S., *The Journal of Organic Chemistry* **2013**, *78*, 2957-2964.
35. Wang, X.; Li, S.-y.; Pan, Y.-m.; Wang, H.-s.; Chen, Z.-f.; Huang, K.-b., *The Journal of Organic Chemistry* **2015**, *80*, 2407-2412.
36. Vardhan Reddy, K. H.; Brion, J.-D.; Messaoudi, S.; Alami, M., *The Journal of Organic Chemistry* **2016**, *81*, 424-432.
37. Liu, K.; Ding, D.; Xing, W.; Liu, L.; Zhang, S.; Meng, Q.; Chen, T., *Organic & Biomolecular Chemistry* **2023**, *21*, 1384-1388.
38. Li, Y.; Shang, J.-Q.; Wang, X.-X.; Xia, W.-J.; Yang, T.; Xin, Y.; Li, Y.-M., *Organic letters* **2019**, *21*, 2227-2230.
39. Li, Y.; Qian, F.; Wang, M.; Lu, H.; Li, G., *Organic Letters* **2017**, *19*, 5589-5592.
40. Yang, K.; Song, M.; Ma, Z.; Li, Y.; Li, Z.; Sun, X., *Organic Chemistry Frontiers* **2019**, *6*, 3996-3999.

41. Dow, N. W.; Pedersen, P. S.; Chen, T. Q.; Blakemore, D. C.; Dechert-Schmitt, A.-M.; Knauber, T.; MacMillan, D. W., *Journal of the American Chemical Society* **2022**, *144*, 6163-6172.

42. Zhao; Yu, Z.; Yan; Wu, S.; Liu, R.; He, W.; Wang, *The Journal of Organic Chemistry* **2005**, *70*, 7338-7341.

43. Cross, R. J.; Green, T. H.; Keat, R., *Journal of the Chemical Society, Dalton Transactions* **1976**, 1150-1152.

44. Quirós Méndez, N.; Arif, A. M.; Gladysz, J., *Organometallics* **1991**, *10*, 2199-2209.

45. Wicht, D. K.; Kovacik, I.; Glueck, D. S.; Liable-Sands, L. M.; Incarvito, C. D.; Rheingold, A. L., *Organometallics* **1999**, *18*, 5141-5151.

46. Joshi, H.; Kharel, S.; Ehnbom, A.; Skopek, K.; Hess, G. D.; Fiedler, T.; Hampel, F.; Bhuvanesh, N.; Gladysz, J. A., *Journal of the American Chemical Society* **2018**, *140*, 8463-8478.

47. Prack, E.; O'Keefe, C. A.; Moore, J. K.; Lai, A.; Lough, A. J.; Macdonald, P. M.; Conradi, M. S.; Schurko, R. W.; Fekl, U., *Journal of the American Chemical Society* **2015**, *137*, 13464-13467.

48. Schiedel, M. S.; Briehn, C. A.; Bäuerle, P., *Angewandte Chemie International Edition* **2001**, *40*, 4677-4680.

49. Dang, Y.; Qu, S.; Wang, Z.-X.; Wang, X., *Journal of the American Chemical Society* **2014**, *136*, 986-998.

50. Zhang, S.; Shi, L.; Ding, Y., *Journal of the American Chemical Society* **2011**, *133*, 20218-20229.

Chapter 5

Conclusions and Future Scope

5.1 General conclusions

Around the world, synthetic chemists consistently hold a crucial role in the design and synthesis of biologically potent fused heterocyclic molecules, which find extensive use in agrochemicals and pharmaceuticals and are frequently encountered in various natural products. However, to achieve these complex bioactive organic molecules with not only minimization of synthetic steps but with high atom economy and utilizing readily available starting materials. In this context, there is a strong emphasis on synthesizing complex heterocyclic structures in a single step. Furthermore, the transition-metal catalyzed C-H activation method has garnered significant attention over traditional methods for constructing complex heterocyclic moieties without pre-functionalization of starting materials.

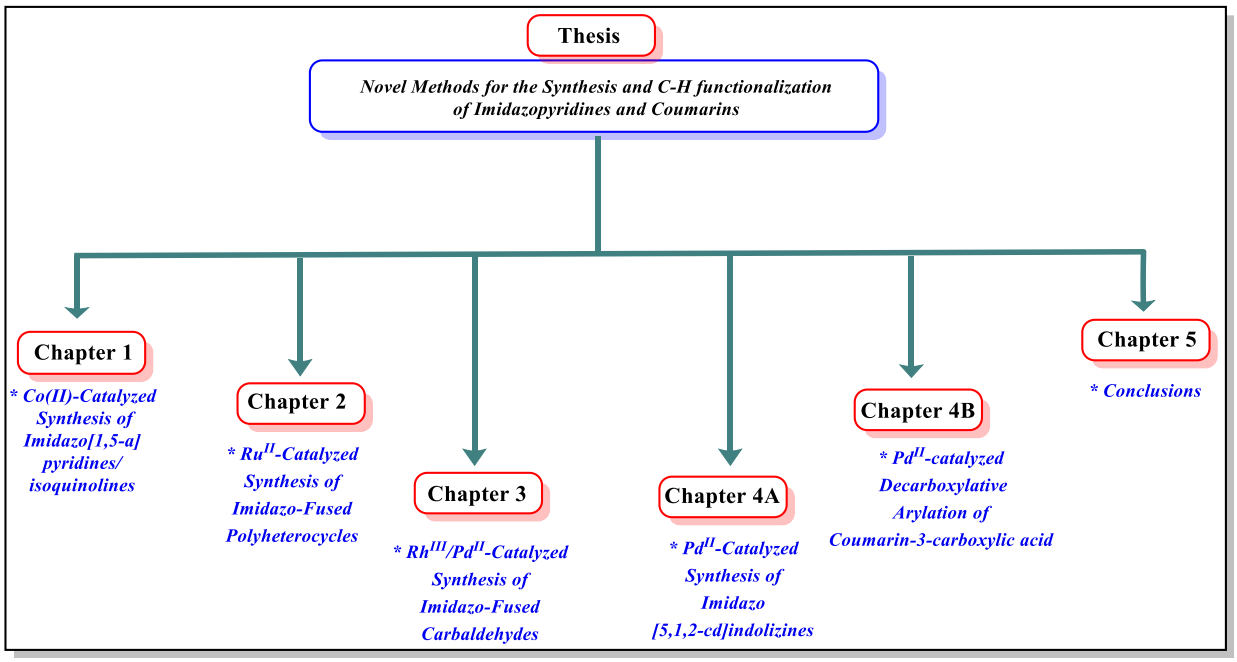

Figure 5.1: A diagram describing a systematic representation of the thesis

In recent years, C–H functionalization reactions have gained significant attention as powerful methods for the formation of C–C and C–X (where X represents heteroatoms like N, O, and S) bonds. These methodologies offer the advantages of high molecular complexity, excellent regioselectivity, and a high tolerance for various functional groups. The thesis entitled **"Novel Methods for the Synthesis and C-H Functionalization of Imidazopyridines and Coumarins"** focuses on the synthesis and functionalization of specific heterocyclic compounds, including

imidazopyridine-fused quinoline, isoquinolines, and coumarin, employing transition-metal catalysts. The thesis is divided into five chapters (**Figure 5.1**).

Chapter 1 of the thesis describes the concise overview of literature reports on C-H functionalization and oxidative C-H/C-H coupling reactions. The plenty of reports of C-H activation provide a valuable chance for the synthetic chemist to synthesize aza-fused heterocycles with diverse functionalities.

Furthermore, the one-pot synthesis of polysubstituted imidazo[1,5-*a*]pyridines and imidazo[1,5-*a*]isoquinolines derivatives. This reaction involves Knoevenagel condensation followed by Co(II)-catalyzed intramolecular direct-alkenylation has been applied for the synthesis of the desired imidazo[1,5-*a*]pyridines and imidazo[1,5-*a*]isoquinolines by using 3-(2-methyl-1*H*-imidazole-1yl)-1-arylpropane-1-ones with β-bromocinnamaldehydes and 2-bromobenzaldehydes, respectively. All synthesized derivatives were characterized by ^{1}H NMR, ^{13}C{^{1}H} NMR, and HRMS spectroscopy, and **25ah** scaffold was unambiguously characterized by single crystal XRD analysis. The developed synthetic approach was conveyed to be operationally simple, using a cost-effective catalyst and easily accessible starting materials that provide a wide range of fused imidazo[1,5-*a*]heterocycles in moderate to good yields with high functional group tolerance. Pleasingly, the current protocol utilized for the synthesis of biologically relevant aroyl- and thiaroyl-substituted imidazo[1,5-*a*]pyridines and imidazo[1,5-*a*]isoquinolines. A putative reaction mechanism of the reaction was proposed on the basis of some control experiments. The intermediate of the reaction and its site selectivity toward cobalt catalyst was mainly investigated. This developed methodology opens a new way to synthesize polysubstituted imidazo-fused pyridine or isoquinoline scaffolds, which could provide a new series of biologically active compounds.

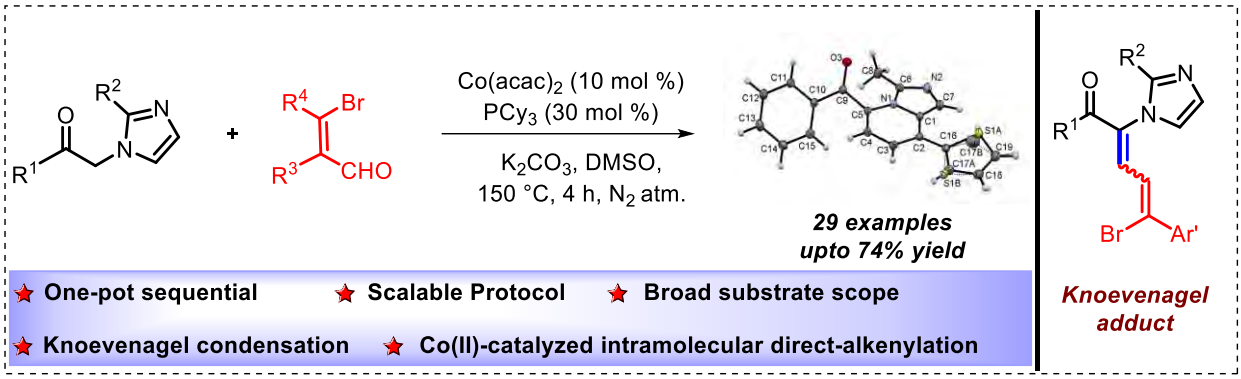

Scheme 5.1: Synthesis of Co(II)-catalyzed imidazo[1,5-*a*]pyridines/isoquinolines derivatives

Chapter 2 deals with the Ru(II)-catalyzed [4+2] annulation reactions of 2-Alkenyl/2-Aryl-imidazoles with maleimides and 1,4-naphthoquinones. The reaction of 2-alkenyl/2-aryl imidazoles with maleimides produced the corresponding derivatives in moderate to good yields. Moreover, 2-alkenyl/2-aryl imidazoles with 1,4-naphthoquinones also reacted smoothly to access the desired annulated products benzo[*g*]imidazo[1,2-*a*]quinoline-6,11-dione in good yields. The synthesized derivatives were well characterized by ^{1}H NMR, ^{13}C{^{1}H} NMR, and HRMS analysis, as well as single X-ray crystal analysis. To gain insight into the mechanism, ruthenacycle I intermediate was successfully synthesized and analyzed by ^{1}H and ^{13}C{^{1}H} NMR. So, on the basis of control experiments and previous reports, a tentative mechanism has been described.

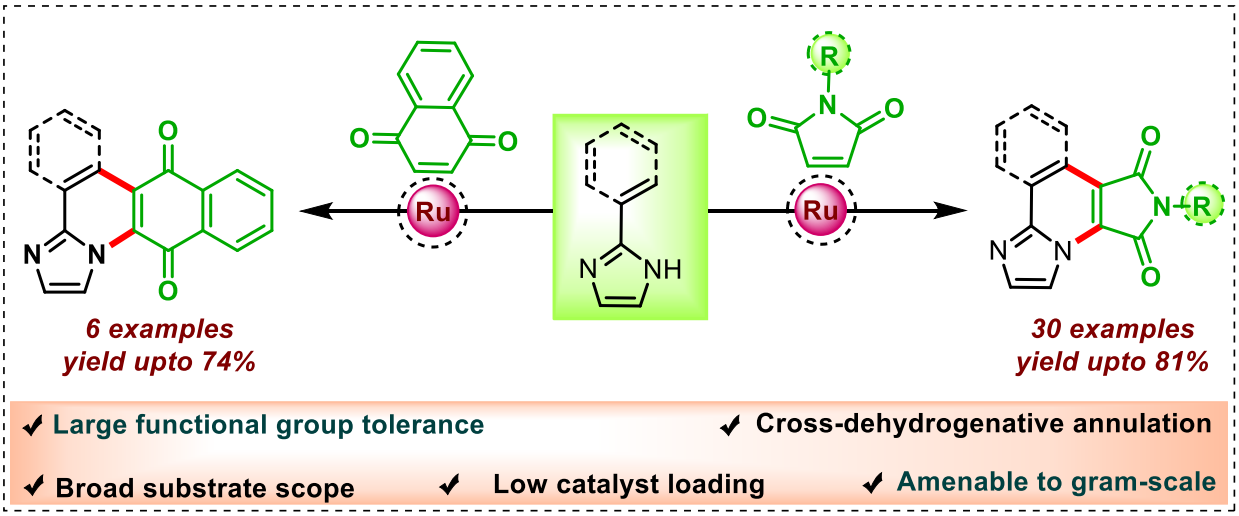

Scheme 5.2: Ru(II)-catalyzed [4+2] annulation of 2-Alkenyl/2-Aryl-imidazoles with Maleimides and 1,4-Naphthoquinones

Chapter 3 elaborates on a catalyst-controlled regioselective oxidative annulation of 2-arylimidaz[1,2-*a*]pyridines with cinnamaldehydes derivatives. The annulation reaction afforded 5-arylnaphtho[1',2':4,5]imidazo[1,2-*a*]pyridine-6-carbaldehydes in the presence of $[RhCp^*Cl_2]_2$ as catalyst while 1,7-diarylimidazo[5,1,2-*cd*]indolizine-6-carbaldehydes were obtained using $Pd(OAc)_2$ as catalyst. This annulation procedure yielded the desired products in high yields and demonstrated a wide range of substrates, showcasing remarkable tolerance toward various functional groups. This method provides access to two distinct isomeric annulated products containing an aldehyde group. These products can serve as versatile starting points for synthesizing diverse compounds with valuable functionalities.

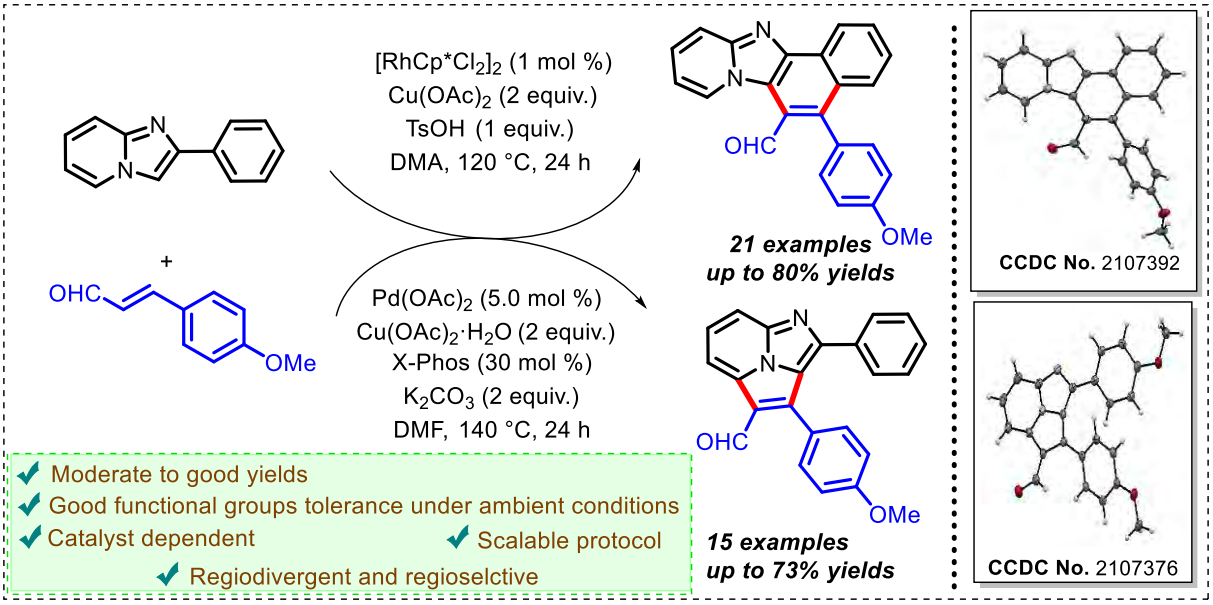

Scheme 5.3: Rh(III)/Pd(II)-catalyzed oxidative annulation of 2-arylimidazo[1,2-*a*]pyridines with trans-cinnamaldehydes

Chapter 4 illustrates the synthesis of selenium coordinated Pd(II)-trans-dichloride molecular rotor as a catalyst. The synthesized palladium complexes were well characterized by ^1H NMR, $^{13}C\{^1H\}$ NMR, HRMS, and IR spectroscopy. Moreover, the Pd(II)-complex was characterized by the single-crystal X-ray analysis, which helps in the identification of the structure of the complex and the bonding of palladium with ligands. The Pd(II)-complex was found to be a very efficient catalyst for the site-selective annulation of 2-arylimidazo[1,2-*a*]pyridines. The catalyst showed high functional group tolerance and only 1.5 mol % of the catalyst loading is required to achieve good yields. The regioselectivity of the catalyst was proven by the DFT study. The results revealed that

the catalyst selectively produced imidazo[5,1,2-*cd*]indolizine. The mechanism of the reaction was proposed on the basis of some control experiments and theoretical studies.

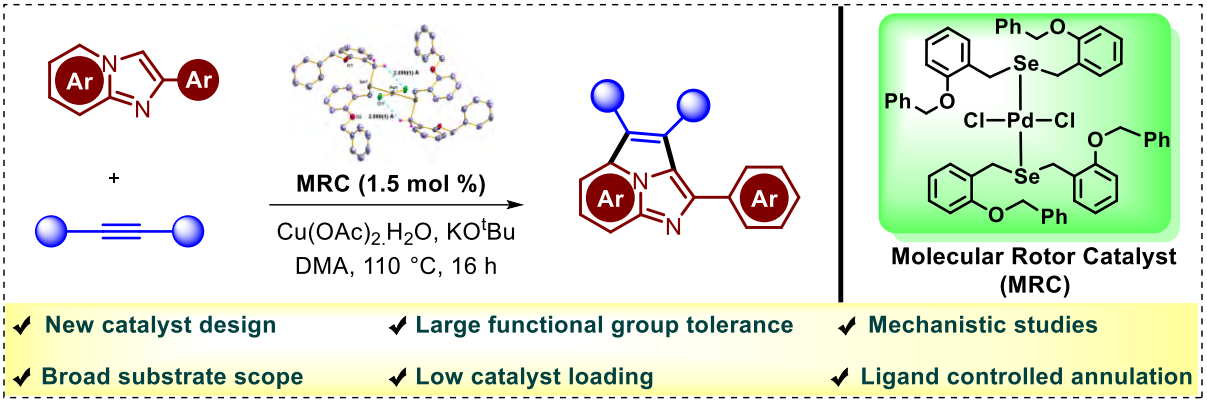

Scheme 5.4: Pd(II)-catalyzed annulation of 2-aryl imidazopyridine with alkynes

Chapter 4B, describes the synthesis of three novel trans-palladium dichloride complexes of bulky selenium ligands. These new ligands and palladium complexes (C1-C3) were characterized through a range of analytical techniques, including ^{1}H, $^{13}C\{^{1}H\}$ NMR, HRMS, UV-Vis., IR, and elemental analysis. Further, the structure of the C2 complex was authenticated by single crystal X-ray studies, which confirmed its square planer geometry with a trans-orientated configuration. The X-ray analysis also revealed intramolecular secondary interactions (SeCH---Cl) between the chlorine of $PdCl_2$ and the CH_2 proton of the selenium ligand. Variable temperature NMR data showed the coalescence of diastereotopic protons, which indicates pyramidal inversion of selenium atom at elevated temperature. The relaxed potential energy scan of C2 suggested a rotational barrier of ~12.5 kcal/mol for the rotation of chlorine atoms through the Cl-Pd-Cl rotor. The complex C3 exhibited dual intramolecular secondary interactions (OCH2---Cl and SeCH2---Cl) with stator ligand. Notably, the molecular rotor C2 was found to be the most efficient catalyst for the decarboxylative Heck-coupling under mild reaction conditions. The protocol proved to be adaptable to a broad range of substrates with large functional group tolerance and low catalyst loading (2.5 mol %). The mechanism behind the decarboxylative Heck-coupling reaction was investigated through both experimental and computational studies. Notably, the reaction was found to proceed under silver-free conditions, reducing the overall cost of the protocol. Furthermore, the catalyst is also effective for decarboxylative arylation and decarboxylative Suzuki-Miyaura coupling reactions, yielding the coupled products with high efficiency.

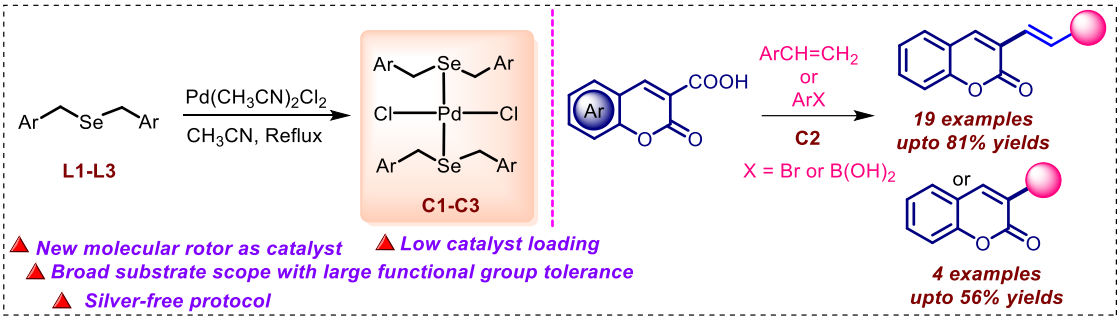

Scheme 5.5: Pd(II)-complex catalyzed decarboxylative coupling of coumarin-3-carboxylic acids with styrenes, aryl bromides and arylboronic acids

5.2 Future scope of the research work

Nitrogen-containing fused heterocyclic compounds have a significant role in organic synthesis due to their wide range of applications in natural products, pharmaceuticals, medicinal chemistry, and material science. The major concern for the access of these potent heterocyclic compounds is the requirement of pre-functionalized starting materials, ultimate multistep synthesis causes low atom and step economy. Thus, transition-metal catalyzed C-H functionalization engrossed more attention in chemical transformations to afford the *N*-fused heterocycles in one-step synthesis from readily available substrate.

Although the thesis is primarily focused on the C-H functionalization of heterocycles, still, there is broad scope for the synthesis of fused aza-heterocycles and their C-H activation. In particular, biologically important 2-arylimidazo[1,2-*a*]pyridines, and coumarin3-carboxylic acid were exclusively explored and used for further C-H functionalization. Some target molecules are demonstrated below, which can be prepared by minor modification of the reaction condition developed for the C-H bond functionalization and annulation reactions (**Figure 5.1**). Furthermore, it would be fascinating to explore the synthesis of the target molecules using the transition-metal catalysts process, which is cheaper and environmentally friendly.

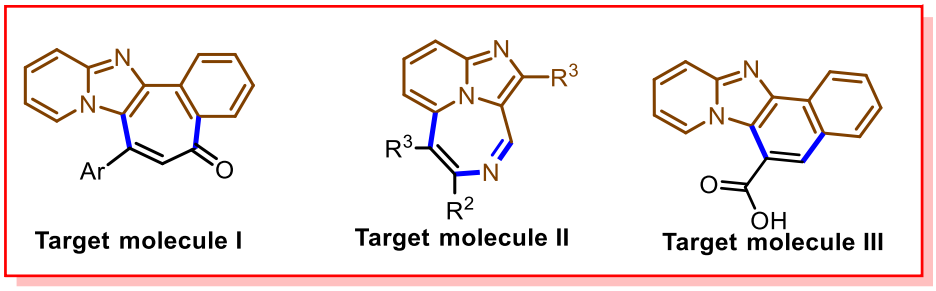

Figure 5.2: Transition metal catalyzed synthesis of fused heterocycles

Appendices

List of Publications *[A-1]*

1. **Neha Meena**, Shobha Sharma, Ramprasad Bhatt, Vikki N. Shinde, Anurag Prakash Sunda, Nattamai Bhuvanesh, Anil Kumar and Hemant Joshi, A selenium-coordinated palladium(II) trans-dichloride molecular rotor as a catalyst for site-selective annulation of 2-arylimidazo[1,2-*a*]pyridines. *Chem. Commun*., **2020**, *56*, 10223-10226.
2. Sonam, Vikki N. Shinde, **Neha Meena**, Dhananjay S. Nipate, Krishnan Rangan, Anil Kumar, Metal-free benzoylation of imidazoheterocycles by oxidative decarboxylation of arylglyoxylic acids. *Org. Biomol. Chem.*, **2020**, *18*, 9072-9080.
3. Vikki N. Shinde, Tapta Kumar Roy, Sonam, Dhananjay S. Nipate, **Neha Meena**, Krishnan Rangan, Anil Kumar, Rhodium(III)-catalyzed annulation of 2-arylimidazo[1,2-*a*]pyridines with maleimides: synthesis of 1*H*-benzo[*e*]pyrido[1',2':1,2]imidazo[4,5-*g*]isoindole-1,3(2*H*)-diones and their photophysical studies. *Adv. Synth. Catal.,* **2020**, *362*, 5751-5764.
4. **Neha Meena**, Sunil Kumar, Vikki N. Shinde, S. Rajagopala Reddy, Himanshi, Nattamai Bhuvanesh, Anil Kumar, and Hemant Joshi, Bulky selenium ligand stabilized trans-palladium dichloride complexes as catalyst for silver-free decarboxylative coupling of coumarin-3-carboxylic acids. *Chem. Asian J*., **2022**, *17*, e202101199.
5. **Neha Meena**, Shiv Dhiman, and Anil Kumar, Cobalt-catalyzed tandem one-pot synthesis of polysubstituted imidazo[1,5-*a*]pyridines and imidazo[1,5-*a*]isoquinolines. *Org. Biomol. Chem.*, **2022**, *20*, 4215-4223.
6. Surabhi Bhatt, **Neha Meena**, Mukesh Kumar, Nattamai Bhuvanesh, Anil Kumar, Anuj K. Sharma, Hemant Joshi, Design and syntheses of ruthenium ENE (E = S, Se) pincer complexes: A versatile system for catalytic and biological applications. *Chem. Asian J.,* **2022**, *17*, e202200736.
7. Srijita Paul Chowdhuri, Shiv Dhiman, Subhendu K. Das, **Neha Meena**, Das, S.; Anil Kumar, Brenubrata Das, Novel pyrido [2′, 1′: 2, 3] imidazo [4, 5-c] quinoline derivative selectively poisons leishmania donovani bisubunit topoisomerase 1 to inhibit the antimony-resistant leishmania infection in vivo. *J. Med. Chem.,* **2023**, *66*, 3411-3430
8. **Neha Meena**, Bhawani, Sonam, Krishnan Rangan, Anil Kumar, A ball-milling-enabled $Zn(OTf)_2$-catalyzed Friedel-Crafts hydroxylation of imidazo[1,2-*a*]pyridines and indoles. *J. Org. Chem.* **2023**, *88*, 3022−3034.
9. Vikki N. Shinde., Bhawani, Dhananjay S. Nipate, Sonam, **Neha Meena**, Krishnan Rangan, Anil Kumar, Manganese-Catalyzed ortho-Hydroalkylation of Aryl-Substituted N-Heteroaromatic Compounds with Maleimides. *Synthesis*, **2023**, *55*, 3632-3643
10. Prakash N. Swami, **Neha Meena**, Krishnan Rangan, and Anil Kumar, Design and Synthesis of Palladium (II) Complex of CNHCNN pincer-type *N*-heterocyclic carbene ligand:

applications towards oxidative amidation of aldehydes with 2-Aminopyridines. *Organometallics* **2023**, *42*, 2359–2368.

11. Neha Meena, Vikki N. Shinde, Sonam, Prakash N. Swami, Krishnan Rangan, and Anil Kumar, Catalyst-controlled regiodivergent oxidative annulation of 2-arylimidazo[1,2-*a*]pyridines with cinnamaldehyde derivatives. *J. Org. Chem.* **2023**, *88*, 12902–12913.
12. Sohan Singh, Vikki N. Shinde, Sunil Kumar, **Neha Meena**, Nattamai Bhuvanesh, Krishnan Rangan, Anil Kumar, Hemant Joshi, Mono and bimetallic palladium pincer complexes of NNSe ligand as catalyst for decarboxylative direct C–H heteroarylation of (hetero)arenes. *Chem. Asian J.* **2023**, *18*, e202300628.
13. **Neha Meena**, Dhananjay S. Nipate, Prakash N. Swami, Krishnan Rangan, and Anil Kumar, Ru(II)-catalyzed [4+2]-annulation of 2-alkenyl/2-aryl-imidazoles with maleimides and 1,4-naphthoquinones: Access to imidazo-fused polyheterocycles. *J. Org. Chem.* **2024**, *89*, 2272-2282
14. Dhananjay S. Nipate, **Neha Meena**, Prakash N. Swami, Krishnan Rangan, and Anil Kumar, *Chem. Commun*., **2024**, *60*, 344-347.

ChemComm

ROYAL SOCIETY OF CHEMISTRY

COMMUNICATION

View Article Online
View Journal | View Issue

Check for updates

Cite this: *Chem. Commun.*, 2024, 60, 344

Received 17th September 2023,
Accepted 27th November 2023

DOI: 10.1039/d3cc04600a

rsc.li/chemcomm

Rh(III)-catalyzed oxidative [4+2] annulation of 2-arylquinoxalines and 2-aryl-2*H*-indazoles with allyl alcohols†

Dhananjay S. Nipate,[a] Neha Meena,[a] Prakash N. Swami,[a] Krishnan Rangan[b] and Anil Kumar*[a]

Synthesis of functionalized benzo[*a*]phenazines and indazolo[2,3-*a*]quinolines has been developed through Rh(III)-catalyzed oxidative annulation of 2-arylquinoxalines and 2-aryl-2*H*-indazoles with allyl alcohols, respectively. The method features a broad substrate scope, excellent functional group tolerance, good to high yields of annulated products, and scaled-up synthesis capability. Based on a preliminary mechanistic investigation, a tentative mechanism of annulation reaction has been proposed.

diverse, and atom-economical method for the synthesis of these important fused heterocycles.

In recent years, transition metal-catalyzed C–H/C–H and C–H/N–H annulation with different coupling partners has become a powerful and attractive method with high atom- and step-economy in organic synthesis to construct diverse carbo- and heterocycles.[7] Among various coupling partners, allyl alcohols have been widely used as alkene partners, equivalent to α,β-

JOC The Journal of Organic Chemistry

pubs.acs.org/joc Article

Ru(II)-Catalyzed [4 + 2]-Annulation of 2-Alkenyl/Arylimidazoles with *N*-Substituted Maleimides and 1,4-Naphthoquinones: Access to Imidazo-Fused Polyheterocycles

Neha Meena, Dhananjay S. Nipate, Prakash N. Swami, Krishnan Rangan, and Anil Kumar*

Cite This: *J. Org. Chem.* 2024, 89, 2272−2282 Read Online

ACCESS | Metrics & More | Article Recommendations | Supporting Information

ABSTRACT: Synthesis of imidazo-fused polyheterocyclic molecular frameworks, viz. imidazo[1,2-*a*]pyrrolo[3,4-*e*]pyridines, imidazo[2,1-*a*]pyrrolo[3,4-*c*]isoquinolines, and benzo[*g*]imidazo[1,2-*a*]quinoline-6,11-diones, has been achieved by the ruthenium(II)-catalyzed [4 + 2] C−H/N−H annulation of 2-alkenyl/2-arylimidazoles with *N*-substituted maleimides and 1,4-naphthoquinones. The developed protocol is operationally simple, exhibits broad substrate scope with excellent functional group tolerance, and provides the desired products in moderate to good yields. The mechanistic studies suggest that the reaction involves the formation of a C−C bond through Ru-catalyzed C(sp^2)−H bond activation followed by intramolecular cyclization.

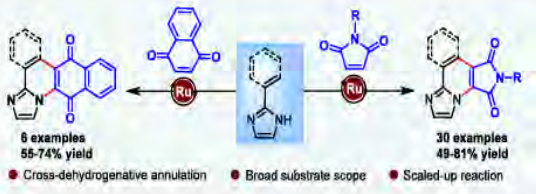

ORGANOMETALLICS

pubs.acs.org/Organometallics Article

Design and Synthesis of a Palladium(II) Complex of a $C_{NHC}NN$ Pincer-Type *N*-Heterocyclic Carbene Ligand: Application towards the Oxidative Amidation of Aldehydes with 2-Aminopyridines

Prakash N. Swami,[‖] Neha Meena,[‖] Hemant Joshi, Krishnan Rangan, and Anil Kumar*

Cite This: *Organometallics* 2023, 42, 2359−2368 Read Online

ACCESS | Metrics & More | Article Recommendations | Supporting Information

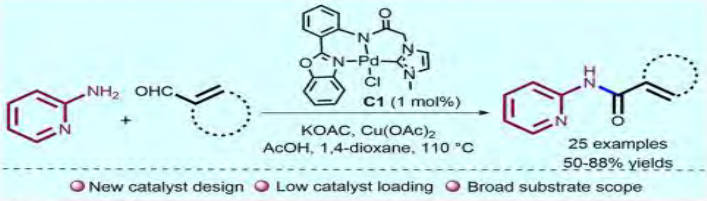

ABSTRACT: This report describes the synthesis of a $[C_{NHC}NN]$-pincer-type palladium(II) complex bearing a *N*-heterocyclic carbene (NHC)-derived pincer CNN ligand. The ligand and palladium pincer complex were characterized with the help of ^{1}H, $^{13}C\{^{1}H\}$ NMR, Fourier transform infrared (FTIR) spectroscopy, high-resolution mass spectrometry (HRMS), ultraviolet−visible (UV−vis) spectroscopy, and X-ray photoelectron spectroscopy (XPS) techniques. The coordination mode of the ligand with the palladium was confirmed using single-crystal X-ray diffraction studies. The complex possesses a distorted square planar geometry around the palladium center. The Pd(II) pincer complex was used as a catalyst for the oxidative amidation of aldehydes with 2-aminopyridines. Notably, only 1.0 mol % catalyst loading is required to activate a wide range of substrates under mild reaction conditions. The protocol showed excellent tolerance toward a diverse range of functional groups with good to very good yields (up to 88%) of amidation products. A plausible mechanism of the amidation reaction is proposed on the basis of control experiments.

JOC The Journal of Organic Chemistry

pubs.acs.org/joc Article

Catalyst-Controlled Regiodivergent Oxidative Annulation of 2-Arylimidazo[1,2-*a*]pyridines with Cinnamaldehyde Derivatives for Construction of Fused N-Heterocyclic Frameworks

Neha Meena,[⊥] Vikki N. Shinde,[⊥] Sonam, Prakash N. Swami, Krishnan Rangan, and Anil Kumar*

Cite This: https://doi.org/10.1021/acs.joc.3c00717 Read Online

ACCESS | Metrics & More | Article Recommendations | Supporting Information

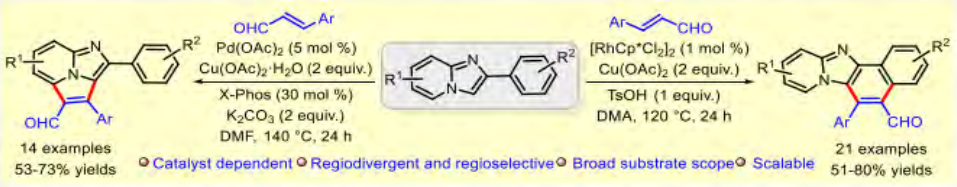

ABSTRACT: Catalyst-dependent regioselective oxidative annulation of 2-arylimidazo[1,2-*a*]pyridines with cinnamaldehyde derivatives to construct fused N-heterocyclic frameworks has been described. The annulation reaction afforded 5-arylnaphtho-[1′,2′:4,5]imidazo[1,2-*a*]pyridine-6-carbaldehydes in the presence of $[RhCp^{*}Cl_2]_2$ as catalyst while 1,7-diarylimidazo[5,1,2-*cd*]indolizine-6-carbaldehydes were obtained using $Pd(OAc)_2$ as catalyst. The reaction produced annulated products in good yields and exhibited broad substrate scope and excellent functional group tolerance. The method provides two different isomeric annulated products bearing an aldehyde functionality which can be elaborated into an array of functionalities leading to valuable compounds.

Journal of Medicinal Chemistry

pubs.acs.org/jmc Article

Novel Pyrido[2′,1′:2,3]imidazo[4,5-*c*]quinoline Derivative Selectively Poisons *Leishmania donovani* Bisubunit Topoisomerase 1 to Inhibit the Antimony-Resistant *Leishmania* Infection *in Vivo*

Srijita Paul Chowdhuri, Shiv Dhiman, Subhendu K. Das, Neha Meena, Sonali Das, Anil Kumar,* and Benu Brata Das*

Cite This: *J. Med. Chem.* 2023, 66, 3411−3430 Read Online

ACCESS | Metrics & More | Article Recommendations | Supporting Information

ABSTRACT: The unique bisubunit structure of *Leishmania donovani* topoisomerase 1B (LdTop1) is a potential drug target in the parasites unlike the monomeric Top1 from its human host counterpart. Here, we report the design, synthesis, and validation of a chimeric pyrido[2′,1′:2,3]imidazo[4,5-*c*]quinoline derivative (**C17**) as a novel antileishmanial agent that poisons topoisomerase 1-DNA covalent complexes (LdTop1cc) inside the parasites and inhibits Top1 religation activity both in the drug sensitive and antimony-resistant *L. donovani* clinical isolates. Importantly, the human Top1 is not sensitive to **C17**. Further, **C17** overcomes the chemical instability of camptothecin (CPT) by generating

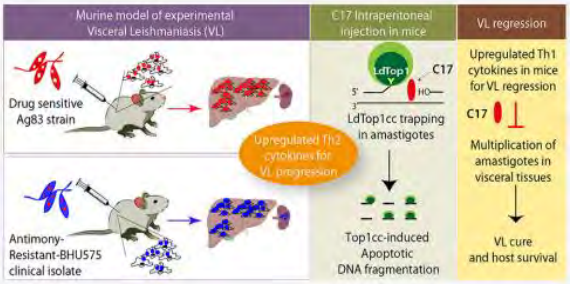

JOC The Journal of Organic Chemistry

pubs.acs.org/joc Article

Ball-Milling-Enabled $Zn(OTf)_2$-Catalyzed Friedel−Crafts Hydroxyalkylation of Imidazo[1,2-*a*]pyridines and Indoles

Neha Meena,§ Bhawani,§ Sonam, Krishnan Rangan, and Anil Kumar*

Cite This: *J. Org. Chem.* 2023, 88, 3022−3034 Read Online

ACCESS | Metrics & More | Article Recommendations | Supporting Information

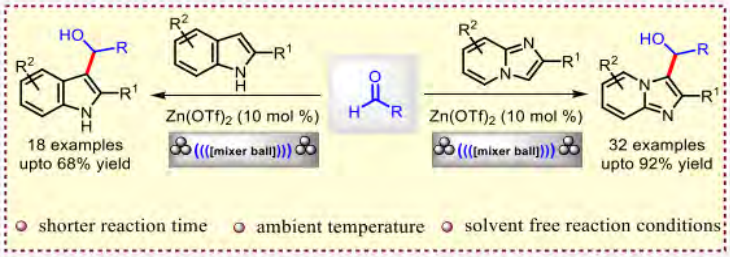

ABSTRACT: A facile and efficient synthetic method for the construction of C3-hydroxyalkylated imidazo[1,2-*a*]pyridines and indoles by a $Zn(OTf)_2$-catalyzed Friedel−Crafts hydroxyalkylation of imidazo[1,2-*a*]pyridines and indoles with carbonyl compounds under mechanochemical conditions is reported. Good product selectivity, shorter reaction time, ambient reaction temperature, tolerance of a wide range of functional groups, broad substrate scope, moderate to good yield of products, and scalability are the salient features of the developed methodology.

ACES Asian Chemical Editorial Society
doi.org/10.1002/asia.202300628
Check for update
CHEMISTRY
AN ASIAN JOURNAL
Research Article
www.chemasianj.org

Mono and Dinuclear Palladium Pincer Complexes of NNSe Ligand as a Catalyst for Decarboxylative Direct C–H Heteroarylation of (Hetero)arenes

Sohan Singh[+],[a] Vikki N. Shinde[+],[b] Sunil Kumar,[a] Neha Meena,[b] Nattamai Bhuvanesh,[c] Krishnan Rangan,[d] Anil Kumar,*[b] and Hemant Joshi*[a]

This report describes the synthesis of a new NNSe pincer ligand and its mono- and dinuclear palladium(II) pincer complexes. In the absence of a base, a dinuclear palladium pincer complex (**C1**) was isolated, while in the presence of Et_3N base a mononuclear palladium pincer complex (**C2**) was obtained. The new ligand and complexes were characterized using techniques like ^1H, $^{13}C\{^1H\}$ nuclear magnetic resonance (NMR), fourier transform infrared (FTIR), high-resolution mass spectrometry (HRMS), ultraviolet-visible (UV-Visible), and cyclic voltammetry. Both the complexes showed pincer coordination mode with a distorted square planar geometry. The complex **C1** has two pincer ligands attached through a Pd–Pd bond in a dinuclear pincer fashion. The air and moisture-insensitive, thermally robust palladium pincer complexes were used as the catalyst for decarboxylative direct C–H heteroarylation of (hetero)arenes. Among the complexes, dinuclear pincer complex **C1** showed better catalytic activity. A variety of (hetero)arenes were successfully activated (43–87 % yield) using only 2.5 mol % of catalyst loading under mild reaction conditions. The PPh_3 and Hg poisoning experiments suggested a homogeneous nature of catalysis. A plausible reaction pathway was proposed for the dinuclear palladium pincer complex catalyzed decarboxylative C–H bond activation reaction of (hetero)arenes.

Organic & Biomolecular Chemistry
ROYAL SOCIETY OF CHEMISTRY
PAPER
View Article Online
View Journal | View Issue
Check for updates
Cite this: *Org. Biomol. Chem.*, 2022, **20**, 4215

Cobalt-catalyzed tandem one-pot synthesis of polysubstituted imidazo[1,5-*a*]pyridines and imidazo[1,5-*a*]isoquinolines†

Neha Meena,‡[a] Shiv Dhiman,‡[a] Krishnan Rangan[b] and Anil Kumar *[a]

Received 19th March 2022,
Accepted 4th May 2022
DOI: 10.1039/d2ob00526c
rsc.li/obc

An efficient cobalt-catalyzed tandem one-pot method has been developed for the synthesis of polysubstituted imidazo[1,5-*a*]-N-heteroaromatics. The method involves Knoevenagel condensation followed by cobalt-catalyzed direct alkenylation to give the desired polysubstituted imidazo[1,5-*a*]pyridines and imidazo[1,5-*a*]isoquinolines in a one-pot manner. This method exhibits a broad substrate scope, provides moderate to good (39–74%) yields and is amenable to scale-up to the gram scale.

Introduction

Over the past few decades, transition metal-catalyzed C–H bond activation and functionalization has made significant properties.[25–27] They have also been used as novel dye structures with promising application as fluorescent probes,[28–32] precursors of N-heterocyclic carbenes,[33–35] and organic light-emitting diodes.[36,37] Thus, the development of novel

ACES Asian Chemical Editorial Society
doi.org/10.1002/asia.202101199
CHEMISTRY AN ASIAN JOURNAL Research Article
www.chemasianj.org

Bulky Selenium Ligand Stabilized *Trans*-Palladium Dichloride Complexes as Catalyst for Silver-Free Decarboxylative Coupling of Coumarin-3-Carboxylic Acids

Neha Meena,[a] Sunil Kumar,[b] Vikki N. Shinde,[a] S. Rajagopala Reddy,[b] Himanshi,[b] Nattamai Bhuvanesh,[c] Anil Kumar,*[a] and Hemant Joshi*[b]

Abstract: This report describes the syntheses of three new *trans*-palladium dichloride complexes of bulky selenium ligands. These complexes possess a Cl–Pd–Cl rotor spoke attached to a Se–Pd–Se axle. The new ligands and palladium complexes (**C1**–**C3**) were characterized with the help of NMR, HRMS, UV-Vis., IR, and elemental analysis. The single-crystal structure of metal complex **C2** confirmed a square planar geometry of complex with *trans*-orientation. The X-ray structure revealed intramolecular secondary interactions (SeCH—Cl) between chlorine of $PdCl_2$ and CH_2 proton of selenium ligand. Variable-temperature NMR data shows coalescence of diastereotopic protons, which indicates pyramidal inversion of selenium atom at elevated temperature. The relaxed potential energy scan of **C2** suggests a rotational barrier of ~12.5 kcal/mol for rotation of chlorine atom through Cl–Pd–Cl rotor. The complex **C3** possesses dual intramolecular secondary interactions (OCH_2—Cl and $SeCH_2$—Cl) with stator ligand. Molecular rotor **C2** was found to be a most efficient catalyst for the decarboxylative Heck-coupling under mild reaction conditions. The protocol is applicable to a broad range of substrates with large functional group tolerance and low catalyst loading (2.5 mol%). The mechanism of decarboxylative Heck-coupling reaction was investigated through experimental and computational studies. Importantly the reaction works under silver-free conditions which reduces the cost of overall protocol. Further, the catalyst also worked for decarboxylative arylation and decarboxylative Suzuki-Miyaura coupling reactions with good yields of the coupled products.

ACES Asian Chemical Editorial Society
doi.org/10.1002/asia.202200736
CHEMISTRY AN ASIAN JOURNAL Research Article
www.chemasianj.org

Design and Syntheses of Ruthenium ENE (E=S, Se) Pincer Complexes: A Versatile System for Catalytic and Biological Applications

Surabhi Bhatt,[a] Neha Meena,[b] Mukesh Kumar,[a] Nattamai Bhuvanesh,[c] Anil Kumar,*[b] Anuj K. Sharma,*[a] and Hemant Joshi*[a]

Abstract: This report describes the synthesis of two ruthenium(II) ENE pincer complexes (E=S, **C1** and E=Se, **C2**) by the reaction of bis(2-(phenylchalcogenyl)ethyl)amine (**L1**, **L2**) with $RuCl_2(PPh_3)_3$. The complexes were characterized with the help of ^1H and $^{13}C\{^1H\}$ NMR, FTIR, HRMS, cyclic voltammetry and elemental analysis techniques. The structure and bonding mode of ligand with ruthenium in **C2** was established with the help of single crystal X-ray diffraction. The complex showed distorted octahedral geometry with two chlorine atoms *trans* to each other. The Ru–Se bond distances (Å) are 2.4564(3)-2.4630(3), Ru–N distance is 2.181(2), Ru–P distance is 2.2999(6), and Ru–Cl distances are 2.4078(6)-2.4314(6). The complexes showed good to excellent catalytic activity for the *N*-alkylation of *o*-phenylenediamine with benzyl alcohol derivatives to synthesize 1,2-disubstituted benzimidazole derivatives. The complexes were also to corresponding aldehydes which are precursors to the bisimines generated in situ during the synthesis of 1,2-disubstituted benzimidazole derivatives. Complex **C2** where selenium is coordinated with ruthenium was found to be more efficient as compared to sulfur coordinated ruthenium complex **C1**. Since ruthenium complexes are getting increasing attention for developing new anticancer agents, the preliminary studies like binding behavior of both the complexes towards CT-DNA were studied by competitive binding with ethidium bromide (EthBr) using emission spectroscopy. In addition, the interactions of **C1**–**C2** were also studied with bovine serum albumin (BSA) using steady state fluorescence quenching and synchronous fluorescence studies. A good stability of Ru(II) state was observed by cyclic voltammetric studies of **C1**–**C2**. Overall these molecules are good examples of bio-organometallic systems for catalytic

ChemComm

ROYAL SOCIETY OF CHEMISTRY

COMMUNICATION

View Article Online
View Journal | View Issue

Check for updates

Cite this: *Chem. Commun.*, 2020, 56, 10223

Received 20th May 2020,
Accepted 9th July 2020

DOI: 10.1039/d0cc03599h

rsc.li/chemcomm

A selenium-coordinated palladium(II) *trans*-dichloride molecular rotor as a catalyst for site-selective annulation of 2-arylimidazo[1,2-*a*]pyridines†

Neha Meena,[a] Shobha Sharma,[b] Ramprasad Bhatt,[a] Vikki N. Shinde,[a] Anurag Prakash Sunda,[c] Nattamai Bhuvanesh,[d] Anil Kumar *[a] and Hemant Joshi *[e]

This report describes the synthesis of a new class of secondary interaction (SeCH···Cl)-controlled molecular rotor having a Cl–Pd–Cl rotor spoke attached onto a Se–Pd–Se axle. NMR data acquired at various temperatures established $\Delta G^{\ddagger}_{298K}/\Delta G^{\ddagger}_{350K}$ values of 15.5 and 17.2 kcal mol^{-1} for a roughly 4.5 Å-long rotor. The molecular rotor molecules.[1b] The Garcia-Garibay, Setaka, and Gladysz groups have explored molecular rotors in depth.

Triptycene rotors are among the very first extensively studied solution-state molecular rotors.[6] The shape, size and symmetry of the rotor unit significantly influence the rotor movement.

Organic & Biomolecular Chemistry

ROYAL SOCIETY OF CHEMISTRY

PAPER

View Article Online
View Journal | View Issue

Check for updates

Cite this: *Org. Biomol. Chem.*, 2020, **18**, 9072

Metal-free benzoylation of imidazoheterocycles by oxidative decarboxylation of arylglyoxylic acids†

Sonam Jaspal,[a] Vikki N. Shinde,[a] Neha Meena,[a] Dhananjay S. Nipate,[a] Krishnan Rangan[b] and Anil Kumar *[a]

Received 6th September 2020,
Accepted 15th October 2020

DOI: 10.1039/d0ob01842b

rsc.li/obc

A simple and straightforward approach has been realized for the direct benzoylation of imidazoheterocycles by oxidative decarboxylation of arylglyoxylic acids in the presence of $K_2S_2O_8$ as an oxidant. Various functional groups were tolerated on both imidazoheterocycles and arylglyoxylic acids and a wide range of C5-benzoyl-imidazoheterocycles were obtained in good to high yields (50–84%). Radical trapping experiments confirmed the involvement of the radical pathway. The developed protocol is amenable for a scale-up reaction.

WILEY-VCH

FULL PAPER

Rhodium(III)-Catalyzed Annulation of 2-Arylimidazo[1,2-*a*]pyridines with Maleimides: Synthesis of 1*H*-Benzo[*e*]pyrido[1',2':1,2]imidazo[4,5-*g*]isoindole-1,3(2*H*)-diones and their Photophysical Studies

Vikki N. Shinde,[a] Tapta Kanchan Roy,[b] Sonam Jaspal,[a] Dhananjay S. Nipate,[a] Neha Meena,[a] Krishnan Rangan,[c] Dalip Kumar[a] and Anil Kumar*[a]

[a] Department of Chemistry
Birla Institute of Technology and Science Pilani, Pilani Campus
Pilani, Rajasthan, 333031 (India)
E-mail: anilkadian@gmail.com and anilkumar@pilani.bits-pilani.ac.in
[b] Department of Chemistry and Chemical Sciences
Central University of Jammu
Rahya Suchani, J&K, 181143 (India)
[c] Department of Chemistry
Birla Institute of Technology and Science Pilani, Hyderbad Campus
Hyderabad, Telangana, 500078 (India)

Supporting information for this article is available on the WWW under https://doi.org/10.1002/adsc.202000960

Abstract: Rhodium(III)-catalyzed dehydrogenative annulation of 2-aryl-imidazo[1,2-*a*]pyridines with maleimides is described. The reaction afforded 1*H*-benzo[*e*]pyrido[1',2':1,2]imidazo[4,5-*g*]isoindole-1,3(2H)-diones in high yields with wide range of functional group tolerance. The reaction proceeds through Rh(III)-catalyzed C-H bond activation, followed by maleimide insertion and intramolecular cyclization. Photophysical properties of 1*H*-benzo[*e*]pyrido[1',2':1,2]imidazo[4,5-*g*]isoindole-1,3(2H)-diones were studied with UV-visible and fluorescence spectroscopy and validated by quantum chemical calculations. All the annulated products showed large Stokes shift values with emission in the range of 530-618 nm, and moderate to high quantum yields.

Keywords: Imidazo[1,2-*a*]pyridine, annulation, rhodium, DFT, photophysical property

annulative coupling of 2-arylimidazo[1,2-*a*]pyridines with diarylalkynes.[6] Later, Fan group reported palladium catalyzed annulation of 2-arylimidazo[1,2-*a*]pyridines with diarylalkynes to obtain a mixture of 5,6-diarylnaphtho[1',2':4,5]imidazo[1,2-*a*]pyridines and 2,3,4-triarylimidazo[5,1,2-*cd*]indolizines (Scheme 1a).[7] Cheng and Song groups independently developed the protocol to access naphtho[1',2':4,5]-imidazo[1,2-*a*]pyridines involving Rh(III)-catalyzed oxidative annulation of 2-arylimidazo[1,2-*a*]pyridines and alkynes.[8] Li group developed a condition controlled synthesis of naphtho[1',2':4,5]imidazo[1,2-*a*]pyridines and fused isoquinolinium derivatives by Rh(III)-catalyzed annulation of 2-arylimidazo[1,2-*a*]pyridines with alkynes (Scheme 1b).[9] Zheng and coworkers utilized a Rh(III)-catalyzed [4 + 2] type oxidative coupling between sulfoxonium ylides and 2-phenylimidazo[1,2-*a*]pyridines to access naphtho[1',2':4,5]-

List of Presentations in Conferences *[A-3]*

1. **Neha Meena**, Bhawani, Anil Kumar, Mechanochemical Zinc-Mediated Hydroxyalkylation of Imidazo[1,2-a]pyridines under Ball Milling Conditions, 29th CRSI National symposium in chemistry, 7th – 9th Jul, 2022, IISER Mohali. **(Best Poster Award)**
2. **Neha Meena**, Vikki N. Shinde, Sonam, Prakash N. Swami, Anil Kumar, Catalyst-Controlled Regiodivergent Oxidative Annulation of 2-Arylimidazo[1,2-*a*]pyridines with Cinnamaldehyde Derivatives, 6th FCASI-2023, 20th-21th April, 2023, Department of Chemistry, University of Rajasthan, Jaipur.
3. **Neha Meena**, Vikki N. Shinde, Sonam, Prakash N. Swami, Anil Kumar, Catalyst-Controlled Regiodivergent Oxidative Annulation of 2-Arylimidazo[1,2-*a*]pyridines with Cinnamaldehyde Derivatives, XVIII-JNOST-2023, October 10th-12th, IISER, Pune.

Brief Biography of the Candidate *[A-4]*

Neha Meena, born in April 1994 in Sardarshahar (Churu), Rajasthan, India, holds a B.Sc (2011-2014) and MSc in chemistry(2015-2014) from Maharaja Ganga Singh University, Bikaner, Rajasthan, India. In December 2016 she was awarded with the Joint CSIR-UGC Test for Junior Research Fellowship and Eligibility for Lectureship (CSIR-NET/JRF) with 124th rank in India held by CSIR New Delhi.

She received CSIR-UGC fellowship by clearing joint CSIR-UGC exam with AIR 124 and joined as a research fellow under the guidance of Prof. Anil Kumar at the Department of Chemistry, BITS Pilani, Pilani Campus, Rajasthan in December 2018. Later, in January 2019, she enrolled for the Ph.D. program at BITS Pilani. In January 2021 she was awarded a Senior Research Fellowship (SRF) for two years. Her research revolves around the C-H bond functionalization of selected azaheterocycles employing transition metal-catalyzed reactions.

Throughout her academic journey, she has published fourteen research articles in peer-reviewed international journals, with seven of them being the first author. She has also actively participated in three international/national conferences, presenting her work as poster presentations. She received best poster award at 29th CRSI- national symposium in chemistry at IISER Mohali.

Brief Biography of the Supervisor *[A-5]*

Dr. Anil Kumar is a professor of chemistry at Birla Institute of Technology and Science (BITS), Pilani, Pilani campus. He completed his PhD from the department of chemistry, University of Delhi, under the esteemed guidance of Professor SMS Chauhan in 2004. During his doctoral research, Dr. Kumar focused on developing heterogeneous catalysts for organic synthesis, with a strong emphasis on green chemistry principles. Following his doctoral studies, Dr. Kumar pursued his postdoctoral research at the department of biomedical and pharmaceutical sciences, University of Rhode Island, Kingston, USA, under the mentorship of Prof. Keykavous Parang. His postdoctoral work involved synthesis of novel Src kinase inhibitory agents and solid-phase synthesis.

In 2006, Dr. Kumar joined the department of chemistry at BITS Pilani as Assistant Professor, and through his dedication and exceptional contributions, he was promoted to Associate Professor in February 2013 and later to Professor in August 2018. Throughout his career, he has displayed outstanding leadership, serving as the Associate Dean for Work Integrated Learning Programmes (WILP) from May 2014 to August 2018, and as the Head of the Department of Chemistry, BITS Pilani, Pilani Campus, from September 2014 to August 2016.

Dr. Kumar is highly regarded for his remarkable achievements and has earned several accolades, including the CRSI Bronze Medal (2020) from CRSI Bangalore, Prof. S. Venkateswaran Faculty Excellence Award (2017) from BITS Alumni Association, Dr. Arvind Kumar Memorial Award (2014) from Indian Council of Chemists, ISCB Young Scientist Award in Chemical Sciences (2013) from ISCB Lucknow, and Harrison McCain Foundation Award (2012) from Acadia University, Canada. He is currently serving as a council member (2023-2026) of CRSI Bangalore. With over 23 years of extensive research experience and more than 17 years of teaching experience, Dr. Kumar's expertise lies in developing novel reaction methodologies using transition metal catalyzed C-C, N, S, O coupling reactions, green chemistry, ionic liquids, and medicinal chemistry. He has an impressive publication record, with over 181 research papers published in reputed international journals and four book chapters covering the areas of synthetic organic chemistry, green chemistry, and medicinal chemistry. He has also co-edited a two volume book on Transition – metal catalyzed C-H functionalization of heterocycles published by Wiley VCH. Prof. Kumar has delivered more than 45 invited lectures at national and international symposiums/conferences.

Brief Biography of the Supervisor *[A-5]*

Dr. Kumar is an accomplished mentor, having supervised thirteen PhD students as supervisor, two as co-supervise and currently, he is supervising six PhD students. He has successfully executed six research projects as Principal Investigator (PI), sponsored by SERB, DST, CSIR, and UGC, and three projects as Co-PI sponsored by SERB, DST and Ranbaxy.

A respected member of various professional organizations, Dr. Kumar is a life member of Chemical Research Society of India, Bangalore; Indian Society of Chemists and Biologists, Lucknow; and Indian Council of Chemists, Agra. He serves as a valuable member of the editorial advisory board for The Open Catalysis Journal and actively contributes as a reviewer for several international journals in organic chemistry.

Dr. Anil Kumar's relentless pursuit of excellence in research and his dedication to imparting knowledge to the next generation of scientists have made him a prominent figure in the field of chemistry, earning him admiration and respect from peers and students alike. His passion for exploring novel chemical transformations and fostering sustainable practices in chemistry continues to inspire and shape the future of the discipline.